The Enterohaemorrhagic *Escherichia coli* Effector EspW Triggers Actin Remodelling in a Rac1 Dependent Manner

Pamela Sandu

Ph.D. Thesis

Imperial College London
Department of Life Sciences

Candidate's declaration

I Pamela Sandu, hereby confirm that this thesis constitutes my own work and that any external contributions are appropriately acknowledged or referenced.

Pamela Sandu

Copyright declaration

Abstract

Enterohaemorrhagic *Escherichia coli* (EHEC) is a diarrheagenic pathogen that colonizes the gut mucosa by forming attaching-and-effacing lesions. EHEC employs a type III secretion system (T3SS) to translocate 50 effector proteins that hijack and manipulate host cell signalling pathways, which contribute to subversion of immune responses, colonization and disease. The role of many effectors during infection remains unclear. This study aimed to identify the function of the T3SS effector protein EspW. Although EspW is an EHEC effector, we found that it is present in the prototypes strains EPEC E11 and B171. Furthermore, screening a collection of clinical EPEC isolates revealed that *espW* is present in 52% of the tested stains, suggesting that EspW is an important virulence factor. We report that EspW modulates actin dynamics in a Rac1-dependant manner. Ectopic expression of EspW results in formation of unique membrane protrusions. Infection of Swiss cells with an EHEC *espW* deletion mutant induces cell shrinkage that could be overcomed by Rac1 activation via expression of the bacterial GEF, EspT. EspW contains a QLSI motif, similar to the QxSI sequence found in the catalytic loops of the effectors EspM and Map, which activate RhoA and Rac-1, respectively. We found that I237 within that motif is essential for the activity of EspW during ectopic expression and infection. Furthermore, using a yeast two hybrid screen we identified the motor protein Kif15 as a potential interacting partner of EspW. Kif15 and EspW co-localized in co-transfected cells, while ectopically expressed Kif15 localized to the actin pedestals following EHEC infection. The data suggest that Kif15 recruits EspW to the site of bacterial attachment, which in turn activates Rac1, resulting in modifications of the actin cytoskeleton that are essential to maintain cell shape during infection.

Acknowledgements

I would like to acknowledge the people without whom this thesis would not have been possible. Firstly thank you to Prof. Gadi Frankel for the opportunity to carry out this research in his laboratory and for the years of support and guidance. I am also very grateful to the Biotechnology and Biological Sciences Research Council for providing the funding for this work.

I would also like to thank both Dr. Valerie Crepin-Sevenou and Dr. Cedric Berger for their invaluable guidance, training and supervision in all aspects of the project. I am extremely grateful for the patience you showed in the day to day teaching, help and advice. Your interest and enthusiasm in bacterial pathogenesis has been a constant source of my own motivation in the subject and gave me the energy to keep going. Thanks also go to Dr. Gunnar Schroeder and Dr. James Collins for their assistance and expertise which they provided me in various aspects of my work. Thank you to Prof. Steve Mathews and Dr. Huw Williams for their guidance and encouragement in their role as my PhD advisors.

I was blessed to share these years with amazing colleagues. Special thanks especially to Corinna, Lukasz, Marianne, Bevin and Mitch with whom I shared the joys and difficulties of the past few years. The Frankel and Filloux groups it was a pleasure to work with you all and also I really enjoyed all the parties and the times spent together outside the lab.

Thank you to my family for their love and support.

Lastly thank you to my many spiritual friends especially Shraddhasiddhi, Cristina, Gabi, Roxana, Elita, David, Livia, Raluca, Siobhan and Suella. Thank you for believing in me and for all your encouragements, love and support. I value your friendship and the time we spend together so much, I know I could not have been who I am today without you.

Table of contents

List of figures

List of Tables

Abbreviations

aa	Amino acid
AAF	Aggregative adherence fimbriae
A/E	Attaching and effacing
Arp2/3	Actin related proteins 2/3
Amp	Ampicillin
ATCC	American type culture collection
aEPEC	atypical EPEC
BFP	Bundle-forming pilus
BSA	Bovine serum albumin
CFA	Colonization factor antigen
Cm	Chloramphenicol
CRIB	Cdc42/Rac interactive binding domain
DH	Dbl Homology
DH-PH	Tandem Dbl-homology-pleckstrin homology
DAEC	Diffuse adherent *E. coli*
DMEM	Dulbecco's modified Eagle's medium
DNA	Deoxyribonucleic acid
DTT	Dithiothreitol
EAEC	Enteroaggregative *E. coli*
ECL	Enhanced ChemiLuminescence
EDTA	Ethylene diamine tetraacetic acid
EHEC	Enterohemorrhagic *E. coli*
EIEC	Enteroinvasive *E. coli*
EPEC	Enteropathogenic *E. coli*
ETEC	Enterotoxigenic *E. coli*
EAF	EPEC adherence factor
ECV	EPEC containing vacuole
ExPEC	Extraintestinal Pathogenic *E. coli*
Esp	*E. coli* secreted protein
F-actin	Filamentous actin
FCS	Fetal calf serum
g	Grams
GAP	GTPase activating protein
GDA	Glutaraldehyde
GDI	GDP-dissociation inhibitor
GDP	Guanine diphosphate
GEF	Guanine nucleotide exchange factor
GST	Glutathione S-transferase
GTP	Guanine triphosphate
h	Hours
HA	Haemmagglutinin (influenza epitope)
HC	Hemorrhagic colitis
HRP	Horseradish peroxidase
HUS	Hemolytic uremic syndrome
IF	Immunofluorescence
IMD	IRSp53/MIM homology domain
InPEC	Intestinal Pathogenic *E.coli*:

IPTG	Iso-propanyl-β-D- thiogalactopyranoside
JNK	c-Jun N terminal Kinase
kb	kilobase
kDa	kilodalton
L	Liters
LB	Luria Bertani
LEE	Locus of enterocyte effacement
LDH	Lactate dehydrogenase
LIMK	LIM kinase
Map	Mitochondrial associated protein
MBP	Maltose binding protein
min	minutes
MOI	multiplicity of infection
Nle	non-LEE encoded
NPY	Asn-Pro-Tyr motif
N-WASP	Wiskott-Aldrich syndrome protein
OD_{600}	Optical density measured at 600 nm
PAI	Pathogenicity island
PBS	Phosphate buffered saline
PCR	Paraformaldehyde
pet	Plasmid encoded toxin
PRD	Proline-rich domain
rpm	Revolutions per minute
Sec	General secretory pathway
SEM	Scanning Electron Microscopy:
Stx	Shiga toxin
SDS-PAGE	Sodium dodecyl sulphate-polyacrylamide gel electrophoresis
T1SS	Type I secretion system
T2SS	Type II secretion system
T3SS	Type III secretion system
T4SS	Type IV secretion system
T5SS	Type V secretion system
T6SS	Type VI secretion system
TBS	Tris Buffered Saline
0.1% TBST	Tris Buffered Saline 0.1% Tween 20
TccP/EspFu	Tir cytoskeleton coupling protein
tEPEC	typical EPEC
Tir	Translocated intimin receptor
U	Unit of enzymes
UPEC	Uropathogenic *E. coli*
V	Volts
Wave2	WASP-like Verprolin-homologous protein 2
WBD	WASP binding domain
WCA	WH2-central-acidic region
WH1/2	WASP-homology 1/2 domain
WHD	Wave homology domain
WT	Wild-type
WxxxE	Trp-xxx-Glu motif
Y2H	Yeast two-hybrid

CHAPTER 1 - **Introduction**

1.1 The Actin cytoskeleton

The cytoskeleton of eukaryotic cells is composed of microtubules, intermediate filaments and actin (Goldmann, 2008). Actin, one of the most abundant proteins in eukaryotic cells, forms major filamentous networks that coordinates cellular morphological changes including maintenance of cell shape, integrity, polarity, cell migration and division, vesicle trafficking, membrane dynamics and cell death (Girao et al., 2008), (Lanzetti, 2007), (Welch, 2002), (Pollard and Cooper, 2009), (Campellone and Welch, 2010).

1.1.1 **Actin polymerisation**

Actin polymerisation and depolymerisation drives the formation of sheet-like lamellipodia, finger-like projections such as filopodia and microvilli as well as stress fibres, ruffles, adhesion sites, phagocytic cups and endocytic pits (Figure 1.1).

Globular-actin (G actin) is a 42 kDa ATP-binding protein that self-assembles whilst releasing inorganic phosphate (Pi) and in this way forms filamentous actin (F-actin) (Pollard, 2007), (Welch, 2002). Actin filaments are polar in nature at the barbed end of the filament (also known as plus (+) end) and it has an increased affinity for ATP bound G-actin. This ATP bound G-actin affinity at the (+) end drives the growth and the extension of the actin filament as is tenfold faster than the slower growing pointed end (also known as minus (-)) (Zigmond, 2004), (Pollard, 1986). The actin filament is highly dynamic as the pointed end ADP bound G-actin is gradually lost allowing the free G-actin subunits to be recycled and further bind ATP (Cooper and Schafer, 2000). The regulation of actin polymerisation relies on a vast number of accessory proteins that will stabilise or destabilise filaments, cap or

uncap pre-existing filaments, sever existing filaments to create free barbed ends, nucleate filaments and crosslinks filaments into networks or bundles (Figure 1.2).

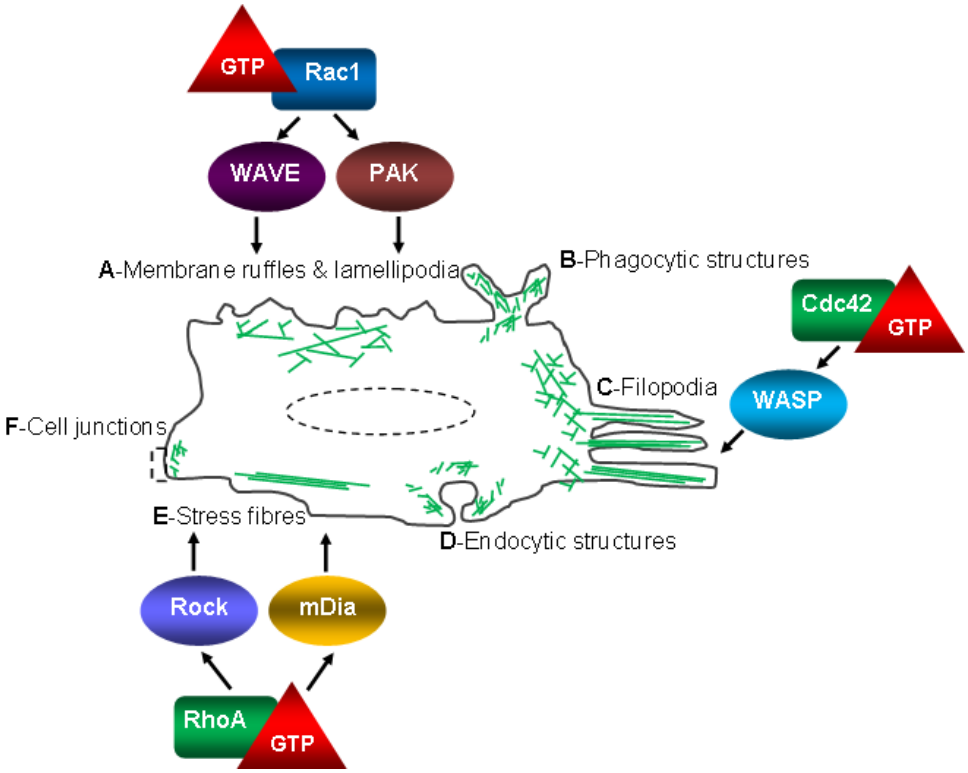

Figure 1.1 - Diagram showing the diverse structures formed by the actin cytoskeleton under the regulation of Rac1, Cdc42 and RhoA

Details in chapter 1.2. Actin filaments in green are nucleated and organised into branched networks by the Arp2/3 complex and its nucleation promoting factors (NPF) or are generated in unbranched forms by formins and tandem WH2-domains (explained in Fig 1.2) **A** - Membrane ruffles and lamellipodia. Active Rac1 further activates the Wave complex resulting in the subsequent recruitments of the actin nucleator Arp2/3. Rac1 also activates the effector PAK which is proposed to play a role in maintaining lamellipodia stability as well as localising Wave to the membrane; **B** – Phagocytic structures; **C** – Filopodia – induced by the GTP-bound Cdc42 and mediated via the WASP proteins and Arp2/3; **D** – Endocytic structures; **E** – Stress fibres induced by GTP bound RhoA via the coordinated activation of Rho coiled coil p160 kinase (ROCK) and the formin mDia. Rock and mDia stimulate an increase in actomyosin contractibility and the nucleation of stress fibres; **F** – Cell junctions.

These accessory proteins include profilins, capping proteins, gelsolins and cofilins. Profilins are G-actin binding proteins that catalyse the exchange of actin bound ADP to ATP, in this way maintaining the levels of ATP bound monomers ready for polymerisation (Condeelis, 2001), (Witke, 2004). Barbed end proteins such as capping proteins keep the barbed ends in low concentrations whilst gelsolins assist in filament binding, capping and severing activities (Condeelis, 2001), (Sun et al., 1999). ADF/cofilin is an actin depolymerizing factor which severs the existing actin filaments, inhibits the ADP-ATP exchange generating an ADP-actin monomeric pool that can be recycled into ATP-actin by profilin (Chan et al., 2009), (Bamburg, 1999).

1.1.1.1 Actin nucleators

The initiation of actin polymerisation from free actin monomers or spontaneous filament nucleation is kinetically unfavourable when compared to actin filaments formation by rapid self-assemble of G-actin monomers. Therefore actin nucleation factors are necessary to stabilise actin dimers and trimers to promote actin polymer formation (Millard et al., 2004), (Campellone and Welch, 2010). There are three classes of actin nucleators including: the Arp2/3 complex, formin and spire classes and the nucleation promotion factors (NPFs) (WAVE/SCAR and WASP-family of NPFs). These factors adopt different mechanisms of nucleation and organise the formed filaments in different types of actin structures such as filopodia, lamellipodia and membrane ruffles (Campellone and Welch, 2010).

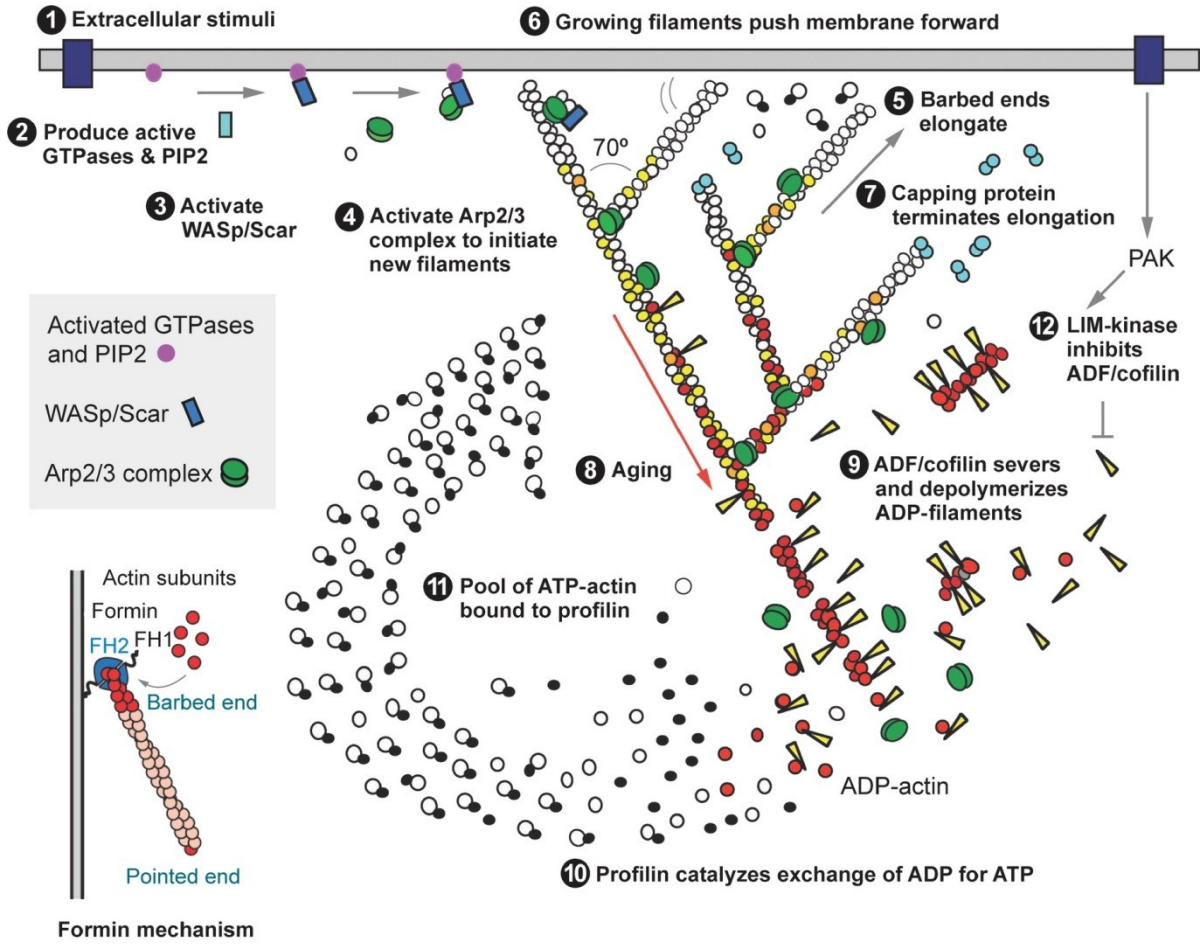

Figure 1.2 - Schematic representation of actin cytoskeleton modulation in response to external stimuli and the functions of Arp2/3 complex and formins.

An extracellular stimulus can result in the activation of nucleation-promoting factors such as WASp and Scar/WAVE. This interaction will bring together Arp2/3 complex with an actin monomer on the side of a filament to nucleate a branch. The free barbed end of the branch grows until it is capped. Formins use their FH2 domain to nucleate unbranched filaments and remain attached to their barbed ends as they elongate. Image taken from (Pollard, 2007).

1.1.1.2 The Arp2/3 complex

The Arp2/3 complex machinery is the best studied actin nucleation factor. It is a 220 kDa heptameric arrangement made up of five actin related proteins (Arp) subunits Arp2, Arp3 and Arp2/3 complex components (ARPC1-5) (Machesky et al., 1994), (Welch, 2002).

Arp2/3 binds to existing F-actin filaments and requires Arp2 phosphorylation and the recruitment of nucleation promoting factors such as WASP to generate branching. Arp2/3 complex binds three subunits from the mother actin filament and forms a 'Y' conformation at a ~ 70° angle (Blanchoin et al., 2000). Repeated Arp2/3-mediated filament assembly can create a highly dynamic branched dendritic network of F-actin generating actin structures such as filopodia, lamellipodia and membrane ruffles (LeClaire et al., 2008), (Campellone and Welch, 2010).

1.1.1.3 Formins

Formins produce unbranched actin linear filaments and represent the second class of actin nucleators. There are ~ 15 mammalian formins (divided in seven subclasses) which are defined by the presence of a conserved formin homology (FH) domains FH1 and FH2. The FH2 domains are sufficient to trigger actin polymerisation *in vitro* (Moseley et al., 2004) and it stabilise actin dimers by preventing their access to capping proteins (Figure 1.2). Furthermore the FH2 domains bind the barbed end of nascent actin polymer and remains bound to the barbed end of the filament whilst moving progressively with the growing actin filament extension (Goode and Eck, 2007), (Otomo et al., 2005). The FH1 domains interact with profilin and accelerate filament elongation by enhancing the delivery of actin monomers at the growing end (Romero et al., 2004).

One of the most widely expressed and best characterised formin is mammalian Diaphanous related formin (mDia) (Campellone and Welch, 2010).

1.1.1.4 Spire, cordon-bleu (Cobl), leiomodin (Lmod) and p53-cofactor JMY (JMY)

This group of actin nucleators contain a tandem of G-actin binding WASP homology 2 (WH2) domains. Spire proteins contain four WH2 domains which are capable of binding four actin monomers in a chain which acts as a template for the addition of further actin monomers. The actin filaments are nucleated by stabilising longitudinal actin tetramers or side-to side formations (Quinlan et al., 2005). This WH2 motif is also conserved in the chimeric NPF p53-cofactor JMY, an NPF that possesses three tandem WH2 domains. Furthermore it was shown to nucleate actin via a spire like mechanism (Zuchero et al., 2009). Cobl also nucleates actin filaments similarly to spire and uses three WASP homology domains to bind actin monomers linearly, with one perpendicular G-actin monomer on a linear dimer (Ahuja et al., 2007). Lmod was shown to have a single WASP homology domain and two actin binding sites (Chereau et al., 2008).

1.1.1.5 Nucleation promoting factors (NPFs)

Nucleation promoting factors control the activation of Arp2/3-mediated actin nucleation pathway. The majority of mammalian NPFs belong to a class I group and act via a WCA/VCA domain which contains the C-terminal WASP-homology 2 (WH2) domain. The WH2 domain is used to recruit G-actin monomers and uses the veroprolin (V), central (C) and acidic (A) domain to activate Arp2/3 (Rodal et al., 2005), (Park et al., 2007).

The WCA binds to the Arp2/3 and actin and induces a conformational change in the Arp2/3 complex resulting in stabilization of Arp subunits Arp2 and Arp3 (Rodal et al., 2005). Class I NPFs include Wiskott-Aldrich syndrome protein (WASP), neuronal-WASP (N-WASP) and WASP-family veroprolin homologue (WAVE) (Figure 1.3 A).

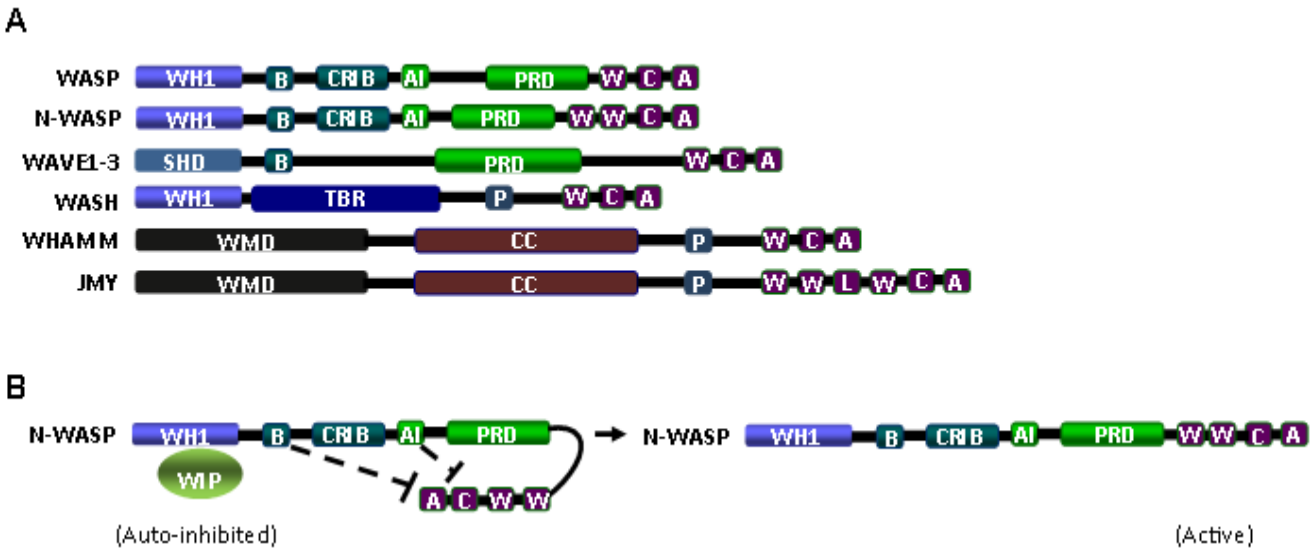

Figure 1.3 - Schematic representation of the Class I NPFs, WASP, N-WASP, WAVE1-3, WASH, WHAMM and JMY with their component domains.

A - Mammalian Class I NPFs contain C-terminal WCA domains that bind G-actin and the Arp2/3 complex, plus diverse N-terminal regulatory regions.
(A, acidic; AI, autoinhibitory; B, basic region; C, connector; CC, coiled-coil; CRIB, Cdc42-Rac-interactive-binding; L, linker; PRD, proline-rich-domain; SHD, Scar-homology-domain; TBR, tubulin-binding region; W, WASP-homology-2 (WH2) domain; WH1, WASP-homology-1; WMD, WHAMM-membrane interaction-domain)
B - Mechanism of activation for N-WASP which is regulated both by autoinhibition and by interactions with proteins from the WIP family.

A. WASP/N-WASP

WASP and Apr2/3 generate highly dynamic branched actin filaments and form structures such as filopodia and lamellipodia. WASP is explicitly expressed in haemopoietic cells while its homologue N-WASP is ubiquitous and with higher prevalence in neuronal cells. (Bosticardo et al., 2009). WASP shares a similar domain architecture with N-WASP; they both contain a WH1 domain, followed by basic (B) region, a GTPase binding domain (GBD) which contains the Cdc42 and Rac interactive binding (CRIB) domain, an autoinhibitory motif followed by a proline rich domain (PRD) and a carboxy-terminal WCA region (Takenawa and Suetsugu, 2007), (Campellone and Welch, 2010) (Fig. 1.3 A). In the inactive form of N-WASP, the GBD domain and the C region of VCA interact forming a closed loop (Figure 1.3 B). In contrast, binding of Rho GTPase Cdc42 to the GBD domain of N-WASP induces the release of the WCA domain and activation of the Arp2/3 complex (Rohatgi, 1999). Furthermore activation can be mediated by interaction of adaptor protein Src-homology 3 (SH3) domains with non catalytic kinases (Nck1 and NcK2) and Abl1 (Innocenti et al., 2005). WASP and N-WASP are found in hetero complexes with the WASP-interacting family of proteins (WIP) which bind WH1 via its WASP-binding domain (WBD) and in this way prevents N-WASP from degradation (de la Fuente et al., 2007). WIP was shown to be required for Cdc42 dependent N-WASP activation and also acts in complex with N-WASP promoting actin polymerisation (Anton et al., 2007).

B. WAVE, WASH and WHAM

WAVE proteins are potentially actin nucleation promoting factors involved in the formation of lamellipodia and membrane ruffles (Suetsugu et al., 2006). There are three WAVE isoforms (WAVE1-3) consisting of an amino-terminal SCAR homology domain (SHD), a basic region which binds to phosphatidylinositol 3,4,5-triphosphate [PI(3,4,5)P_3], a central PRD and carboxy-terminal WCA (Gautreau et al., 2004).

The WAVE family of proteins are regulated via protein-protein interaction. The SHD domain of WAVE forms complexes with Nck-associated protein 1 (NAP1), Abelson-interacting protein-1 and 2 (Abi1/Abi2), HSPC300 and specifically Rac-associated 1 (SRA-1) (Kunda et al., 2003), (Gautreau et al., 2004). Interaction of Nap1 with Nck and of Rac1 with SRA-1 was shown to enhance the actin polymerisation activity of the WAVE complex (Eden et al., 2002), (Steffen et al., 2004). Furthermore, the interaction between VCA of WAVE and PI(3,4,5)P_3 strongly enhances actin polymerisation activity at the cellular membrane (Suetsugu et al., 2006). Regulation by Rac can also be mediated by indirect binding of insulin receptor substrate p53 (IRSp53) to Rac and binding of IRSP53 to the PRD domain of WAVE2 via its SH3 domain (Suetsugu et al., 2006).

WASH was first identified as a WASP family member encoded in the subtelomeric region of chromosomes (Linardopoulou et al., 2007). WHAMM is a WASP homolog which was shown to have actin nucleation activity and microtubule binding capacity (Campellone et al., 2008).

1.2 Tubulin and Human Kinesin-12 (Kif15)

Microtubules are a key component of eukaryotic cell cytoskeleton and are involved in many essential cellular processes, including structural support, intracellular transport and mitosis (Bergen and Borisy, 1980). Microtubules are long, filamentous, tube-shaped protein polymers composed of heterodimers of α- and ß-tubulin (Waterman-Storer and Salmon, 1997). These filamentous structures present two ends, a (+) end which attaches ß-tubulin, and a (-) end, where the α-tubulin subunit is exposed to the solvents. To form microtubules, the dimers of α- and ß-tubulin bind to GTP and assemble into the (+) end of microtubules forming a short region called GTPcap which prevents the microtubule from disassembly (Kaur et al., 2014). Microtubules are destabilised following the hydrolysis of tubulin-bound GTP into GDP through inter-dimer contacts along the microtubule protofilament (Nogales, 2001). Whether the β-tubulin member of the tubulin dimer is bound to GTP or GDP influences the stability of the dimer in the microtubule. Dimers bound to GTP tend to assemble into microtubules, while dimers bound to GDP tend to fall apart and in this way the GTP cycle is essential for the dynamic instability of the microtubules (Kollman et al., 2011), (Downing and Nogales, 2010). The switch from growing or paused state to shortening state is called 'catastrophe' and the switch in opposite direction is called 'rescue' (Nogales and Wang, 2006). This ability to assemble and disassemble is critical in cell shape maintenance, intracellular transportation and cell division and mitosis.

The microtubule behaviour is affected by a large family of kinesin motor proteins, which move on these cytoskeletal tracks in order to perform diverse activities including 'catastrophe', crosslinking and movement of microtubules relative to one another in order

to 'self-organize' (Conde and Caceres, 2009). Motor proteins such as kinesin and dynein use ATP hydrolysis to generate force for transport along microtubules (such as axonal transport) or for cell motility (such as ciliary or flagellar motion) (Rath and Kozielski, 2012).

A conventional kinesin consists of a heavy chain (KHC) dimer and two associated kinesin light chains (KLC) that are involved in substrate recognition and binding. The heavy chain comprises an N-terminal motor domain (MD) (comprising an ATP binding pocket) followed by an elongated stalk and a small, intrinsically disordered C-terminal tail domain (Figure 1.4 A) (Hirokawa et al., 1989), (Seeger et al., 2012), (Yang et al., 1989).

Human Kif15 (which will become relevant later in this study) belongs to the kinesin family and is a dimeric protein of 1388 residues. It has an N-terminal motor domain (residues 19–375) followed by a long alpha-helical rod-shaped stalk predicted to form an interrupted coiled coil. The C-terminal region has been shown to contain a putative interacting region for actin (residues 743–1333) (Figure 1.4 B) (Klejnot et al., 2014). This plus-end directed microtubule motor protein is expressed in all cells during mitosis and in postmitotic neurons undergoing axon growth (Matuliene et al., 1999). In dividing cells, it promotes spindle assembly by cross-linking and sliding along microtubules creating a separation between centrosomes. Moreover in Hela cells, Kif15 has been shown to concentrate on spindle poles and microtubules in early mitosis and to localize with actin in late mitosis (Buster et al., 2003). One possibility is that Kif15 truly switches affinity from one filament system to the other, while another possibility is that Kif15 may associate with the more abundant cytoskeletal filament system. Potentially, Kif15 could utilise its myosin tail homology domain located in the coiled-coil to associate with an actin-based motor and through this interaction contact actin, though this theory has not yet been diligently investigated.

The activity of Kif15 might have clinical implications. Tubulin has additional target sites for anticancer drugs including interference with the binding and function of microtubule associated proteins and interference with motor proteins which are essential for the transport of substances within the cell such as Kif15. Because many of these microtubule associated proteins have an ATP binding site, both computer-aided design and combinatorial chemistry techniques can be used to make agents to interfere with their function. Currently there are a number of such agents that are undergoing clinical trials (Pellegrini and Budman, 2005).

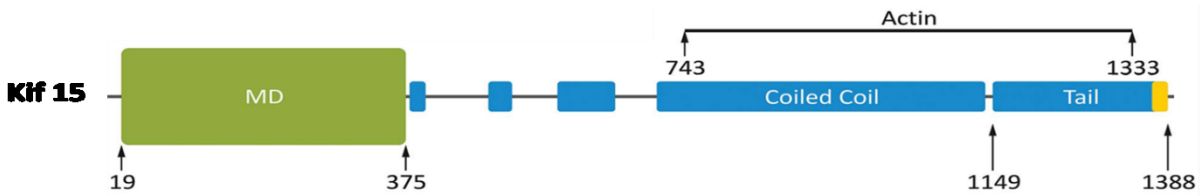

Figure 1.4 - Schematic representation of human kinesin Kif15

The motor domain (MD) shown in green is followed by a neck region and coil-coil regions and a putative tail (in blue). The leucine zipper is presented in yellow (Klejnot et al., 2014).

1.3 Rho GTPases

Rho-GTPases which belong to the family of Ras-related small GTPases have emerged as key regulators in various cellular processes including actin polymerisation, microtubule dynamics, vesicle trafficking, cell polarity and cytokinesis (Heasman and Ridley, 2008).

There are ~22 Rho family GTPases including Rho (A, B, C, D, E, G, H, BTB1, BTB2), Rac (1, 2,

3), Cdc42, Rnd (1, 2), TC10, TCL, Chp, Wrch1, Rif and Miro (1, 2) (Jaffe and Hall, 2005). These small Rho GTPases share a characteristic G-domain structure responsible for GTP binding and hydrolysis, two flexible switch loops (I and II) able to undertake conformational shifts, a phosphate loop (P-loop) involved in the activity and regulation of interaction proteins and an Mg2+ pocket required for high affinity binding of nucleotides at the switch region (Rossman et al., 2005).

1.3.1 **Regulation of Rho GTPases**

Rho-GTPases can switch from an inactive GDP bound state to an active GTP bound state and this exchange is regulated by guanine nucleotide exchange factors (GEFs). The switch from the active GTP to an inactive GDP bound state is regulated by GTPase-activating proteins (GAPs). The guanine nucleotide dissociation inhibitors (GDIs) prevent membrane localization and maintain the GTPases in an inactive state in the cytosol (Hoffman et al., 2000), (Jaffe and Hall, 2005) (Figure 1.5).

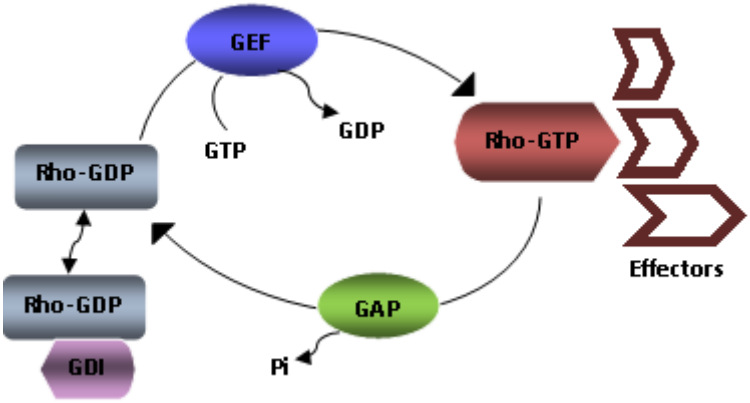

Figure 1.5 - Rho GTPase cycle

Guanine exchange factors (GEFs), GTPase-activating proteins (GAPs) and guanine nucleotide dissociation inhibitors (GDIs) mediate the classical Rho GTPases switch from the inactive (GDP-bound) to active (GTP-bound); Activated Rho GTPases interact with target effector proteins to initiate downstream signalling.

In their GTP-bound the conformation of the switch regions change dramatically altering the structure of Rho-GTPases and allows them to interact with and activate downstream target effector proteins such as serine/threonine kinases, tyrosine kinases, lipid kinases, lipases, oxidases, and scaffold proteins. Rho GTPases are also post translationally modified at their C-terminal CAAX motif, allowing them to be anchored in the cellular membrane (Roberts et al., 2008).

1.3.1.1 Rho guanine nucleotide exchange factors (GEFs)

Rho GEFs promote the exchange of GDP for GTP within the switch region by promoting the release of Mg^{2+} and GDP. The majority of mammalian Rho GEFs belong to the Dbl family, characterised by the presence of a Dbl Homology catalytic domain (DH) which contains 10-15 alpha helices with three conserved regions (CR1, CR2 and CR3) (Rossman et

al., 2005). The DH domain interacts with Switch I and II resulting in a conformational change that releases the GDP and leaves the nucleotide pocket available for GTP. Rho GEFs also contain a Pleckstrin Homology (PH) domain that binds phosphoinositols and localises the GEF GTPase complex to the cell membrane (Olson and Cuff, 1997).

Another family of Rho GTPase GEFs are the dedicator of cytokinesis (DOCK) family of Rho GEFs which are classified based on the presence of two conserved DOCK homology regions DHR1 and DHR2 (Cote and Vuori, 2007). In comparison with the DH domain that binds both switches (I and II), the DHR2 domain interacts with the switch I region without altering the switch II (Yang et al., 2009). This interaction will also result in the conformational change required for GTP binding.

1.3.1.2 Rho GTPase-activating proteins (GAPs)

Rho GAPs have a role in increasing GTP hydrolysis and activating the switch between GTP-bound active form and the GDP-bound inactive form and turns off GTPase signalling.

There are ~70 human GAP proteins, grouped into ~23 subfamilies according to their structure and function (Peck et al., 2002), (Tcherkezian and Lamarche-Vane, 2007). GAPs bind GTPases and insert a loop called arginine finger which contains a primary arginine residue that acts as electron acceptor during the hydrolysis reaction (Fidyk and Cerione, 2002). After GTP hydrolysis, Rho GAP are released from the GTPase. There are different GAP regulation activities including protein-protein interaction, localisation and phosphorylation (Roof et al., 1998).

1.3.1.3 Rho GDP dissociation inhibitors (GDIs)

Human Rho GDIs are grouped in three categories: Rho GDIα, Rho GDIß and Rho GDIγ. GDIα is ubiquitously expressed, GDIß is haematopoietic and GDIγ s selectively expressed, mainly in lung, brain and testis (Dovas and Couchman, 2005). Rho GDIs associate with both GTP and GDP bound GTPases, preventing GTP and GDP exchange and maintain the Rho GTPases in an inactive form in accordance with cellular needs. It has an inhibitory effect and bind to the GTP form of Rho GTPases to prevent GTP hydrolysis and interaction with downstream effector proteins (Dovas and Couchman, 2005). Furthermore GDIs prevents localisation of the GTP-bound Rho GTPases at the plasma membrane by sequestering active Rho GTPase into the cytosol away from activating membrane bound GEFs (Olofsson, 1999). This is a result of the interaction between the C-terminal domain of the Rho GDIs and the CAAX motif of Rho GTPases (Gosser et al., 1997).

GDI regulation is mediated by proteins, such as Ezrin Radixin Moesin family of proteins (ERM), GDI displacement factors, lipids, tyrosine kinase Etk (Kim et al., 2002) or directly by phosphorylation by protein kinase C or PAK (DerMardirossian and Bokoch, 2005).

1.3.2 **Modulation of actin dynamics by RhoA, Rac1 and Cdc42 Rho GTPases**

The best characterised members of the family of small Rho GTPases are RhoA, Rac1 and Cdc42 with a pivotal role in actin dynamics. Their activation leads to the assembly of stress fibres (RhoA), lamellipodia/ruffles (Rac1/Cdc42) and filopodia (Cdc42) (Hall, 1998).

1.3.2.1 RhoA

RhoA induces actomyosin contractibility and the formation of stress fibers, which results in modifications in the structural aspects of the cell architecture (Figure 1.1). Stress fibers form at focal adhesions and are highly ordered unbranched long polymers of actin, held together by the actin cross-linking protein α-actinin (Pellegrin and Mellor, 2007). The actomyosin system is formed of myosin family proteins which interact with actin to act as molecular motors that drive motility and contraction, cytoskeletal reorganisation vesicle transport and phagocytosis (Walker et al., 2000). Stress fibers are categorised in three groups: ventral stress fibers (which lie across the base of the cell and interact with focal adhesions at both ends), dorsal stress fibers (one end is connected with focal adhesions at the base of the cell and the other terminates at the dorsal surface) and transverse arcs (that form beneath the dorsal surface) (Cramer, 1997).

Activated RhoA interacts with down-stream effector proteins formin mDia and Rho coil coil p160 serine-threonine kinase (ROCK) (Fig. 1). ROCK phosphorylates both the Myosin Light Chain (MLC) and the Myosin Binding subunit (MBS) of the MLC phosphatase to form increased thick parallel stress fibres (Amano et al., 1996). Furthermore ROCK targets LIM kinase (LIMK) which subsequently phosphorylates and inhibits cofilin resulting in stabilisation of actin filaments (Jaffe and Hall, 2005), (Maekawa et al., 1999).

1.3.2.2 Rac1

Rac1 induces the formation of membrane ruffles and lamellipodia which are associated with cellular movement (Hall, 1998). Lamellipodia are a network of actin rich

extensions which projects from the leading end of cells (Nobes and Hall, 1995) facilitating the crawling movement of cells. Membrane ruffles are waves of sheet like structures formed from lamellipodia that failed to establish stable adhesions. It also has a role in cellular movement, macro-pinocytosis and receptor recycling (Fukata et al., 2003). The actin filaments from lamellipodia branch at a 70° angle and is Arp2/3 complex dependant. Activated Rac1 interacts with downstream effector proteins including WASP-like Verprolin homologous protein 2 (WAVE2) and the P21 activating kinase (PAK) family of Ser/Thr kinases (Eden et al., 2002), (Hall, 1998) (Figure 1.1, Figue 1.6). PAK also phosphorylates LIMK and inhibits cofilin activity (Edwards et al., 1999). Furthermore Rac1 mediated PAK activation was shown to enhance lamellipodia stability by activating Erk1/2 (Smith et al., 2008).

Rac1 does not bind WAVE2 directly, but interacts in a complex together with the GTPase in order to induce lamellipodia and membrane ruffling formation. This complex that mediates Rac1 binding includes WAVE2, Abi1 and accessory proteins PIR121 and Nap1 (Steffen et al., 2004), (Innocenti et al., 2005). Furthermore, interaction of Rac1 with Steroid receptor RNA activator 1 (SRA-1) was shown to enhance the actin polymerisation activity of the WAVE complex (Steffen et al., 2004) (Figure 1.6). Regulation of actin filament formation by Rac1 can also be mediated by indirect binding of insulin receptor substrate p53 (IRSp53) to Rac1 and binding of IRSP53 to the PRD domain of WAVE2 via its SH3 domain (Suetsugu et al., 2006).

1.3.2.3 Cdc42

In a similar way as Rac1, the Cdc42 dependent actin polymerisation is mainly mediated by the Arp2/3 complex, through the binding and activation of WASP and WAVE family NPFs (Rohatgi, 1999). Cdc42 induces the formation of filopodia which are finger like projections that extend from the cell membrane and contain cross-linked actin bundles (Figure 1.1). Filopodia provides the resistance required for the lamellipodia to drive the cell during migration and also in contacting neighbouring cells (Faix and Rottner, 2006), (Ridley, 2001). Activated Cdc42 interacts with downstream effector proteins by direct binding with the CRIB domain of WASP and N-WASP. This results in the release of the autoinhibitory conformation of WASP and N-WASP and allows actin nucleation in an Arp2/3 manner. Furthermore WASP and N-WASP interacts with profilin and enhances actin polymerisation activity (Takenawa and Suetsugu, 2007). Cdc42 also interacts with PAK in a similar way to Rac1 (Kurokawa et al., 2004).

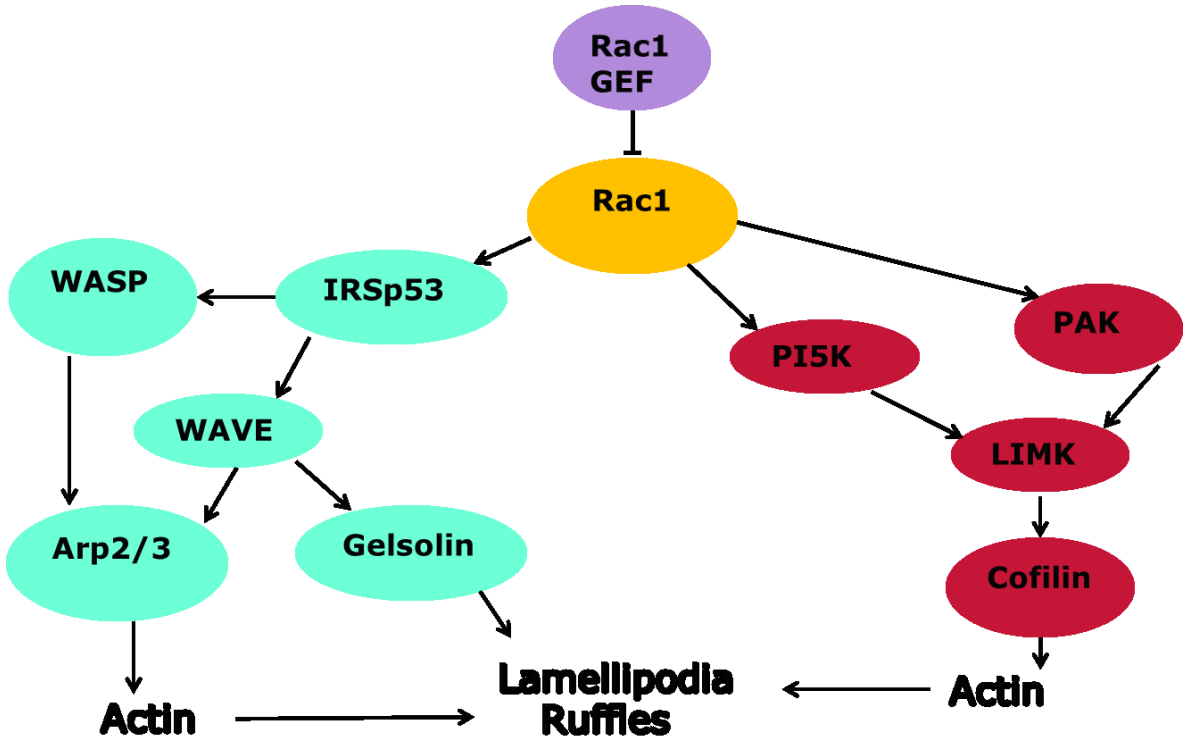

Figure 1.6 - Schematic representation of the regulation of actin dynamics that might be related to the project

Activated Rac1 interacts with downstream effector proteins including PAK which in turns activates LIMK leading to cofilin phosphorilation resulting in lamellipodia and membrane ruffling formation. Regulation of actin filament formation by Rac1 can also be mediated by indirect binding of IRSp53 to Rac1 and binding of the PRD domain of WAVE2.

1.4 Pathogenic Escherichia coli

Escherichia coli is a Gram-negative bacteria amongst the facultative anaerobic intestinal flora which has an important role in maintaining the gut physiology (Siitonen, 1992). Although most *E. coli* are beneficial for the gut homeostasis, several clones have acquired (via horizontal transfer) small gene clusters and pathogenicity islands associated with virulence, and are referred to as pathogenic (Kaper et al., 2004).

The pathogenic *E. coli* strains are able to employ different infection strategies causing gastro-intestinal infections, urinary tract infections (UTIs), and systemic infections (leading to sepsis, meningitis and renal failure) (Nataro and Kaper, 1998). Their capacity to infect and disseminate are attributed to the presence of virulence factors such as toxins, adhesins and secreted effector proteins. Pathogenic *E. coli* strains were first characterized according to the serology of their surface characteristics (Kauffmann, 1974) by O (lipopolysaccharide, LPS) and H (flagellar) antigens where O antigen defines serogroups and O:H defines a serotype (Figure 1.7). Currently there are 174 *E. coli* O and 53 *E.coli* H antigens (DebRoy et al., 2011).

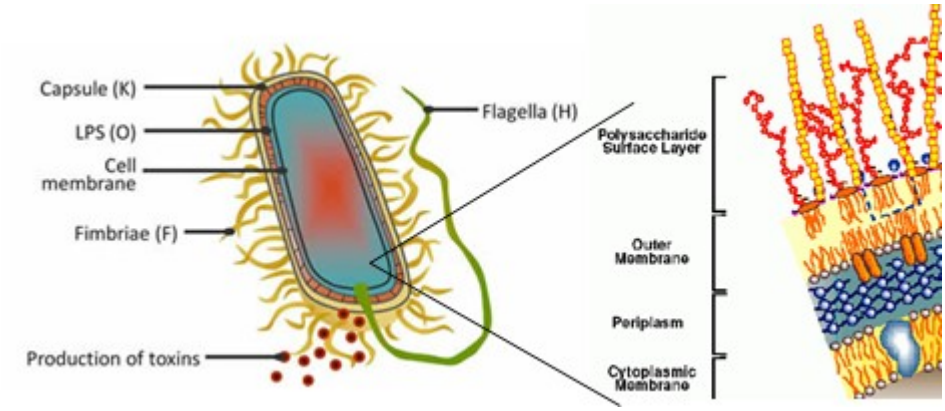

Figure 1.7 - Schematic representation of E.coli outer surface

E. coli is classified in different serotypes based on somatic (O), capsular (K), fimbrial (F) and flagellar (H) antigens. It has two double lipid bilayer membranes with a periplasmic space in between. (This figure is reproduced courtesy of www.ecl-lab.com/en/ecoli/index.asp and 2007.igem.org/BerkiGEM2007Present4 online resources).

A pathotype is defined as a group of microorganisms of the same species that have the same pathogenicity on a specified host. As some serotypes can belong to more than one pathotype (most recently, the pathogenic *E. coli* were grouped into three major categories: Extraintestinal Pathogenic *E. coli* (ExPEC), Intestinal Pathogenic *E.coli* (InPEC) and

commensal *E. coli* (that can act as opportunistic pathogens at lower immunity) (Russo and Johnson, 2000). There are six types of InPEC: Enteropathogenic *E.coli* (EPEC), Enterotoxigenic *E.coli* (ETEC), Enteroinvasive *E.coli* (EIEC), Diffusely Adherent *E.coli* (DAEC), Enterohaemorrhagic *E.coli* (EHEC) and Enteroaggregative *E.coli* (EAEC), each having distinct histopathological and clinical characteristics (Figure 1.8).

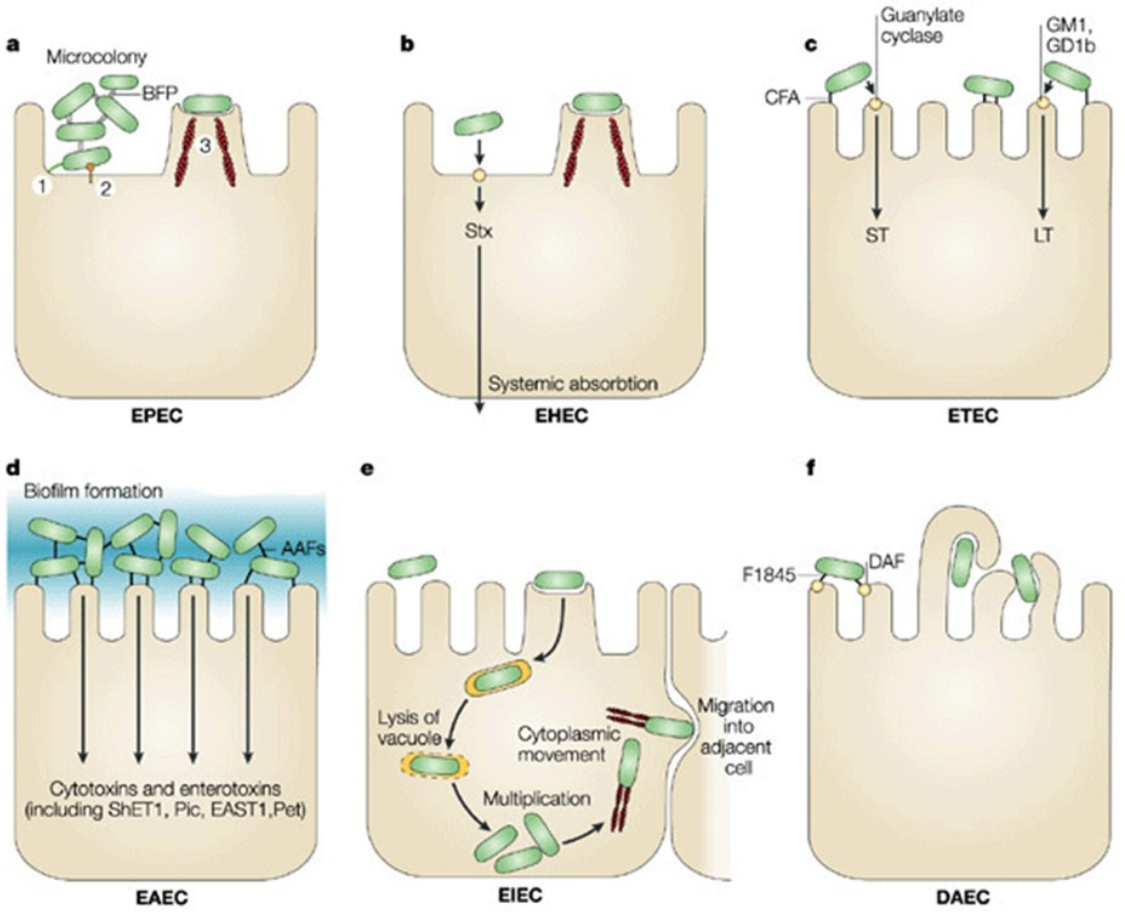

Figure 1.8 - Schematic representation of diarrhoeagenic *E.coli*

There are six categories of diarrhoeagenic *E.coli* that employ different infection strategies: **a** – EPEC adhere to small bowel enterocytes (1), translocates bacterial proteins using a type three secretion system (2), resulting in attaching and effacing lesions (3); **b** – EHEC produce and release Shiga toxin (Stx); **c** – ETEC colonises the brush border via CFA (colonization factor antigen) and uses heat-labile (LT) and/or heat stable (ST) enterotoxins to induce watery diarrhea; **d** – EAEC forms a thick biofilm via AAF (aggregative adherence factors) and releases various cytotoxins and enterotoxins such as ShET1 (*Shigella* enterotoxin 1), Pic, EAST1 (Enteroaggregative *E. coli* ST1) and Pet; **e** – EIEC invades host cells and once internalized escape from their vacuole, multiply in the cytoplasm and nucleates actin microfilaments for lateral spread into an adjacent cell; **f** - DAEC induces the formation of long finger-like projections that wrap the bacteria. BFP (bundle-forming pilus); DAF (decay-accelerating factor) (Kaper et al., 2004)).

1.5 Enteropathogenic *E. coli* (EPEC), Enterohaemorrhagic *E. coli* (EHEC): Attaching and effacing pathogens

EHEC and EPEC along with rabbit EPEC (REPEC) and the murine pathogen *Citrobacter rodentium* belong to a family of pathogens that form attaching and effacing (A/E) lesions, characterised by effacing of microvilli and intimate adherence between the bacteria and host epithelial cell membrane (*in vivo*) (Frankel et al., 1998a), (Knutton et al., 1987b) (Figure 1.9 A). *In vitro* it also leads to the formation of actin-rich 'pedestal' like structure underneath bacterial attachment site (Knutton et al., 1989), (Rosenshine et al., 1996) (Figure 1.9 B and C).

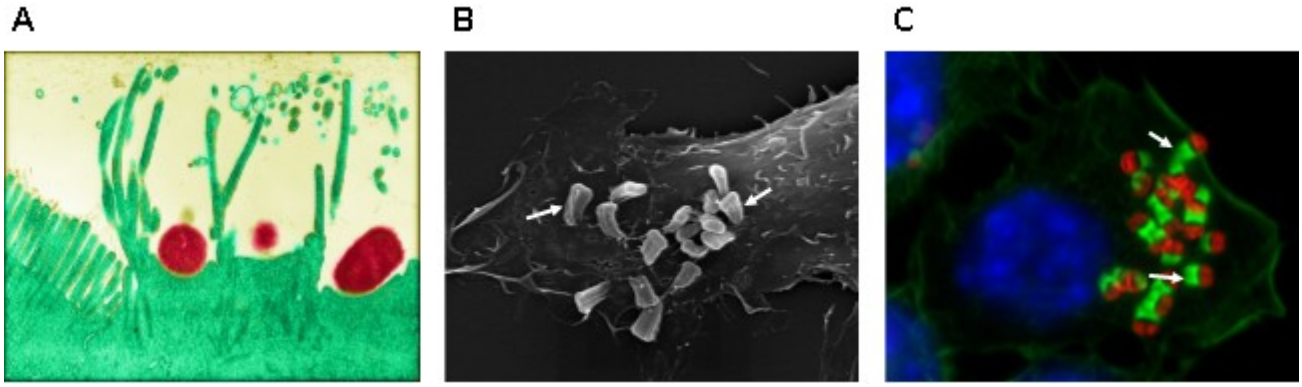

Figure 1.9 - A/E lesions

A- Electron micrograph of human colonic IVOC (*in vitro* organ culture) infected with the EPEC strain showing intimate attachment of the bacteria and the altered microvilli beneath them (A/E lesions) (Knutton et al., 1987a); **B** - Scanning electron micrograph of pedestals induced by adherent bacteria in vitro (arrows); **C** – Immunofluorescence imaging of EHEC infected Swiss cells (nuclei (blue), actin pedestal (in green (arrows)) and bacteria (red)). Images B and C taken in this study

A pathogenicity island referred to as the Locus of Enterocyte Effacement (LEE) is the genetic determinant required in order to induce the formation of A/E lesions (McDaniel et al., 1995a). The LEE island encodes the functional and structural components of a type 3

secretion system (T3SS), associated chaperones and seven T3SS effector proteins which are translocated into host cells (McDaniel et al., 1995a) (detailed explanation in section 1.7.6 and 1.7.7).

1.5.1 **Enteropathogenic *E. coli* (EPEC)**

EPEC, the first *E. coli* to be associated with human disease (Levine et al., 1978), is a major cause of infantile diarrhoeal disease (younger than 5 years) in the developing world (Nataro and Kaper, 1998), with over 750 000 deaths each year (Liu et al., 2012).

This pathogen is transmitted via fecal-oral route, with contaminated water, hands and fomites serving as vehicles. EPEC strains are differentiated as typical and atypical. Typical EPEC are defined by the presence of the locus of enterocyte effacement (LEE) Pathogenicity Island (McDaniel et al., 1995a), and the EPEC adherence factor (EAF) plasmid (Baldini et al., 1983), that carries the transcriptional regulator locus *per* (Mellies et al., 1999), and encodes the type IV bundle-forming pilus (BFP) (Girón et al., 1991). Typical EPEC are further divided into two distinct evolutionary lineages known as EPEC 1 and EPEC 2 (Orskov et al., 1990). EPEC1 is characterized by the presence of flagellar antigens H6 and H34 and the adhesin intimin subtype α (Adu-Bobie et al., 1998). EPEC2 express the flagellar antigen H2 or can be H^-, and encodes the adhesin intimin subtype ß and the effector protein TccP2. Atypical EPEC lacks the EAF plasmid (Trabulsi et al., 2002). Both animals and humans can be reservoirs for atypical EPEC however for typical EPEC the only reservoir is humans. The World Health Organisation has assigned typical EPEC to serogroups O26, O55, O111, O114, O119, O125, O127, O128, O142 and O158 (Chen and Frankel, 2005). The archetypal strain of EPEC1 is

E2348/69 and its genome contains only a fraction of the virulence factors associated with EPEC2 strains such as B171 O111:H$^-$.

1.5.2 **Enterohaemorragic *E. coli* (EHEC)**

Epidemiology studies identified the bovine intestinal tract the main EHEC reservoir, which only incidentally causes disease in humans (Vega and Ridley, 2007). It affects industrialised and developed countries and requires a very low infectious dose (estimated to be < 100 cells), facilitating person-to-person transmission (Karch et al., 2005). Outbreaks are also associated with consumption of undercooked meat and a variety of contaminated foods such as radish sprouts and lettuce (Kaper et al., 2004). In 2012 there were reported around 800 cases of O157:H7 related infections in England and Wales (Public Health England). The largest outbreak reported to date occurred in 1996 in Osaka, Japan causing 9,000 cases and 11 deaths (WHO).

The cardinal trait of EHEC is their ability to produce and release phage encoded cytotoxins (also known as Shiga toxins) Stx1 and Stx2 (Nataro and Kaper, 1998), similar to that of *Shigella dysenteriae* (Herold et al., 2004). Stx1 and Stx2 have cytotoxic activity which leads to bloody diarrhoea (hemorrhagic colitis), and hemolytic uremic syndrome (HUS), the major cause of pediatric renal failure (Karch et al., 2005).

EHEC is divided in two main lineages: EHEC1 O157:H7 serotype (expressing Intimin-γ) and EHEC2 O26 and O111 serogroups (expressing Intimin-ß). The archetypal strain of EHEC is O157:H7 strain EDL933 (Perna et al., 2001).

The most prevalent EHEC strain associated with outbreaks is O157:H7, although serogroups O26, O111 and O145 are also prevalent (Frankel et al., 1998b). EHEC O157s are often segregated based on their ability to ferment sorbitol. The non-sorbitol fermenting (nsf) O157 EHEC were associated with severe disease, however recently has been reported an increase in the prevalence of sorbitol fermenting (sf) O157 caused infections (Eklund et al., 2002).

1.6 Other intestinal pathogenic *E.coli* (InPEC)

1.6.1 Enterotoxigenic *E. coli* (ETEC)

ETEC is a major cause of infantile and traveller's diarrhoea, in regions associated with poor sanitations, where uncontaminated water is not ready available (Qadri et al., 2005). Symptoms vary from mild watery diarrhoea to cholera-like profuse diarrhoea. ETEC colonises the gut via adhering to enterocytes using colonisation factors (CF) and, to date, over 25 antigenic specific fimbrial CFs have been identified (Turner et al., 2006). ETEC secretes Heat-stable toxin (ST) and Heat-labile toxin (LT) which bind to host receptors and increase intestinal secretion of water and electrolytes, in this way modifying host cell homeostasis (Qadri et al., 2005). LT possess 80% homology with the cholera toxin (CT) and display the same ADP rybosylase activity (Spangler, 1992). STs are small toxins (less than 20 amino acids in length) which include STa and STb and are present in 75% of ETEC isolates (Wolf, 1997). STa mimics the intestinal hormone guanylin, and activates the guanylate cyclase receptor, leading to increased cGMP levels whilst STb increases intracellular calcium

levels (Nataro and Kaper, 1998). The most prevalent ETEC serogroups are: O6, O8, O11, O15, O20, O25, O27, O78, O128, O148, O149, O159 and O173 (Stenutz et al., 2006).

1.6.2 **Enteroaggregative *E. coli* (EAEC)**

EAEC is an emerging pathogen of concern causing persistent diarrhoeal outbreaks in both developing and industrialised countries, most notably the May 2011 outbreak in Germany (Rasko et al., 2011). Intestinal mucosal damage and diarrhoea are facilitated by the elaboration of enterotoxins and cytotoxins. These include *Shigella* enterotoxin 1 (shET1), the plasmid-encoded toxin (Pet) and the heat stable enteroaggregative *E. coli* ST1 toxin (EAST1) (Harrington et al., 2006), (Fasano et al., 1995). EAEC adhere to Human epithelial type 2 (Hep-2) cells in an auto-aggregative 'stacked brick' pattern (Nataro and Kaper, 1998), mediated by the aggregative adherence fimbriae (AAF) and other adherence factors such as AAF/I, AAF/II and AAF/III (Huang et al., 2006) encoded on the aggregative adherence plasmid (pAA) (Boisen et al., 2008). The EAEC serogroups identified include: O3, O7, O15, O44, O77, O68, O111, O126, and O127 (Stenutz et al., 2006).

1.6.3 **Diffusely Adhering *E. coli* (DAEC)**

DAEC are characterised by their diffusely adherent pattern on Hep-2 cells (Nataro and Kaper, 1998) and formation of finger-like projections that wrap around the bacteria without complete internalisation. The adherence pattern is mediated by fimbrial adhesins F1845 which binds to the decay accelerating factor (DAF) which is then relocalised around

attached bacteria (Guignot et al., 2000). DAEC can be divided into two groups, those expressing Afa/Dr adhesins (Afa/Dr/DAEC), primarily associated with urinary tract infections and those expressing AIDA-1 adhesins, associated with infantile diarrhoea (Servin, 2005).

1.6.4 **Enteroinvasive *E. coli* (EIEC)**

EIEC is the only InPEC pathovar that invades the host cells, the rest of the *E. coli* pathovars being considered extracellular. EIEC pathovar comprises fourteen distinct O antigens: O28ac, O29, O112ac, O124, O136, O143, O144, O152, O159, O164 (Stenutz et al., 2006). The O112ac, O124 and O152 are genetically and pathogenically related to *Shigella* species (Peng et al., 2009), causing diarrhoea and dysentery through invasion of enterocytes or macrophages (Torres et al., 2005). These bacteria further escape from the endocytic vacuole, multiply intracellularly and spread through adjacent cells within the epithelial cell layer via actin nucleation (Kaper et al., 1998) (Philpott et al., 2000). Furthermore, these bacteria uses a T3SS to translocate multiple effector proteins inside these cells to manipulate host cell signalling events such as inflammatory pathways, actin cytoskeleton, uptake, lysis of the endocytic vacuole, cell adhesion and cell cycle progression (Sasakawa, 2010). EIEC invasive effector proteins activate Rho family GTPases, inducing actin rearrangement resulting in engulfment and bacterial internalisation (Kepp et al., 2009).

1.7 Secretion Systems in Gram negative bacteria

Gram negative bacteria are comprised of an inner cytosolic membrane and an outer membrane enriched with lipopolysaccharides and separated by a periplasmic space with a thin peptidoglycan layer. Bacteria uses a plethora of specialised transport systems designed to deliver proteins by translocation across the bacterial inner membrane (IM), periplasm and the outer membrane (OM) to the cell surface, extracellular milieu or even directly into the host cells. There are six main secretion systems (Type 1 to 6) described in the Gram-negative bacteria that mediate the transport of effector proteins across the inner and outer membrane (Figure 1.10). This transport can be achieved in a single step (T1SS, T3SS, T4SS and T6SS) or in two-steps, firstly into the periplasm via secretory pathways Sec and Tat, and after translocated across the OM via other secretion systems (T2SS and T5SS) (Tseng et al., 2009). Several secretion system T1SS, T2SS and T5SS secrete proteins from the bacterial cell cytoplasm to the extracellular space, whilst T3SS, T4SS and T6SS deliver proteins across the bacterial cell and directly into the host cytosol. The proteins secreted through these systems are termed effectors and have an important role in pathogenesis (Kenny and Valdivia, 2009).

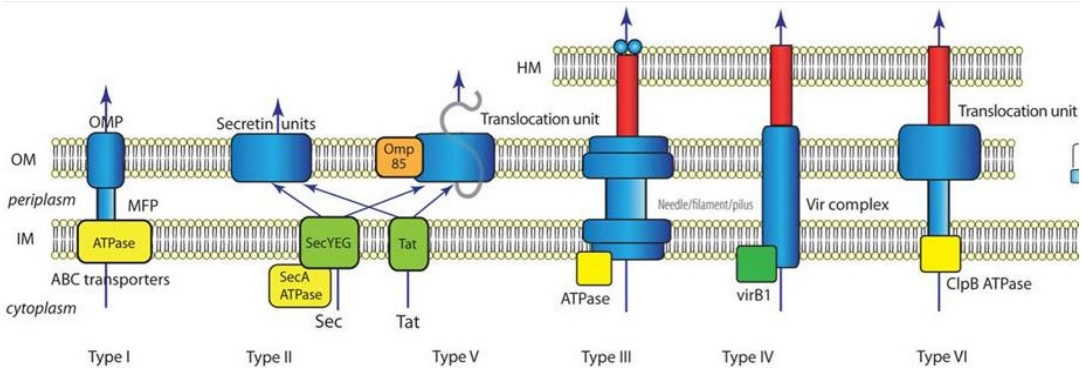

Figure 1.10 - Summary on the different Sec-dependent (T2SS and T5SS) and Sec-independent (T1SS, T3SS and T4SS) secretion systems and their chaperons required for protein translocation

(HM-host membrane, OM-outer membrane, IM-inner membrane, MM-mycomembrane, OMP-outer membrane protein, MFP-membrane fusion protein, ATPases and chaperones are showed in yellow, translocons in red and secretion apparatus in blue) Image used with permission from (Tseng et al., 2009)

1.7.1 The general secretory (Sec) and two-arginine transport (Tat) system

There are two general secretory pathways: the universal secretory pathway (Sec) or Two-arginine (Tat) system (Tseng et al., 2009), (Driessen and Nouwen, 2008). The Sec pathway consists of several proteins, a multifunctional protein SecA and three integral proteins SecY, SecE and SecG that assemble the membrane spanning translocase channel which is inserted into the inner membrane (Brundage et al., 1990). SecA is an ATPase that binds SecY to provide the energy required for translocation (Papanikou et al., 2007). The Sec translocase transports unfolded pre-proteins across the inner membrane after they are recognised by a trigger factor (TF) and a signal recognition particle (SRP) (Luirink et al., 2005). SecA recognises the presence of an N-terminal signal sequence of the unfolded proteins to be translocated and further guides them to the SecYEG translocase (Economou and Wickner, 1994). Each successive round of ATP hydrolysis facilitates the movement of

around 20 residues of the pre-protein (Schiebel et al., 1991). After translocation, the signal sequence is cleaved and the protein is either released into the periplasm or remains associated with the bacterial inner membrane.

Folded proteins can be transported across the bacterial inner membrane via the twin arginine transport system (Tat), so called based on the presence of two adjacent arginine residues within the signal sequence. The Tat translocase consists of three integral membrane proteins (TatA, TatB and TatC) and is powered via the proton motive force (Natale et al., 2008). TatA is considered the major pore-forming subunit of the translocase and TatC is involved in substrate recognition (Muller, 2005). The Tat pathway recognises an N-terminal twin-arginine motif (from the S-R-R-x-F-L-K sequence) on folded proteins and uses proton motive force to translocate proteins into the periplasm (Yahr and Wickner, 2001). Proteins are then further secreted by the Sec dependent T2SS and T5SS.

1.7.2 **The Type II and V Secretion System**

The Type II Secretion System (T2SS) spans the periplasm connecting the inner and outer membranes and translocates proteins that were first transported into the periplasmic space using the Sec pathway (Filloux, 2004). Examples of such proteins include: *E. coli* heath-labile toxin (LT), *Pseudomonas aeruginosa* Exotoxin A and *Vibrio cholera* cholera toxin (Korotkov et al., 2012), (Filloux, 2004), (Tauschek et al., 2002)). The T2SS is composed of 12-16 core components which include the outer membrane secretin (GspD), inner transmembrane protein (GspF), cytoplasmic ATPase (GspE), pseudo-pilins (GspG-K) (which exhibit homology to Type IV pilins) and connector proteins (GspL and GspM) which facilitate the attachment of ATPase to the inner membrane (Cianciotto, 2005), (Filloux, 2004). It is

hypothesised that pseudo-pilins undertake conformational changes and extend from the inner membrane platform within the periplasm, thereby pushing proteins through the outer membrane channel, or retracts, to allow access to the central opening (Douzi et al., 2011), (Filloux, 2004).

The Type V Secretion System utilises the Sec pathways, is conserved throughout Gram negative bacteria. It is divided into three subsystems (a-c): the autotransporter protein system (T5aSS), the two-partner system (T5bSS) and an oligomeric autotransporter system (T5cSS) (Dautin and Bernstein, 2007). The T5SS proteins consists of an N terminal passenger domain carrying the N-terminal signal sequence for Sec transport and a conserved ß-barrel C-terminal domain involved in translocation (Dautin and Bernstein, 2007). The C-terminal ß-barrel domain of the substrate (T5aSS) or its partner (T5bSS) then forms a pore in the outer membrane allowing the substrate to pass through outer membrane (Henderson et al., 2004). The N-terminal signal peptide of the substrate is cleaved during secretion and translocated into the extracellular space. The T5cSS consists of pairs of proteins (the two-partner system) where the passenger proteins are produced as two separate proteins, bears the ß-barrel domain, whilst the other is secredted. (Henderson et al., 2004).

Unlike the T5SS and T2SS, the Type I, III, IV and VI systems transport effectors in a single step directly across the inner and outer membrane.

1.7.3 The Type I Secretion System

The Type I Secretion System (T1SS) secreted unfolded proteins such as small peptides, complex carbohydrates and large proteins in one step, from the bacterial cell

cytoplasm to the extracellular space. Is composed of three proteins: an outer membrane protein (OMP), an ATP-binding cassette (ABC) transporter and an adaptor protein (the membrane fusion protein MFP) (Holland et al., 2005), (Delepelaire, 2004). The T1SS is commonly exemplified by the *E. coli* haemolysin secretion system TolC-HlyD-HlyB complex, that exports haemolytic toxin HlyA (Koronakis et al., 2004).

1.7.4 **The Type IV Secretion System**

The Type IV Secretion System (T4SS) is found in gram negative bacteria and has the ability to transport nucleic acids (horizontal transfer of DNA) as well as proteins (virulence factors) inside eukaryotic host cells (Zechner et al., 2012). The best studied T4SS core effectors are VirB/Dot from *Agrobacterium tumefaciens* which transfer DNA to target plant cells (Christie and Cascales, 2005). This is regulated by three ATPases (VirB4, VirB11 and VirD4) which are involved in substrate recognition, assembly of the T4SS and secretion (Fronzes et al., 2009a). T4SS forms a multi protein core complex consisting of VirB7, VirB9, VirB10 which is thought to span both bacterial membranes and the periplasm. VirB6 and VirB8 form the inner-membrane pore and VirB2 and VirB5 complete the T4SS assembly by forming the extracellular pilus of the secretion channel (T-pilus) (Fronzes et al., 2009b), (Christie et al., 2014). The pilus is essential for cell to cell contact and comprises the needle-like structure to which the pore forming protein is attached (Gauthier et al., 2003).

1.7.5 **The Type VI Secretion System**

The Type VI Secretion system (T6SS) resembles the tail spike complex of the T4 bacteriophage and it plays an important role in virulence in animal plant and human pathogens (Filloux et al., 2008), as well as in biofilm formation (Bordi et al., 2010). It is encoded on approximatively 15 genes and is composed of an ATPase, a channel extending across both inner and outer membrane, an injectosome, a putative outer membrane lipoprotein and inner membrane proteins (Filloux et al., 2008). Hcp and VgrG proteins have been shown to be secreted in the majority of organisms encoding a T6SS (Mougous et al., 2006). Hcp resembles structural and sequence homology with the phage tail component which in the T6SS forms a channel for protein delivery and has been shown to form hexameric rings that docks beneath the phage tail-like tip. It further polymerise into tubular structures formed upon remodelling of VipA and VipB (in *Vibrio cholerae*) (Mougous et al., 2006). VgrG share homology with the phage tail spike proteins which form a pointed complex for injecting the bacterial envelope (Pukatzki et al., 2009). The tip detaches from the T6SS enabling effector protein delivery (Pukatzki et al., 2009). T6SS is powered by the cytoplasmatic chaperone ATPase ClpV (Filloux et al., 2008), (Felisberto-Rodrigues et al., 2011).

1.7.6 **The Type III Secretion System**

The Type III Secretion System is a one step process utilised by many Gram negative pathogens, including *Salmonela* spp., *Citrobacter rodentium*, *Yersinia*, *Shigella*, *Pseudomonas,* as well as EHEC and EPEC to interact with eukaryotic host cells (Wang et al., 2004). It is a complex macromolecular machinery which translocates effector proteins directly from bacteria, to host cell cytoplasm, in this way, modulating host cell functions. When visualised by transmission electronic microscopy, different T3SS needle complexes show a similar structure as exemplified in Figure 1.11 C.

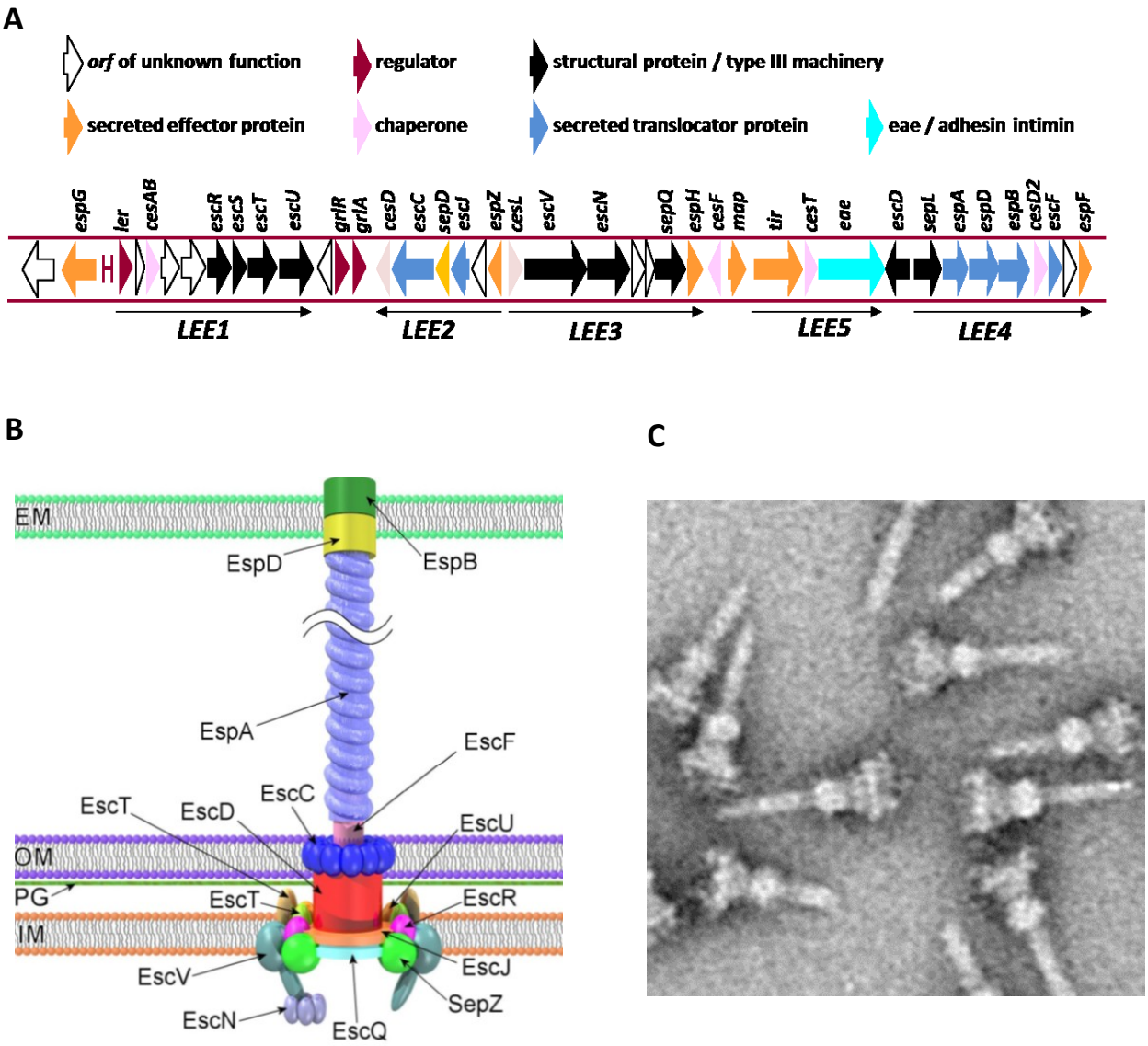

Figure 1.11 - EPEC/EHEC LEE and the T3SS

A – Genetic organisation of the EPEC/EHEC LEE (Garmendia et al., 2005) ; **B** - Graphical representation of EPEC/EHEC type III secretion apparatus encoded within LEE with their component proteins; EM; eukaryotic membrane, OM; outer membrane, PG; peptidoglycan layer, IM. Image used with permission from (Pallen et al., 2005); **C** - Type III secretion needle complex in *Salmonella typhimurium* shown by electron microscopy (Schraidt et al., 2010).

The T3SS requires several types of proteins:

- Structural proteins (T3SS needle proteins (EscF) and inner rod components (EscI)) – these are secreted first to form the injectosome.

- Translocator proteins – are secreted after the needle and inner rod components but before the effectors as they are needed to translocate the effectors into host cells (EspA, EspB and EspD).
- Effector proteins – secreted into eukaryotic cells in a programmed temporal hierarchy by the T3SS, as some effectors have opposing functions, and their secretion may be required at different stages of infection (Map, EspF, EspG, EspH and SepZ).
- Chaperones – assist in the unfolding and secretion of effector proteins (CesAB, CesD, CesD2, CesF and CesT).
- Regulatory proteins – control the expression of the T3SS and secretion of translocators and effectors (Ler, GlrA and GlrR).

Assembly of the T3SS is sequential, first involving the export of membrane–bound components using the Sec pathway to form a basal structure (approximatively 20 proteins), followed by the addition of needle and filament components, then of the cytosolic components that energise and promote the injection of the effector in the host cell (translocation) (Cornelis, 2006). The basal body consists of two ring structures associated with the inner membrane inner ring 1 (IR1) and 2 (IR2) and two outer membrane rings, outer ring 1 (OR1) and 2 (OR2) (Yip et al., 2005a). In EPEC and EHEC, structural proteins EscC, a membrane secretin form the outer membrane structure and EscD and EscJ form the inner membrane structure. EscJ lipoprotein was shown to act as a bridge between the inner and outer membrane protein rings (Crepin et al., 2005) and EscF is the needle which is extended out from the outer membrane EscC structure by the EspA filament, providing a channel for protein secretion (Crepin et al., 2005), (Knutton et al., 1998b) (Figure 1.11 B) The EspA filament is composed of EspA monomers that polymerise at the distal end of the growing

filament, in a way similar to flagellar elongation (Crepin et al., 2005). Membrane-bound components EscV together with EscR, EscS, EscT and EscU form the inner membrane ring structure and EscQ forms a cytoplasmic facing ring, providing a binding site for the ATPase EscN (Garmendia et al., 2005), (Akeda and Galan, 2005). The translocator proteins EspD and EspB (Kresse et al., 1999) form the pore in the host cytoplasm in order to allow translocation of effector proteins, whilst EscN ATPase provides the energy required by the T3SS machinery for protein secretion (Daniell et al., 2003), (Gauthier et al., 2005). SepD and SepL are required for the secretion of the translocators EspA, EspB, and EspD, and mutation of either SepD or SepL abolishes secretion of the translocators and leads to hypersecretion of the effectors (Deng et al., 2015). SepL has been shown to bind Tir, suggesting that SepL may prevent Tir secretion before the translocators are secreted (Wang et al., 2008).

The correct assembly of the T3SS is orchestrated by a series of cytosolic chaperones. Class I chaperones might play a role in hierarchy, directing the substrates of the T3SS (called effectors) to the injectosome where they dissociate. Furthermore, Class I chaperones bind effector proteins maintaining them in a secretion competent conformation and usher them to the membrane associate ATPase (EscN) (Creasey et al., 2003b). Class II chaperones bind to the translocator proteins at an uncleaved N-terminus chaperone recognition site (Galan and Wolf-Watz, 2006), in order to inhibit their toxicity in the bacterial cell. They are also involved in mediating the correct assembly of the T3SS injectosome, preventing premature assembly of the complex by masking oligomerization domains (Yip et al., 2005a).

The proteins secreted via the T3SS carry targeting signals usually located at the N-terminal 20 or so aminoacid residues, although the T3S targeting signals are located in the mRNA of some effectors (Niemann et al., 2013). Several proteins such as EscU, SepD and SepL have

been implicated in the regulation of the secretion hierarchy in these pathogens (Munera et al., 2010), which appears to happen at the posttranslational level (Deng et al., 2005). However (Deng et al., 2015) showed that T3S hierarchy of certain substrates is determined by signals other than the N-terminal secretion and translocation signal.

1.7.7 **A/E lesion and the Locus of Enterocyte Effacement (LEE)**

The A/E lesion phenotype, characterized by destruction of cellular microvilli on the intestinal epithelial cells surface is encoded by a chromosomic 35-kb pathogenicity island (PAI) termed the locus of enterocyte effacement (LEE) region. The T3SS of EPEC, EHEC and *C. rodentium* is also encoded by genes on LEE (McDaniel and Kaper, 1997) and is required for the A/E lesion formation and the assembly of the T3SS (McDaniel et al., 1995a) (Figure 1.11 A).

LEE is conserved among the A/E pathogens and contains 41 open reading frames (ORF) arranged in five polycistronic operons LEE1 to LEE5 (Elliott et al., 1998) (Fig. 9A). These genes encode LEE functional proteins (SepD, SepL and EscN), the T3SS apparatus (described in chapter 1.5.5) (Jerse et al., 1990), the *eae* encoding adhesin intimin (α and ß in EPEC and γ in EHEC), its translocated intimin receptor Tir (translocated intimin receptor) (Kenny and Finlay, 1997), as well as regulator proteins, effector proteins and their associated chaperones (Elliott et al., 1998).

Regulation of LEE gene expression is a highly complex and coordinated process, dependent on environmental conditions, quorum sensing, and several regulators and regulatory pathways in a direct or indirect way. LEE is subjected to various levels of regulation,

including transcriptional and posttranscriptional regulators located both inside and outside of the pathogenicity island (Franzin and Sircili, 2015).

The LEE- encoded regulator proteins include the locus of enterocyte effacement-encoded regulator (Ler), Global regulator of LEE activator (GrlA) and global regulator of LEE repressor (GrlR) (Iyoda et al., 2006).

Ler is a 15 kDa protein encoded in the Open reading frame 1 on the LEE1 operon, which was shown to be essential for the formation of A/E lesions (Berdichevsky et al., 2005). Elliot *et. al* showed that *ler* mutants of EPEC and EHEC were unable to form A/E lesions on Hep-2 cells. Furthermore these *ler* mutants failed to express type 3 secreted proteins, implying that all genes known to be important in A/E lesion formation are regulated by Ler.

GrlA binds the LEE1 promoter and activates LEE expression through Ler and in this way maintaining an appropriate level of Ler to activate LEE gene expression. In contrast GrlR binds GrlA, preventing it to bind LEE1 promoter which results in the repression of Ler/LEE expression (Franzin and Sircili, 2015).

Many of the type III secreted proteins are dependent on specific chaperones for stabilization in the bacterial cytosol prior to secretion and prevention of premature interactions with secreted proteins and/or with parts of the secretion and translocation machinery (Akeda and Galan, 2005). In addition, chaperones have been shown to be required for the exportation of translocator and effector proteins. The chaperones encoded within the LEE region are CesAB, CesD, CesD2, CesL, CesF and CesT (Parsot et al., 2003).

CesD is a chaperone for EspB and EspD (Neves et al., 2003), CesT a bivalent chaperone that binds to, and is required for translocation of, both Tir (Yip et al., 2005b), and Map (Creasey et al., 2003a) and CesF, which specifically interacts with EspF (15). CesD2 is a second LEE-encoded chaperone for EspD (Neves et al., 2003), CesL a chaperone for the type III secretion

gatekeeper protein SepL (Younis et al., 2010) and CesAB a chaperone for EspA and EspB (Creasey et al., 2003b).

The secreted translocator proteins include EspA, EspB and EspD and effector proteins: Map, EspF, EspG, EspH and SepZ (Goosney et al., 1999), (Elliott et al., 1998), (Garmendia et al., 2005).

1.7.8 Subversion of host cell signalling by A/E pathogen's LEE and non-LEE encoded effectors

After initial adherence of bacteria to epithelial cells, A/E pathogens hijack and manipulate host cell signalling pathways allowing infection of host cells, evasion of host immune responses and efficient colonisation which ultimately leads to disease (Wong et al., 2011), (Dean and Kenny, 2009). These pathogens use a type III secretion system (T3SS) described previously, that acts as a macromolecular syringe to inject effector proteins directly into infected cells (Garmendia et al., 2005). There are seven effectors encoded by LEE- EspB (Chiu and Syu, 2005), EspZ (Kanack et al., 2005), Map (Kenny and Jepson, 2000), EspH ((Tu et al., 2003), EspG (Elliott et al., 2001), EspF (McNamara and Donnenberg, 1998) and Tir (Kenny et al., 1997), which are conserved in both EPEC and EHEC (Frankel et al., 1998b), (McDaniel et al., 1995a). In addition to these, there are several non-LEE encoded effectors (Nle) (with genes carried on prophages or integrative elements) that vary significantly in distribution between EPEC and EHEC strains (Iguchi et al., 2009). Example of Nle effectors include TccP (Campellone et al., 2004a), the WxxxE effectors - EspT and EspM (Arbeloa et al., 2009), and EspW (which is the focus of this study).

Most of these non-LEE-encoded effectors genes are located outside the LEE pathogenicity island within lambda-like prophages or integrative elements. Although not all A/E effectors have been functionally characterized, it is now evident that these proteins exert diverse, cooperative, and redundant functions once translocated into the host cells and have variable degrees of importance during infection (Dean and Kenny, 2009). To coordinate the spatiotemporal expression of these T3SE genes during the course of an infection, regulatory mechanisms would have been acquired to allow their coexpression with other LEE genes in order to have the effectors readily available for secretion upon assembly of the T3SS. As mentioned in chapter 1.7.7 LEE genes are regulated by the LEE-encoded regulators Ler, GrlA and GrlR (Mellies et al., 2007a).

Although the function of the non-LEE encoded effector is expanding, the regulatory mechanisms controlling their expression is not fully understood. Previous studies indicate that the quorum-sensing regulator QseA and the two-component signaling system QseEF regulate the expression of *espFu* (also called *tccP*) in EHEC in a cascade fashion (Reading et al., 2007) and that NleA is heterogeneously expressed together with Tir and EspA in a Ler-dependent manner (Roe et al., 2007). In contrast, the expression of *nleG* in EPEC, as well as that of the *espJ-espFu* (*tccP*) operon in EHEC, has been shown not to depend on Ler (Garmendia and Frankel, 2005). In addition, expression of *nleA*, but not *nleD* or *espJ*, responds to SOS signaling in EPEC (Mellies et al., 2007b).

Furthermore, (Garcia-Angulo et al., 2012) identified the presence of a common novel DNA motif named *nle* regulatory inverted repeat (NRIR) located in the regulatory regions of several *nle* genes coding for different effector proteins of A/E pathogens. This conserved

DNA region consists of a 13-bp inverted repeat separated by a conserved 5-bp spacer. NRIR-containing genes include *nleG*, *nleH1*, *nleH2*, and *nleB2*.

Between all pathogenic A/E strains, there are 21 conserved effectors deemed important for pathogenesis (referred to as the core effectors) whilst other effectors are strain-specific and may have an effect on virulence, competitiveness or host range. The number of translocated effector proteins varies from one strain to another. The development of next generation sequencing revealed that EPEC, EHEC and *C. rodentium* genomes contain genes that encode a variety of additional putative virulence factors. Furthermore Tobe *et al*., (Tobe et al., 2006) identified over 50 proteins in EHEC O157 to be T3SS effectors including EspW.

One of the major mechanisms for genome evolution of EHEC O157 is phage-mediated horizontal gene transfer, which can include new virulence genes (Dobrindt et al., 2010), (Cooper et al., 2014). (Cote et al., 2015) showed that the genome of the EHEC O157:H7 strain SS17 contains 22 phage-bearing regions distributed across the entire genome Figure 1.12.

Region 2 contains non-LEE encoded (Nle) secreted effectors *nleB1*, *nleC*, *nleH1*, and *nleD*. The Nle-encoded type III secreted effectors, *espX7* and *espN* are located in the fifth; *nleA*, *nleH2*, and *nleF* are located in the eighth region, while *nleG7* is encoded in the ninth region. Region 11 contains *espJ* and *tccP* and region 19 the *nleB2* and *nleE* genes. The LEE-encoded genes including *eae*, *tir*, and *ler* are located in region 20 (Cote et al., 2015).

The genes *espW* and *espM2* were shown to be located in close proximity on Region 18 in EHEC O157:H7 strain SS17 and Region Sp17 in EHEC O157:H7 strain Sakai (Cote et al., 2015), (Tobe et al., 2006).

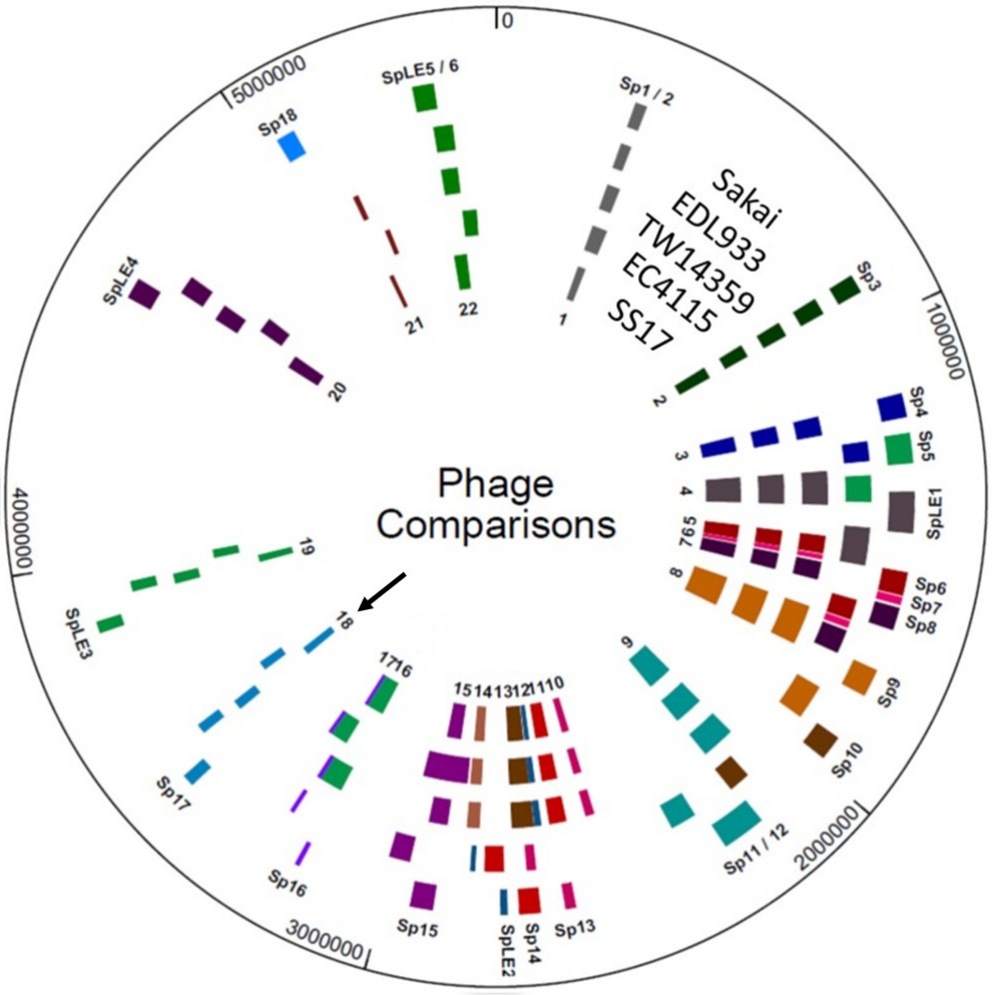

Figure 1.12 - Phage comparisons between EHEC O157:H7 strain SS17 and reference strains Sakai, EDL933, TW14359 and EC4115

Location of phage regions for SS17, EC4115, TW14359, EDL933 and Sakai determined in each strain are colour coordinated based on insertion sites and similarities. Inner ring - number designation for SS17 phage regions; Outer ring - S-loop numbers for Sakai phage. The black arrow indicate region 18 of phage (24,157 bp) that houses espW and espM2 genes (Cote et al., 2015).

In comparison EPEC E2348/69 encodes 21 T3SS effector proteins (Iguchi et al., 2009) and *C. rodentium* encodes 29 T3SS effector proteins (Petty et al., 2010) (Table 1.1- adapted from (Wong et al., 2011). There are some effectors such as Tir essential for colonisation and many

others target different cellular compartments and in this way are believed to increase the fitness of the A/E pathogens (Garmendia et al., 2005), (Hemrajani et al., 2008), (Mundy et al., 2004).

The function of these effector proteins can be divided in several categories with more details shown in Table 1.1:

a) inhibition of cell cycle G2/M phase transition (Cif)
b) inhibition of vesicular transport between the Golgi apparatus and the endoplasmic reticulum (EspI)
c) inhibition of phagocytosis (EspB, EspF, EspJ)
d) mitochondrial damage (EspF, Map)
e) disruption of intestinal barrier function (EspF, EspI, Map)
f) subversion of the host cell cytoskeletal system – microtubule, actin and intermediate filament networks (EspB, EspG, EspH, Tir, Map)
g) apoptosis: pre-apoptotic proteins (EspF) and anti-apoptotic proteins (NleH)

Table 1.1 - Summary of the Type III secretion system effector proteins

Effector	**EHEC O157:H7 Sakai**	**EPEC O127:H6 E2348/69**	***C. rodentium***	**Function**
Tir	1	1	1	Intimin receptor, pedestal formation, down regulates Map-dependent filopodia formation (Vingadassalom et al., 2009), (Weiss et al., 2009), (Berger et al., 2009), (Crepin et al., 2015)
TccP	2	0	0	Promotes Nck independent actin assembly (Campellone et al., 2004b). Required for actin assembly beneath adherent EHEC O157:H7 *in vitro* but dispensable for A/E lesion formation *in vivo* (Tu et al., 2003), (Lai et al., 2013)
EspB	1	1	1	Pore component for translocation, binds myosins to inhibit phagocytosis (Iizumi et al., 2007), (Hamaguchi et al., 2008),

				(Deng et al., 2015)
EspF	1	1	1	TccP/EspFu homolog, Localises at mitochondria with role in mitochondrial disruption, tight junctions disruption, induce membrane remodelling, binds and activates N-WASP, inhibits PI3K-dependent phagocytosis (Viswanathan et al., 2004), (Alto et al., 2007), (Dean et al., 2010), (Hodges et al., 2008), (Zhao et al., 2013)
EspG	1	2	1	Disrupts microtubule network (Shaw et al., 2005), (Smollett et al., 2006) and blocks ARF GTPase signalling and alters paracellular permeability (Selyunin and Alto, 2011), (Matsuzawa et al., 2004), (Glotfelty et al., 2014)
EspH	1	1	1	Blocks RhoGTPase signalling and modulates host actin cytoskeleton structure (Tu et al., 2003), (Dong et al., 2010), (Wong et al., 2012a)
EspJ	1	1	1	Localises at mitochondria, homologus to P*seudomonas syringae* effector HopF. Required for clearance of *C. rodentium* from the mouse colon Not required for A/E lesion formation *in vitro* or *ex vivo* (Dahan et al., 2005). Inhibits FCγR-mediated and CR3-mediated trans-phagocytosis (Marches et al., 2008), (Kurushima et al., 2010), (Young et al., 2014)
EspK	1	0	1	Homologous to Salmonella T3SS effector GogB. Not required for A/E lesion formation. Shows a diffuse cytoplasmic localisation in eukaryotic cells (Vlisidou et al., 2006), (Bonanno et al., 2015)
EspL	4	3	1	Enhances the cross linking of actin filaments via activation of host cell protein annexin2 (Miyahara et al., 2009).
EspM	2	0	3	RhoA GEF, activates stress fiber formation (Arbeloa et al., 2010), (Arbeloa et al., 2008).
EspN	1	0	3	Unknown
EspO	2	1	1	Stabilises focal adhesions (Kim et al., 2009)
EspR	4	0	0	Unknown
EspT	0	0	1	Localises at mitochondria; Induces membrane ruffles and lamellipodia by activating Rac1 and Cdc42 (Bulgin et al., 2009b)
EspV	1	0	1	Present in cytosol with role in cytoskeleton modulation (Arbeloa et al., 2011)
EspW	1	0	0	Actin remodelling via Rac1 (this study)
EspX	6	0	1	Unknown
EspY	5	0	0	Unknown
EspZ	1	1	1	inhibits apoptosis and cellular cytotoxixity (Shames et al., 2010)
Map	1	1	1	Mitochondrial localisation, Cdc42 GEF that promotes filopodia formation, mitochondrial disruption and tight junction disruption (Alto et al., 2006), (Martinez et al., 2010), (Dean et al., 2006), (Berger et al., 2009), (Thanabalasuriar et al., 2010a).
NleA	1	1	1	Localises at Golgi, it inhibits COPII-dependent protein export from ER, disrupts TJ and is required for virulence in mice (Gruenheid et al., 2004), (Lee et al., 2008), (Thanabalasuriar

				et al., 2010b), (Kim et al., 2007), (Yen et al., 2015)
NleB	3	3	2	Associated with non-O157 EHEC outbreaks and HUS (Wickham et al., 2006); Inhibits TNF-induced NF-kB activation (Newton et al., 2010), (Nadler et al., 2010) necessary for colonisation and mortality in mice (Kelly et al., 2006), (Pearson et al., 2015)
NleC	1	1	1	Not required for A/E lesion formation or colonisation (Marches et al., 2005); cleaves p65, c-Rel, p50 and IkB to inhibit NF-kB activation (Yen et al., 2010), (Muhlen et al., 2011), (Pearson et al., 2011), (Hodgson et al., 2015)
NleD	1	1	2	Not required for A/E lesion formation or colonisation (Marches et al., 2005); inhibits AP-1 activation by cleaving JNK (Baruch et al., 2011)
NleE	1	3	1	Required for colonisation and mortality in mice (Wickham et al., 2007). Associated with outbreaks (and HUS) of non-O157 EHEC (Wickham et al., 2006); OspZ homologue that blocks IkB degradation to inhibit NF-kB activation (Newton et al., 2010); (Nadler et al., 2010), (Yao et al., 2014)
NleF	1	1	1	Required for colonisation of mouse and piglet colon (Wickham et al., 2007), (Echtenkamp et al., 2008), (Pallett et al., 2014)
NleG/NleI	14	1	5	Ubiquitin ligase (Wu et al., 2010)
NleH	2	3	1	Homologous to *Shigella* effector OspG. Involved in activation of NF-kB in host cells to optimise host gut inflammatory response (Hemrajani et al., 2008), (Hemrajani et al., 2010). Required for colonisation of mice (Garcia-Angulo et al., 2008), (Grishin et al., 2014)
NleK	0	0	1	Unknown
Cif	0	1	0	Deaminates NEDD8 and inhibits CRL activity; inhibits cell cycle G2/M phase transition (Chavez et al., 2010), (Morikawa et al., 2010), (Taieb et al., 2006).
Total	62	27	35	

Effectors may function individually, synergistically or antagonistically with other effectors within the host cell to perturb normal cell processes. Although the understanding of T3SS has expanded over the last years, many of the effectors have not yet been characterised.

1.7.9 **A/E lesion formation and Tir mediated actin polymerisation**

1.7.9.1 Modulation of actin cytoskeleton

Actin is one of the most conserved proteins in the eukaryotic cell. The ability of a cell to co-ordinate the assembly and disassembly of its actin cytoskeleton is essential for cell integrity, motility, membrane trafficking and shape changes (Millard et al., 2004). Several bacterial pathogens including *Salmonella*, *Shigela*, *Listeria*, *Yersinnia*, EPEC and EHEC are known to subvert the actin cytoskeleton during pathogenesis to facilitate attachment, intracellular entry and motility (Campellone and Welch, 2010).

1.7.9.2 Tir and N-WASP-Arp2/3 complex

As previously mentioned, an important stage in EPEC and EHEC infection is characterised by enterocyte effacement, intimate bacterial attachment to the host cell and actin pedestal formation. The binding of adhesin intimin at the surface of bacteria to Tir (inserted in the host cell membrane) directly links extracellular EPEC and EHEC to the epithelial membrane and it links the pathogen to the host cell actin and cytoskeleton network (Frankel et al., 2001), (Chen and Frankel, 2005). Tir is the key effector protein that is required for the A/E lesions *in vivo* and the formation of the pedestal in culture cells (Kenny et al., 1997). The interaction between Tir and intimin results in clustering of Tir and polymerisation of actin beneath adherent bacteria, which *in vitro* cell culture results in pedestal formation underneath bacteria. (Jenkins et al., 2000), (Frankel and Phillips, 2008) (Figure 1.13).

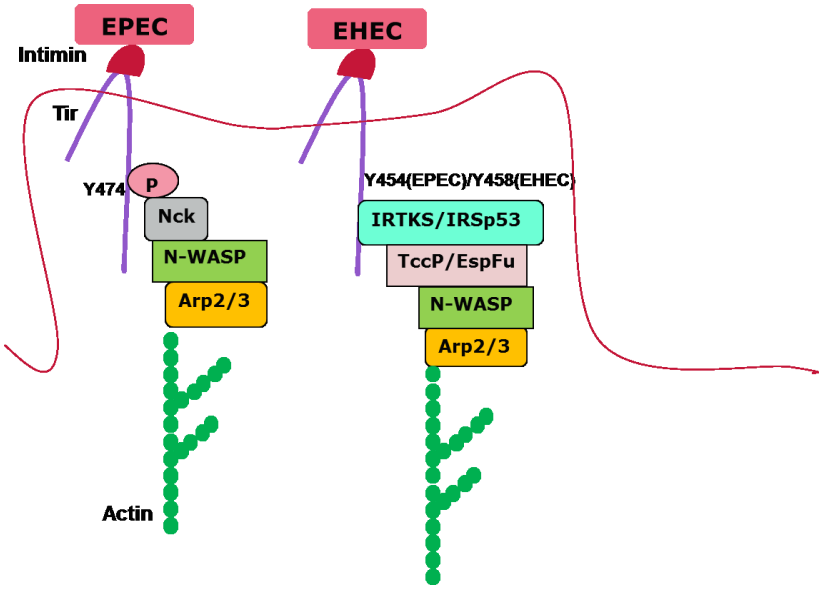

Figure 1.13 - EPEC O127:H7 and EHEC O157:H7 pedestal formation pathways

EPEC intimate attachment is mediated by the interaction between intimin and Tir. Tir is phosphorylated (at Y474) by host tyrosine kinases, leading to recruitment of Nck, N-WASP and ARP2/3 complex to mediate actin rearrangements and pedestal formation. In EHEC infections Tir is not phosphorylated, and pedestal formation is Nck-independent. The actin rearrangements that are necessary for pedestal formation are mediated by Tir cytoskeleton-coupling protein (TccP; also known as EspFU), which is linked to Tir through IRTKS/IRSp53 and interacts with N-WASP to activate the ARP2/3 complex.

Although Tir_{EHEC} and Tir_{EPEC} have relatively high level of Tir sequence homology (~ 70 %), the C-terminal domains that are responsible for binding intracellular actin signalling molecules, exhibit only 44% sequence identity (DeVinney et al., 1999). Therefore EHEC and EPEC employ different approaches to direct actin pedestal formation. Tir contains two transmembrane domains and forms a hairpin-like topology such as both the N- and C-termini are located within the host cell (Hartland et al., 1999), (Kenny, 1999). Two Tyrosine residues of EPEC Tir, Y454, (Y458 in EHEC) and Y474, are involved in triggering actin polymerisation to form pedestals (Bommarius et al., 2007), (Campellone and Leong, 2005).

The C-terminus of Tir from EPEC is phosphorylated by various host tyrosine kinases such as c-Fyn (Hayward et al., 2009), (Phillips et al., 2004). Phosphorylation at Y474 induces the recruitment of the adaptor protein Nck1/2 (Campellone et al., 2002), (Gruenheid et al., 2001). Nck then activates N-WASP and the Arp2/3 complex to stimulate actin polymerisation and initiation of the characteristic pedestal (Lommel et al., 2001) (Fig. 1.13). Actin polymerisation can also be weakly activated by the Y454 Tir residue (Kalman et al., 1999).

In EHEC Tir lacks Y474, is not phosphorylated and pedestals formation is Nck independent; it utilises a conserved Asn-Pro-Tyr (NPY458) motif to recruit IRTKS (Vingadassalom et al., 2009) and/or IRSp53 (Weiss et al., 2009), (Campellone and Leong, 2005), which in turn will recruit the non LEE encoded effector Tir cytoskeleton-coupling protein (TccP- also known as EspFu). TccP activates N-WASP by interacting with its GTPase binding domain (GBD), further recruits the ARP2/3 complex and stimulates actin polymerization, leading to pedestal formation (Garmendia et al., 2006).

Whale *et al*., (Whale et al., 2007) identified a group of atypical EPEC strains (including EPEC O111:NM B171) which utilise both the Nck dependent and TccP mediated pathway to polymerise actin pedestals.

Interestingly previous studies showed that A/E lesions formation can occur independently of both Nck and Tccp mediated actin polymerisation and that A/E lesion formation and actin pedestal formation might be unrelated (Frankel and Phillips, 2008).

Actin pedestal like structures can be detected by immuno-fluorescence microscopy using the fungal toxin phalloidin coupled to a fluorophore or by SEM whilst A/E lesions can be visualised by TEM (Figure 1.11).

1.7.9.3 Subversion of Rho GTPase signalling by A/E pathogens

As mentioned previously the family of small Rho GTPases RhoA, Rac1 and Cdc42 have an important role in actin dynamics. Their activation leads to the assembly of stress fibers, lamellipodia/ruffles and filopodia respectively (Hall, 1998) (Figure 1.1 and Figure 1.5).

Rho GTPases are common targets for bacterial toxins and secreted effector proteins due to their pivotal role in the regulation of the actin cytoskeleton along with a wide range of other cellular processes. Bacterial factors which modulate Rho GTPase signalling can be divided into three categories:

a) Enzymes which chemically modify GTPases, such as Toxin A and B from *Clostridium difficile* which modify RhoA, Rac1 and Cdc42 (Jank et al., 2007) and toxin C3 from *Clostridium botulinum* with ribosyltransferase activity specific to RhoA which prevents the interaction with its GEF (Vogelsgesang et al., 2007).

b) Factors which indirectly modulate GTPase activity. Protein effectors such as EspG of the A/E pathogens can activate endogenous mammalian Rho GEFs. EspG depolymerises microtubules resulting in the liberation of GEFH1 which subsequently activates RhoA resulting in the formation of stress fibres (Matsuzawa et al., 2005).

c) Proteins which are mimics of host Rho GTPases (details below).

1.7.9.4 Bacterial mimics of host Rho GTPases

As small Rho GTPases have a central role in eukaryotic biology, many secreted bacterial effectors have evolved functional or structural characteristics of GEFs, GAPs, and GDIs in order to mimic their cellular activities and to subvert GTPase signalling to the benefit of the bacteria (Boquet, 2000), (Finlay, 2005). Effectors may function individually, synergistically or antagonistically with other effectors within the cell to manipulate different signalling pathways.

For example, the T3SS effectors SopE and SptP of *Salmonella* counteract each other. SopE acts as a GEF of Cdc42 and Rac1 and induces the formation of membrane ruffles allowing bacterial invasion in host cells (Hardt et al., 1998). SptP has GAP activity towards Cdc42 and Rac1, acts in an antagonistic way by restoring normal cytoskeletal function and down regulates ruffle formation after Salmonella invasion (Fu and Galan, 1999). Other bacterial GAPs such as Yersinia YopE have been demonstrated to have a similar fold to SptP (Evdokimov et al., 2002).

1.7.9.5 The WxxxE Family of Effectors

Alto *et al*. (Alto et al., 2006), grouped several known T3SS effectors into a family where, members possess an invariant structural motif consisting on an invariant Tryptophan (W) and Glutamic acid (E residue separated by three variable amino acids (WxxxE) motif (Figure 1.14). Members include: SifA and SifB in *Salmonella enterica*, *Shigella* proteins IpgB1 and IpgB2 (Kenny and Jepson, 2000) as well as Map, EspM and EspT in EPEC and EHEC (Kenny and Jepson, 2000), (Arbeloa et al., 2009), (Bulgin et al., 2009a). Previous studies

showed that EHEC and EPEC translocate the effector EspH which inactivates host Rho-GEFs (Wong et al., 2012b).

Figure 1.14 - Alignment of bacterial protein effectors that belong to the WxxxE family

(Image modified with permission from (Bulgin et al., 2010))

The WxxxE motif confers Rho GTPase GEF activity which facilitates the activation of mammalian Rho GTPases.

Previous studies showed that in ~ 1000 of EHEC and EPEC clinical and environmental strains Map is conserved among all A/E pathogens, EspM is found in ~ 50 % of EPEC and EHEC strains (mainly in the serogroups that are linked to severe human infections), while espT is found in less than 2% of EPEC and none of the EHEC strains tested (Arbeloa et al., 2009).

1.7.9.6 Map (Mitochondrial-associated protein)

Map is a multifunctional effector containing two functional domains: a C-terminal class I PDZ motif (Alto et al., 2006) and an N-terminal mitochondrial targeting sequence (Kenny and Jepson, 2000), (Papatheodorou et al., 2006). Map activates the small GTPase Cdc42 in order to induce the formation of filopodia at early times during infection (Berger et al., 2009), (Huang et al., 2009), (Kenny and Jepson, 2000). Map is also known to interact with PDZ-containing Na^+/H^+ exchange regulator factor 1 (NHERF1) in this way regulating

filopodial dynamics (Alto et al., 2006), (Martinez et al., 2010). Deletion of the DTRL C-terminal region of Map which is a consensus PDZ binding motif resulted in a reduction in the longevity of filopodia (Berger et al., 2009), (Simpson et al., 2006b). It has also been demonstrated that depletion of NHERF1 from cells can abolish Map mediated filopodia formation (Alto et al., 2006).

1.7.9.7 EspM

EspM exhibits GEF activity for RhoA and induces formation of stress fibres in infected host cells (Arbeloa et al., 2008). Furthermore modulates pedestal biogenesis by diminishing pedestal formation during EPEC and EHEC infection (Luo et al., 2000). It also affects epithelial monolayer architecture in vitro by inducing a bulging phenotype that is dependent on activation of ROCK, a downstream effector of RhoA (Simovitch et al., 2010).

1.7.9.8 EspT

EspT directs GEF activity towards both Cdc42 and Rac1 to induce membrane ruffling and the formation of lamellipodia, resulting in the invasion of host cells (Bulgin et al., 2009a). From inside an EPEC-containing vacuole, the bacteria utilise Tir to induce the formation of actin-rich pedestals that contribute to intracellular bacterial survival (Bulgin et al., 2009a). EPEC strains are considered exclusively extracellular, however, the EspT-dependent invasion of host cells may explain previous reports that some atypical EPEC strains could invade non-phagocytic cells (Donnenberg and Kaper, 1992), (Hernandes et al., 2008), (Simpson et al., 2006b).

Aims and Objectives

Tobe *et al*., identified over 50 proteins in EHEC O157 to be T3SS effectors including EspW (Tobe et al., 2006). EspW is a 352 aa non-LEE encoded effector that has not been previously characterised.

The aim of this study was to:

- characterise the function and localisation of the non LEE encoded T3SS EspW in eukaryotic cells during EHEC infection and ectopic expression
- Determine host cell binding partners and signalling pathway affected
- Investigate the distribution of *espW* in clinically significant EPEC isolates

CHAPTER 2 - **Materials and Methods**

2.1 Primers, strains and plasmids

All plasmids, primers and strains used in this study can be found in Tables 2.1 - 2.4.

Table 2.1 - List of strains

Strain	Description	Source/Reference
ICC608	EHEC O157:H7, str 85-170	(Tzipori et al., 1987)
ICC1111	EHEC O157:H7, str 85-17085-170 Δ*espW,* Kan^r	This study
ICC735	EHEC O26:H11 3801	Frankel
ICC736	EHEC O26:H11 B3#44	Frankel
ICC737	EHEC O26:H11 B3#42	Frankel
ICC738	EHEC O26:H11 B3#38	Frankel
ICC533	EHEC O157:H7 EDL933	Frankel
ICC504	EHEC O157:H7 Sakai	(Hayashi et al., 2001)
ICC734	EHEC O26:H- EC740	Frankel
ICC608	EHEC O157:H7 85-170	Frankel
ICC689	EHEC O157:H7 CB1556	Frankel
-	EPEC O111:H9 E110019	(Viljanen et al., 1990)
ICC481	EPEC O127:H6 str E2348/69	(Levine et al., 1978)
ICC920	REPEC 82/215-2 (O8:H-)	Frankel
ICC923	REPEC 82/183 (O128:H2)	Frankel
ICC767	REPEC O103:H2 E22	Frankel
ICC922	REPEC 82/123 (O109:H2)	Frankel
ICC921	REPEC 84/110-1 (O103:H2)	Frankel
ICC168	*Citrobacter rodentium*, Nal^r	(Barthold et al., 1976)
AH109	*S. cerevisiae* MATα mating type with ADE2, HIS3, MEL1 and LacZ reporters for interaction and TRP1 and LEU2 selection markers	Clontech
Y187	*S. cerevisiae* MATα mating type with MEL1 and LacZ reporters and TRP1 and LEU2 selection markers	Clontech
E. coli Top10	Cloning strain	Invitrogen
BL21 Star™(DE3)	F- ompT hsdSB (rB-mB-) gal dcm rne131 (DE3)	Invitrogen
BL21 Star™(DE3)pLysS	F- ompT hsdSB (rB-mB-) gal dcm rne131 (DE3) pLysS	Invitrogen

Kan^r, Kanamycin resistance 50 μg/ml, Nal^r, Nalidixic acid

Table 2.2 - List of plasmids and primers

Plasmid and derivative(s)	**Description**			**Source**
pRK5-HA	**Vector for the expression of proteins with N-terminal HA tag in mammalian cells, Amp^r**			**(Dolezal et al., 2012)**
pRK5-HA-derivative	*Expressed protein*	*Primers 5' → 3'*	*RS*	
		Primers 5' → 3' (EHEC O157:H7, str. 85-170 genomic DNA used		

		as template)		
pICC1727	HA-EspW	CGCGGATCCATGCCCAAAATATCATCAGTTGTATC CCGGAATTCTTAATTTCTAACCAAGGGGTCCC	*BamHI* *EcoRI*	This study
pICC1728	HA- $EspW_{1-206}$	CGCGGATCCATGCCCAAAATATCATCAGTTGTATC CCGGAATTCTCAATCAGAACTAATATTTTCGAACATTCTTACG	*BamHI* *EcoRI*	This study
-	HA-$EspW_{20-352}$	CCGGGATCCATGCTTTCAAATGAAACAACAATGACG CCGGAATTCTTAATTTCTAACCAAGGGGTCCC	*BamHI* *EcoRI*	This study
-	HA-$EspW_{20-206}$	CCGGGATCCATGCTTTCAAATGAAACAACAATGACG CCGGGATCCtcaATCAGAACTAATATTTTCGAACATTCTTACG	*BamHI* *EcoRI*	This study
		Phosphorylated Primers 3' → 5'(pICC1727-used as template)		
pICC1730	HA-$EspW_{Q234A}$	AGCGCTTTATCAATTCGTTACTTACCC GAGTTTTATTACATTCCCTGA	N/A	This study
pICC1731	HA-$EspW_{I237A}$	AGCGCTCGTTACTTACCCAATATCAGCTCAATC TAACTGACTGAGTTTTATTAC	N/A	This study
pICC1396	HA-Cherry	N/A	N/A	Frankel
pRK5-Myc	**Vector for the expression of proteins with N-terminal Myc tag in mammalian cells, Amp^r**			**Clontech**
pRK5-Myc-derivative	*Expressed protein*	*Primers 5' → 3'*	*RS*	
pICC563	Myc-GFP	N/A	N/A	(Clements et al., 2011)
-	Myc-PAK1	N/A	N/A	Frankel
-	Myc-$Rac1^{N17}$	N/A	N/A	(Pelletier et al., 2005)
-	Myc-Rac1	N/A	N/A	(Pelletier et al., 2005)
-	Myc-$RhoA^{N19}$	N/A	N/A	(Pelletier et al., 2005)
-	Myc-$Cdc42^{N17}$	N/A	N/A	(Pelletier et al., 2005)
-	Myc-Cdc42(L61)	N/A	N/A	(Caron et al., 2006a)
-	Myc-Rac1(L61)	N/A	N/A	(Nobes and Hall, 1999)
-	Myc-RhoA(L63)	N/A	N/A	(Caron et al., 2006a)
pICC1914	Myc-$Kif15_{1092-1368}$	*Primers 5' → 3' to amplify kif15 (pICC1723 used as template)* CCGGAATTCcATGGAACTGACCAAGAAGGAAGCC CCCAAGCTTTTACTCAGCAAGCCTGACATTTTCC	*EcoRI* *HindIII*	This study
-	Myc-Kif15	*Phosphorylated Primers 3' → 5' to amplify pRK5-myc* GACTGACCATTTGTCACGCTGCGTAACTCAGTTTTGCAGCCGGGTG CCATcaggtcctcctcggagatc AAGGAAAAGAAAAGAAGTGAATCTtgaTCGggatcccgggtcgCGAgcc *Primers 5' → 3' to amplify kif15 (pCATE-eGFP-3F-KIF15 used as template)* CGATTGAATTGGCCACCatggagcagaagctgatctccgaggaggacctgATG GCACCCGGCTGCAAAAC AGTTGGGCCATGGCGGCCAAGCTTCTGCAGGAATTcgcgacccgggat ccTTAAAAATACATTTTCGGCACGCAA ***Kif15 sequence check primers 5' → 3'*** CTGGGTCAGCTGATGGAGAG GAGCTTGCTTCAGGACAGAC GCGGCAAGAAGTTTCTCAGC AGTTCTTGAGGCTGTACGTC CTGGCTCCTGCAAGGTCAG GCTACCTAGGCATCACCTTG	N/A	This study

pCATE-eGFP-3F-KIF15	**Vector for the expression of Kif15 with N-terminal GFP and FLAG tag in mammalian cells, Kan^r**			**(Drechsler et al., 2014)**
pSA10	**pKK177-3 derivative containing *lac^I*, IPTG inducible, Amp^r**			**(Schlosser-Silverman et al., 2000)**
pSA10-derivative	*Expressed protein*	*Primers 5' → 3'*	*RS*	
pICC1732	EspW	*Primers 5' → 3' (pICC1727-used as template)* CCGGAATTCATGCCCAAAATATCATCAGTTGTATC TGCACTGCAGTTAATTTCTAACCAAGGGGTCCC	*EcoRI* *PstI*	This study
pICC1906	EspW$_{I237A}$	*Primers 5' → 3' (pICC1731-used as template)* CCGGAATTCATGCCCAAAATATCATCAGTTGTATC TGCACTGCAGTTAATTTCTAACCAAGGGGTCCC	*EcoRI* *PstI*	This study
pICC461	EspT	N/A	N/A	(Bulgin et al., 2009b)
pICC1205	EspW$_{W/A}$	N/A	N/A	(Bulgin et al., 2009b)d
pSA10-2HA	**pKK177-3 derivative containing *lac^I*, IPTG inducible, Amp^r**			**Frankel**
pSA10-2HA derivative	*Expressed protein*	*Primers 5' → 3'(pICC1727-used as template)*	*RS*	
-	EspW-2XHA	CCGGAATTCATGCCCAAAATATCATCAGTTGTATC CCGCTCGAGATTTCTAACCAAGGGGTCCC	*EcoRI* *XhoI*	This study
pSA10-4HA	**pKK177-3 derivative containing *lac^I*, IPTG inducible, Amp^r**			**Frankel**
pSA10-4HA derivative	*Expressed protein*	*Primers 5' → 3'(pICC1727-used as template)*	*RS*	
-	EspW-4XHA	CCGGAATTCATGCCCAAAATATCATCAGTTGTATC CCGCTCGAGATTTCTAACCAAGGGGTCCC	*EcoRI* *XhoI*	This study
pACYC184	***E. coli* plasmid clonig vector containing the p15A origin of replication Cm^r**			**Clontech**
pACYC184-derivative	*Expressed protein*	*Primers 5' → 3'(pSA10-EspW-4XHA-used as template)*	*RS*	
-	EspW-4XHA	TTTGATATCAAGAAGGAGATATACCTACGTAATGCCCAAAATATCA TCAGTTGTATC CGCCGGCCGTGGCTGCAGGTCGACGGATCC	*EcoRV* *EagI*	This study
-	EspW$_{1-206}$ - 4XHA	TTTGATATCAAGAAGGAGATATACCTACGTAATGCCCAAAATATCA TCAGTTGTATC ccgCTCGAGATCAGAACTAATATTTTCGAACATTCTTACG	*EcoRV* *XhoI*	This study
pKD46	**Coding for the lambda red recombinase Amp^r**			**(Datsenko and Wanner, 2000b)**
pSB315	**Coding the kanamycin resistance *aphT* cassette Kan^r**			**(Galan et al., 1992)**
pGEM-T	**System for cloning of PCR products Amp^r**			**Invitrogen**
pGEM-T-derivative	*Insert*	*Primers 5' → 3' (EHEC O157:H7, str. 85-170 genomic DNA used as template)*		
-	EspW$_{EHEC85-170}$ with flanks	TTTCCTGTACTGAGGAACATC CCGATAACGCTGGACACAC	N/A	This study
		Primers 3' → 5'(inverse PCR using pEGMT-5'flank-espW-3'flank as template)		
-	EspW$_{EHEC85-170}$ flanks	CCGGAATTCGGGCATAAATAGTCTCCTCG CCGGAATTCCATGGGACCCCTTGGTTAG	*EcoRI* *EcoRI*	This study
		Primers 5' → 3'(pEGMT-5'flank-aphT-3'flank used as template)		
-	EspW$_{EHEC85-170}$ flanks with	TTTCCTGTACTGAGGAACATC CCGATAACGCTGGACACAC	N/A	This study

	Kan cassette (aphT)			
		aphT insertion (sequence check) primers 5′ → 3′		
		AGACAACTTAACGGAGGTAAC TCAGAGTGTCATGGCAGAAC		
pET28a(+)	**Bacterial expression vector with T7 lac promoter; N-terminal 6X His tag with thrombin cleavage site or C-terminal 6X His tag, Kan^r**			**Novagen**
pET28a(+)-derivative	*Expressed protein*	*Primers 5′ → 3′*	*RS*	
	EspW-6X His	CATGCCATGGATCCCAAAATATCATCAGTTGTATC CCAAGCTTATTTCTAACCAAGGGGTCCC	*NcoI* *HindIII*	This study
	6X His-EspW$_{20-352}$	CGCCATATGCTTTCAAATGAAACAACAATGACG CCAAGCTTATTTCTAACCAAGGGGTCCC	*NdeI* *HindIII*	This study
	6X His-EspW$_{20-206}$	CGCCATATGCTTTCAAATGAAACAACAATGACG CCAAGCTTTCAATCAGAACTAATATTTTCGAACATTCTTACG	*NdeI* *HindIII*	This study
pMAL-c2x	**Bacterial vector for expression and purification of desired proteins with an N-terminal maltose binding protein (MBP) tag, Amp^r**			**NEB**
pMAL-c2x-derivative	*Expressed protein*	*Primers 5′ → 3′*	*RS*	
-	EspW	CGCGGATCCATGCCCAAAATATCATCAGTTGTATC CCAAGCTTTTAATTTCTAACCAAGGGGTCCC	*BamHI* *HindIII*	This study
-	EspW$_{1-206}$	CGCGGATCCATGCCCAAAATATCATCAGTTGTATC CCAAGCTTTCAATCAGAACTAATATTTTCGAACATTCTTACG	*BamHI* *HindIII*	This study
pBiFC-VC155	**Eukaryotic protein expression vector with EGFP-C +HA-tag, Amp^r**			**Addgene**
pBiFC-VC 155-derivative	*Expressed protein*	*Primers 5′ → 3′(pRK5-Myc-Rac1, pRK5-Myc-* Rac1^{N17A}*, pRK5-Myc- Rac1^{Q61L} used as templates)*	*RS*	
-	Rac1	CCGGAATTCCGATGCAGGCCATCAAGTGTGTGG CGGGGTACCCAACAGCAGGCATTTTCTCTTCC	*EcoRI* *KpnI*	This study
-	Rac1^{N17A}	CCGGAATTCCGATGCAGGCCATCAAGTGTGTGG CGGGGTACCCAACAGCAGGCATTTTCTCTTCC	*EcoRI* *KpnI*	This study
-	Rac1^{Q61L}	CCGGAATTCCGATGCAGGCCATCAAGTGTGTGG CGGGGTACCCAACAGCAGGCATTTTCTCTTCC	*EcoRI* *KpnI*	This study
pBiFC-VN173	**Eukaryotic protein expression vector with EGFP-N +Flag tag, Amp^r**			**Addgene**
pBiFC-VC173-derivative	*Expressed protein*	*Phosphorylated primers 3′ → 5′ (inverse PCR - pBiFC-VC173-used as template)*	*RS*	
-	CRIB of PAK	AAATCTGAAGGGAGAGAAAT CGAACACACAATTCATGTCGGTTCGGTACCAGTCGACTCTAGAAG	N/A	This study
-	PAK1	*Primers 5′ → 3′ (pRK5-Myc-PAK1-used as template)* CCGGAATTCCATGTCAAATAACGGCCTAGA CGGGGTACCCCCTGTAGCAGCTCTTTAGCTG	*EcoRI* *KpnI*	This study
pGBKT7	**Yeast vector for expression of proteins fused to amino acids 1-147 of the GAL4 DNA binding domain, Kan^r**			**Clontech**
pGBKT7-*derivative*	*Expressed protein*	*Primers 5′ → 3′*	*RS*	
-	EspW	CCGGAATTCATGCCCAAAATATCATCAGTTGTATC CCGGGATCCTTAATTTCTAACCAAGGGGTCCC	*EcoRI* *BamHI*	This study
pGBT9	**Yeast vector for expression of proteins fused to amino acids 1-147 of the GAL4 DNA binding domain, Amp^r**			**Clontech**
pGBT9-derivative	*Expressed protein*	*Primers 5′ → 3′ (pICC1727 used as template)*	*RS*	
pICC1714	EspW	CCGGAATTCATGCCCAAAATATCATCAGTTGTATC	*EcoRI*	This study

		CCGGGATCCTTAATTTCTAACCAAGGGGTCCC	*BamHI*	
pICC1715	$EspW_{1-206}$	CCGGAATTCATGCCCAAAATATCATCAGTTGTATC CCGGGATCCtcaATCAGAACTAATATTTTCGAACATTCTTACG	*EcoRI* *BamHI*	This study
-	$EspW_{206-352}$	CCGGAATTCatgGATACAGATAAGATAACAGGAAGG CCGGGATCCTTAATTTCTAACCAAGGGGTCCC	*EcoRI* *BamHI*	This study
-	$EspW_{20-352}$	CCGGAATTCatgCTTTCAAATGAAACAACAATGACG CCGGGATCCTTAATTTCTAACCAAGGGGTCCC	*EcoRI* *BamHI*	This study
-	$EspW_{93-352}$	CCGGAATTCatgGATAAACGCTCCCGAATAGACAT CCGGGATCCTTAATTTCTAACCAAGGGGTCCC	*EcoRI* *BamHI*	This study
-	$EspW_{1-93;207-352}$	*Phosphorylated primers 3' → 5' (inverse PCR – pGBT9-espW-used as template)* GATGATACAGATAAGATAACAGGAAG ATCACTGTTTATGGCATAGTATTGG	N/A	This study
		Primers 5' → 3' (pICC1730 and pICC1731 used as templates)		
pICC1721	$EspW_{Q234A}$	CCGGAATTCATGCCCAAAATATCATCAGTTGTATC CCGGGATCCTTAATTTCTAACCAAGGGGTCCC	*EcoRI* *BamHI*	This study
pICC1722	$EspW_{I237A}$	CCGGAATTCATGCCCAAAATATCATCAGTTGTATC CCGGGATCCTTAATTTCTAACCAAGGGGTCCC	*EcoRI* *BamHI*	This study
pGAD-T7-AD	**Yeast vector for expression of proteins fused to amino acids 768-881 of the GAL4 DNA activation domain; N-terminal HA tag, Amp^r**			**Clontech**
pGAD-T7-AD-derivative	*Expressed protein*	*Primers 5' → 3'*	*RS*	
N/A		***pGAD-T7-AD Y2H screening primers 5' → 3'*** CTATTCGATGATGAAGATACCCCACCAAACCC GTGAACTTGCGGGGTTTTTCAGTATCTACGAT	N/A	
pICC1723	$Kif15_{1092-1368}$	N/A	*N/A*	This study
		Primers 5' → 3' (pICC1723 used as template)		
pICC1724	$Kif15_{1142-1347}$	CGCCATATGatgAAGACACCACCTCACTTTCAAAC CGGTCGATTGGTGACCTACCAACTTTCCA	*NdeI* *XhoI*	This study
pICC1725	$Kif15_{1092-1347}$	CGCCATATGATGGAACTGACCAAGAAGGAAGCC CGGTCGATTGGTGACCTACCAACTTTCCA	*NdeI* *XhoI*	This study
pICC1726	$Kif15_{1142-1368}$	CGCCATATGatgAAGACACCACCTCACTTTCAAAC CCGCTCGAGCTCAGCAAGCCTGACATTTTCC	*NdeI* *XhoI*	This study
pICC1752	$Kif15_{1092-1142}$	*Phosphorylated primers 3' → 5' (inverse PCR – pICC1723-used as template)* TCGAGCTGCAGATGAATCGTAG GAGGACTCTGGGGATCCTC	N/A	This study
pEGFP-C1-N-WASP	**Mammalian vector expressing N-WASP; N-terminal EGFP tag, Kan^r/Neo^r**			**(Caron et al., 2006a)**
N/A		***espW screening primers 5' → 3'*** AATATCATCAGTTGTATCATCATG AGCGTTTATCATCACTGTTTATG	N/A	
N/A		***$espW_{1-206}$ screening primers 5' → 3'*** ATGGTTGGCTACAGCTAAAACTC CCAGAAGAACAATTACCTTGTG	N/A	
N/A		***tccP screening primers 5' → 3'*** ATGATTAACAATGTTTCTTCACTT TCACGAGCGCTTAGATGTATTAAT	N/A	
N/A		***tccP2 screening primers 5' → 3'*** ATGATAAATAGCATTAATTCTTT TCACGAGCGCTTAGATGTATTAAT	N/A	

Table 2.3 - List of antibodies used in this study

Antibody/Conjugate	Application	Dilution	Source
Primary Antibodies			
Haemagglutinin (HA) (Mouse)	IF	1:500	Covance
Myc (Mouse)	IF	1:500	BD Biosciences
O157 EHEC (Rabbit)	IF	1:500	R. La Ragione
Tubulin (Mouse)	IF/WB	1:1000	DSHB University of Iowa
Secondary antibodies			
Donkey Anti-mouse Cy2	IF	200	Jackson ImmunoResearch
Donkey Anti-rabbit Cy5	IF	200	Jackson ImmunoResearch
Donkey Anti-mouse RRX	IF	200	Jackson ImmunoResearch
Rabbit anti Mouse HRP	WB	1:2000	Invitrogen
Anti-mouse AMCA	IF	50	Jackson ImmunoResearch
Chemicals			
Oregon Green Phalloidin	IF	100	Invitrogen
Texas Red Phalloidin (TRITC)	IF	500	Sigma
Alexa647 Phalloidin	IF	100	Invitrogen
DAPI	IF	1000	Sigma

Table 2.4 - List of 132 clinical EPEC isolates used in this study (isolated in Spain, Brazil and Bolivia)

Serogroup	Serotype (no. of strains)
ONT (3)	H7(1) ; H45(1); H-(1)
O13(1)	H-(1)
O26 (13)	H-(8); H11(5)
O49(1)	H-(1)
O55(24)	H-(11); H6(5); H7(5); H34(3)
O86(5)	H8(2); H34(3)
O104(1)	H2(1)
O109(1)	H9(1)
O111(12)	H-(4); H2(3); H9(1); H12(1); H21(1); H25(2)
O114(3)	H-(1); H2(2)
O119(29)	H2(11); H4(1); H6(17)
O123(1)	H-(1)
O125(3)	H6(3)
O126(4)	H-(1); H27(3)
O127(8)	H-(1); H6(3); H27(1); H40(3)
O128(6)	H-(1); H2(4); H35(1)
O142(7)	H6(3); H34(4)
O153(1)	H-(1)

O154(1)	H9(1)
O177(1)	H11(1)

2.2 Tools used to characterise EspW at the aa level

The diagrammatic representation of the genes in the region surrounding *espW* was obtained from the Xbase genome database UK website. *espW* homology was checked using BLAST and the DNA nucleotide and primary protein sequences were aligned using ClustalW v2.0 software.

2.3 Bacterial strains and growth conditions

The bacterial strains used in this study and their origin are listed in Table 1. *E. coli* and *C. rodentium* were grown from a single colony in Luria-Bertani (LB) broth in a shaking incubator (200 rpm) at 37°C for 18 h or on agar supplemented with the appropriate antibiotics: ampicillin (100 μg/ml), kanamycin (50 μg/ml) or chloramphenicol (30 μg/ml).

2.4 Molecular biology techniques

2.4.1 PCR, digestion and ligation reactions

The plasmids constructs, plasmid and DNA templates and primers used in this study are listed in Table 2.2. All synthetic primers used in polymerase chain reactions (PCR) were synthesised by Thermofisher (UK). Oligonucleotide primers were resuspended in deionised

water to a stock of 100 pmol/µl and used at a final concentration of 10 pmol/µl. The genes of interest were amplified from their corresponding DNA template (outlined in Table 2.2) by PCR using KOD Hot Start polymerase (Novagen).

The KOD Hot Start DNA polymerase kit (Novagen) was used in a mix of 1.5 µl forward and reverse primers (10 pmol/µl), 50 ng/50 µl of plasmid DNA, 3 µl of MgSO4 (25 mM, Novagen), 5 µl of dNTP (2 mM, Novagen), 5 µl KOD polymerase buffer (1U/µl, Novagen) all resuspended in sterile dH2O to give 50 µl reaction volume.

A typical PCR run consisted of an initial denaturation step of 93°C for 3 min, followed by 30 cycles of 93°C for 20 s (denaturation), 60°C for 30 s (annealing), and 74°C for 1 min/kb (70°C, 15 s/kb for KOD) (elongation), before a further 5 min at 74°C (70°C for KOD) to finish any incomplete reactions.

The vectors and PCR products were digested overnight at 37°C in a final volume of 100 µl using 1 µg of DNA template, 10 U of each appropriate restriction enzymes (NEB UK) and 10 µl of restriction buffer (NEB UK). After digestion the DNA products were column washed using Qiagen Gel extraction kit. Ligation was performed with a ratio vector to insert of 1:3, 2 µl of T4 10X ligation buffer (50 mM Tris-HCl pH 7.5, 10 mM MgCl2, 10 mM DTT, 1 mM ATP, 25 µg/ml BSA) (NEB UK) and 40 U/µl T4 DNA ligase (NEB UK) in a final volume of 20 µl at 14°C overnight.

2.4.2 *espW*$_{Q234A}$ and *espW*$_{I237A}$ point mutagenesis

espW$_{Q234A}$ and *espW*$_{I237A}$ point mutagenesis was carried out by inverse PCR using KOD Hot Start polymerase and phosphorylated primers outlined in Table 2.2

For *espW, espW*$_{1\text{-}206,}$ *tccp* and *tccp2* PCR screening of *E. coli* strains (Table 2.1 and Table 2.4) was performed using One Taq Quick-Load 2XMaster mix with stand buffer (NEB UK), according to the manufacturer's instructions. The PCR conditions consisted of an initial denaturation step at 95°C followed by 30 cycles of 95°C for 30 s (denaturation), 60°C for 30 s (annealing) and 68°C for 2 min (elongation).

The pRK5-myc-*kif15* was constructed using the Gibson Assembly Master Mix (Neb). Briefly primers were designed to amplify the full length *kif15* from pCATE-eGFP-3F-KIF15 and the pRk5-myc vector with appropriate overlaps (Table 2.2). The fragments were amplified by PCR using using the KOD Hot Start DNA polymerase kit (Novagen) then further run on agarose gels, and gel-purified using QIAPrep Gel Extraction kit (Qiagen). The concentration of resulted DNA fragments (vector and insert) was determined by Nanodrop. The DNAs (3 µl of vector (200 ηg/µl) and 1.5 µl of insert (200 ηg/µl) were added to the 10 µl Gibson Assembly Master Mix with 5.5 µl of water giving a final volume of 20 µl. After 1 h incubation at 50°C, 2 µl of the solution containing the assembled DNA was transformed into 50 µl of chemically competent *E. coli* Top10 cells by heath shock (at 42°C for 30 s) and followed by transfer on ice for 2 min. 950 µl of room temperature SOC media was added and the cells were recovered at 30°C for 1.5 h. 100 µl of bacterial cells was plated on Amp supplemented plates and incubated at 30°C overnight.

The resulted *kif15* full length sequence was checked by sequencing using six primers outlined in Table 2.2.

2.4.3 **Agarose gel electrophoresis**

Following purification or PCR-amplification, the PCR products were run on agarose gels, and then gel-purified using QIAPrep Gel Extraction kit (Qiagen). Gels were cast using 0.8-1.2% agarose gels, and a 1:10000 dilution of SYBR Safe™ DNA gel stain (Invitrogen) was added for PCR product visualisation. PCR products were mixed with 6X loading buffer (40% (w/v) sucrose, 0.25% (w/v) bromphenol blue, 0.25% (w/v) Xylene cyanol FF) prior to gel loading; gels were run in 1xTAE buffer (40mM Tris-acetate, 1mM EDTA) using a constant voltage of 120V. DNA bands were visualised using a Safe Imager™ blue light transilluminator (Invitrogen) and images were acquired using the Synegene BioImaging software. DNA fragment size was estimated using 1kb or 2-log ladder (NEB). DNA purification was performed by removing using a scalpel of the agarose containing the DNA of interest followed by DNA purification using a gel extraction kit (Quiagen) according to manufacturer's protocol. Briefly, the agarose containing the DNA was melted at 55°C in high salt containing buffer and further purified on silica-gel membranes to remove contaminants. DNA was eluted in 50 µl of sterile deionised water and stored at -20°C or processed for ligation.

All constructs were confirmed by sequencing using GATC Biotec (Germany) services. DNA was sequenced using primers corresponding to the flanking regions of the DNA fragment of interest using 50-100 ng/µl DNA and 10pmol of primer. Sequences were analised using BioEdit and SerialCloner2 software.

2.4.4 Plasmid extraction

Plasmid extractions were carried out from 5 ml bacterial overnight cultures with QIAPrep Spin Miniprep kits (Qiagen) or 150 ml cultures with QIAPrep Spin Midiprep kits (Qiagen) according to manufacturer's instructions. Briefly, bacteria were harvested and resuspended in an alkaline solution containing sodium dodecyl sulphate (SDS) and RNase. These conditions resulted in the lysis of bacteria as well as the denaturation of genomic and plasmid DNA. Neutralisation of the solution led to re-annealing of plasmid DNA and precipitation of genomic DNA. Bacterial debris and precipitated DNA were aggregated by centrifugation of flotation. Plasmid DNA was then purified and concentrated on silica-based resins. Following a washing step with 70% ethanol, plasmid DNA were eluted with sterile dH2O. Plasmid DNA concentration was assessed using a NanoDrop ND-1000 reader (Thermo Scientific).

2.5 Bacterial transformation

2.5.1 Bacterial transformation using chemically competent Top 10 *E.coli*

The transformation of ligated products into chemically competent Top 10 *E.coli* (Invitrogen) was achieved by heath-shock. The cells were first made chemically competent by inoculating 1:100 of overnight TOP10 cultures in fresh LB broth and grown to mid-log phase (OD600 0.4 – 0.5) before harvest by centrifugation at 4000 x g, 4°C for 7 min. Cells were resuspended in 0.4X volume of ice-cold TFBI buffer (30 mM potassium acetate, 10 mM CaCl2, 50 mM MnCl2, 15% (v/v) glycerol, pH 5.8) and then incubated on ice for 5 minutes

before pelleted by centrifugation as before. Cells were re-suspended in ice cold TFBII buffer (10 mM MOPS, 75 mM CaCl2, 10 mM RbCl2, 15% (v/v) glycerol, pH 6.5) and then stored at -80°C for long-term use. Unless stated otherwise, 50 µl of chemically competent cells were incubated at 4°C with 5–10 µl of ligated products for at least 30 min before heat-shocking for 90 seconds in a 42°C water bath. The cells were then transferred immediately to 4°C to allow recovery for 5 minutes before 1 ml of LB broth without antibiotics was added. Cells were allowed to recover at 37°C for 1-3 h before plating 300 µl of the mix on LB agar with the appropriate selection of antibiotic and incubated at 37°C overnight.

2.5.2 **Bacterial transformation using electrically competent Top 10 *E.coli***

Some of the purified recombinant plasmid DNAs were transformed into *E. coli* strains also by electroporation. Bacteria were made electrocompetent by first being grown in LB broth (1 ml of ON growth into 50 ml broth) to mid-log phase and further cooled to 4°C for 30 min. The culture was pelleted down by centrifugation before re-suspension in 20 ml 15% (v/v) glycerol at 4°C. This step was repeated twice before resuspension into a final volume 80 µl of 15% (v/v) glycerol was added. The 80 µl resuspension was mixed with 4 µl recombinant plasmid in an electroporation cuvette of 0.2 cm width (Bio-Rad). Electroporation was performed using the GenePulser™ electroporation system (Bio-Rad) using the following parameters: resistance (200 Ω for *E. coli*), voltage (2.5 kV) and capacity (25 µF). 800 µl of LB broth without antibiotics was then added immediately. The transformation mix was incubated at 37°C shaking for 90 min before 300 µl of the mix was plated onto LB plates containing the appropriate antibiotics and incubated at 37°C

overnight.

2.6 Yeast-2-Hybrid analysis

2.6.1 Yeast transformation

Plasmids were transformed in to yeast using the LiAc method. Briefly, a 10 ml overnight culture was diluted 1:10 and grown in 50 ml YPD media for 4 h at 30 °C at 200 rpm. Cells were centrifuged for 5 min at 4000 rpm, washed in 10 ml H_2O, and resuspended in 500 µl 100 mM LiAc. 50 µl aliquots were used for each transformation: 240 µl PEG, 25 µl SS-DNA, 25 µl 1M LiAc, 50 µl H_2O and 5 µl of each plasmid were added to the yeast and incubated at 30 °C for 30 min then heat shocked at 42 °C for 20 min before plating on selective SD media (double drop out (DDO) –Leu, -Tryp; triple DO (TDO) –Leu, -Tryp, -Ade; quadruple (DO) QDO –Leu, -Tryp, -Ade, -His).

2.6.1 Yeast-2-Hybrid and Direct Yeast-2-Hybrid screens

Saccharomyces cerevisiae (AH109) were grown in YPDA medium (20 g/L Difco peptone, 10 g/L yeast extract 2% glucose and 0.003% adenine hemisulfate) for 48 h at 30°C. For the Yeast-2-hybrid screen, the following selective media was required: SD minimal media (6.7 g/L Yeast nitrogen base without amino acids, 2% glucose, 100 ml 10 X Drop Out solution.

The Yeast-2-Hybrid screen was performed using Mate & Plate™ Library - HeLa S3 (Normalized) (Clontech) as described previously (Simpson et al., 2006b). This library was

constructed from HeLa S3 cDNA library transformed into yeast strain Y187 and for this experiment we used the pGBT9 plasmid with GAL4 DNA-BD fused to EspW (as bait) transformed into AH109. AH109 cultures were grown into YPDA medium (20 g/L Difco peptone, 10 g/L yeast extract 2% glucose and 0.003% adenine hemisulfate) overnight. For the Yeast-2-hybrid screen, the following selective media was required: SD minimal media (6.7 g/L Yeast nitrogen base without amino acids, 2% glucose, 100 ml 10 X Drop Out solution. The Drop Out solution contains a mixture of specific amino acids and nucleosides and missing one or more of the nutrients required by untransformed yeast to grow on SD medium: quadruple drop-out (QDO) (-Ade, -His, -Leu, -Trp), triple drop-out (TDO) (-His,-Leu,-Trp), double drop-out (DDO) (-Leu, -Trp) and single drop-out (SDO) (-Trp).

The genes and primers used to make the constructs used in the Y2H assays are outlined in Table 2.2.

The transformed AH109 strain with pGBT9-EspW presented three reporter genes: ADE2, HIS3 and MEL1 (encoding for α-galactosidase and β-galactosidase), under the control of GAL4. Because α-galactosidase is a secreted enzyme, the transformants were assessed for MEL1 activation directly on X-α-Gal indicator plates, which employed blue/white screening. The EspW protein was assessed for toxicity when expressed in yeast by measuring growth curves. If the bait is toxic to the yeast cells, both solid and liquid cultures will grow more slowly.

The pGBT9-EspW containing AH109 was mated with the library according to the manufacturer's instructions and the mated culture was plated on TDO media containing X-α-Gal, which selects for colonies containing both bait and prey and activates two of three interaction promoters. Each positive blue colony was streaked onto QDO plates containing

X-α-Gal that selects for the activations of all promoters. The new positive blue colonies were passaged thrice by further streaking onto QDO plates.

The colonies were screened by PCR for the positive targets using primers outlined in Table 2.2 and further sent for sequencing for target identification. Sequencing results were analysed using blastx searches for protein identification.

2.7 Construction of EHEC *ΔespW* mutant

The EHEC *ΔespW* mutant was generated using a Lambda red-based mutagenesis system (Datsenko and Wanner, 2000b) where *espW* gene was replaced by a kanamycin cassette. The primers used to make the different constructs used in this assay are outlined in Table 2.2. Plasmid pSB314 (Galan et al., 1992) was the source of the kanamycin resistance gene (*aphT*) which was excited using EcoRI restriction site. Briefly, the *espW* gene with up flanking region (380 bp) at the 3' end and down flanking region (348 bp) at the 5' end was amplified from *E. coli* O157:H7 (85-170) genomic DNA; the generated DNA fragment was inserted into TOPO Blunt II (Invitrogen) by blunt-end ligation and transformed into Top10 cells. An inverse PCR reaction was set up using the best pGEMT-3'flank-espW-5'flank clone (checked by sequencing). In order to remove the bacterial DNA, the PCR reactions were treated with DpnI (5 µl of Dnp1 per 50 µl and incubate at 37°C for 3-4 h) and gel purified. To prevent the pEGMT vector containing the flanking regions of *espW* and the EcoRI restriction sites from self-ligation, the samples were further dephosphorylated using CIP (1.5 µl per 30 µl of sample with 3 µl of Buffer 4 (NEB) for 1 h at 37°C.

The pGEMT-3'flank-aphT-5'flank vector was constructed by the insertion of the *aphT* cassette at the EcoRI site. The orientation of the kanamycin cassette was verified by PCR and clones were verified by sequencing. The 3'flank-aphT-5'flank DNA fragment was amplified from pGEMT-3'flank-aphT-5'flank. The PCR products were further electrophorated into EHEC 85-170 containing the lambda Red recombinase following induction with 1mM arabinose (Datsenko and Wanner, 2000b). Strains containing pKD46 were incubated at 30°C as the plasmid is heat-sensitive. Transformants were selected on kanamycin plates and the insertion of the kanamycin cassette mutant confirmed by PCR and DNA sequencing.

2.8 PCR screen for the distribution of *espW* in pathogenic *E. coli* strains

E. coli strains available in the laboratory and a collection of 132 EPEC clinical isolates (Table 2.4) were screened for the presence of *espW* by PCR. PCR settings of 30 cycles at 94°C for 30 s, 58°C for 30 s and 68°C for 1 min. The primers used for screening are outlined in Table 2.2.

We screened first for the presence of *espW* followed by a screen of all the *espW* full length negative strains for the presence of $espW_{1\text{-}206}$. EHEC O157:H7 (85-170) and EPEC E2348/69 were used as positive and negative controls respectively.

2.9 Infection of Swiss 3T3 and HeLa cells

For cell infections, EHEC strain were grown in LB in a shaking incubator (200 rpm) at 37°C for 8 h and then subculture (1/500) in DMEM with low glucose and grown overnight at 37°C without agitation in 5% CO2 incubator.

Swiss NIH 3T3 and HeLa cells were maintained in DMEM with 4500 mg/ml glucose (Sigma) or DMEM with 1000 mg/ml glucose (Sigma), respectively, supplemented with 10% (vol/vol) heat-inactivated foetal bovine serum FCS (Gibco),4 mM GlutaMAX (Gibco) and 0.1 mM nonessential amino acids at 37°C in 5% CO2.

Forty-eight hours prior to infection cells were seeded in 24-well plates containing 13-mm glass coverslips (VWR International) at a density of 5x105 cells per well and maintained in DMEM supplemented with 10% FCS at 37°C in 5% CO2. Bacteria were primed for infection by diluting 1:50 overnight culture in 1000 mg L^{-1} serum free DMEM (SIGMA). The cultures were incubated statically at 37°C in a 5% CO2 incubator for 8 h. Before infection the cells were washed 3 times with PBS, the media replaced with fresh DMEM without FCS. Cells in 24-well plates were infected with 20 µl of prime cultures. The plates were then centrifuged at 200 rpm for 5 min at room temperature to synchronize infection and incubated for 3 h at 37°C in 5% CO2 without agitation. After infection, cells were washed at least ten times in PBS to remove the bacteria and before fixing in 3% paraformaldehyde (PFA) in PBS for 15 min, followed by two more washes with PBS. The coverslips were kept in the second wash until immunofluorescence staining. For Sphingosine 1-phosphate (S1P) (Sigma-Aldrich) treatment, S1P dissolved in dimethyl sulfoxide (DMSO) (Sigma-Aldrich) was added to DMEM media to attain a final concentration of 100 nM per well.

2.10 Transfection assays

The cells were split around 80-90% confluence and seeded onto glass coverslips at 5×104 density of cells per well into 24-well tissue culture plates for 24 h. Swiss cells were transfected using Lipofectamine 2000 (Invitrogen) according to the manufacturer's instructions and HeLa cells were transfected using GeneJuice (Merck Millipore) according to the manufacturer's recommendations. Swiss transfected cells were incubated at 37°C in a humidified atmosphere containing 5% CO2 for 4 h, washed twice with PBS before having their media replaced with DMEM and incubated for further 24h. Transfected HeLa cells were incubated for 24 h in the same conditions.

For cotransfection experiments we used a ratio of EspW to dominant negative Rho GTPases of 60% : 40%. As positive control the cells were cotransfected using pRK5-HA-EspW with pRK5-HA-GFP and as negative control the cells were cotransfected using pRK5-HA with dominant negative $Rac1^{N17}$, $RhoA^{N19}$ and $Cdc42^{N17}$.

2.11 Immunofluorescence and microscopy

Coverslips were washed three times in PBS and fixed with 3% Paraformaldehyde (PFA) for 15 min before washing 3 more times with PBS. Cells were quenched for 10 min with 50 mM NH4Cl then permeabilized for 4 min in PBS 0.2% Triton X-100, and washed 3 times in PBS. The coverslips were blocked for 15 min in 0.2% bovine serum albumin (BSA)-PBS before incubation with primary and secondary antibodies. The primary antibody mouse anti Haemagglutinin (HA) (Cambridge Bioscience), chicken anti Myc (Millipore), polyclonal

anti O157 (Roberto la Ragione, Veterinary Laboratory Agency, United Kingdom) were used at a dilution of 1:500. Coverslips were incubated with the primary antibody for 1 h, washed 3 times in PBS and incubated with the secondary antibodies. AMCA-, Cy2-, RRX- or Cy5-conjugated donkey anti-mouse and anti-rabbit antibodies (Jackson ImmunoResearch) were used as secondary antibodies. All dilutions were in PBS/0.2% BSA. Actin was detected with tetramethyl rhodamine isothiocyanate (TRITC)-conjugates phalloidin (1:500 dilution) (Sigma). DNA was stained with 4',6-diamidino-2-phenylindole (DAPI) (1:1,000 dilution). Coverslips were mounted on slides using ProLong® Glod antifade reagent (Invitrogen) and examined by conventional epifluorescence microscopy using a Zeiss Axio LSM-510 microscope. Images were deconvoluted, processed using the Axio Vision 4.8 LE software (Zeiss) and trimmed using Adobe Photoshop CS4.

2.12 LDH Cytotoxicity assay

Swiss cells grown in 96-well plates were infected with 1 ml of primed EPEC culture (MOI 1:200) in phenol red-free DMEM media and centrifuged for 4 min at 200 g to synchronize infection. Cells were incubated for 30 min, washed once with PBS and then incubated with 200 µg ml-1 gentamicin (Sigma) in phenol red-free DMEM media for a further 4 hours. LDH release during EPEC infection was assayed using a CytoTox96® cytotoxicity assay kit (Promega) according to manufacturer's instructions. Briefly, the supernatant containing LDH of lysed cells was collected and combined with 1:1 ratio of the substrate mixture for 30 min in the dark. Total LDH is assessed by addition of 1% Tween-20 to an uninfected well to trigger cell permeabilization. Cytotoxicity was assayed using a 96-

well plate reader at 492 nm, and calculated as a percentage of (experimental LDH activity – basal LDH activity) / (total LDH activity – basal LDH activity).

2.13 Scanning electron microscopy

Coverslips from transfection and infection assays (described above) were washed 3 times in phosphate buffer pH 7.4 and then fixed with 2.5% glutaraldehyde in phosphate buffer pH 7.4 at 4°C overnight. The following day coverslips were washed thrice for five min with 500 µl 0.2 M phosphate buffer pH 7.4 and further post fixed in 1% Osmium Tetraoxide for 1 h. Cells were then washed 3 times in phosphate buffer before being dehydrated for 15 min in sequence of 50%, 75%, 85%, 95% and 100% aqueous ethanol solutions. The cells were then transferred to an Emitech K850 Critical Point drier and processed according to the manufacturer's instructions. The coverslips were mounted on aluminium stubs and sputter-coated with gold/palladium mix for 90 seconds using the Emitech Sc762 mini sputter. Samples for scanning electron microscopy (SEM) were then examined blindly at an accelerating voltage of 25 kV using a Jeol JSM-6390.

2.14 Protein expression and analysis

EspW and $EspW_{1-206}$ were expressed from Top10 with pMAL-c2X plasmid by addition of isopropyl-ß-D-thiogalactopyranoside (IPTG) to the culture. The BL21 (DE3) star strain containing expression plasmids was grown overnight at 37°C in 50 ml in LB broth containing the appropriate antibiotic. Overnight cultures were diluted 1:100 in LB with the appropriate

antibiotics and grown until OD_{600} of 0.4 - 0.6, then induced for 3 h at 30°C, 37°C and ON at 25°C and 18°C with a concentrations of IPTG of 0.5 mM. Uninduced cell cultures were used as control. Bacterial cells were harvested by centrifugation at 4°C at 3000 x g for 15 min. The supernatant was then discarded and bacterial pellets were either processed immediately for protein purification, or stored at –20°C.

For expression test, whole cell lysates were generated by resuspending bacterial pellets from 1 ml of induced and uninduced cultures in SDS buffer (50% glycerol, 1M Tris pH 6.8, 10% SDS, B-mercaptoethanol and 0.05% bromphenol blue). Protein loading was normalised according to the optical density of the bacteria to make sure that the same amount of protein was loaded onto the 12% polyacrylamide SDS- gel (BioRad).

Protein samples were boiled for 10 min at 90°C, loaded on the SDS gel and separated by electrophoresis at 120 V.

2.14.1 **Protein purification**

2.14.1.1 Purification of MBP-tagged proteins

For protein purification 1L of culture were centrifuged at 4000 RPM for 20 min and the bacterial pellet resuspended in 40 ml MBP protein buffer (50 mM Tris, 0.2 M NaCl, 1 mM EDTA and 1 mM DTT (DL-Dithiothreitol) at pH 7.4) and cOmpleteTM EDTA-free protease inhibitors (Roche) and bacteria were lysed with three passes through an Emulsiflex B-15 (Avestin). Samples were clarified at 12 000 RPM for 20 min and the supernatant loaded onto MBP-bind resin (Novagen) pre-equilibrated in 8 ml MBP protein buffer. Resin was

washed with 30 ml MBP protein buffer and the sample eluted with MBP protein buffer containing 10 mM maltose. 1 ml fractions were collected in 1.5 ml eppendorf tubes and stored at 4°C.

2.14.1.2 Purification of His-tagged proteins

For His-tagged protein purifications, the bacterial pellet was resuspended in 3 ml of binding buffer (50 mM Tris-HCl, pH 7.8, 500 mM NaCl, 30 mM imidazole) and lysed as previously described using the Emulsiflex B-15 (Avestin). The supernatant was loaded into a 15ml column containing 2ml Nickel- NTA resin (NEB), pre-charged with 50 mM NiSO4 in a 15 ml column and equilibrated in binding buffer. Following loading of the cell lysate onto the resin, columns were washed with 20 ml of binding buffer followed by 30 ml of washing buffer (50 mM Tris-HCl, pH 7.8, 500 mM NaCl, 60 mM imidazole). Proteins were eluted with eluting buffer (50 mM Tris-HCl, pH 7.8, 500 mM NaCl, 250 mM imidazole); 1 ml fractions were collected in 1.5 ml Eppendorf tubes and stored at 4°C.

2.14.1.3 Purification of GST-tagged proteins

The bacterial pellet was resuspended in 3 ml of GST column buffer (50 mM Tris-HCl, pH 7.4, 150 mM NaCl, 1 mM EDTA, 1 mM DTT) and lysed as previously described. The supernatant was loaded onto 2ml glutathione resin (GE Healthcare), equilibrated in GST column buffer, in a 15 ml column. After the cell lysate had completely entered the resin, the columns were washed with 30 ml of GST column buffer. Proteins were eluted with GST

column buffer supplemented with 25 mM glutathione; 1 ml fractions were collected in 1.5 ml Eppendorf tubes and stored at 4°C.

2.14.1.4 Quantification of protein concentration (BCA assay)

Cells in tissue culture flasks (BD Biosciences) or 24-well plates (BD Biosciences) were lysed with cold RIPA buffer (25 mM Tris-HCl pH 7.6, 150 mM NaCl, 1% (v/v) NP-40, 1% (v/v) sodium deoxycholate, 0.1% SDS) supplemented with protease inhibitor cocktail (Roche) for 45 min. Lysates were harvested using cell scrapers and centrifuged at 14,000 rpm at 4°C for 20 min to remove insoluble debris. Protein concentration of cleared lysates was quantified using Pierce bicinchoninic acid (BCA) Protein Assay kit (Thermo Scientific) according to manufacturer's protocol. Briefly, the protein samples were added to the BCA reagent at a ratio of 1:1 and incubated for 30 min at 37°C. Samples were read at 562 nm using a 96-well plate reader (Biorad). Protein concentration of samples was determined using a 0.1 – 1.0 mg BSA standard ladder. Absorbance of BSA standard samples (0 to 500 µg/ml BSA) at A_{562} was assessed in parallel, to plot a standard curve and determine the concentration of unknown samples. All measurements were performed in duplicate.

2.14.2 **SDS-PAGE**

Resolving gels were cast using 8 – 12 % acrylamide in Tris-SDS buffer (0.375 M Tris-HCl pH 8.8, 0.1 % SDS), while stacking gels were cast using 4% acrylamide in Tris-SDS buffer (0.125 M Tris-HCl pH 6.8, 0.1 % SDS). 0.1 % (w/v) ammonium persulfate and 0.1 % (v/v) TEMED were added to induce acrylamide polymerization. After polymerisation, gels were

positioned in a gel electrophoresis tank (Biorad) with 1 X running buffer (3 g/l Tris, 14.4 g/l glycine, 0.1% SDS). Protein samples were boiled in 5X Laemmli buffer (60 mM Tris-HCl pH 6.8, 2% SDS, 10% (v/v) glycerol, 5% (v/v) β-mercaptoethanol, 0.01% (w/v) bromophenol blue) for 8 – 10 min prior to loading. Samples were separated on the polyacrylamide gel between 90 – 200 V in 1X Tris-Glycine-SDS buffer (Bio-Rad). Molecular weight of protein samples was estimated using a prestained broad range protein marker (NEB UK).

2.14.3 **Coomassie staining**

For Coomassie staining the gels were incubated for 1 h at room temperature with gentle agitation in 0.125% (w/v) Coomassie blue stain (0.25 g Coomassie powder, 30% methanol 100% (v/v), 10% acetic acid 100% (v/v) and 40% sterilised Milli-Q water). After staining the gels were washed in destaining solution (30% methanol 100% (v/v), 10% acetic acid 100% (v/v) and 40% sterilised Milli-Q water) for as long as it was necessary. After destaining the gels were kept in Milli-Q water.

2.14.4 **Western blotting**

For detection of proteins with specific antibodies, a wet western blot analysis was done after the separation via SDS-PAGE. The transfer onto onto the PVDF membrane (GE Healthcare) was performed at 300 mA for 1.5 h. To avoid unspecific binding of the antibodies the membrane was blocked overnight in PBS-T (PBS with 0.1% Tween) and 3% milk. The primary antibody was diluted in blocking buffer as indicated and added to the

membrane. After incubation for at least 1 h the membrane was washed three times for 10 min in PBS-T and incubated for 1-1.5 h with the appropriate secondary HRP-conjugated antibody diluted in PBS as indicated. After three additional washing steps with PBS-T the membrane was incubated for 1 min with EZ-ECL reagent (GE Healthcare) and developed by the LAS-3000 imager (Fuji).

2.14.5 **Statistical analysis**

Statistical analysis of the data was performed using Prism software (Version 5, GraphPad Software, San Diego, CA, USA). All experiments represent at least three biological replicates. Data is presented as mean ± SD. For the unpaired Stuent t-test and ANOVA with n=3, the difference between the means of the groups were considered significant for p values below 0.05 ($p< 0.05$).

CHAPTER 3 - **Results**

3.1 Characterisation of EspW at the aa level and screening of *espW* in EPEC clinical isolates

3.1.1 Genomic context of EspW

The T3SS is employed by many bacterial pathogens of plants and animals to inject effector proteins into the eukaryotic cells (Galan and Wolf-Watz, 2006). The large numbers of effectors that have been identified and characterized in recent years have revealed broad diversity in terms of both functions and mechanisms. A/E pathogens contain many genetic elements that encode T3SS effector proteins reviewed in (Wong et al., 2011), (Frankel et al., 1998b).

One of the major mechanisms for genome evolution of EHEC O157 is phage-mediated horizontal gene transfer, which can include new virulence genes (Dobrindt et al., 2010), (Cooper et al., 2014). Analysis of the EHEC O157:H7 strain SS17 genome revealed 22 phage-bearing regions distributed across the entire genome (Figure 1.12). The genes *espW* and *espM2* were shown to be located in close proximity on Region 18 in EHEC O157:H7 strain SS17 and Region Sp17 in EHEC O157:H7 strain Sakai (Cote et al., 2015), (Tobe et al., 2006).

EspW is a 352 aa prophage encoded effector present in EHEC strains (Cooper et al., 2014), with no homologs amongst other bacterial species. xBASe revealed that in the genome of *E.coli* O157:H7 strain TE14359, *espW* is located in vicinity of two genes encoding for non-LEE encoded T3SS effectors EspM2 and NleG (Figure 3.1).

To find if *espW* was reported in other bacterial species, TBLASTX was used to search NCBI databases for EspW amino acid sequence. Out of all database, *espW* was found to be present in five EHEC O157:H7 strains (Xuzhou2, TW14359, EC4115, EDL933 and Sakai) and in four non-O157:H7 strains (two O111:H$^-$, one of which is strain 11128, O26:H11 strain 11368 and O103:H2 strain 12009). In addition, a shorter version of EspW (containing only the first 206 aa) was identified in two EPEC O55:H7 strains: CB9615 and RM12579 (Table 3.1).

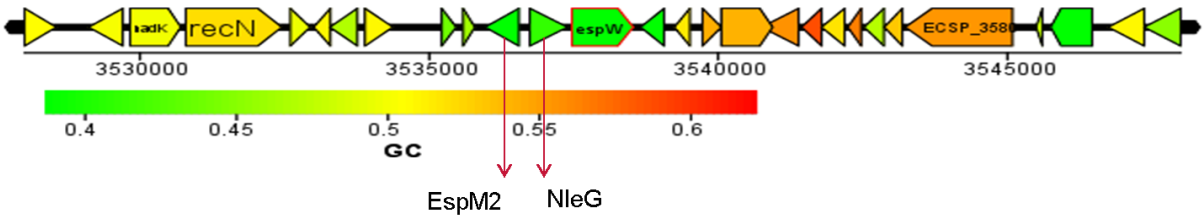

Figure 3.1 - EspW non-LEE-encoded Type 3 Secreted effector gene organisation of EHEC O157:H7 str. TE14359

Genome position: 3537470-3538528; Length: 1059 bp - 352 amino acids). The genes are coloured by GC% content. (http://www.xbase.ac.uk/genome/escherichia-coli-o157h7-str tw14359/NC_013008/ECSP_3569;espW/viewer

Table 3.1 - List of full length *espW*$_{1-352}$ and truncated *espW*$_{1-206}$ positive *E. coli* strains identified by BLAST

		espW$_{1-352}$	*espW*$_{1-206}$
EHEC O157:H7	str. Xuzhou21	+	-
	str. TW14359	+	-
	str. EC4115	+	-
	str. EDL933	+	-
	str. Sakai	+	-
EHEC non O157:H7	O111:H- str. 11128	+	-
	O26:H11 str. 11368	+	-
	O103:H2 str. 12009	+	-
	O111:H-	+	-
EPEC	O55:H7 str. CB9615	-	+
	O55:H7 str. RM12579	-	+

Nucleotide BLAST analysis against NCBI database, showed that EspW shares 29% identity with the C-terminal domain of HopPmaA/HopW, a protein with unknown function identified in *Pseudomonas syringae*. Furthermore EspW shares 55% identity with an uncharacterised protein in *Salmonella enterica* subsp. *salamae* (Figure 3.2).

```
EspW     MPKISSVVSSCYHLFSEHQQLSNETTMTNPVSRRIVHKEYGISLKSVPVWLATAKTPLAL  60
         M  ++S  SSC+++  E+++LS ETT++  +SRR+ H E    L++ PVWL TAK PL L
S.prot   MLNVTSFFSSCFNVLQENRELSRETTISPSISRRVTHIENPPLLRTPPVWLVTAKIPLPL  60

EspW     LNGRHTRSHSFIIAGTPGMGSRSGAQYYAINSDDKRSRIDIDSLFLKKLNNVRNQNKFPI  120
         LNGRHTRSHSF++ G PG GS SGAQYYAINSDDKRSR+ ID  F++K NN    + F
S.prot   LNGRHTRSHSFVMVGDPGKGSNSGAQYYAINSDDKRSRVIIDDSFIQKTNNNHRHHNFSN  120

EspW     DVKETVIKLQGQKFTCIEDFYKRYNETRLKANTNIQQEQIADEVKSLTYLIPSEKKEMWI  180
         + +  V  L G+ F+CIE F+K Y   R K   NI   ++ +EVK+LT+LIPSE KEMWI
S.prot   NTRAAVESLLGRNFSCIEGFHKTYTNIRQKQEPNISPNKLMEEVKALTFLIPSEHKEMWI  180

EspW     YKNNGKDNAKPNLGERDVRMFENISSDDTDKITGRKFSELGEYLYSGNVIKLSQLSIRYL  240
         Y+NNGK++ KPNLGERDVRMFEN+   + DK+  +  SEL  ++ SG  IK S+L++RYL
S.prot   YENNGKESTKPNLGERDVRMFENVDLSEIDKVNVKSKSELYSHMLSGEPIKTSKLTLRYL  240

EspW     PNISSISLIETKQSLLLHRLYSDEVLQRNGTLIPTPLHEEKSIPADNIKTMLNNIPTYKM  300
         PN   I+LIE K+ LLL RLY DE+ +RNGTL+P     +  +P D +  + N  PTYKM
S.prot   PNTDPIALIEAKRDLLLQRLYMDELYERNGTLLPCSEPNKGFVPPDILSQIQNKTPTYKM  300

EspW     LPPFTETQGNCSSGAATFLRKSGAEEKDILACSPRNYGLHHNIKTWDPLV  350
         LPPFT  QGNCS+GAAT LRK+G +E+DILACSPRNYGLHH +  W P++
S.prot   LPPFTPLQGNCSTGAATILRKAGTKEEDILACSPRNYGLHHPMYFWKPIL  350
```

Figure 3.2 - Alignment of EspW from EHEC O157:H7 strain TW14359 and an uncharacterised effector in *Salmonella enterica* subsp. *salamae*.
These two proteins share 55% identity (NCBI-BLAST).

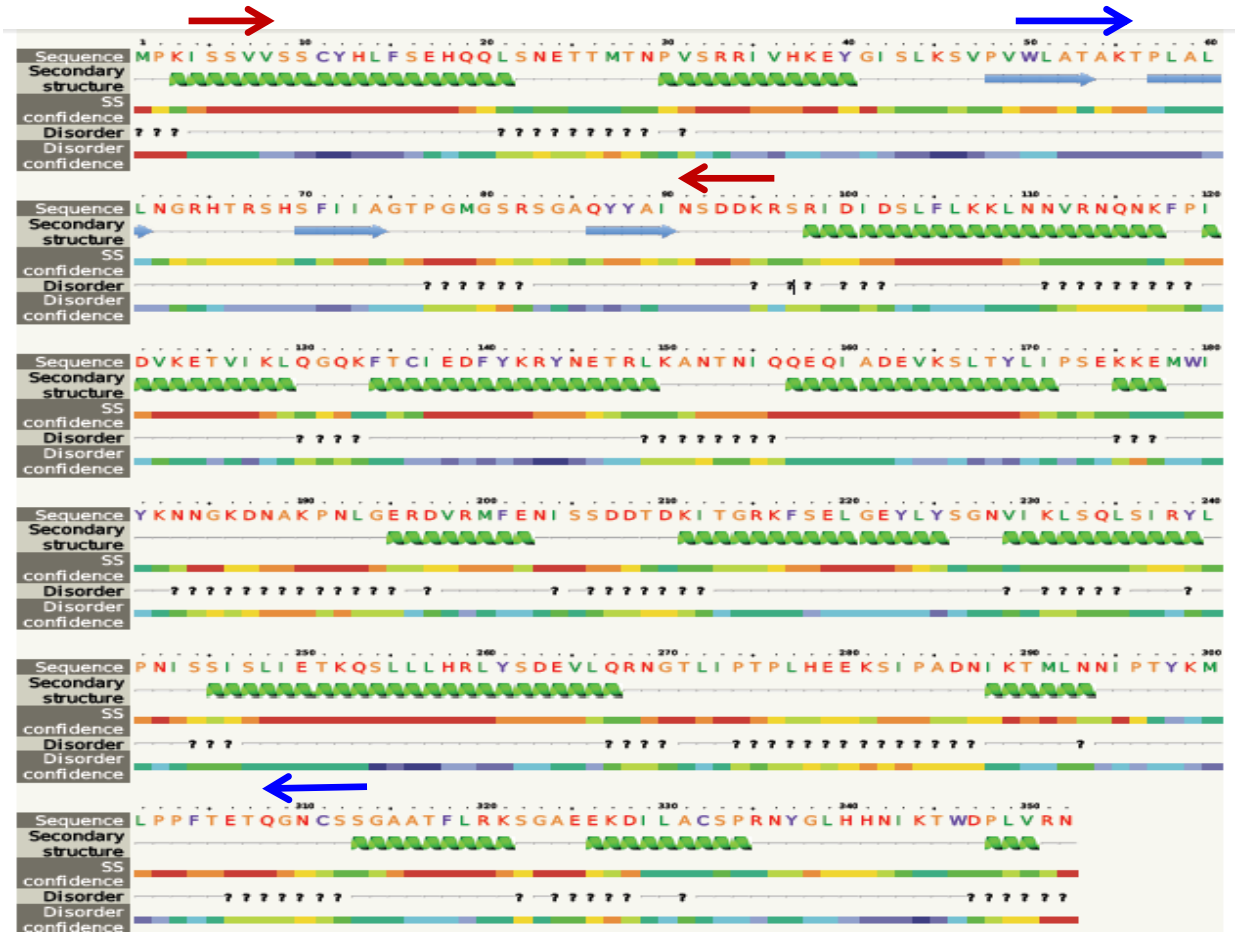

Figure 3.3 – Predicted secondary structure for EspW

The Phyre2 software predicted that EspW secondary structure contains 15 alpha helixes (in green) and four beta seets (blue arrows).

The * marks the last residue of *espW*$_{1\text{-}206}$; the primers used to screen clinical isolates for the presence of *espW* are marked with blue arrows and for *espW*$_{1\text{-}206}$ are marked in red.

The secondary structure of EspW (Figure 3.3) revealed that it is rich in alpha helices however the Phyre 2 software could not determine any predictive structure matching any portion of the EspW protein. No structure domains similarities and no homologues with any other already reported protein domains could be found.

In order to have a more elaborated view of the distribution of the *espW* we screened by PCR the collection of pathogenic *E. coli* strains available in Frankel's laboratory (Table 3.2).

The presence of *espW* was confirmed amongst nine EHEC strains out of which four O157:H7 (EDL933, Sakai, 85-170 and CB1556) and five non-O157:H7 strains O26:H11 (3801, B3#38, B3#42, B3#44 and EC740). *espW* was also present in five REPEC strains screened O8:H- (82/215), O128:H2 (82/183), O103:H2 (E22), O109:H2 (82/123) and O103:H2 (84/110-1). *Citrobacter rodentium* (ICC168) and EPEC O127:H6 E2348/69 were *espW* negative but EPEC O111:H9 (E110019) and EPEC O111:H- (B171) were *espW* positive. Here we are reporting for the first time that *espW* is present not only in EHEC, but in REPEC and EPEC too.

Table 3.2 - Distribution of *espW* in 18 pathogenic *E. coli* strains
(Prof. Frankel's collection). REPEC (rabbit pathogen), *C. rodentium* (murine pathogen)

Pathotype and serotype		*espW*
REPEC	82/215-2 (O8:H-)	+
	82/183 (O128:H2)	+
	O103:H2 E22	+
	82/123 (O109:H2)	+
	84/110-1 (O103:H2)	+
EHEC	O26:H11 3801	+
	O26:H11 B3#44	+
	O26:H11 B3#42	+
	O26:H11 B3#38	+
	O157:H7 EDL933	+
	O157:H7 Sakai	+
	O26:H- EC740	+
	O157:H7 85-170	+
	O157:H7 CB1556	+
Citrobacter rodentium	ICC168	-
EPEC	O127:H6 E2348/69	-
	O111:H9 E110019	+
	O111:H- (B171)	+

3.1.2 **Screening of *espW* in 132 EPEC clinical isolates**

In order to investigate further the presence of *espW* in EPEC strains, we screened by PCR a collection of 132 clinical EPEC strains isolated in Spain, Brasil and Bolivia (Table 3.3).

We took into account the information obtain by BLAST with regards to the two types of *espW* (full-length and truncated (*espW*$_{1-206}$)) and we used two sets of primers for the PCR screening outlined in Table 2.2 and marked on Figure 3.3, to amplify the full length or the truncated version of *espW*.

We screened first for the full length *espW*, followed by a second round of PCR employed to screen all the full length *espW* negative strains for the presence of the truncated version of the gene.

As shown in Table 3.3 *espW* was present in 52% of the tested strains. Furthermore, *espW*$_{1-206}$ was found in 10 out of 132 (8%) of the strains tested. Interestingly nine out of these ten *espW*$_{1-206}$ genes were present in the O55:H7 strains as those identified by BLAST (Table 3.1).

Table 3.3 - Distribution of *espW* and *espW*$_{1-206}$ among 132 clinical EPEC strains.

Serogroup	*espW*	Serotype (no. of strains)
ONT (3)	3	H7(1/1) ; H45(1/1); H-(1/1)
O13(1)	1	H-(1/1)
O26 (13)	9	H-(4/8); H11(5/5)
O49(1)	1	H-(1/1)
O55(24)	10	H-(3/11); H6(5/5); H7(1/5); H34(1/3)
O86(5)	3	H8(0/2); H34(3/3)
O104(1)	1	H2(1/1)
O109(1)	1	H9(1/1)
O111(12)	5	H-(2/4); H2(3/3); H9(0/1); H12(0/1); H21(0/1); H25(0/2)
O114(3)	2	H-(0/1); H2(2/2)
O119(29)	14	H2(4/11); H4(0/1); H6(10/17)
O123(1)	1	H-(1/1)
O125(3)	1	H6(1/3)
O126(4)	1	H-(1/1); H27(0/3)
O127(8)	3	H-(1/1); H6(2/3); H27(0/1); H40(0/3)
O128(6)	4	H-(0/1); H2(4/4); H35(0/1)
O142(7)	5	H6(3/3); H34(2/4)
O153(1)	1	H-(1/1)
O154(1)	1	H9(1/1)
O177(1)	1	H11(1/1)

67 of these strains were isolated in Spain and Brasil and 65 strains were kindly given by Jeannette Adu-Bobie. The presence of *espW* was verified by PCR. All *espW* negative strains were further screened for the presence of the truncated version of the gene containing the first 206 amino acids at the N terminus. The *espW* gene was present in 68 out of 132 EPEC strains screened; Furthermore 10 out of the 64 PCR negative strains (O26:H-(1); O55:H-(5) AND O55:H7(4)) were *espW*$_{1-206}$ positive. The following strains were *espW* and *espW*$_{1-206}$ negative: O2:H49(1), O6:H19(2), O45:H-(1); O85:H-(1) and O118:H5(2).

3.2 Kif15 identified as putative binding partner for EspW

3.2.1 A Yeast-2-Hybrid Screen identified Kif15 and RHAMM as interacting partners of EspW

Identifying binding partners of EspW would give important information about its mechanism of action and so a Yeast-2-Hybrid (Y2H) screen was used to identify interacting host cell proteins. EHEC EspW was fused to the GAL4 binding domain in a pGBKT7 and

pGBT9 vectors and transformed into *S. cerevisiae* AH109 strain. This construct was used as bait against a Human Normalised cDNA library pre-transformed into *S. cerevisiae* Y187 (Clonetech). The interaction between bait and prey proteins will result in the activation and transcription of four reporter genes ADE2, HIS3, MEL1 and LacZ and expression of the essential amino acids adenine (Ade), histidine (His) and of α-galactosidase and ß-galactosidase. The α-galactosidase reacts with the chromogenic substrate provided by the X-α-Gal supplemented in the agar media resulting in a blue coloration of the mated colonies.

The autoactivation tests performed in order to test for the ability of pGBKT7-EspW and pGBT9-EspW to activate the reporter genes in the absence of a prey protein were negative (data not shown). Cytotoxicity tests were performed in order to determine if the pGBKT7-EspW and pGBT9-EspW constructs were toxic for *S. cerevisiae* AH109 strain compared to the empty pGBKT7 and pGBT9 vectors. Growth curves were obtained over 12 h period for AH109-pGBKT7-EspW, AH109-pGBKT7, AH109-pGBT9-EspW and AH109-pGBT9 grown in YPDA medium lacking the amino acid Tryptophan (Trp). As shown in Figure 3.4, the growth rate of AH109-pGBKT7-EspW clones was reduced comparing to the AH109-pGBKT7, showing that the pGBKT7-EspW was toxic to AH109. In contrast, the pGBT9-EspW was not toxic and the growth curves were similar to AH109-pGBT9. The mating efficiency was more than 3% for both constructs.

As pGBT9 was not toxic, AH109 yeast strains transformed with pGBT9-EspW were mated to with a Human Normalised cDNA library (Clonetech) and the mated colonies were plated onto a medium stringency triple dropout and X-α-Gal selective medium that selected for the presence of bait plasmid (-Trp), prey plasmid (-Leu) and two specific markers for interaction (-His and the colorimetric MEL1 reporter for X-α-Gal).

The Y2H resulted in 83 blue colonies and 59 white colonies; however re-streaking (three times on QDO media which adds a third reporter –Ade, in addition to –His and MEL1) reduced the number of positive clones to 72. All the 72 clones were positive when screened for the presence of pGAD plasmid by colony PCR (using primers shown in Table 2.2). The possible interaction partners were identified after sequencing using the T7 promoter primers. The results for the Hits are shown in Table 3.4. The highlighted hits Kif15 and RHAMM might be of interest as they relate to cytoskeleton dynamics

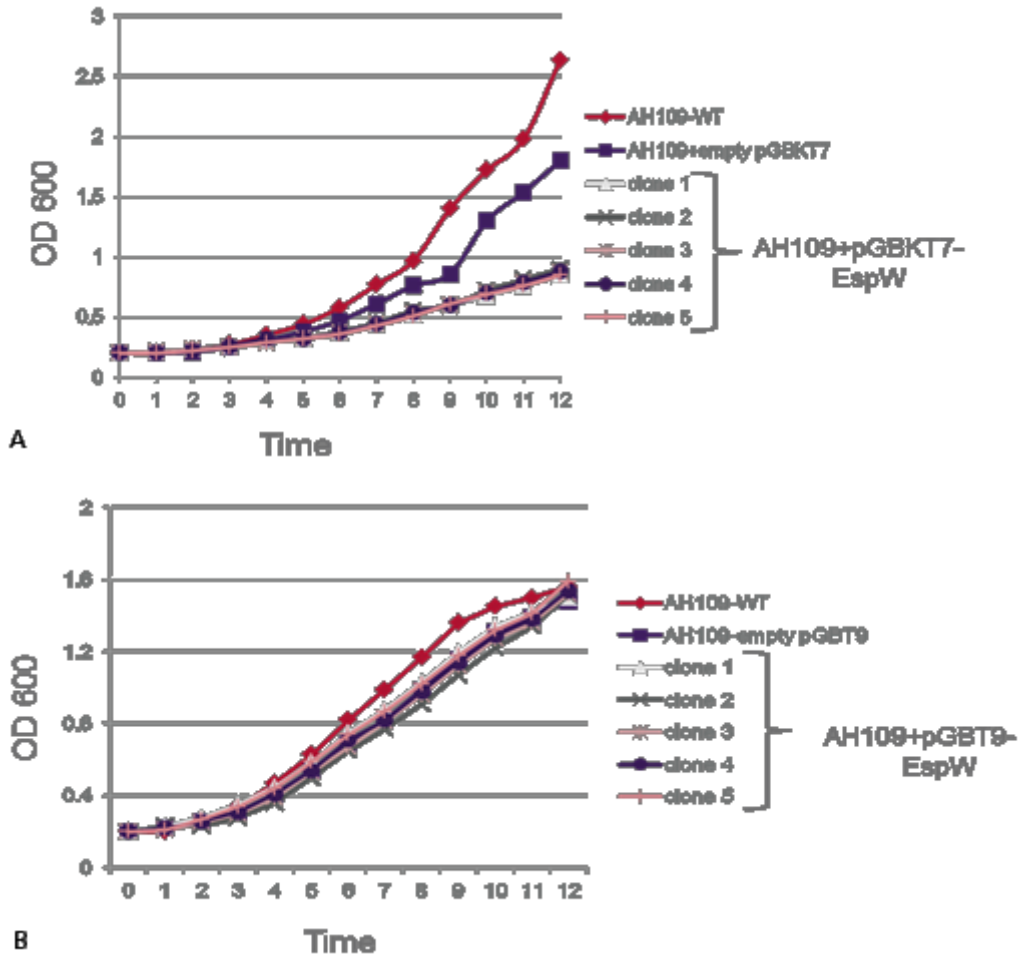

Figure 3.4 - Growth curves for cytotoxicity assay for AH109-pGBKT7-EspW, AH109-pGBT9-EspW and AH109-pGBT9

These constructs were grown in YPDA medium lacking the amino acid Tryptophan (Trp); growth kinetics was analysed by taking the OD_{600} every hour. There was a significan difference between the growth rate of AH109 expressing EspW in comparison to the AH109 transformed with empty pGBKT7 vector (A) The expression of EspW in AH109 was not toxic for pGBT9 (B)

Table 3.4 - Y2H positive clones sequences.
Positive clones were confirmed for the presence of pGAD plasmid using AD-LD FW/RV primers and sequenced using the T7 promoter. A blastx search was conducted to identify the sequenced targets. The highlighted hits might be of interest as they relate to microtubule dynamics.

Hit	Gene ID	Total hits
ATP synthase mitochondrial F1 complex assembly factor 1	64756 ATPAF1	46
Pan troglodytes aspartyl-tRNA synthetase	459634 DARS	3
Scm-like with four mbt domains 2, transcript variant 2	57713 SFMBT2	2
IMP2 inner mitochondrial membrane peptidase-like (*S. cerevisiae*), transcript variant 2	83943 IMMP2L	1
Interferon-induced protein with tetratricopeptide repeats 1, transcript variant 5	3434 IFIT1	1
TAF7 RNA polymerase II, TATA box binding protein (TBP)-associated factor, 55kDa	6879 TAF7	2
Kinesin family member 15	56992 KIF15	3
Hyaluronan-mediated motility receptor (RHAMM), transcript variant 3	3161 HMMR	4
no significant similarity found		10

3.2.2 Kif15 was confirmed as putative interaction partner of EspW by Direct Y2H screen

The pGAD-T7-AD-Kif15 and pGAD-T7-AD-RHAMM constructs containing the Y2H Kif15 and RHAMM clones were directly transformed into AH109 with pGBT9-EspW. The results showed that only the transformants containing Kif15 with EspW grew on QDO, confirming protein interaction . The transformants containing RHAMM with EspW did not grow and we concluded that RHAMM is a false positive (Figure 3.5 - A).

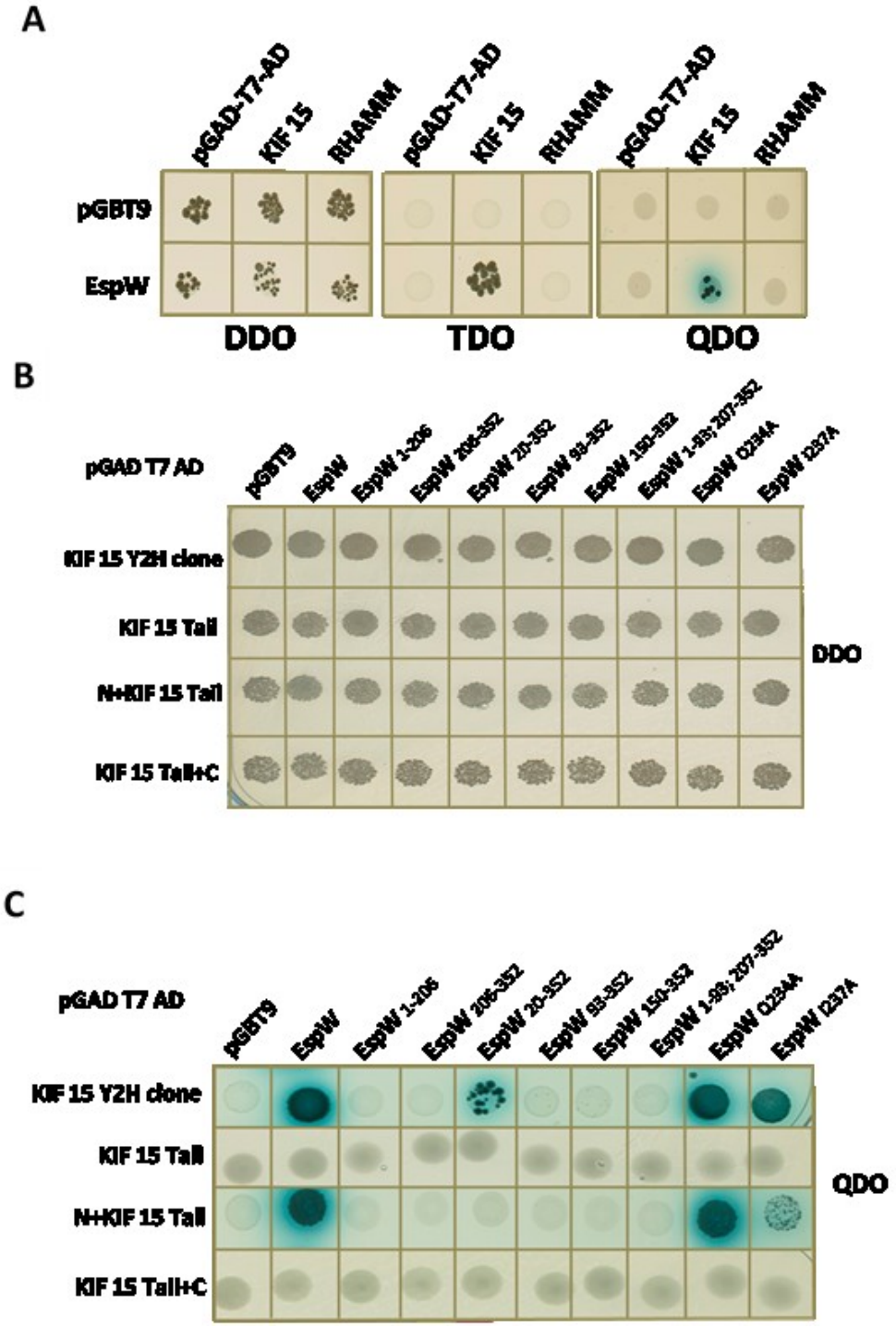

Figure 3.5 - Direct yeast-two hybrid analysis

S. cereviseae AH109 was co-transformed with pGBT9 and PGAD-T7-AD vectors either encoding test proteins or as empty vector controls and grown on DDO, TDO and QDO drop out minimal media was assessed. **A** - EspW and interacts with Kif15 but not with RHAMM Y2H clones. **B** – Colonies growth on DDO plates; **C** - Colonies growth on QDO plates: $Kif15_{1092-1368}$ (Kif15 Y2H) clone interacts with EspW, $EspW_{1-206}$, $EspW_{Q234A}$, $EspW_{I237A}$ and $EspW_{20-352}$, but not with $EspW_{206-352}$, $EspW_{93-352}$ and $EspW_{1-93;207-352}$; $Kif15_{1092–1142}$ (Kif15-N) is essential for the interaction between EspW and Kif15. EspW interacts with $Kif15_{1092–1347}$ (Kif15-N+Tail) and $Kif15_{1092–1142}$ (Kif15-N) only, but not with $Kif15_{1142-1347}$ (Kif15-Tail) and $Kif15_{1142–1368}$ (Kif15-Tail+C).

3.2.3 **EspW interacts with the C-terminus of Kif15**

The Kif15 Y2H clone identified contained aa $Kif15_{1092-1368}$ which represents C-terminal portion of the human Kif15 full length protein. In order to narrow down the putative binding domain of EspW to Kif15, further direct Y2H experiments were performed using various truncations of EspW (Figure 3.6 B) as bait together with PGAD-T7-AD- $Kif15_{1092-1368}$ (Y2H clone) and PGAD-T7-AD-$Kif15_{1142-1347}$ (Kif15-Tail) as bait. The PGAD-T7-AD-$Kif15_{1142-1347}$ vector was constructed using $Kif15_{1092-1368}$ amplified from $Kif15_{1092-1368}$ (Kif15 Y2H clone). Truncations were designed based on the EspW and Kif15 secondary structure predictions using Phyre2 software. Importantly, $Kif15_{1092-1368}$ interacted with the long version of EspW (Figure 3.5) but not with $EspW_{1-206}$. To further map the binding site of EspW to Kif15, a set of Kif15 truncation has been generated and tested by DY2H (Figure 3.5). An empty pGAD-T7 plasmid was used as a negative control. No growth was observed on selected media (QDO) when yeast were co-transformed with EspW and $Kif15_{1142-1347}$, $Kif15_{1142-1368}$ or with the negative control; in contrast, growth was seen following co-transformation with EspW and $Kif15_{1092-1347}$ or $Kif15_{1092-1142}$ (Fig. Figure 3.5 C), suggesting that the C-terminus of the coil-coil domain of the Kif15 plays an important role in the interaction with EspW.

We further showed that Kif15 binds $EspW_{Q234A}$, $EspW_{I237A}$ and $EspW_{20-352}$, therefore protein interaction is not affected after removal of the first 20 amino acids of EspW or after point mutations in Q234A and I237A. These point mutations will become more relevant later in the study.

The fact that $EspW_{1-206,}$ $EspW_{206-352,}$ $EspW_{93-352}$ and $EspW_{1-93;207-352}$ transformants did not bind with Kif15 might suggest that these truncations could affect the protein fold, and in this way the interaction is impeded.

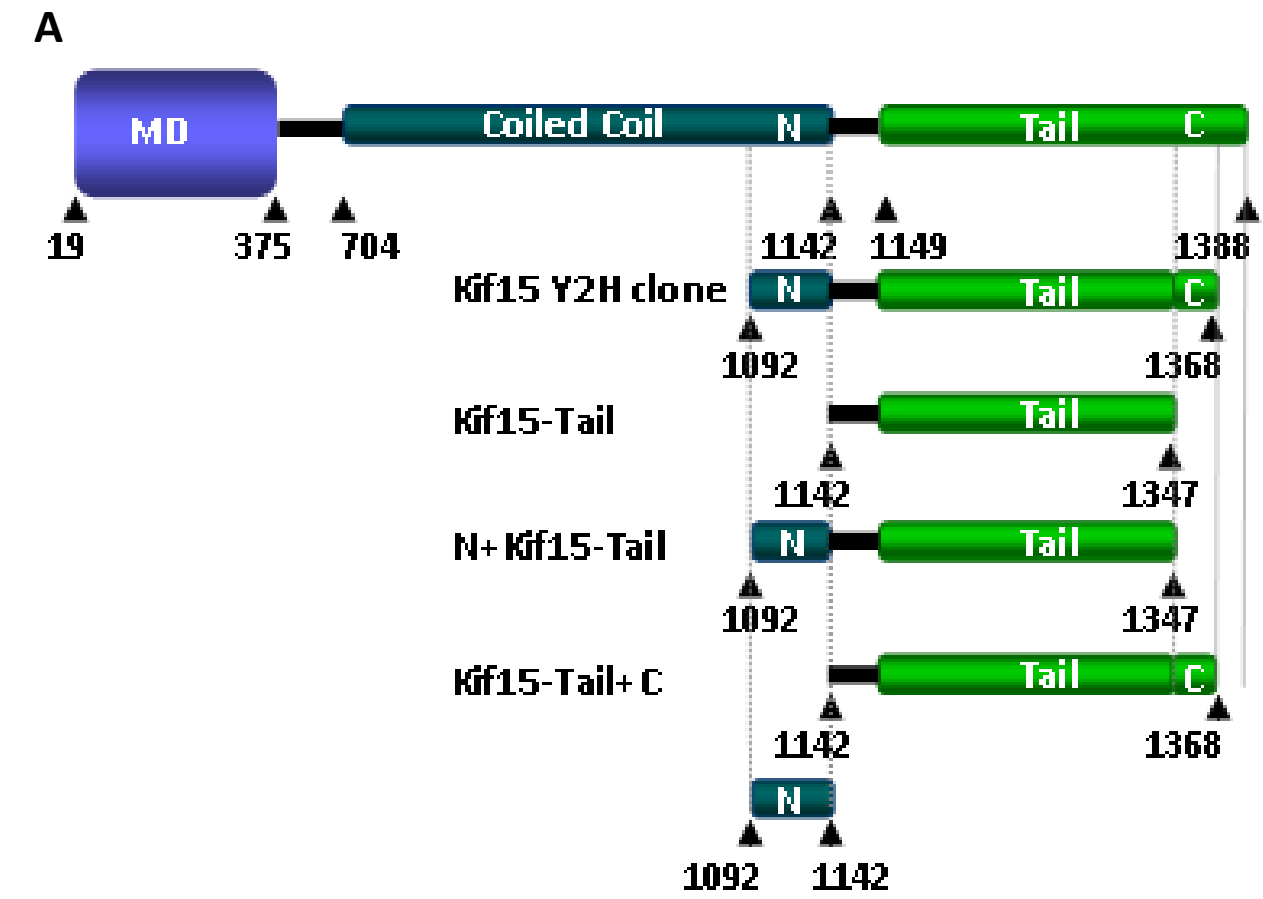
A
MD
Coiled Coil
N
Tail
C
19
375
704
1142
1149
1388
Kif15 Y2H clone
1092
1368
Kif15-Tail
1142
1347
N+ Kif15-Tail
1092
1347
Kif15-Tail+ C
1142
1368
1092
1142

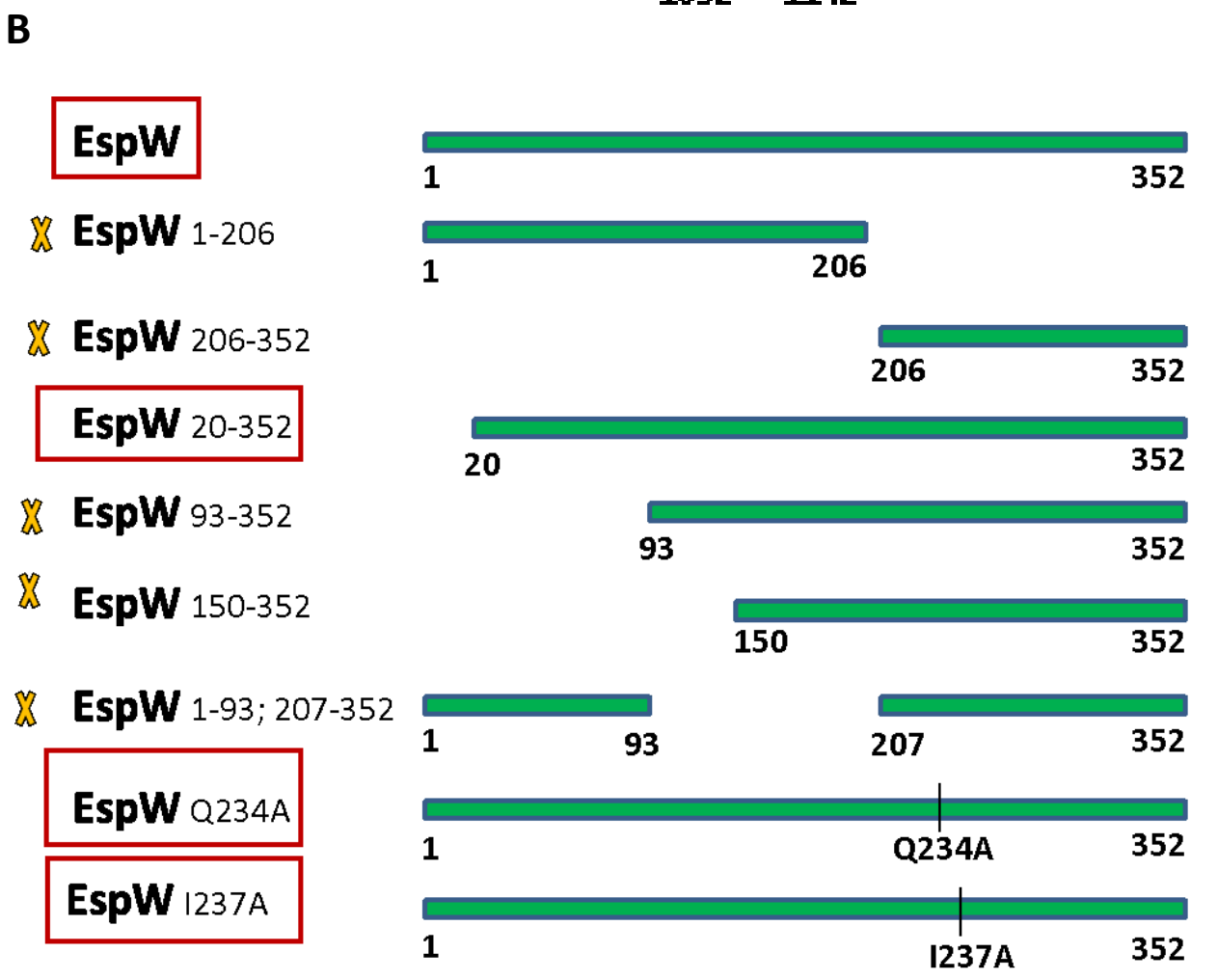
B
EspW
1
352
EspW 1-206
1
206
EspW 206-352
206
352
EspW 20-352
20
352
EspW 93-352
93
352
EspW 150-352
150
352
EspW 1-93; 207-352
1
93
207
352
EspW Q234A
1
Q234A
352
EspW I237A
1
I237A
352

Figure 3.6 - Schematic representation of Kif15 and EspW
A- Kif15 and of the subsequent clones we used to identify its binding domain with EspW: $Kif15_{1092\text{-}1368}$ (Kif15-Y2H clone), $Kif15_{1142\text{-}1347}$ (Kif15-Tail), $Kif15_{1092–1347}$ (Kif15-N+Tail), $Kif15_{1142–1368}$ (Kif15-Tail+C) and $Kif15_{1092–1142}$ (Kif15-N). Direct Y2H: *kif15* genes were cloned in yeast expression vector pGAD-T7 and the *espW* genes were cloned in pGBT9.
B - Schematic representation of protein truncations used to identify the EspW putative binding domain with Kif15. EspW truncated proteins in the red square interacted with Kif15, whereas the ones marked by yellow cross did not.

3.2.4 **Upon transfection, Kif15 colocalizes with EspW**

As we showed previously by DY2H that $Kif15_{1092\text{-}1368}$ (Kif15-Y2H) interacts with EspW We next aimed to determine if Kif15 and EspW co-localized. For this, we first tried to HA-tag EspW in EHEC, however, no signal could be detected by immunofluorescence (results provided later in the manuscript). Therefore we co-transfected cells with pRK5-HA-*espW* and pRK5-Myc-$Kif15_{1092\text{-}1368}$. pRK5-HA-*mCherry* was used as a negative control. Whereas no co-localization was observed between mCherry and Kif15, EspW and Kif15 co-localized (Figure 3.7). Interestingly, EspW and Kif15 are also present at membrane site showing actin reorganisation.

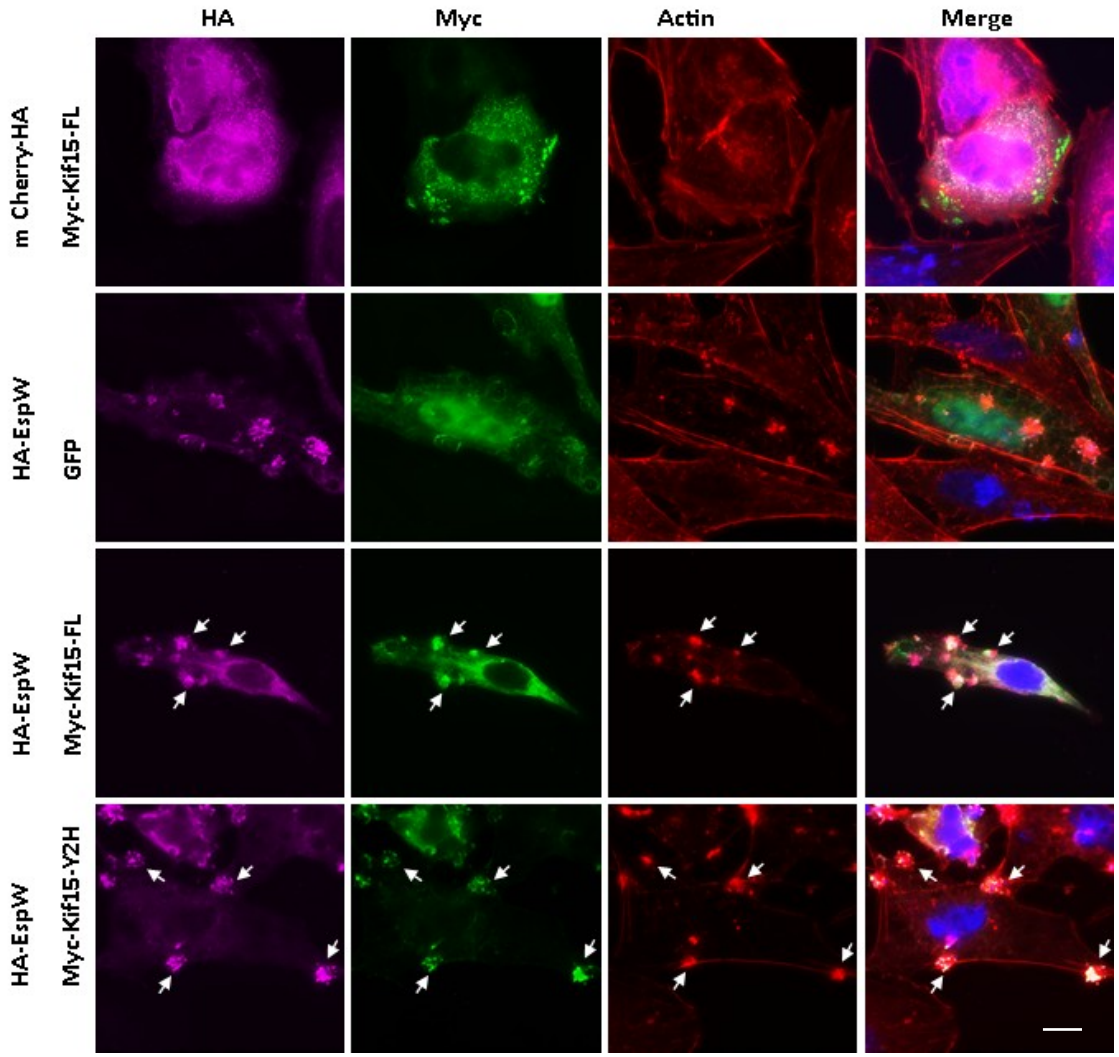

Figure 3.7 - Upon transfection Kif15 colocalises with EspW

Colocalization shown with white arrows. Swiss cells were co-transfected with myc-Kif15 and HA-EspW for 24 h. Co-transfection with myc-Kif15 and HA-mCherry was used as control. Immunofluorescence staining: anti-HA antibody (magneta), anti-myc antibody (green), actin with TRITC-phalloidin (red) and nuclei were stained with DAPI (blue). Bar = 5 µm.

3.2.5 **Kif15$_{1092\text{-}1368}$, localises at the actin pedestals induced by EHEC infection**

We showed previously (Figure 3.7) that upon cotransfection with EspW, full length Kif15 and Kif15$_{1092\text{-}1368}$ (Kif15-Y2H) is present at the actin rearrangement sites. We wanted to determine whether or not upon transfection Kif15 and Kif15$_{1092\text{-}1368}$ (Kif15-Y2H) are present at actin pedestals induced by EHEC infection. We transfected Swiss 3T3 cell lines with mammalian transfection vectors pRK5-Myc-Kif15 and pRK5-Myc-Kif15$_{1092\text{-}1368}$ (Kif15-Y2H) for 24 h and infect the transfected cells for 3 h with WT EHEC. As shown in Figure 3.8, Kif15$_{1092\text{-}1368}$ (Kif15-Y2H) colocalises with actin pedestals; however this was not the case with full length Kif15 and in control pRK5-Myc-GFP transfected cells that were infected with WT EHEC. This was due to the fact that Kif15 is a large protein (160 kDa) and the transfection efficiency of full length Kif15 was too low (data not shown).

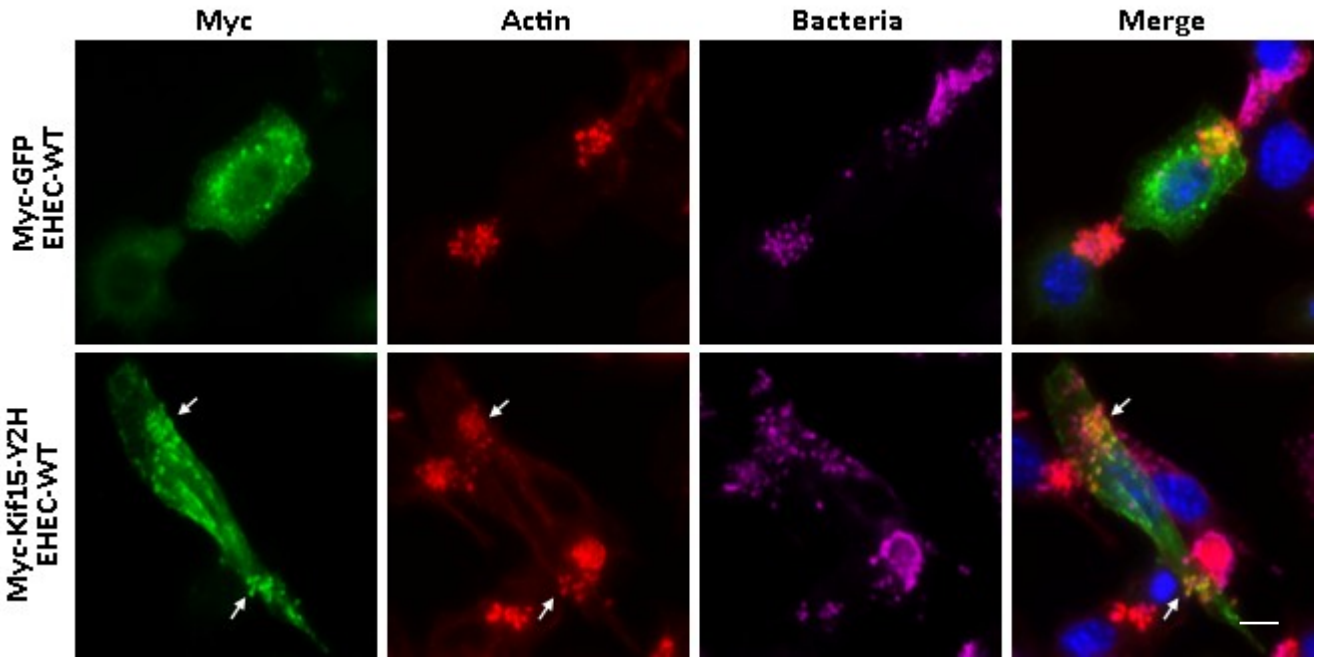

Figure 3.8 - Ectopically expressed Kif15 localised at the pedestals upon EHEC infection
Transfection of Kif15 followed by infection with EHEC in Swiss cells (colocalization shown with white arrows). Immunofluorescence microscopy of Swiss 3T3 cells transfected with myc-Kif15-Y2H clone and infected with WT EHEC for 3 h. Bacteria was visualised with anti-E85/170 antibody (magneta), myc-Kif15-Y2H with anti-myc antibody (green), actin was detected with TRITC-Phalloidin (red) and nuclei were stained with DAPI (blue). Myc-GFP was used as control. Bar = 5 µm.

3.3 Ectopic expression of EspW in eukaryotic cells

3.3.1 EspW triggers membrane ruffles formation and actin remodelling

In order to determine the role of EspW is Swiss cells were transfected with pRK5-HA-*espW*, pRK5-HA-*espW*$_{1\text{-}206}$, or pRK5 encoding HA-GFP as a control, for 24 h. IF straining revealed that the full length EspW triggered formation of membrane ruffles and flower-shaped structure, which were rich in actin and co-localized with EspW. EspW$_{1\text{-}206}$ showed aggregative localisation dispersed within the cell with an actin structure similar to those

seen in the GFP control cells (Figure 3.9).

However it was difficult to determine if this rearrangement is inside or outside the transfected cells. In order to analyse any structural changes on the surface we processed EspW transfected cells for scanning electron microscopy (SEM). SEM images revealed flower like structures on the cell surface of pRK5-HA-*espW* transfected cells which is likely to correspond to the actin rearrangement observed by immunofluorescence (Figure 3.9). The cells transfected with $EspW_{1-206}$ did not reveal any noteworthy surface structures when compared with the negative control. These results showed that EspW can induce actin remodelling and the formation of actin rich structures at the cell surface.

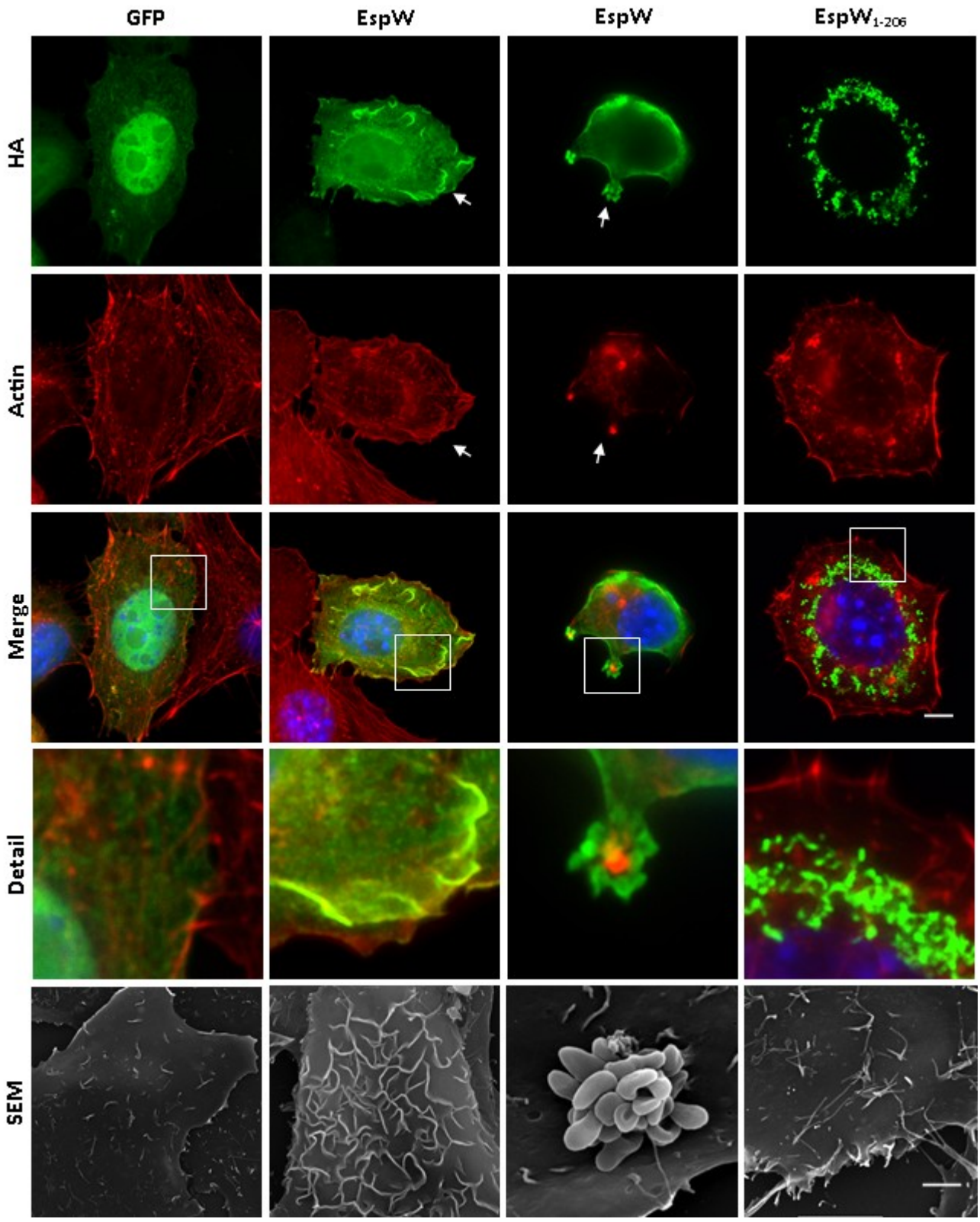
GFP
EspW
EspW
EspW1-206
HA
Actin
Merge
Detail
SEM

Figure 3.9 - Ectopic expression of EspW in Swiss 3T3 cells
EspW induces actin rearrangement upon transfection; furthermore EspW colocalises with actin
Immunofluorescence microscopy of Swiss 3T3 cells transfected with HA-GFP, HA-EspW and HA-$EspW_{1-206}$ for 24 h. HA-tagged proteins were visualised with anti-HA antibody (green), actin with TRITC-phalloidin (red) and nuclei were stained with DAPI (blue). Ectopic expression of EspW, but not $EspW_{1-206}$ and GFP induced membrane ruffles and actin rearrangement resembling a flower like structure. Upon transfection EspW colocalises with actin (white arrows). $EspW_{1-206}$ localisation was dispersed within the cell.
Scanning electron microscopy (SEM) of Swiss 3T3 cells transfected with HA-GFP, HA-EspW and HA-$EspW_{1-206}$ for 24 h. Cells transfected with HA-EspW presented membrane ruffles and membrane remodelling in a flower like pattern resembling the structure of HA-EspW transfected cells observed by immunofluorescence. There were no patterns observed on the surface of the cells transfected with HA-GFPand HA-$EspW_{1-206}$ Bar = 5 µm.

3.3.2 **EspW does not colocalise with microtubules**

We identified by Y2H that Kif15 is the putative binding partner of EspW. Previous studies showed that Kif15 is a motor protein that associates with microtubules in order to transport molecules in eukaryotic cells. Furthermore in dividing eukaryotic cells, it promotes spindle assembly by cross-linking and sliding along microtubules creating a separation between centrosomes (Buster et al., 2003).

To evaluate whether or not EspW transfection results in microtubule rearrangement (along with actin) the same transfection assays (as described previously) were performed and stained for tubulin instead of actin. We also wanted to investigate where the microtubules are localised in relation to the 'flower' actin phenotype observed by IF. There was no difference in tubulin IF staining in EspW transfected cells when compared to the negative control and there was no colocalisation of EspW and tubulin staining. We concluded that the 'flower like' actin structure phenotype was not a consequence of microtubule rearrangement, confirming that EspW is involved in the actin pathway. (Figure 3.10).

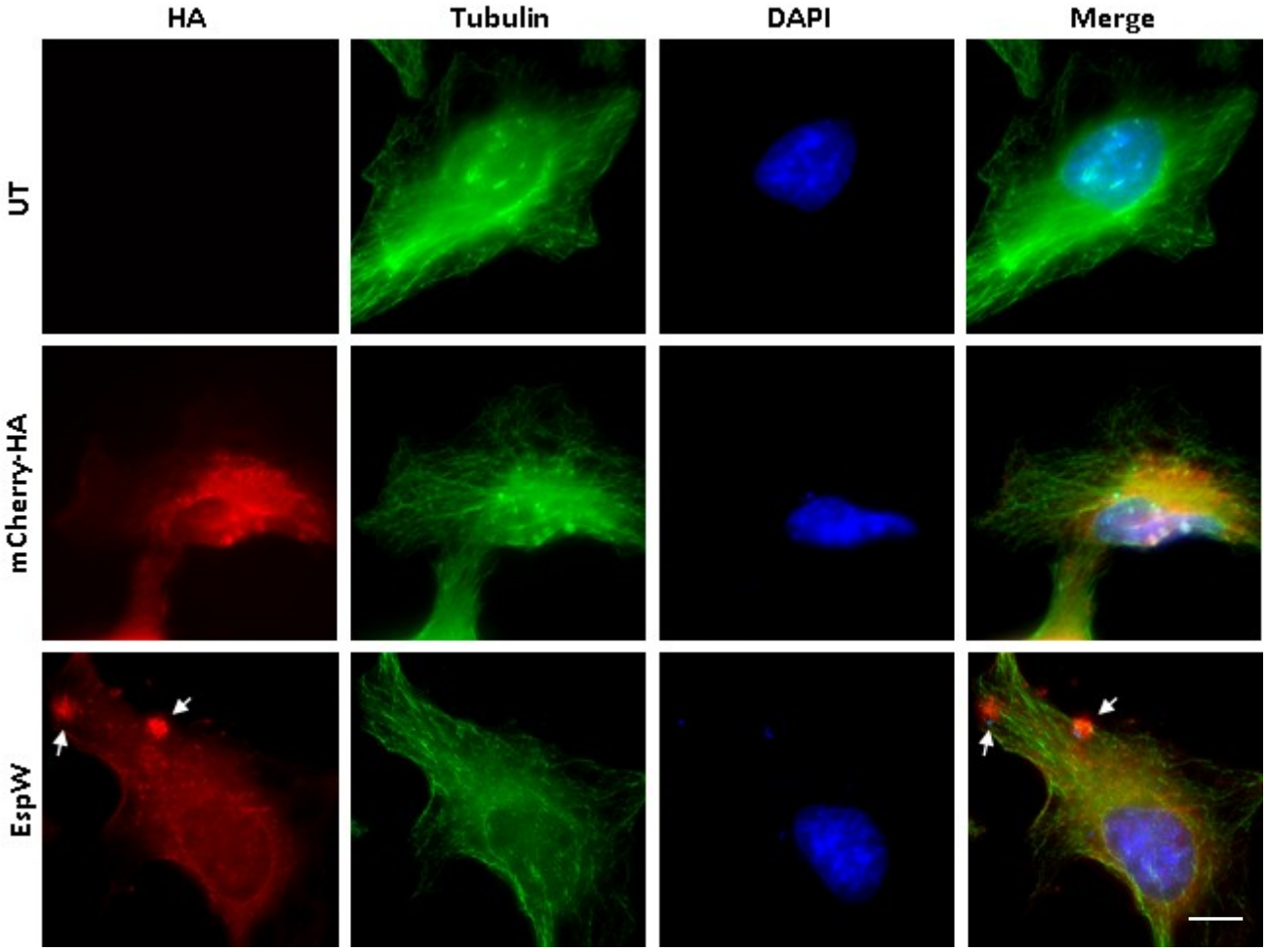

Figure 3.10 - Tubulin staining of Swiss 3T3 cells upon overexpression of EspW
Swiss 3T3 cells were transfected with HA-GFP, HA-EspW for 24 h. pRK5-mCherry-HA was used as negative control. HA-tagged proteins were visualised with anti-HA antibody (red), tubulin with anti-tubulin (green and nuclei were stained with DAPI (blue). EspW showed granulated staining resembling the actin 'flower' like phenotype (white arrows); however there were no modifications in microtubule structures when compared to the negative control Bar = 5 µm.

3.3.3 **Actin remodelling requires Rac1**

We have shown that EspW might be involved in an actin signalling pathway. As Rho GTPases such as Rac1, RhoA and Cdc42 are key regulators of actin and cytoskeleton

dynamics we investigated whether any of these small Rho GTPases regulate the actin pathway in which EspW might be involved. We performed cotransfection experiments using pRK5-HA-*espW* with dominant negative $Rac1^{N17}$, $RhoA^{N19}$ and $Cdc42^{N17}$. The dominant-negative Rho-GTPases contain a substitution mutation that allows them to bind to their GEFs but inhibits downstream interactions with their effector proteins, therefore titrating out the GEFs that bind to the native Rho GTPase.

The co-transfected cells were assessed by IF for the presence of actin-rich flower shaped structures. This revealed that inactivation of either RhoA or Cdc42 had no effect on the ability of EspW to induce actin reorganisation (Figure 3.11). In contrast, inhibition of Rac1 significantly compromised the ability of EspW to induce actin rearrangements (Figure 3.11). Overall, where present, the size of the actin flower pattern was similar in all transfected cells. We concluded that EspW might be involved in an actin rearrangement pathway regulated by Rac1.

A

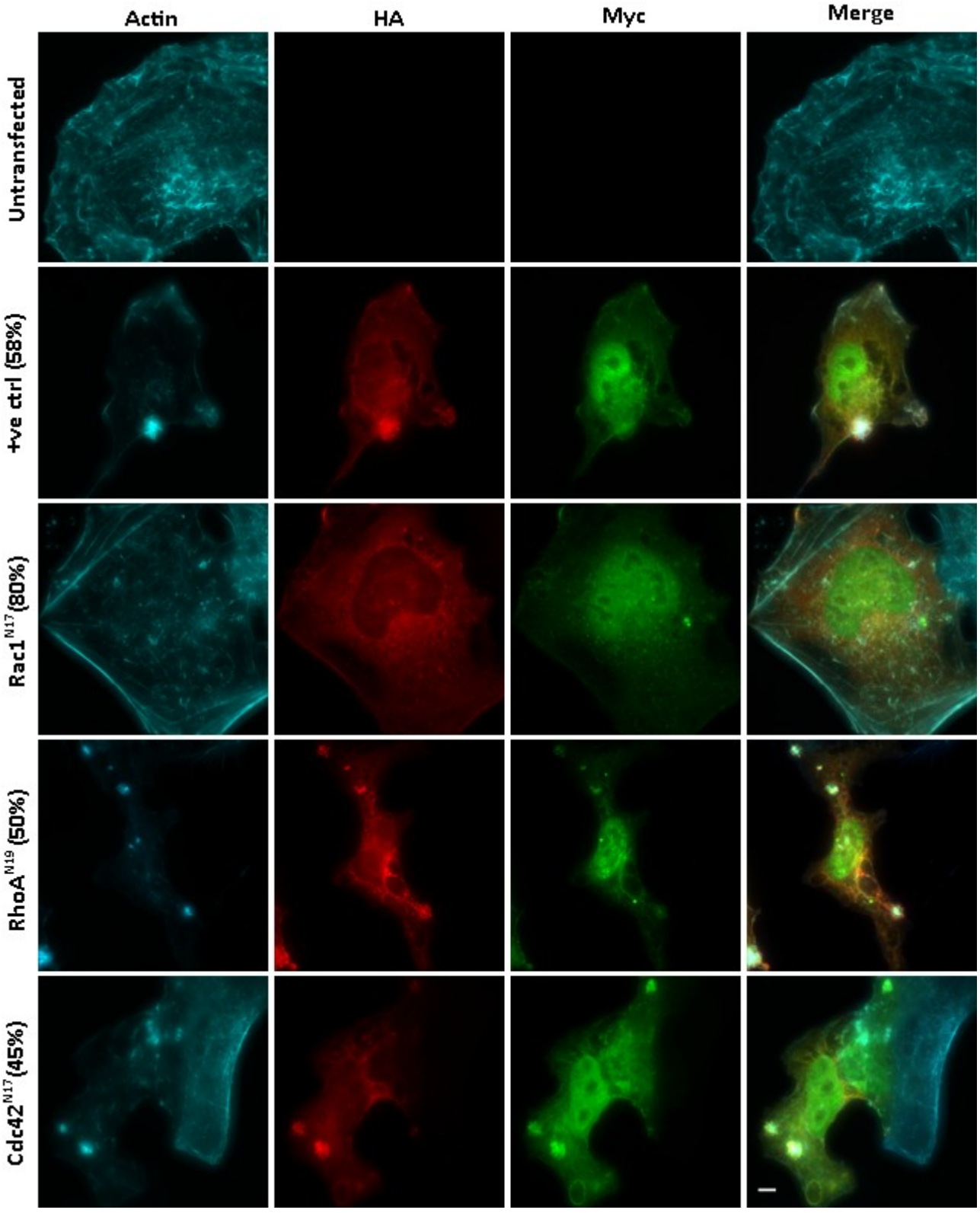
Actin
HA
Myc
Merge
Untransfected
+ve ctrl (58%)
Rac1N17 (80%)
RhoAN19 (50%)
Cdc42N17 (45%)

B

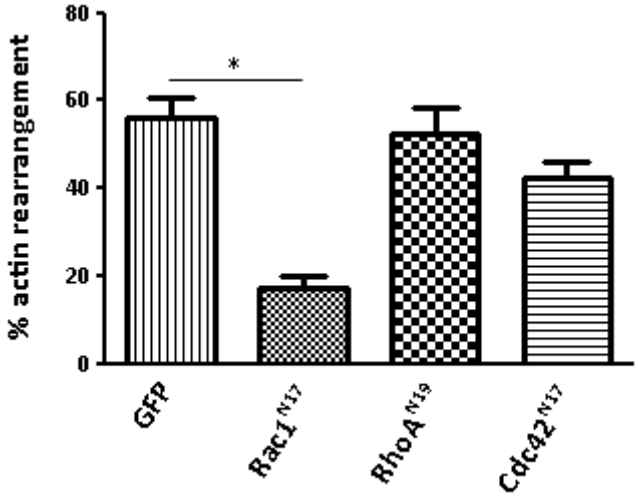

Figure 3.11 - The actin 'flower like' phenotype is Rac1 dependant
A - HeLa cells were co-transfected with dominant negative GTPases and EspW for 24 h. Co-transfection with EspW and GFP was used as a positive control. Actin was stained with AMCA 350 (cyan), the myc-tagged GTPases with mouse anti-myc (green) and HA-tagged EspW with anti-HA antibody (red). Flower like actin structures that co-localises with EspW were observed in the positive control and in the cells co-transfected with EspW and $Cdc42^{N17}$ and $RhoA^{N19}$. In contrast, co-transfection of EspW with $Rac1^{N17}$ inhibited the formation of flowers Bar = 5 µm.
B - Quantification of the percentage of co-transfected HeLa cells with actin flower like structure. The percentage was calculated out of one hundred transfected cells in triplicate from three independent experiments. Results are presented as means ± SD. The formation of actin flower like structures is affected by expression of $Rac1^{N17}$, but not by expression of $Cdc42^{N17}$ or $Rac1^{N17}$

3.3.4 **RhoGTPase Biosensors assays**

To investigate whether or not EspW activates Rac1, a RhoGTPase Biosensors assay was adapted. Previously this method has been used to visualise protein interaction in living cells. It uses the BiFC (biomolecular fluorescence complementation) technique whereby two different plasmid (containing two fragments of a fluorescent protein (e.g GFP)) are brought together by an interaction between two proteins that are each encoded on one of the pBiFC

plasmids (Figure 3.12). This would allow the visualisation of the subcellular location of specific cellular interaction in the normal cellular environment such as the activation of Rac1. As the CRIB (Cdc42/Rac1 interacting binding) domain of PAK is known to bind specifically to the effector region of active GTP-bound Rac1 and Cdc42 the aim was to cotransfect cells overexpressing EspW with BiFC constructs and check whether or not the levels of active Rac1 in the cells will be significantly increased when compared to cells that were previously transfected with a negative control. To validate this assay control test were performed where Swiss cells were cotransfected with pBiFC-VN173-Crib of PAK and pBiFC-VC155-$Rac1_{T17N}$ as negative control and pBiFC-VN173-Crib of PAK with pBiFC-VC155-$Rac1_{Q61L}$ as positive control (Figure 3.12 A). In the case of the negative control the $Rac1_{T17N}$ mutant was not expected to interact with the Crib of PAK domain and therefore no fluorescence should be observed. Unfortunately both negative and positive control showed fluorescence by IF which suggests that the negative control was not suitable for this assay (Figure 3.12 B). This might be due to the fact that the Crib of PAK fragment was too short (only 14 aa in length) and therefore the N-GFP and GFP-C from the two plasmid constructs used in this assay were in close proximity at all times and resulted in their interaction and fluorescence emission. These results were taken into consideration and the experiment was repeated using the pBiFC-VN173 vector overexpressing PAK1 which is 562 aa in length (Figure 3.13 A). Unfortunately there was still fluorescence present in more than 20% of the cotransfected cells with the negative control and we concluded that this assay was also not suitable to use for our purpose (Figure 3.13 B).

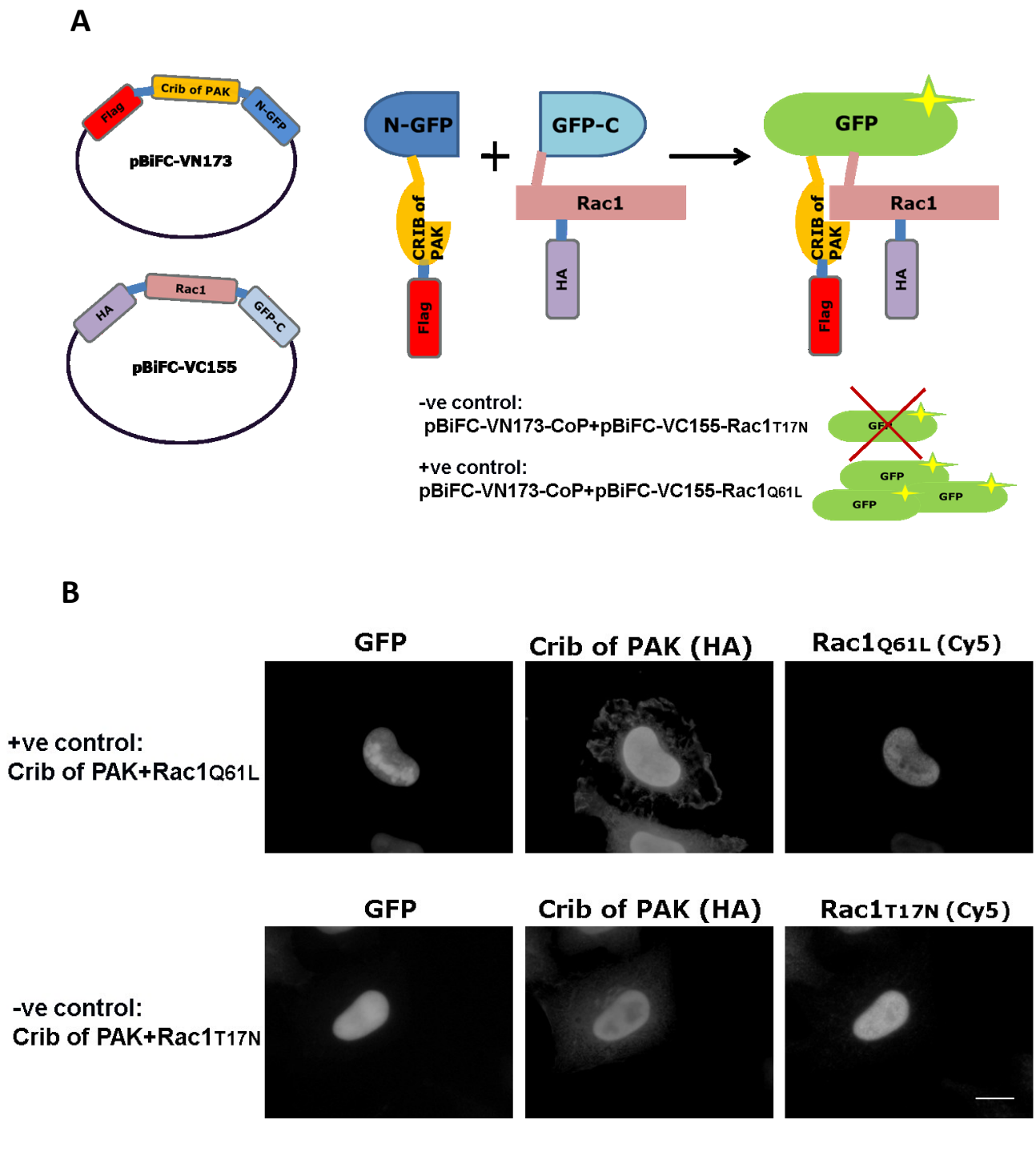

Figure 3.12 - BiFC assay using Crib of PAK.

A - Schematic representation of pBiFC constructs. **B** - Swiss cells were cotransfected with pBiFC-VN173-Crib of PAK and pBiFC-VC155-Rac1$_{T17N}$ as negative control and pBiFC-VN173-Crib of PAK with pBiFC-VC155-Rac1$_{Q61}$L as positive control. HA-tagged EspW was stained with anti-HA antibody and Flag tagged Rac1Q61L and Rac1T17N with anti-Flag antibody. The results showed GFP fluorescence in both negative and positive controls Bar = 5 µm.

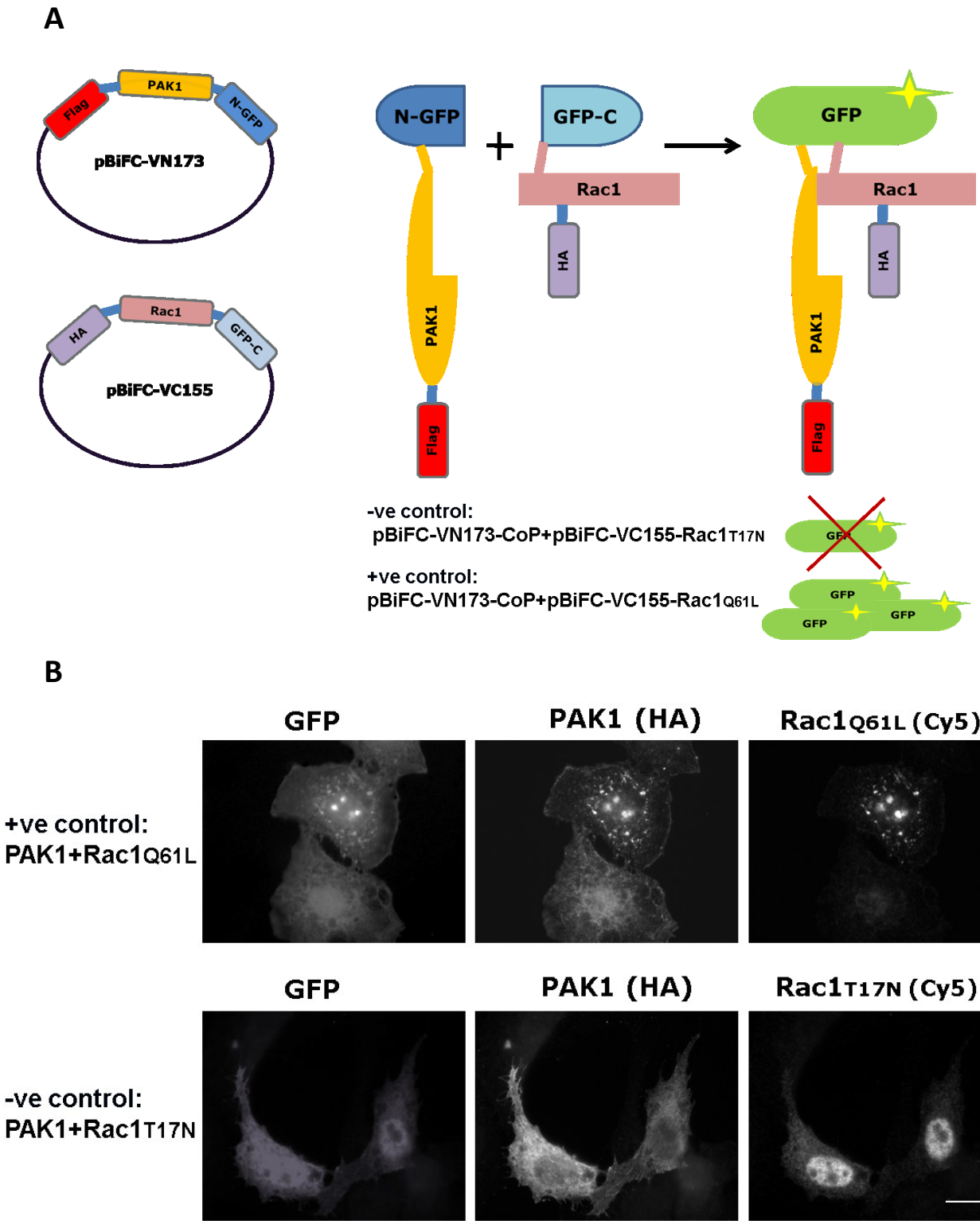

Figure 3.13 - BiFC assay using PAK1

A - Schematic representation of BiFC constructs (biomolecular fluorescence complementation). **B** - Swiss cells were cotransfected with pBiFC-VN173-PAK1 and pBiFC-VC155-Rac1$_{T17N}$ as negative control and pBiFC-VN173-Crib of PAK with pBiFC-VC155-Rac1$_{Q61L}$ as positive control. HA-tagged EspW was stained with anti-HA antibody and Flag-tagged Rac1$_{Q61L}$ and Rac1$_{T17N}$ with anti-Flag antibody. The results showed GFP fluorescence in both negative and positive controls Bar = 5 µm.

3.3.5 No actin 'flower like' structures were observed following ectopic expression EspW$_{I237A}$

We showed that Rac1 regulates the actin rearrangement upon EspW transfection and this could suggest that EspW is a GEF. Sequence analysis showed that the residue important for the actin rearrangement induced by bacterial GEFs EspM2 (EHEC), EspT (*C. rodentium*), IpgB2 (*Shigella flexneri*) may be present in EspW.

Previous studies showed that the glutamine (Q_{124}) and isoleucine (I_{127}) residues from the putative catalytic loop and flanking regions of the WxxxE protein EspM2 were important for its function (Arbeloa et al., 2010). As EspW appears to contain a similar QxSI motif, including residues Q_{234} and I_{237} (Figure 3.14 A), single mutation were generated and tested by DY2H for binding Kif15 (explained in Chapter 3.2.3, Figure 3.5 and Figure 3.6) and by transfection for actin reorganization. Whereas neither mutation affected the binding of EspW to Kif15 (DY2H) (Figure 3.5), EspW$_{I237A}$ did not induce any actin rearrangement (Figure 3.14 B). The fact that that EspW$_{I237A}$ does not induce actin rearrangements suggests that I_{237} residue is involved either directly in the protein function or is important for the integrity of the protein fold. In addition the localisation of EspW$_{I237A}$ differs considerably from the localisation of EspW, shown as small aggregates dispersed within the cell (Figure 3.14 B).

Taken together these results indicate that the conserved Isoleucine residue cannot be substituted with Alanine suggesting that it may play a role in maintaining the structure or function of EspW.

A

```
EspM2   96   MISKDFGIKLDARSAQSSINHIITGNGSFG
IpgB2   91   QVEKDYHISLDINAAQSSINHLVSGSSYFK
EspT    89   RASFHCGFSLDVRCAQTSTHHMILNSLYFQ
SifB   218   ENTNLKNAAFEPNYAQSSVTQIVYSCLFKN
EspW   234   ELGEYLYSGNVIKLSQLSIRYLPNISSISL
```

B

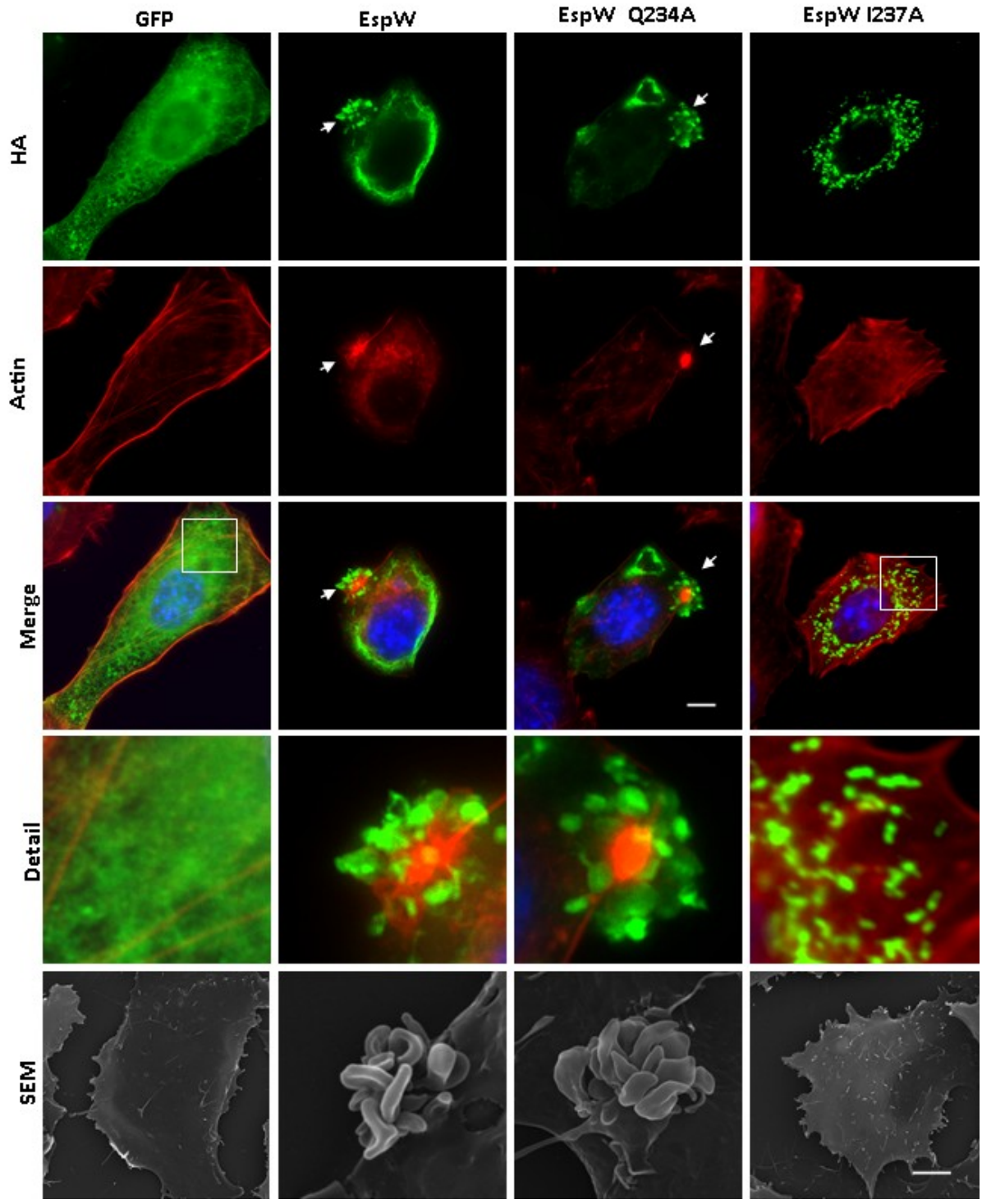

Figure 3.14 - EspW and the QxSI motif

A - Sequence alignment of the putative catalytic loop and flanking regions of the WxxxE proteins: IpgB2 from *Shigella flexneri*, SifB from Salmonella Typhimurium, EspM2 from EHEC O157:H7 Sakai and EspT from *C. rodentium*. EspW from EHEC O157:H7 85-170 shares similar residues Q234 and I237 highlighted in grey; in this study these residues were selected for mutagenesis**. B -** The effect of site-directed mutagenesis on actin flower formation Immunofluorescence microscopy of Swiss 3T3 cells transfected with pRK5 encoding HA-tagged GFP, EspW and derivative mutants $EspW_{Q234A}$ and $EspW_{I237A}$ for 24 h. HA-tagged proteins were visualised with anti-HA antibody (green), actin with TRITC-phalloidin (red) and nuclei were stained with DAPI (blue). Ectopic expression of EspW and $EspW_{Q234A}$ (results not shown) but not GFP and $EspW_{I237A}$ induced actin rearrangement resembling a flower like structure. Upon transfection with EspW and $EspW_{Q234A}$ colocalises with actin (white arrows). $EspW_{I237A}$ localisation is shown as agglomerates dispersed within the cell. Bar = 5 µm.

Scanning electron microscopy (SEM) of Swiss 3T3 cells transfected with HA-GFP, HA-EspW and HA-$EspW_{I237A}$ for 24 h. Cells transfected with EspW and $Espw_{Q237A}$ (results not shown) showed membrane remodelling in a flower like pattern resembling the images of EspW and $EspW_{Q234A}$ transfected cells observed by immunofluorescence. There were no patterns observed on the surface of the cells transfected with HA-GFP and $EspW_{I237A}$ Bar = 5 µm.

3.4 Localisation of EspW upon EPEC and EHEC infection

3.4.1 No phenotype observed after EPEC E69 overexpressing EspW infection in Swiss cells

An infection assay using EPEC E69 overexpressing EspW-2XHA was used to understand the role of EspW in infection. Recombinant EPEC/E69 WT and EPEC/E69 *ΔescN* were used to infect Swiss 3T3 as described in material and methods. EPEC/E69 *ΔescN* was used as negative control as the mutation in the *escN* gene results in the inability of the EPEC to translocate effector proteins. Actin staining presented no phenotypic modifications in terms of pedestals and cellular cytoskeleton and there was no HA signal detected for EspW localisation. As we were not able to detect any HA signal (Figure 3.15) we decided to repeat

this experiment with a new pSA10-espW construct with 4XHA tags (pSA10-espW-4XHA) in order increase sensitivity.

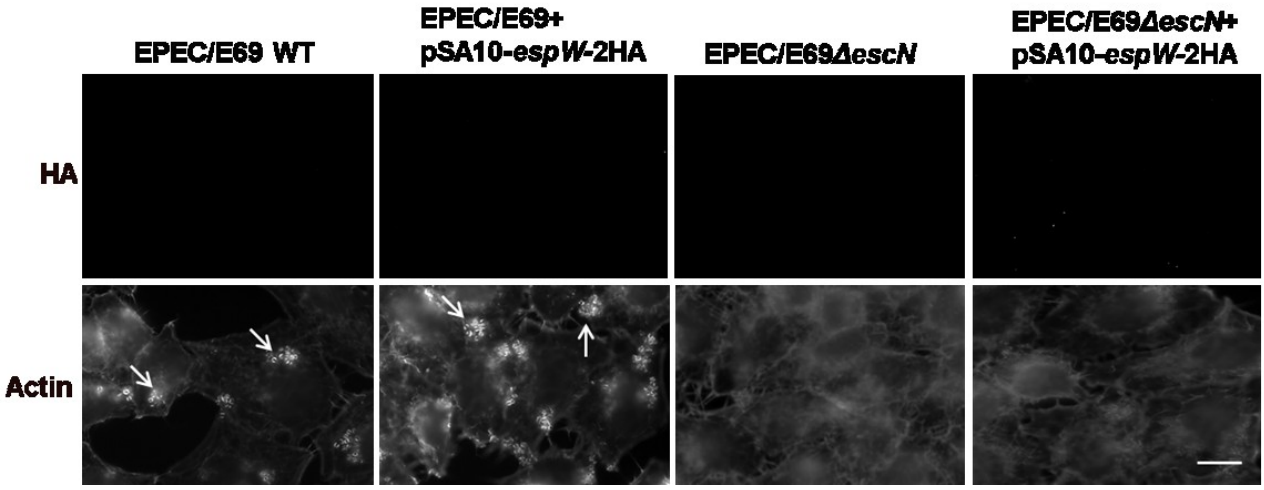

Figure 3.15 - IF of EPEC E69 overexpressing EspW-2XHA infection in Swiss cells
Swiss 3T3 cells infected with EPEC/E69 WT and EPEC/E69*ΔescN* with and without pSA10-*espW*-2XHA. The cells were induced 2.5 h post infection with 0.05 mM IPTG for 30 min. Coverslips were fixed and stained with anti-HA (green), TRITC for actin (red) and rabbit anti-E2348/69 antibody followed by anti-rabbit Cy5 conjugate (far red) for bacteria (not shown). EPEC/E69*ΔescN* and EPEC/E69*ΔescN* complemented with pSA10-2XHA-*espW* were used as negative control. The HA signal was not detected therefore we were not able to determine visually where EspW is found upon Swiss cells infection with EPEC/E69 WT and EPEC/E69*ΔescN* overexpressing EspW-2XHA. Actin pedestals marked with arrows. There was no pedestal formation observed in the cells infected with EPEC/E69*ΔescN* and complemented EPEC/E69*ΔescN* Bar = 5 µm.

We repeated the infection assay where EPEC/E69 and EPEC/E69 *ΔescN* strains were transformed with pSA10 plasmid allowing the expression of EspW fused to 4XHA tags. The immunofluorescence images showed that induction with IPTG was needed in order to visualise EspW; however EspW did not seem to be translocated but remained localised inside the bacteria. There is a common technical problem experienced in the laboratory where different effectors overexpressed using the pSA10 vector block the translocation of

other effectors needed for pedestal formation. It therefore seems reasonable that over-expression EspW effector protein would disrupt the translocation through this system and have implications during infection (Figure 3.16).

We concluded that the settings for the infection experiment were wrong and for future experiments we decided to use lower copy plasmids for expression of EspW-4XHA such as pACYC.

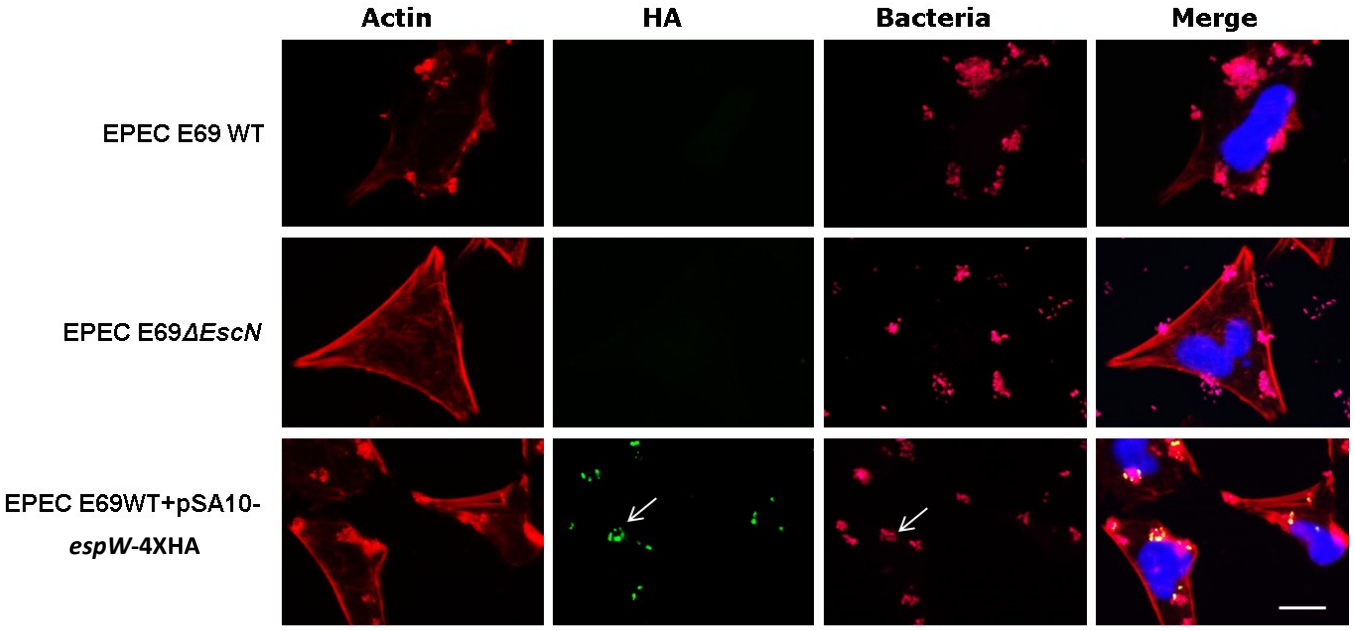

Figure 3.16 - IF of EPEC E69 overexpressing EspW-4XHA infection in Swiss cells
Representative images of HeLa ATCC cells infected with with EPEC/E69 WT and EPEC/E69 *ΔescN* with and without pSA10-*espW*-4XHA (IPTG 0.05mM). The cells were induced 2.5 h post infection with different concentration of IPTG (0.05 mM and 1 mM) for 30 min. Coverslips were fixed and stained with anti-HA (green), TRITC for actin (red), Phalloidin 350 AMCA (blue) for nuclei and rabbit anti-E2348/69 antibody followed by anti-rabbit Cy5 conjugate (far red) for bacteria. Immunofluorescence staining showed that EspW was not translocated as it was localised inside bacteria (white arrows) Bar = 5 µm.

3.4.2 No difference in pedestals formation and cellular actin cytoskeleton upon EHEC and EPEC infection in Swiss cells

We previously showed that after infection of Swiss cells with EPEC/E69 overexpressing EspW-4XHA, EspW was localised inside the bacteria.

We concluded that the settings for the infection assay were wrong and we repeated the experiment using a lower copy number plasmid for expression of EspW such as pACYC in two cell lines HeLa and Swiss 3T3. We investigated the effects of EPEC/E69 and EHEC 85-170 infection in both Swiss 3T3 and HeLa cell in different conditions outlined in Figure 3.17 in order to detect actin cytoskeleton modifications (in early or late infection). We thought that the HA tag could interfere with the function of EspW so we performed these infection experiments after removing the HA tag and looked at the effects on actin cytoskeleton. No morphology difference between the pedestal and actin cytoskeleton induced by EPEC E69, EHEC 85-170 strains overexpressing EspW was observed when compared to the negative control (Figure 3.18).

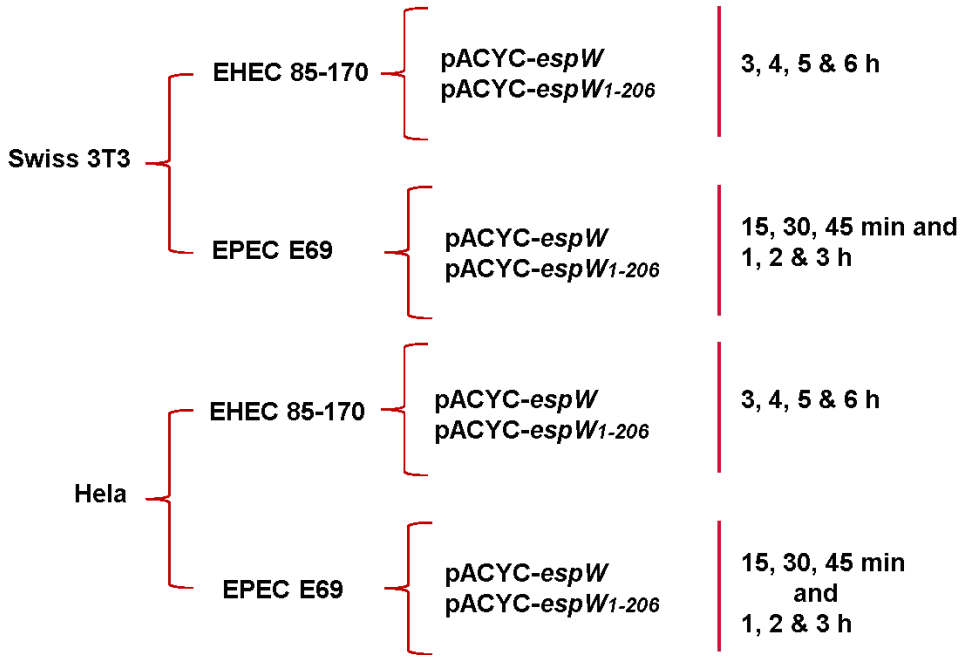

Figure 3.17 - Schematic representation of the different conditions used in order to investigate the actin phenotype induced by EspW upon EHEC and EPEC infection
Swiss 3T3 and HeLa cell lines were infected with EHEC 85-170 and EPEC/E69 WT strains and EHEC 85-170 and EPEC/E69 overexpresing *espW* and $espW_{1-206}$ respectively. The infection time varied from 15 min to 3h.

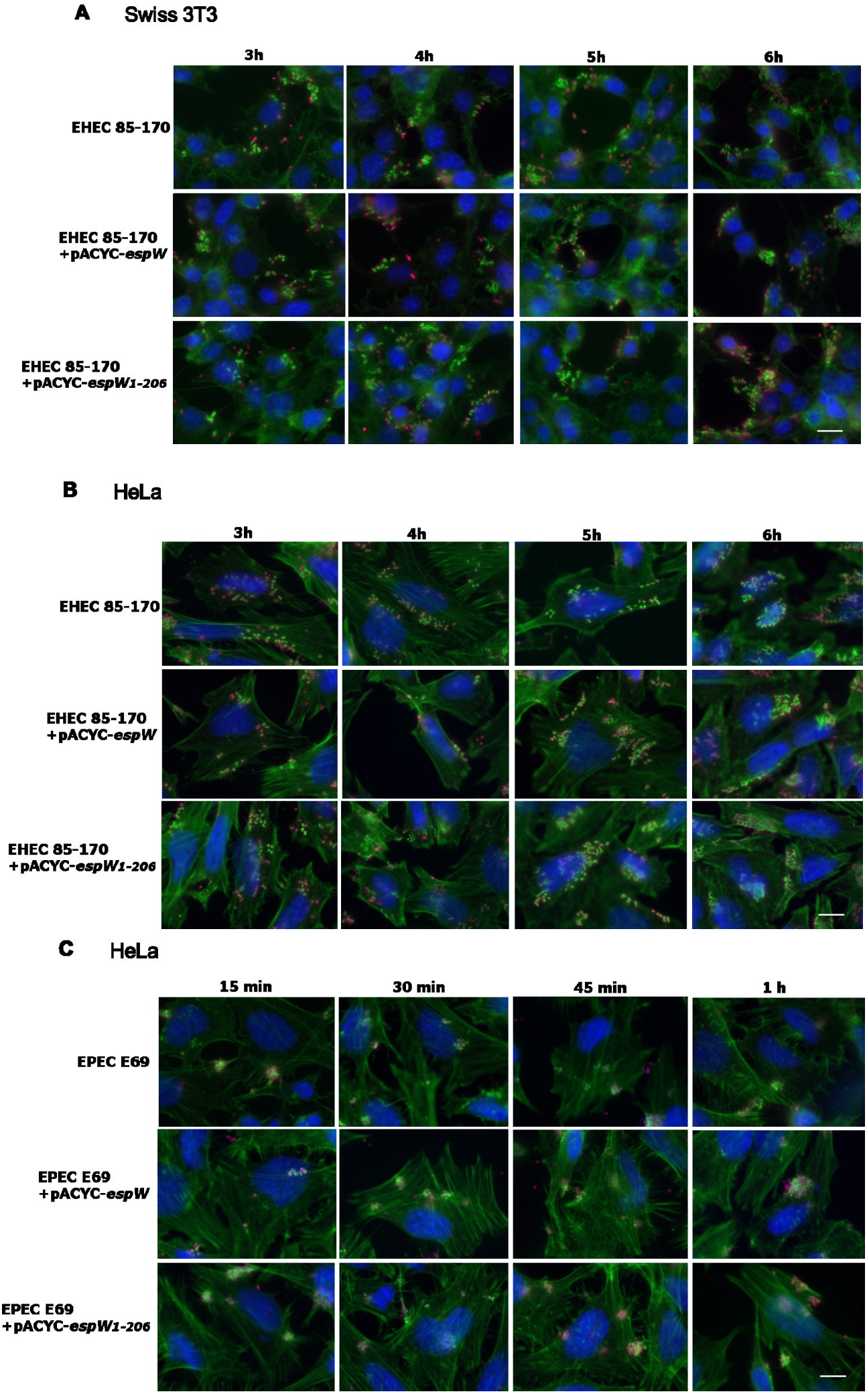
A
Swiss 3T3
3h
4h
5h
6h
EHEC 85-170
EHEC 85-170
+pACYC-espW
EHEC 85-170
+pACYC-espW1-206
B
HeLa
3h
4h
5h
6h
EHEC 85-170
EHEC 85-170
+pACYC-espW
EHEC 85-170
+pACYC-espW1-206
C
HeLa
15 min
30 min
45 min
1 h
EPEC E69
EPEC E69
+pACYC-espW
EPEC E69
+pACYC-espW1-206

Figure 3.18 - IF examples of different conditions used to look at the actin phenotype induced by EspW upon EHEC and EPEC infection
A – Swiss 3T3 cells infected (for 3,4,5 and 6 hours) with EHEC 85-170 WT and EHEC 85-170 overexpressing EspW and $EspW_{1-206}$. **B** – HeLa cells infected (for 3, 4, 5 and 6 hours) with EHEC 85-170 WT and EHEC 85-170 overexpressing EspW and $EspW_{1-206;}$ **C** – HeLa cells infected with EPEC/E69 WT and EPEC/E69 overexpressing EspW and $EspW_{1-206}$. Coverslips were fixed and stained with phalloidin green for actin, DAPI (blue) for nuclei and rabbit anti-E2348/69 antibody followed by anti-rabbit Cy5 conjugate (far red) for bacteria. Immunofluorescence staining showed that there was no difference in the cell morphology in either HeLa or Swiss cells after infection with EPEC/E69 and EHEC 85-170 overexpressing EspW and $EspW_{1-206}$ when compared with cells infected with EPEC/E69 and EHEC 85-170 WT strains Bar = 5 µm.

As we did not observe any morphology changes in pedestal and actin cytoskeleton morphology upon EPEC/E69 and EHEC 85-170 overexpressing EspW and $EspW_{1-206}$ infection we further performed western blot to check whether or not these constructs express EspW. We found that there was no EspW-4HA protein expression in HeLa cell lysates after infection with with EHEC 85-170 overexpressing EspW-4XHA (using pACYC plasmid) when compared with the expression of EspW-4XHA using the pSA10 plasmid (results not shown). However, there was expression of $EspW_{1-206}$-4XHA but at low levels. We repeated the experiments using EPEC/E69 overexpressing EspW-4XHA and there was no protein expression observed. We concluded that the EspW protein expression from pACYC plasmid is really low and might explain the fact that there was no phenotype observed by infection.

3.4.3 Transfection with EspW followed by EHEC 85-170 infection in Swiss 3T3 cells

The aim of this experiment was to look at phenotypic modifications in Swiss 3T3 cells after ectopic expression of EspW followed by EHEC 85-170 WT infection. The results showed a transfection efficiency of less than 5% and this was low when compared with the transfection efficiency upon ectopic expression of EspW without infection which was 45%. The reduced number of EspW transfected cell most probably was due to cellular stress caused by both transfection and infection assay which could have causes cell death.

There were only a few cells left on the coverslip that were positive for transfection and infection. EspW transfected cells showed actin rearrangement in a 'flower like pattern', however the actin pedestals normally induced by EHEC infection were difficult to differentiate Figure 3.19. The experiment was inconclusive as there were not enough representative samples to draw any conclusion.

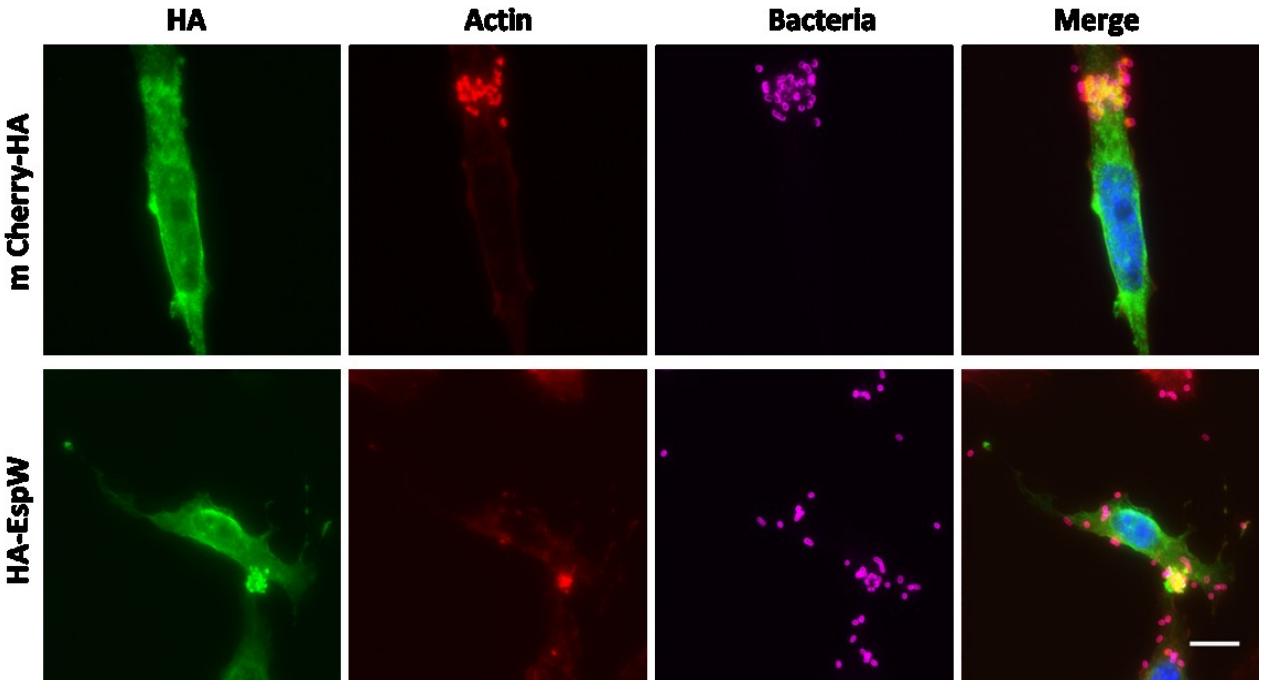

Figure 3.19 - Transfection with pRK5-HA-*espW* (4 h) followed by 3 h EHEC 85-170 infection in Swiss cells

Swiss 3T3 cells were mock transfected or transfected with HA tagged EspW for 4 h prior to infection with wild type EHEC 85-170. Ectopic expression of EspW showed actin rearrangement in a flower like pattern (white arrow) and the pedestal were not clearly visible when compared with the negative control (red arrows).

Immunofluorescence staining: anti-HA antibody (green), bacteria was visualised with anti-E85/170 antibody (magneta), actin was detected with TRITC-Phalloidin (red) and nuclei were stained with DAPI (blue) Bar = 5 µm.

3.5 Construction of EHEC 85-170 *ΔespW* mutant

The EHEC *ΔespW* mutant was generated using a Lambda red-based mutagenesis system as described in material and methods section. A schematic representation of the workflow is shown Figure 3.20 A. We assessed the growth of two EHEC *ΔespW* mutant clones in comparison with EHEC 85-170 WT strain in three different types of media: cell culture (DMEM), rich LB medium and minimal M9 medium. We used M9 minimal medium to highlight possible housekeeping genes defects that is difficult to observe after growth in nutrient rich medium. As M9 contains just basic nutrients, the bacteria needs to produce its

own amino acids in order to grow. If one of the genes that is critical for bacterial function is missing, the mutation will have a strong effect and the rate of bacterial growth will be reduced. The results showed that the replacing of *espW* with kanamycin cassette does not influence the bacterial growth (Figure 3.20 B).

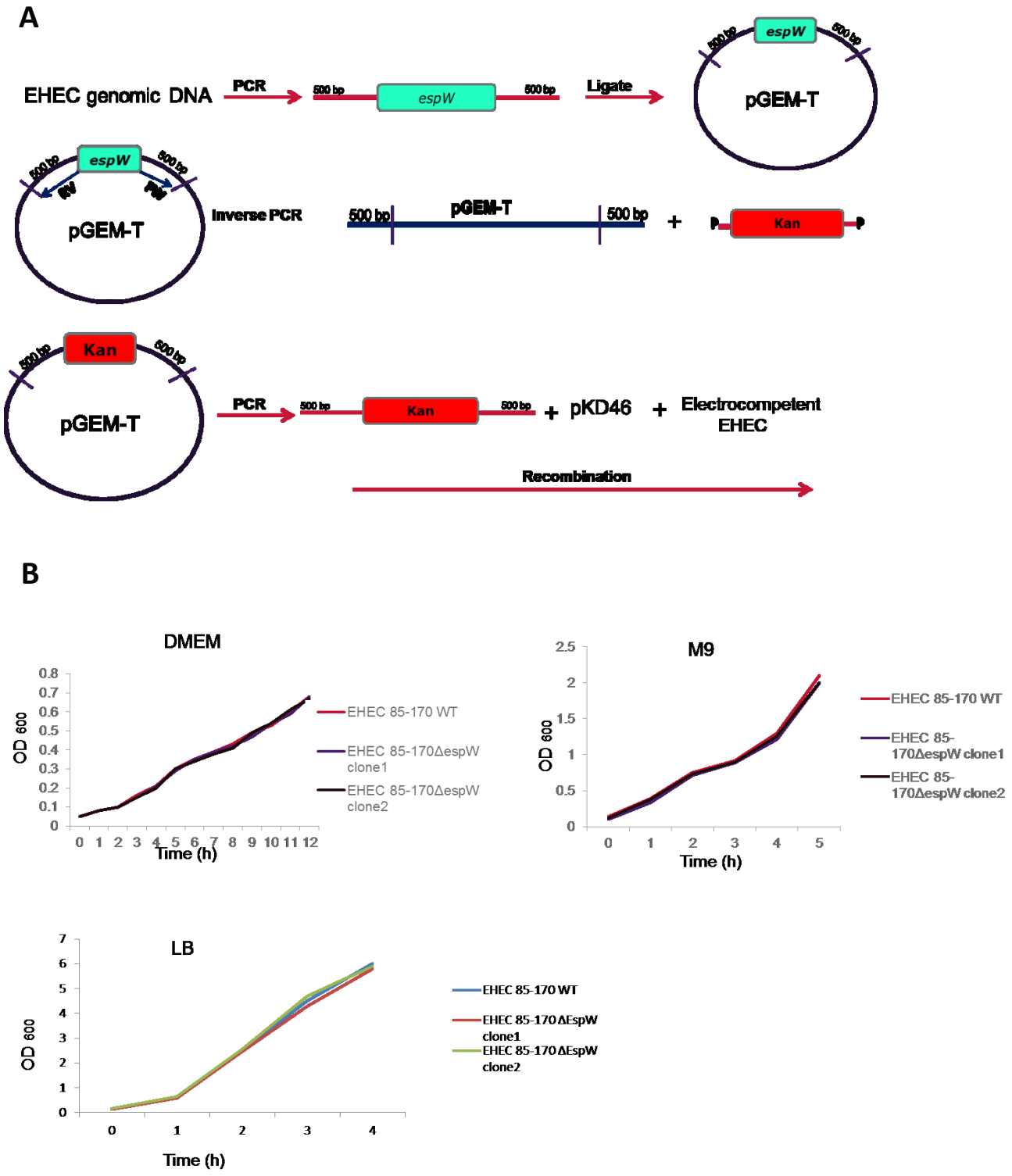

Figure 3.20 - Construction of EHEC 85-170 ΔespW mutant

A – Schematic representation of the steps taken to generate the EHEC87-170 *ΔespW* construct using Lambda red recombinase (as described in material and methods). **B** - Growth curve assays EHEC *ΔespW* mutants and EHEC 85-170 WT strains grew in a similar way regardless of the growth media used (DMEM, M9 or LB).

3.5.1 **Deletion of *espW* induces cell shrinkage that could be overcome by Rac1 activation**

To assess the role of EspW during infection, Swiss 3T3 fibroblasts were infected for 3 h with wild-type EHEC, EHEC *ΔespW* or EHEC *ΔespW* complemented with pSA10-*espW* and pSA10-$espW_{I237A}$. Cell infected with EHEC Δ*espW* showed a marked increase in cells that appear shrunk by immunofluorescence when compared to those infected with WT EHEC (Figure 3.21 A). EHEC Δ*espW* was found to induce 56±0.5% cell shrinkage; however, complementation of the mutant with pSA10-*espW* reduced the level of cell shrinkage to 32±1.5% relative to that of the WT EHEC control (12±1%) (Figure 3.21 B).

We further wanted to address the question whether or not these morphological modifications observed after EHEC Δ*espW* infection are Rac1 dependent.

Previously characterised EspT effector has been reported to induce the formation of lamellipodia and membrane ruffles by activation of Rac1 (Bulgin et al., 2009a). In order to determine if the cell shrinkage was caused by a lack of Rac1 activation, we complemented EHE CΔ*espW* with both pSA10-*espT* (Rac1 activator) and its inactive counterpart pSA10-$espT_{W/A}$, and calculated the percentage of cells shrunk after infection. Indeed, the later complementation reduced the number of shrunk cells to 31±1%. This was not the case after complementation with pSA10-$espT_{W/A}$ (50±1.5%). We concluded that overexpression of EspT during EHEC Δ*espW* infection results in a full complementation functionality suggesting that EspW as well might be a Rac1 GEF.

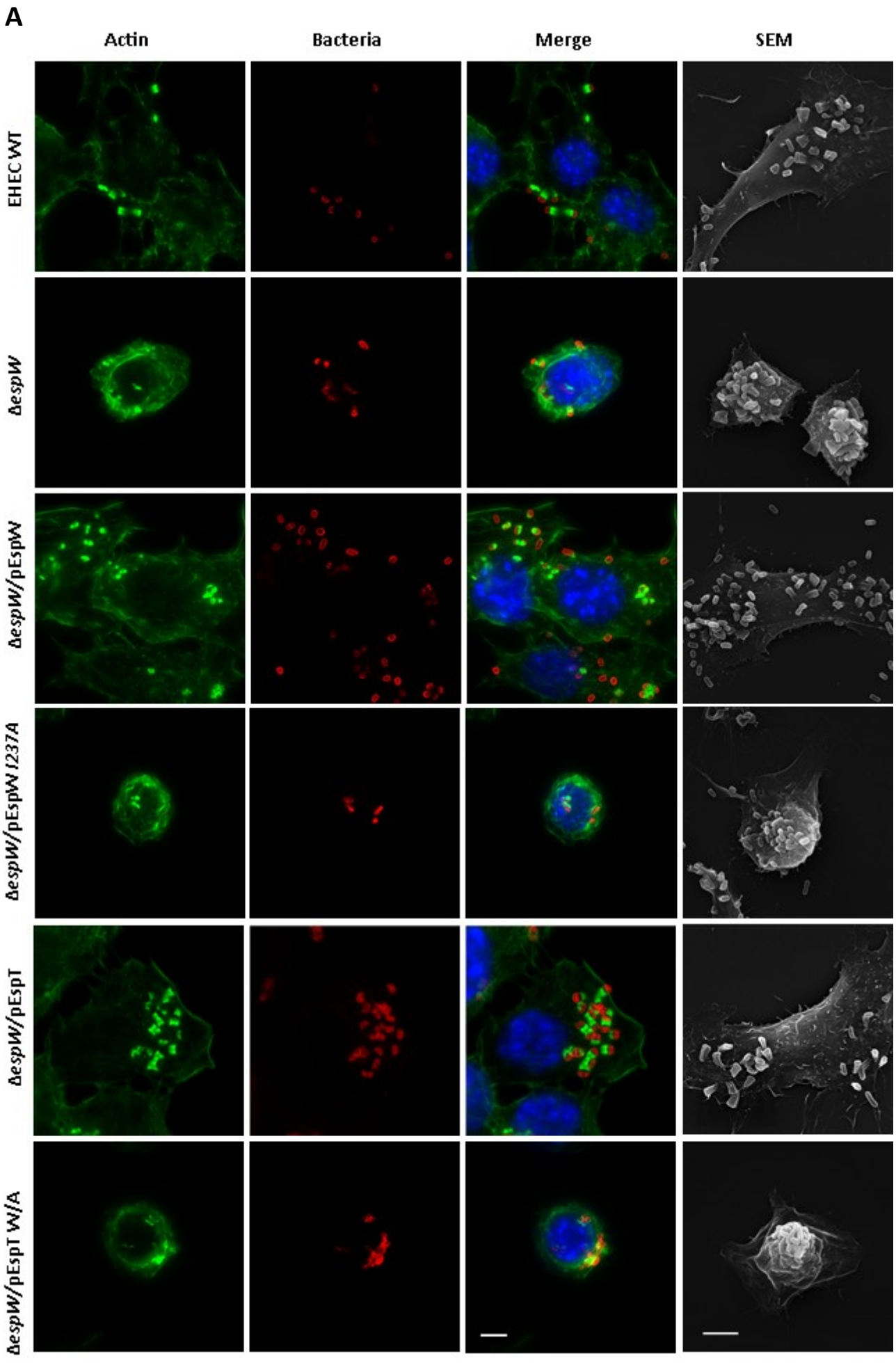
A
Actin
Bacteria
Merge
SEM
EHEC WT
ΔespW
ΔespW/pEspW
ΔespW/pEspW I237A
ΔespW/pEspT
ΔespW/pEspT W/A

B

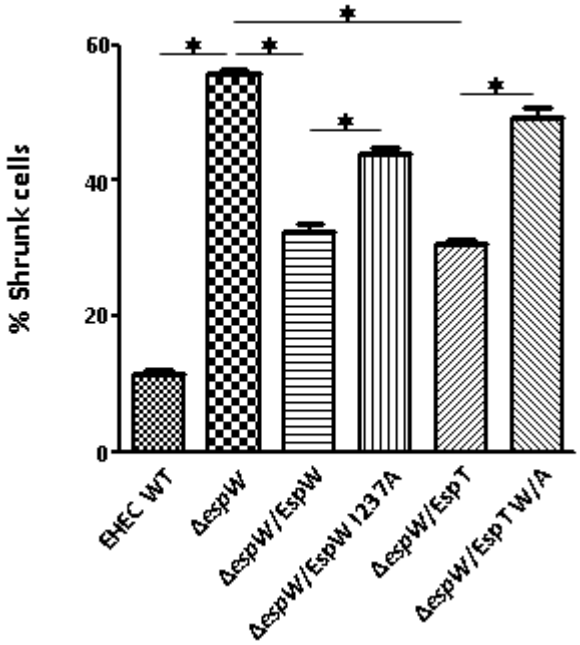

Figure 3.21 - EHEC 85-170 *ΔespW* Infection assay

A - Immunofluorescence microscopy of Swiss 3T3 cells infected with WT EHEC, EHEC*ΔespW*, EHEC*ΔespW* overexpressing EspW, $EspW_{I237A}$, EspT and $EspT_{W/A}$ for 3 h. Bacteria was visualised with anti-EHEC 85-170 antibody (red), actin was detected with TRITC-Phalloidin (green) and nuclei were stained with DAPI (blue).The EHEC *ΔespW* mutant induced Swiss cell shrinkage after 3 h of infection compared to WT EHEC. Complementation with pSA10-*espW* and pSA10-*espT* but not with pSA10-$espW_{I237A}$ and pSA10-$espT_{W/A}$ resulted in a reduction in the number of shrunk cells when compared to EHEC *ΔespW* alone. 100 infected cells were counted in triplicate Bar = 5 µm.

B - Quantification of shrunk Swiss cells infected with WT EHEC, EHEC*ΔespW*, EHEC*ΔespW* overexpressing EspW, $EspW_{I237A}$, EspT and $EspT_{W/A}$.

One hundred infected cells were counted in triplicate. Results are means plus standard deviations (SD) of three independent experiments. The number of shrunk cells was significantly higher after EHEC*ΔespW* when compared to WT EHEC. Complementation with pSA10-*espW* and pSA10-*espT* restored the phenotype, but not completely. This was not the case after complementation with pSA10-$espW_{I237A}$ and pSA10-$espT_{W/A}$.

3.5.2 **Chemically activation of Rac1 using Sphingosine-1-phosphate (S1P) resulted in a reduction of shrunk Swiss cells upon EHEC *ΔespW* infection**

Sphingosine-1-phosphate (S1P) is a bioactive lysophospholipid that induces a variety of biological responses in diverse cell types. Previous studies showed that S1P induce an increase in the amount of the GTP-bound active form of Rac in eukaryotic cells (Gonzalez et al., 2006).

In order to confirm that the cell shrinkage was caused by the lack of Rac1 activation, we chemically induced activation of Rac1 during infection by adding 100nM S1P to the culture medium and quantify the number of shrunk cells after infection (Figure 3.22). S1P treatment significantly reduced cell shrinking of cells infected with EHEC ΔespW from 53±1.5% to 33±2%. These results suggest that EspW activates Rac-1 to maintain the shape of infected cells.

A

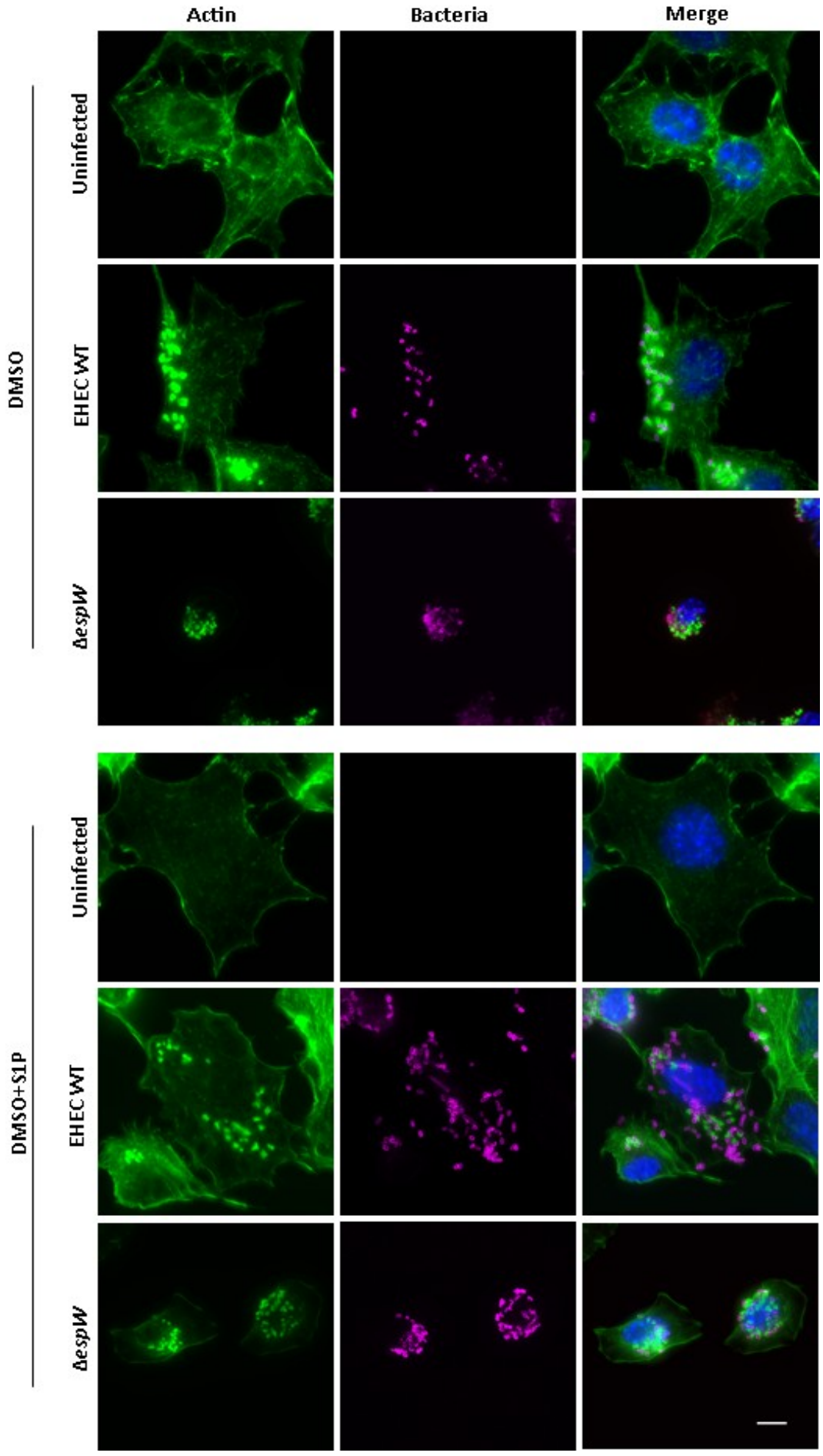
Actin
Bacteria
Merge
DMSO
Uninfected
EHEC WT
ΔespW
DMSO+S1P
Uninfected
EHEC WT
ΔespW

B

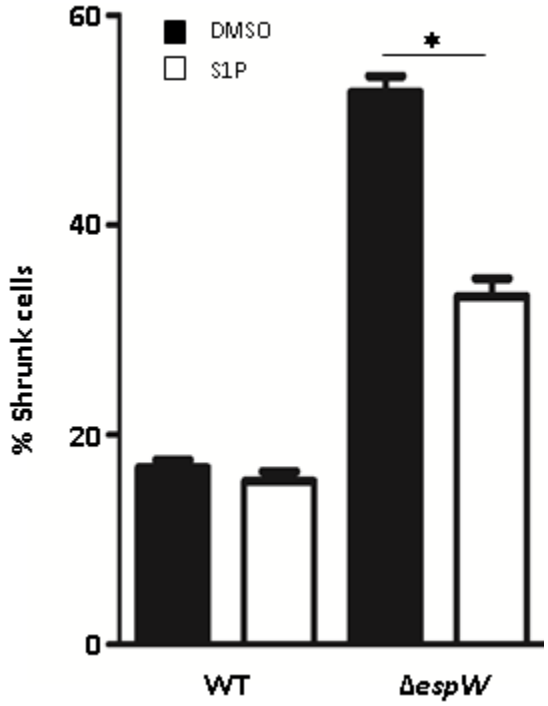

Figure 3.22 - In the presence of Sphingosine-1-phosphate (S1P) the shrinkage of Swiss cells is significantly reduced after 3h infection with EHEC *ΔespW*

A - Immunofluorescence microscopy of Swiss 3T3 cells infected with WT EHEC and EHEC *ΔespW* for 3 h in the presence of 100nM of S1P. DMSO was used as a solvent for S1P and the concentration used was not toxic to the cells. Bacteria was visualised with anti-E85/170 antibody (magneta), actin was detected with TRITC-Phalloidin (green) and nuclei were stained with DAPI (blue). The number of Swiss cells shrinkage induced after 3 h infection with EHEC *ΔespW* in the presence of S1P was significantly reduced when compared to infection with EHEC *ΔespW* in the presence of DMSO only. 100 infected cells were counted in triplicate Bar = 5 µm.

B - Quantification of shrunk Swiss cells infected with WT EHEC and EHEC *ΔespW* in the presence of DMSO only and DMSO with 100nM S1P for 3 h. The number of shrunk cells after 3 h infection with EHEC *ΔespW* in the presence of 100nM of S1P was significantly reduced when compared with the infection in the presence of DMSO. One hundred infected cells were counted in triplicate. Results are means plus standard deviations (SD) of three independent experiments.

3.5.3 **LDH Cytotoxicity tests negative upon EHEC *ΔespW* infection in Swiss 3T3 cells**

To check whether the shrunk cells was a result of cell death we decided to use LDH assay to measure the release of LDH into the media from damaged cells as a biomarker for cellular cytotoxicity and cytolysis. Briefly Swiss 3T3 were infected with EHEC, EHEC *ΔespW*, EHEC *ΔespW* complemented with pSA10-*espW* and pSA10-*espW*-4XHA. The supernatant was extracted and analysed for Lactose dehydrogenase (LDH release) using Cytotox 96 non-radioactive cytotoxicity assay (Promega), following the manufacturer's instructions. As positive control for total LDH, cell lysis buffer (1% Triton-X100/PBS) was added for 30 min at 37°C directly to the medium and cell layer. Absorbance was measured at 490 nm using the FluoStar Omega plate reader and results are displayed as percentage of total release. As negative control 0.05% TritonX-100/PBS supplemented with 3.3 μg/ml propidium iodide was added for 15 min at 37°C. As shown in Figure 3.23 the LDH Cytotoxicity tests were negative therefore we concluded that the shrunk cells resulted upon Swiss 3T3 cells infection with EHEC *ΔespW* are not a consequence of cell death.

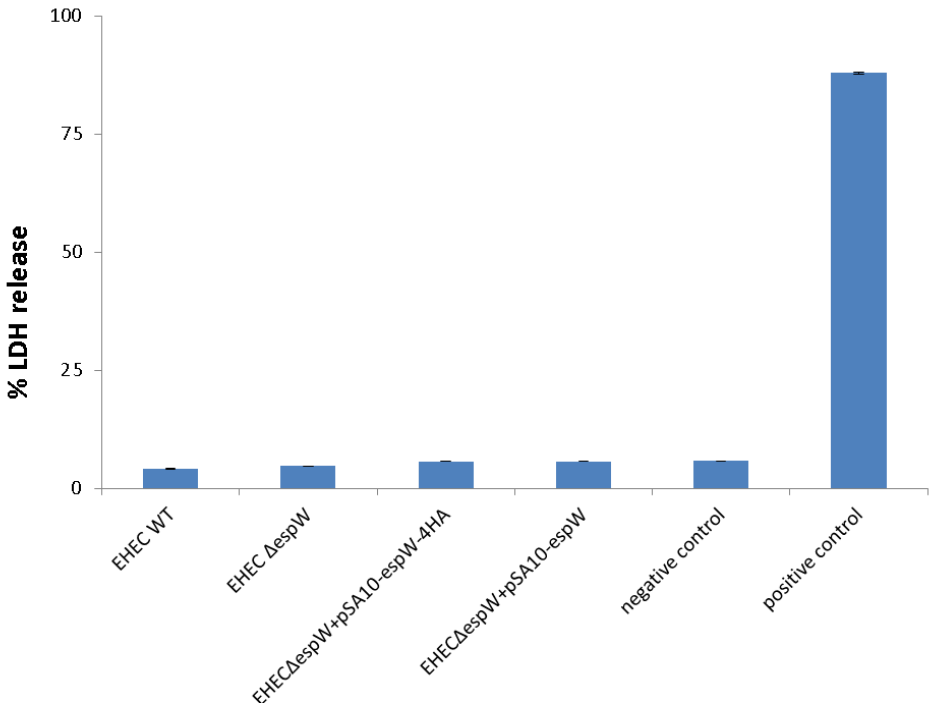

Figure 3.23 - LDH Cytotoxicity assay
Swiss 3T3 cells infected with EHEC 85-170, EHEC *ΔespW*, EHEC *ΔespW* complemented with pSA10-*espW* and pSA10-*espW*-4HA (with no induction with IPTG) were spun for 5 min and Gen 100 µg/ml was added after 2.5 h of infection. As positive control for total LDH, cell lysis buffer (1% Triton-X100/PBS) was added for 30 min at 37°C directly to the medium and cell layer. Absorbance was measured at 490 nm using the FluoStar Omega plate reader and results are displayed as percentage of total release. As negative control 0.05% TritonX-100/PBS supplemented with 3.3 µg/ml propidium iodide was added for 15 min at 37°C.

3.6 EspW protein expression and purification

As EspW is a novel effector, there was no information in published researched literature with regards to its structure. Therefore we attempted to purify EspW for antibody and for possible structural work. In order to optimise EspW expression we used different bacterial strains such as BL21 DE3 star and BL21 DE3 plysS and different tag localisation such as pET28a-EspW with –C and -N terminal His-tag. The strains were induced with different

concentrations of IPTG (0.05 mM to 1 mM) at different incubation temperature for different lengths of time (as described in Material and methods section) followed by Coomassie staining and Western blotting analysis (Figure 3.24 A). As the N-terminal ~20 residues of T3SS effectors function as a secretory signal and are generally unstructured (Munera et al., 2010), constructs were made lacking the first 20 amino acids (Figure 3.24 B). Despite those various conditions none of the systems above gave satisfactory results in terms of amount of recombinant protein expressed and protein solubility and led to poor purification level (Figure 3.25).

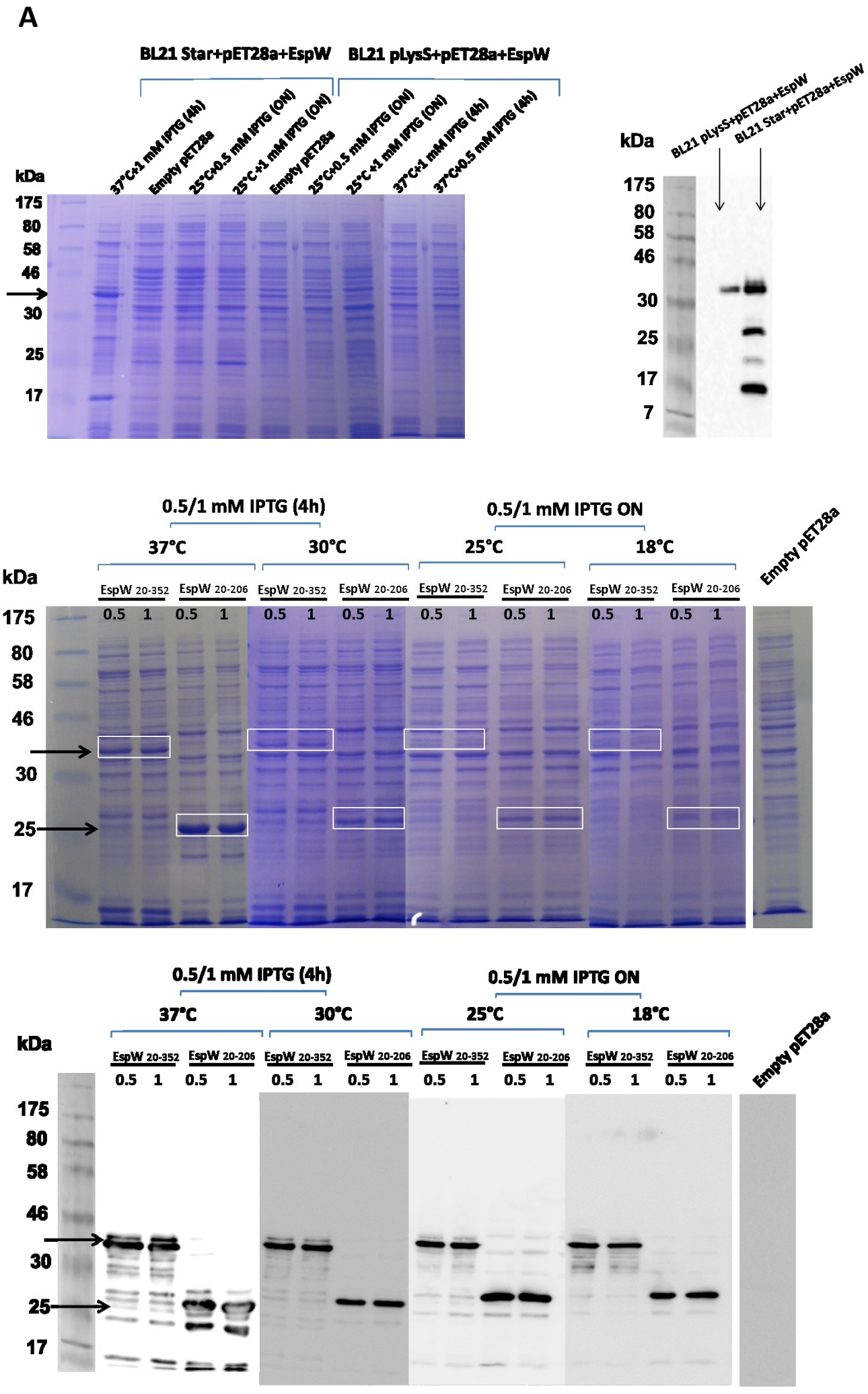
A
BL21 Star+pET28a+EspW
BL21 pLysS+pET28a+EspW
37°C+1 mM IPTG (4h)
Empty pET28a
25°C+0.5 mM IPTG (ON)
25°C+1 mM IPTG (ON)
Empty pET28a
25°C+0.5 mM IPTG (ON)
25°C+1 mM IPTG (ON)
37°C+1 mM IPTG (4h)
37°C+0.5 mM IPTG (4h)
kDa
175
80
58
46
30
25
17
kDa
BL21 pLysS+pET28a+EspW
BL21 Star+pET28a+EspW
175
80
58
46
30
25
17
7
0.5/1 mM IPTG (4h)
0.5/1 mM IPTG ON
37°C
30°C
25°C
18°C
Empty pET28a
kDa
EspW 20-352
EspW 20-206
0.5
1
175
80
58
46
30
25
17
0.5/1 mM IPTG (4h)
0.5/1 mM IPTG ON
37°C
30°C
25°C
18°C
Empty pET28a
kDa
EspW 20-352
EspW 20-206
0.5
1
175
80
58
46
30
25
17

Figure 3.24 - EspW protein expression

(Coomassie stained polyacrylamide gel and Western blotting using anti His tag (PolyHis-HRP 1:10000)) **A** - BL21 star (λDE3 lysogen) and BL21 plysS (pET28a-*espW*) cultures were induced with 0.5 mM and 1 mM of IPTG and grown at 37 °C for 4 h and at 25 °C overnight. The concentration of the EspW protein produced was low and protein degradation was present. Western blotting – cultures induced with 1mM IPTG for 4 hours. Gels were loaded with 15 µl of samples diluted to similar protein concentration. Purification assay using Ni-NTA His-bind resin where BL21 strains with empty pET28a was used as negative control. **B**- $espW_{20\text{-}352}$ and $espW_{20\text{-}206}$ were cloned into pET28a and further transformed into BL21 DE3 Star and BL21 DE3 pLysS for expression as N-terminal 6-His tagged $EspW_{20\text{-}352}$ and $EspW_{20\text{-}206}$. EspW was unstable and appeared in many bands, corresponding to the full length effector and for degradation products (black arrows). Gels were loaded with 15 µl of samples diluted to similar protein concentration. Purification assay using Ni-NTA His-bind resin where BL21 strains with empty pET28a was used as negative control.

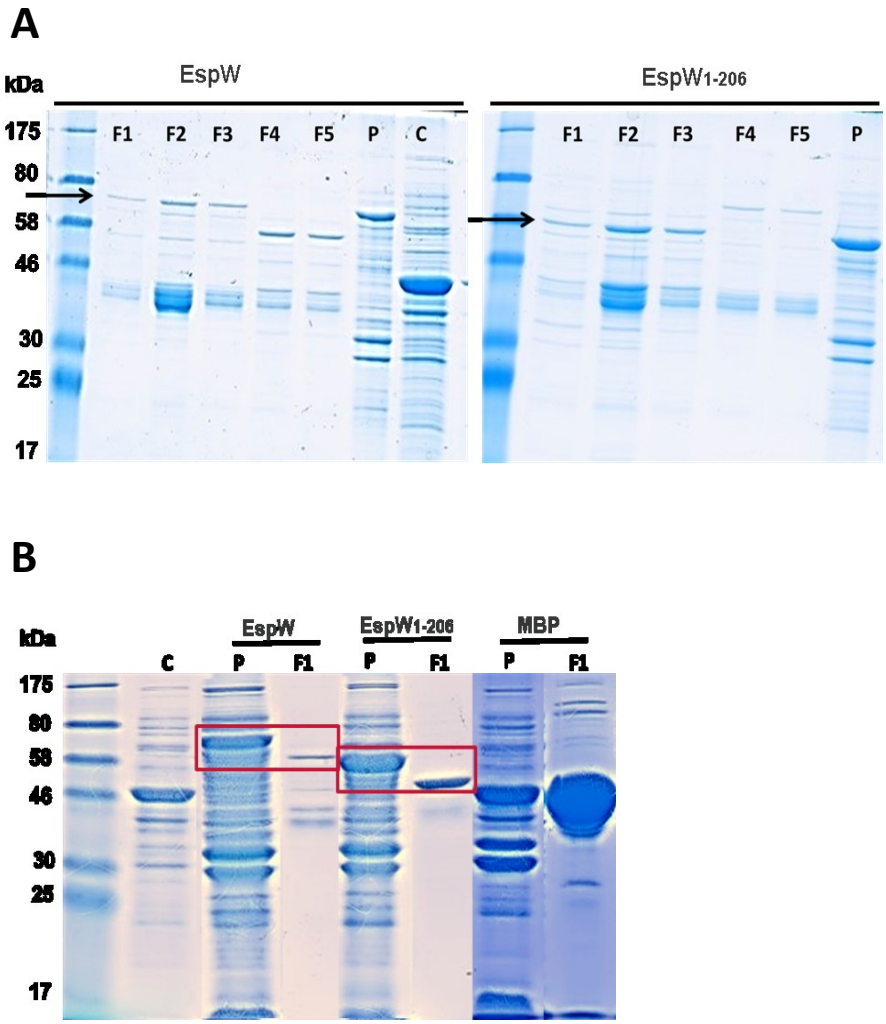

Figure 3.25 - EspW protein purification
Protein expression from Top10-pMALc2x-*espW*/*espW*$_{1-206}$ was induced with 0.5mM IPTG for 4 h. Expression and purification of EspW-MBP and EspW$_{1-206}$-MBP was analysed by Coomassie stained polyacrylamide gel (Molecular weight: MBP- 42.5 kDa, MBP-EspW - 77 kDa and MBP-EspW$_{1-206}$ - 55.9 kDa); F- elution fractions, P-pellet, C-MBP as control; **A** - 50 ml culture, **B** - 1 L culture.

The full length *espW* and *espW*$_{1-206}$ sequences were further cloned into pMALc2x for expression as a fusion protein with the maltose binding protein (MBP). The expression and purification of EspW-MBP and EspW$_{1-206}$-MBP was tested from 50 ml Top10 *E.coli* cultures (Figure 3.25 A). Following purification the elution fractions were analysed by Coomassie staining which showed additional bands that suggested protein degradation. The experiment was scaled up to 1 L culture (Figure 3.25 B), and in order to remove the aspecific binding the stringency of the wash was improved by increasing the buffer salt concentration and the number of washes. The results showed that the amount of EspW-MBP detected in the pellet was much higher when compared to the amount retrieved following purification suggesting that either cell lysis was not optimal or that the EspW-MBP is hardly soluble and therefore difficult to purify. Moreover on the SDS gel, the size of the proteins in the soluble fractions was lower than in the pellet, suggesting protein degradation. Despite trying out different protein purification strategies, EspW was insoluble and degraded, therefore unable to be purified.

3.7 The correlation between the presence of EspW and other effectors with role in cytoskeleton modulation in EPEC

3.7.1 No correlation between the distribution of *espW* and *espT*, *espM* and *espV* in EPEC

Proteins such as the WxxxE effector Map is conserved in all EPEC and EHEC strains. The number of T3SS effector proteins is highly variable between different A/E pathogen strains ranging from 26 in EPEC/E69 to over 50 in EHEC Sakai. The *espW* gene is carried on a phage encrypted region and it is present in all EHEC strains. We have showed that *espW* is present in 52% of clinical EPEC isolates (Table 2.4) and we demonstrated the role of EspW in the reorganisation of actin cytoskeleton. We wanted to investigate possible correlations between the presence of *espW* and other genes for protein effector proteins with role in the modulation of cytoskeleton in eukaryotic cells such as EspM (RhoA GEF, activates stress fiber formation (Arbeloa et al., 2010), (Arbeloa et al., 2008)), EspT (induces membrane ruffles and lamellipodia by activating Rac1 and Cdc42 (Bulgin et al., 2009b)) and EspV (Present in cytosol with role in cytoskeleton modulation (Arbeloa et al., 2011)). Arbeloa *et al*., performed large screens in order to determine the prevalence of EspM, EspT and EspV effectors among clinical EPEC and EHEC strains for a better understanding of their impact on infection (Arbeloa et al., 2009).

In this chapter we compared *espW* distribution in 42 EPEC clinical isolates with the results published by Arbeloa *et*. *al* (Arbeloa et al., 2009). We look for any associations for the presence of *espW* with the presence of the *espM*, *espT* and *espV*. Although the results show that there might be a correlation between the presence of *espW* in the *espM*, *espV* and *espT*

positive strains, the number of biological samples needs to be significantly higher in order to prove that this is indeed the case (Figure 3.26).

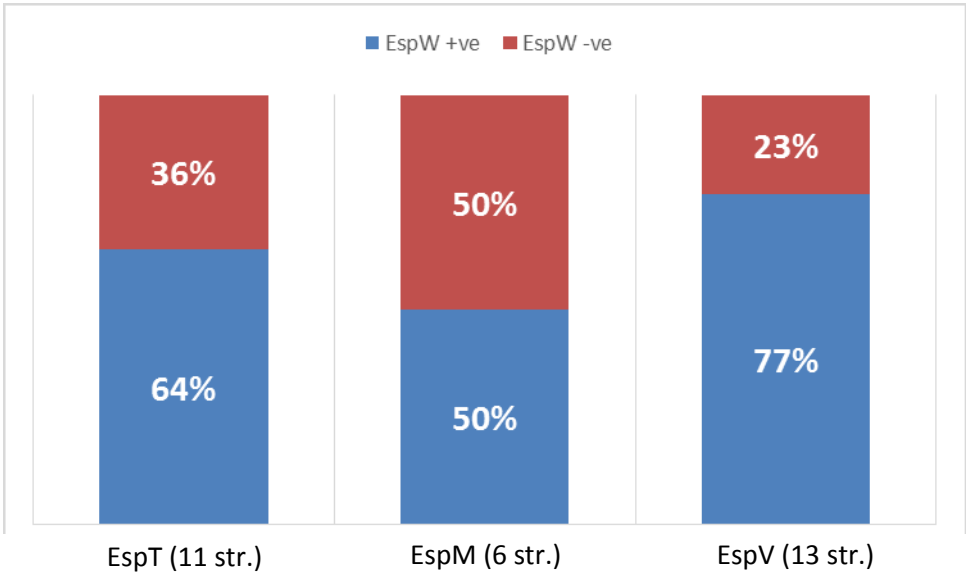

Figure 3.26 - Comparison of the distribution of *espW* and *espT*, *espM* and *espV* in EPEC
There might be a correlation between the presence of *espW* and *espT*, *espM* and *espV*, however the number of samples that we had access to for screening was low. The presence of *espW* amongst the 42 out of 132 EPEC strains screened was contrasted with the presence of *espM*, *espT* and *espV* found in previous studies (Arbeloa et al., 2009) and (Arbeloa et al., 2011). Out of these 42 EPEC strains screened, there were 11 *espT*, 6 *espM* and 13 *espV* known positive strains. *espW* was present in 64% of the *espT* positive strains, 50% of the *espM* positive strains and 77% of the *espV* positive strains.

3.7.2 There was no correlation between the presence of *espW* and *tccp* and *tccp2* in EPEC

In this study we have shown that EspW has a role in the reorganisation of actin cytoskeleton. As *tccp* is a major player in EHEC infection in terms of actin remodelling we wanted to find out if there is any correlation between the presence of *tccp* and *espW*. Along with *espW* and $espW_{1\text{-}206}$ 90 EPEC clinical samples (strains kindly given by Jeannette Adu-

Bobie Appendix Table 1) were screened for the presence of *tccp* and *tccp2*. Out of the 90 clinical EPEC isolates screened, the percentage of *espW* positive strains was 47%, $espW_{1\text{-}206}$ 8%, *tccp* 14% and *tccp2* 24% (Figure 3.27.)

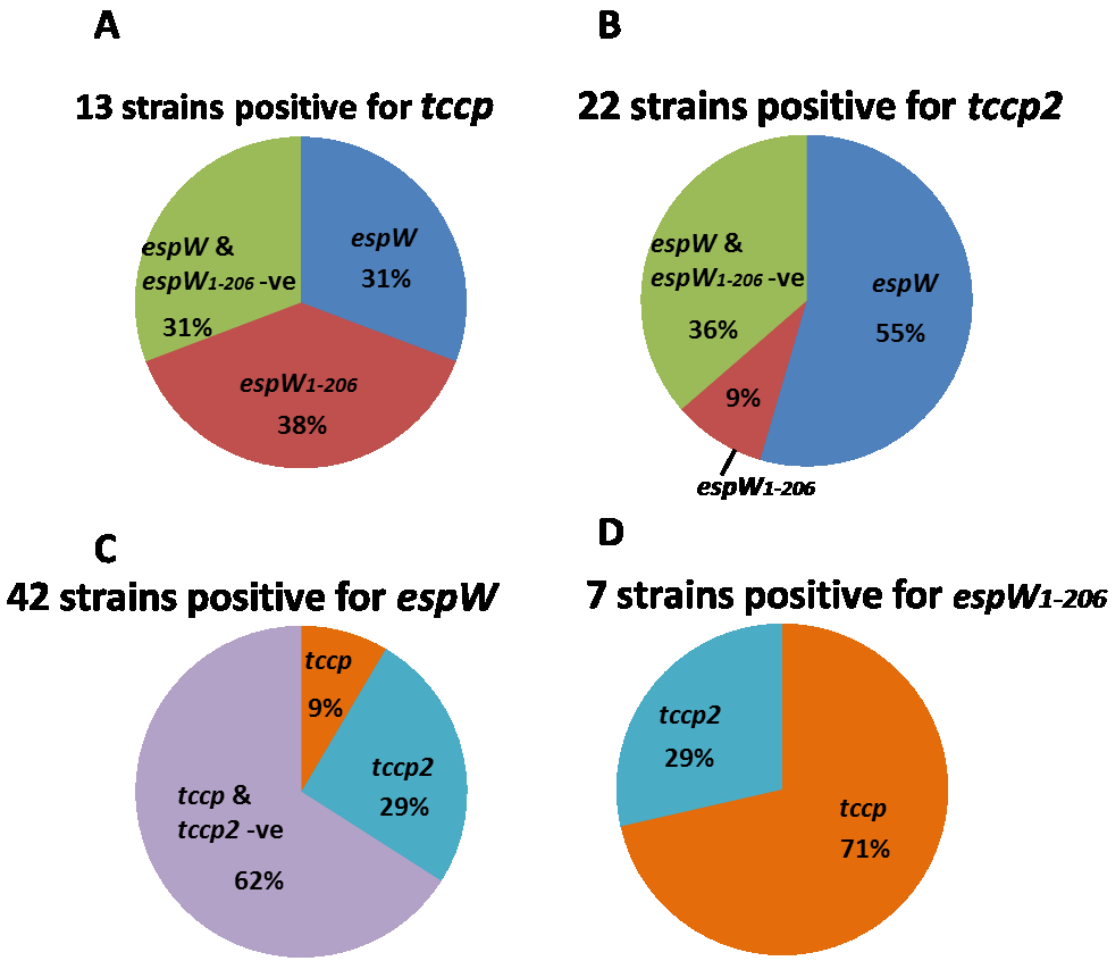

Figure 3.27 - Comparison of the distribution of *espW*, *tccp* and *tccp2*
There might be a correlation between the presence of *espW* and *tccp2* in EPEC. 90 clinical isolates were screened by PCR for the presence of *espW*, $espW_{1\text{-}206}$, *tccp* and *tccp2* and we looked for correlations. **A** - Out of the 13 *tccp* positive strains 31 % were also positive for *espW* and 38 % for $espW_{1\text{-}206}$; **B** - Out of the 22 *tccp2* positive strains 55 % were also *espW* positive and only 9 % had $espW_{1\text{-}206}$. **C** - Out of the 42 EPEC *espW* positive strains screened, there were 4 *tccp* (9 %) and 12 *tccp2* (29 %) positive strains. **D** - Seven (out of 90) EPEC clinical strains were $espW_{1\text{-}206}$ positive, out of which 5 had *tccp* (71%) and 2 had *tccp2* (29%).

3.7.3 **EspW colocalises with N-WASP**

N-WASP is a Class I NPF, found along WASP in hetero complexes with the WASP-interacting family of proteins (WIP). WIP was shown to be required for Cdc42 dependent N-WASP activation and also acts in complex with N-WASP promoting actin polymerisation (Anton et al., 2007). As Kif15-Y2H is EspW binding partner which is found at the pedestal after wild type EHEC85-170 infection, we wanted to look at possible links between the players involved in pedestal formation and EspW. N-WASP is activated by TccP(EspFu) and recruits ARP2/3 complex which stimulates actin polymerization, leading to pedestal formation (Garmendia et al., 2006).

We performed a cotransfection experiment in Swiss cells using pRK5-HA-*espW* and pEGFP-*N-WASP* and the immunofluoresce imaging revealed that EspW colocalises with N-WASP (Figure 3.28). It will be interesting to address the question that EspW triggers actin rearrangement not only in a Rac1 dependant manner but perhaps in a Cdc42 as well. Rac1 utilizes a plethora of downstream effectors in order to regulate cytoskeletal dynamics (reviewed in (Etienne-Manneville and Hall, 2002)). Several GTPase effectors including IRSp53, N-WASP, Pak, Wave2 and Abi1 have been previously been implicated in formation of membrane ruffles (Innocenti et al., 2005), (Legg et al., 2007), (Machuy et al., 2007), (Miki et al., 2000), (Sasaki et al., 2000). As EspW triggers the formation of membrane ruffles it will be interesting to investigate whether it uses the pathway that involves N-WASP.

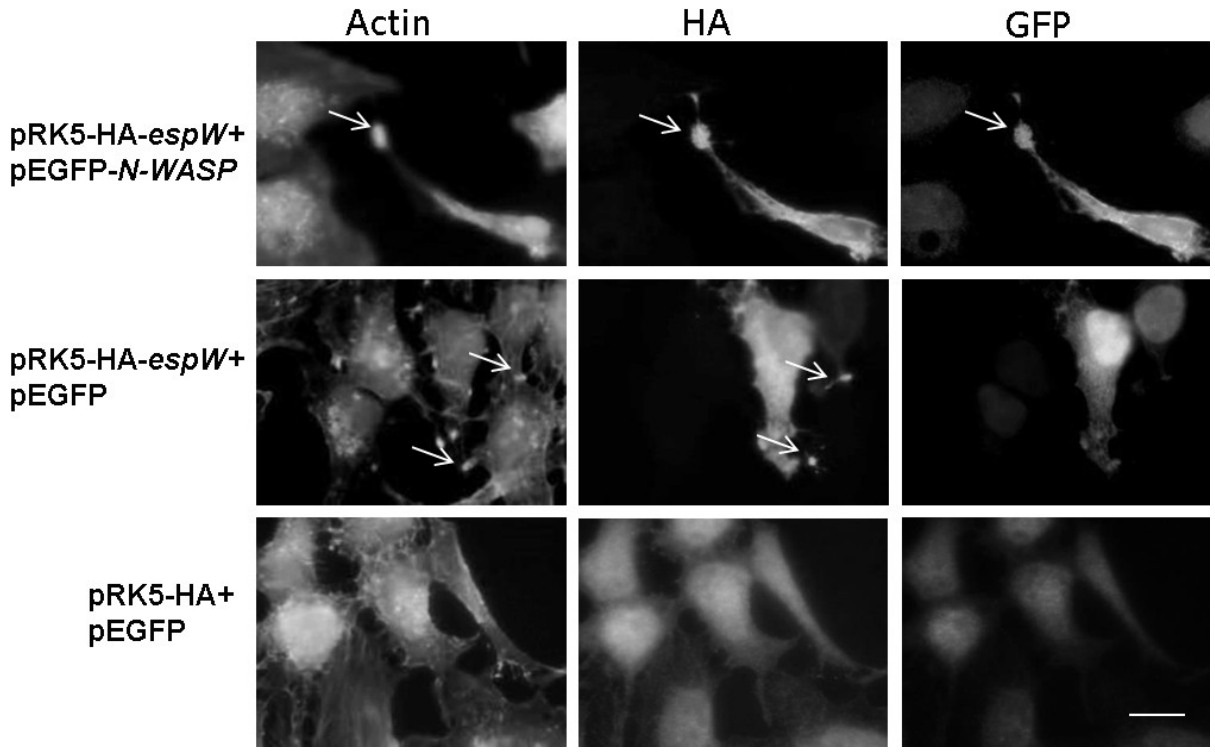

Figure 3.28 - EspW colocalises with N-WASP

Swiss 3T3 were cotransfected with pRK5-HA-*espW* and pEGFP-*N-WASP.* Cells cotransfected with pRK5-HA-*espW* and pEGFP were used as positive control and cells cotransfected with pRK5-HA and pEGFP-*N-WASP* as negative control. Actin was stained with AMCA (Blue), N-WASP was detected with a GFP (green) and HA was visualized using polyclonal rabbit antibody (Red). Transfected cells presented 'flower' like actin structures which colocalises with EspW and N-WASP Bar = 5 µm.

CHAPTER 4 - **General discussion**

EHEC belongs to a family of A/E pathogens which upon infection, hijack and manipulate host cell signalling pathways allowing infection of host cells, evasion of host immune responses and efficient colonisation which ultimately leads to disease (Wong et al., 2011), (Dean and Kenny, 2009). These pathogens use a type III secretion system (T3SS) described previously, that acts as a macromolecular syringe to inject effector proteins directly into infected cells (Garmendia et al., 2005). Previous research on characterisation of A/E pathogens effectors has expanded our understanding of the infection strategy of A/E pathogens; however to date, the functional role of many effectors still remains unknown.

In this study we have characterised the host interacting partners and the functional role of the EHEC non-LEE encoded T3SS effector EspW.

Firstly we investigated EspW at the aa level to try and find clues on its structure and functionality. Our searches did not provide us with enough information due to the lack of previous research studies.

EspW shares 29% identity with the C-terminal domain of HopPmaA/HopW, a protein with unknown function identified in *P. syringae*. Some preliminary data showed that the plant extracellular pathogen *P. syringae* injects HopW1 effector into host cells to disrupt the actin cytoskeleton and reduce vesicle movement in order to elude defence responses. Furthermore, in some Arabidopsis accessions, HopW1 was shown to cause resistance via an actin-independent mechanism (Jelenska et al., 2014). HopW1 has no similarity to any proteins of known functions but has a common domain at the N-terminal region of HopAE *from P. syringae* pv. *Syrinagae*. Interestingly the C-terminal domain of HopW1 is present in

EspW (Figure 4.1). In this paper (Jelenska et al., 2014) suggested that it is possible that EspW is another *E. coli* effector that targets actin and that it might have actin-disrupting activity similar to HopW1.

```
HopW1      MNPAQITRLSQSFLPSISPA---SFEAESSHA----------------------------
EspW       -------------MPKISSVVSSCYHLFSEHQQLSNETTMTNPVSRRIVHKEYGISLKSV
                        :*.** .   .:.  *.*
HopW1      -------------QSPQQTRPHAFVASGELNAAFGRTSTSPTQDFTRLLGAVQRELESES
EspW       PVWLATAKTPLALLNGRHTRSHSFIIAGTPGMG----SRSGAQYYAINSDDKRSRIDIDS
                         . ::** *:*: :*    .    * * :* ::      : .:: :*
HopW1      TSFPAVAELANQLAEAAMGEHWPGHDEQQV--LKGVIDRCTSQLAH----TPVSHPSRDA
EspW       LFLK-------KLNNVRNQNKFPIDVKETVIKLQGQKFTCIEDFYKRYNETRLKANTNIQ
             :        :* :.   :::* . :: *  *:*    * .:: :    * :.  :.
HopW1      LSQVCESLKTAR-------LHQSISHMLGESHA-TVRGVPDLLALIHIDPKVLADKPVSM
EspW       QEQIADEVKSLTYLIPSEKKEMWIYKNNGKDNAKPNLGERDVRMFENISSDD--TDKITG
            .*:.:.:*:          .  * :  *:..*    *  *:  : .*. .    . ::
HopW1      PSHVKFGSFICLARARAAQLSESLNSNSGDVARLLHPHADTLLGLEKLPEALAALTENCP
EspW       RKFSELGEYLY----------------SGNVIKLSQ------LSIRYLPN----------
            .. ::*.::                 **:* :* :      *.:. **:
HopW1      DTSTQDDLRALAEEAGGLLQQLRSTGLLPRSGEVSGELAETLVPSCEVVEPKLTLGQALL
EspW       -IS---SISLIETKQSLLLHRLYSDEVLQRNGTLI--------PT-------------PL
             *   .:  :  : . **::* *  :* *.* :          *:              *
HopW1      KAGGDGPLDGQRVHLDGL---RHAPTHVA---SSDSGSRAPARAAGDSQK--------AA
EspW       HEEKSIPADNIKTMLNNIPTYKMLPPFTETQGNCSSGAATFLRKSGAEEKDILACSPRNY
           :   . * *  :. *: :   :  * ..    ...**: :  * :* .:*
HopW1      GLYAEKKRTNWTHATGVAGKIAHKIESLLGMRDAQSRVQAFVAFMADGKGKADATTLDLG
EspW       GLH--HNIKTWDPLV---------------------------------------------
           **:  :: ..*   .
HopW1      DGWMRVTRVIKGGDGFDRLQVRQ
EspW       -------RN--------------
```

Figure 4.1 - Protein alignment: HopW1 from *P. syringae* pv. *Syrinagae* and EspW from EHEC O157:H7 str. TW14359
(Clustal-Omega)

Despite the fact that EspW shows limited sequence identity with HopW1, in this study we showed that EspW has the ability to remodel the mammalian actin cytoskeleton.

A common theme in A/E pathogen subversion of host signalling is the modulation of the eukaryotic cytoskeleton. We have demonstrated that EspW is one of the modulators of the host cell actin cytoskeleton amongst other previously identified effectors such as Map, EspM2, IpgB2 and EspT.

Map, IpgB1, IpgB2, EspM2 and EspT, bacterial Rho GEFs that mimic the function of human Dbl GEFs, are grouped together based on a conserved structural WxxxE motif (Alto et al., 2006). Substitution of either the Trp or Glu residues abolishes binding to the cognate Rho GTPase and inhibits the exchange of GDP for GTP (Alto et al., 2006), (Arbeloa et al., 2010). In particular, Map and IpgB2 activate Cdc42 (Alto et al., 2006), (Berger et al., 2009), (Kenny, 2002), EspM2 and IpgB1 activate RhoA (Alto et al., 2006), (Arbeloa et al., 2010) and EspT activates Rac1 (Bulgin et al., 2009a). Huang *et al*. have shown that specificity of the WxxxE bacterial GEFs is achieved via differential pairing with the ß2-3 patch of Cdc42, Rac1 or RhoA (Huang et al., 2009). Moreover, these effectors share the motif AQxSI, which comprises the catalytic loop and the adjacent α-helix. In Map residues Ala127 and Q128, found in the catalytic loop, form hydrogen bonds with Cdc42-Phe37 within the switch one interface. Huang *et al*. have also shown that a catalytic loop deletion in Map, MapΔAQSSI, and the point mutant MapQ128Y were unable to trigger filopodia formation. Interestingly, while searching for additional EHEC effectors that might target Rho GTPases we identified an SQLSI motif in the effector EspW.

Using a two-hybrid screen we identified Kif15 as a specific partner protein of the long version of EspW. Human Kif15 is a dimeric protein of 1388 residues which belongs to the kinesin family (Drechsler et al., 2014). It has an N-terminal motor domain (19–375) followed by a long alpha -helical rod-shaped stalk predicted to form an interrupted coiled coil. The C-terminal region has been shown to contain a putative interacting region for actin (residues 743–1333) (Klejnot et al., 2014). Moreover in Hela cells, Kif15 has been shown to concentrate on spindle poles and microtubules in early mitosis and to localize with actin in late mitosis (Buster et al., 2003). One possibility is that Kif15 switches affinity from one

filament system to the other, while another possibility is that Kif15 may associate with the more abundant cytoskeletal filament system (Buster et al., 2003). In this study we mapped the EspW binding to a segment of Kif15, amino acids 1092-1142.

This segment is a known binding site for both Ki-67 (1017-1237) and actin (743-1333). The exact role of Kif15 during infection is still unclear as labelling of EspW in EPEC did not allow us to localize the effector during infection. However, its recruitment to the pedestal during EPEC infection is independent of EspW. We therefore hypothesize that Kif15 recruits EspW and determines its spatial distribution, similar to the function of NHERF1 or NHERF2 towards the effector Map (Martinez et al., 2010).

This scenario resembles that of Map, which contains a carboxy terminal PDZ (PSD-95/Dlg/ZO-1)-binding motif (Tonikian et al., 2008) that mediates binding of Map to the PDZ domain of Na+/H+ exchanger regulatory factor (NHERF1) (Alto et al., 2006), (Simpson et al., 2006b), which targets Map to the apical membrane. Depleting cells of NHERF1 abolished Map-induced filopodia formation, while deleting the PDZ-binding motif of Map resulted in a significant decrease in number of filopodia 30 min post infection (Berger et al., 2009). Unfortunately, we were unable to knockdown Kif15 and therefore it was not possible to establish a direct link between Kif15 and EspW-induced actin rearrangements however, $EspW_{I237A}$ is still able to bind Kif15 without inducing any actin reorganization suggesting that EspW used Kif15 to localize in a specific area.

Ectopic expression of EspW led to the formation of actin ruffles and aggregates in flower-shaped structures, reminiscent of those induced by Rac1. Indeed, in the presence of dominant negative Rac1 the ability of EspW to trigger formation of ruffles and flower-shaped structures was significantly attenuated.

The hallmark of EPEC and EHEC infection of cultured cells is formation of actin pedestal -like structures underneath the attached bacteria. In EPEC, formation of these structures is dependent on the effector Tir and activation of N-WASP and independent of activation of mammalian Rho GTPases (Ben-Ami et al., 1998). However, EspH, which is a global inhibitor of endogenous mammalian GEFs (Dong et al., 2010), is required for efficient actin pedestal elongation (Tu et al., 2003) suggesting that Rho GTPases may be partially involved in this process. Importantly, EPEC and EHEC translocate several effectors, belonging to the SopE family, which have a GEF activity towards mammalian Rho GTPases (Bulgin et al., 2010). In vitro, EspT which activates Rac1 triggers formation of ruffles or lamelipodia and in vivo it induces expression of KC and TNF-α (Raymond et al., 2011). In this study, we found that EspW also appears to activate Rac1, either directly or indirectly, in compartmentalised fashion; this is in contrast to EspT which has a more global effect.

Nonetheless, the phenotype of espW deletion could be partially complemented by *espT*, suggesting some activity overlap. Due to a poor solubility, we were not able to identify whether EspW directly activates Rac1. Importantly, multiple biological systems revealed that activation or inhibition of the Rho GTPase has to be fine-tuned both spatially and temporally. Their over activation or inhibition have detrimental effects leading to activation of alarm signals (Keestra et al., 2013) or apoptosis (Fiorentini et al., 2003). During EPEC infection activation of Cdc42 is limited to the bacterial binding sites (Berger et al., 2009); followed by rapid inhibition by Tir (Berger et al., 2009). The effector EspO expressed by a selection of EPEC and EHEC strains has been reported to inactivate EspM2 (RhoA GEF). Interestingly, deletion of *espO1* and *espO2* leads to cell shrinkage, in an EspM2 dependant manner (Morita-Ishihara et al., 2013). Rac1 and RhoA have antagonistic effects (Chauhan et

al., 2011). Interestingly, we found that cells infected with EHEC expressing EspM1 and EspM2 but missing EspW undergo cell shrinkage. This cell shrinkage phenotype was not associated with decreased cell attachment or with any signs of cell death, including nucleus condensation, loss of membrane permeability, or membrane blebbing, for the duration of the experiment. Interestingly, we found that EPEC and EHEC strains expressing EspM also express either EspT or EspW, suggesting that activation of RhoA and Rac1 need to be coordinated during infection. Furthermore, deletion of Rac1 impairs focal adhesion complex formation and cell spreading (Guo et al., 2006). Taken together, these observations suggest that EPEC and EHEC have developed a complex mechanism to control cell shape by manipulating the localization and activation of RhoA and Rac1. Any dysregulation leading to an uncontrolled activation leads to dramatic cell morphology changes. Further studies will be needed in order to understand the spatiotemporal regulation of the Rho GTP ase during EPEC and EHEC infections.

Despite sharing limited sequence identity with other effectors involved in actin dynamics, EspW has a QLSI motif similar QSSI motif of EspM2 and IpgB2. Substitution of Q124, located within the QSSI catalytic loop of EspM2, with alanine, greatly attenuated the RhoA GEF activity *in vitro* and the ability of EspM2 to induce stress fibres upon ectopic expression (Arbeloa et al., 2010). We investigated whether or not the Q234 and I237 residues in the QLSI motif of EspW are important for its activity. Ectopic expression of $EspW_{I237A}$, but not $EspW_{Q234A}$, does not induce the typical EspW actin rearrangements. Furthermore, complementation of the EHEC *ΔespW* mutant with a plasmid encoding $EspW_{I237A}$ did not reduce cell shrinkage in infected cells, despite the fact that it still binds Kif15 in yeast. In

accordance with these results we concluded that I237 residue is involved either directly in the protein function or is important for the integrity of the protein fold.

EHEC has developed sophisticated mechanisms to subvert Rho GTPase signalling pathways in a functionally co-ordinated manner. More work is required to dissect the mechanisms by which EspW activates Rac1.

In this study we found that *espW* is common amongst clinical EHEC and EPEC isolates. The majority of the EPEC strains contain the full length espW gene, while others, mainly belonging to EPEC O55:H7, encode a truncated EspW isoform. Although the truncated form of EspW does not induce actin reorganization, it is possible that it has other biological functions.

The fact that *espW* is not present in all EPEC clinical strains can suggest that it is still an emerging effector which might be acquire through horizontal gene transfer. A possible explanation for the presence of a shorter version of *espW* is in some of the EPEC strains might be that a part of the gene was lost during the phage-mediated lateral gene transfer processes.

Together these results add to our understanding of the pathogenesis and virulence mechanisms employed by EHEC during infection and demonstrate novel functions of EspW effector. Finally more screening and examination of EspW positive strains is required in order to fully understand its contribution to the clinical outcome of disease caused by the A/E pathogens.

Conclusion

In conclusion we have demonstrated that the novel A/E pathogen EspW triggers actin remodelling in a Rac1 dependent manner.

We hypothesise that that Kif15 recruits EspW to the pedestal where it locally activates Rac1.

References

ADU-BOBIE, J., FRANKEL, G., BAIN, C., GONCALVES, A. G., TRABULSI, L. R., DOUCE, G., KNUTTON, S. & DOUGAN, G. 1998. Detection of intimins alpha, beta, gamma, and delta, four intimin derivatives expressed by attaching and effacing microbial pathogens. *J. Clin. Microbiol.,* 36**,** 662-8.

AHUJA, R., PINYOL, R., REICHENBACH, N., CUSTER, L., KLINGENSMITH, J., KESSELS, M. M. & QUALMANN, B. 2007. Cordon-bleu is an actin nucleation factor and controls neuronal morphology. *Cell,* 131**,** 337-50.

AKEDA, Y. & GALAN, J. E. 2005. Chaperone release and unfolding of substrates in type III secretion. *Nature,* 437**,** 911-5.

ALTO, N. M., SHAO, F., LAZAR, C. S., BROST, R. L., CHUA, G., MATTOO, S., MCMAHON, S. A., GHOSH, P., HUGHES, T. R., BOONE, C. & DIXON, J. E. 2006. Identification of a bacterial type III effector family with G protein mimicry functions. *Cell,* 124**,** 133-45.

ALTO, N. M., WEFLEN, A. W., RARDIN, M. J., YARAR, D., LAZAR, C. S., TONIKIAN, R., KOLLER, A., TAYLOR, S. S., BOONE, C., SIDHU, S. S., SCHMID, S. L., HECHT, G. A. & DIXON, J. E. 2007. The type III effector EspF coordinates membrane trafficking by the spatiotemporal activation of two eukaryotic signaling pathways. *J Cell Biol,* 178**,** 1265-78.

AMANO, M., ITO, M., KIMURA, K., FUKATA, Y., CHIHARA, K., NAKANO, T., MATSUURA, Y. & KAIBUCHI, K. 1996. Phosphorylation and activation of myosin by Rho-associated kinase (Rho-kinase). *J Biol Chem,* 271**,** 20246-9.

ANTON, I. M., JONES, G. E., WANDOSELL, F., GEHA, R. & RAMESH, N. 2007. WASP-interacting protein (WIP): working in polymerisation and much more. *Trends Cell Biol,* 17**,** 555-62.

ARBELOA, A., BLANCO, M., MOREIRA, F. C., BULGIN, R., LOPEZ, C., DAHBI, G., BLANCO, J. E., MORA, A., ALONSO, M. P., MAMANI, R. C., GOMES, T. A., BLANCO, J. & FRANKEL, G. 2009. Distribution of espM and espT among enteropathogenic and enterohaemorrhagic Escherichia coli. *J Med Microbiol,* 58**,** 988-95.

ARBELOA, A., BULGIN, R. R., MACKENZIE, G., SHAW, R. K., PALLEN, M. J., CREPIN, V. F., BERGER, C. N. & FRANKEL, G. 2008. Subversion of actin dynamics by EspM effectors of attaching and effacing bacterial pathogens. *Cell Microbiol,* 10**,** 1429-41.

ARBELOA, A., GARNETT, J., LILLINGTON, J., BULGIN, R. R., BERGER, C. N., LEA, S. M., MATTHEWS, S. & FRANKEL, G. 2010. EspM2 is a RhoA guanine nucleotide exchange factor. *Cell Microbiol,* 12**,** 654-64.

ARBELOA, A., OATES, C. V., MARCHES, O., HARTLAND, E. L. & FRANKEL, G. 2011. Enteropathogenic and enterohemorrhagic Escherichia coli type III secretion effector EspV induces radical morphological changes in eukaryotic cells. *Infect Immun,* 79**,** 1067-76.

BALDINI, M. M., KAPER, J. B., LEVINE, M. M., CANDY, D. C. A. & MOON, H. W. 1983. Plasmid-mediated adhesion in enteropathogenic *Escherichia coli*. *J Pediatr Gastroenterol,* 2**,** 534-38.

BAMBURG, J. R. 1999. Proteins of the ADF/cofilin family: essential regulators of actin dynamics. *Annu Rev Cell Dev Biol,* 15**,** 185-230.

BARTHOLD, S. W., COLEMAN, G. L., BHATT, P. N., OSBALDISTON, G. W. & JONAS, A. M. 1976. The etiology of transmissible murine colonic hyperplasia. *Lab Anim Sci,* 26**,** 889-94.

BARUCH, K., GUR-ARIE, L., NADLER, C., KOBY, S., YERUSHALMI, G., BEN-NERIAH, Y., YOGEV, O., SHAULIAN, E., GUTTMAN, C., ZARIVACH, R. & ROSENSHINE, I. 2011. Metalloprotease type III effectors that specifically cleave JNK and NF-kappaB. *EMBO J,* 30**,** 221-31.

BERDICHEVSKY, T., FRIEDBERG, D., NADLER, C., ROKNEY, A., OPPENHEIM, A. & ROSENSHINE, I. 2005. Ler is a negative autoregulator of the LEE1 operon in enteropathogenic *Escherichia coli*. *J Bacteriol,* 187**,** 349-57.

BERGEN, L. G. & BORISY, G. G. 1980. Head-to-tail polymerization of microtubules in vitro. Electron microscope analysis of seeded assembly. *J Cell Biol,* 84**,** 141-50.
BERGER, C. N., CREPIN, V. F., JEPSON, M. A., ARBELOA, A. & FRANKEL, G. 2009. The mechanisms used by enteropathogenic Escherichia coli to control filopodia dynamics. *Cell Microbiol,* 11**,** 309-322.
BLANCHOIN, L., POLLARD, T. D. & MULLINS, R. D. 2000. Interactions of ADF/cofilin, Arp2/3 complex, capping protein and profilin in remodeling of branched actin filament networks. *Curr Biol,* 10**,** 1273-82.
BOISEN, N., STRUVE, C., SCHEUTZ, F., KROGFELT, K. A. & NATARO, J. P. 2008. New adhesin of enteroaggregative Escherichia coli related to the Afa/Dr/AAF family. *Infect Immun,* 76**,** 3281-92.
BOMMARIUS, B., MAXWELL, D., SWIMM, A., LEUNG, S., CORBETT, A., BORNMANN, W. & KALMAN, D. 2007. Enteropathogenic Escherichia coli Tir is an SH2/3 ligand that recruits and activates tyrosine kinases required for pedestal formation. *Mol Microbiol,* 63**,** 1748-68.
BONANNO, L., LOUKIADIS, E., MARIANI-KURKDJIAN, P., OSWALD, E., GARNIER, L., MICHEL, V. & AUVRAY, F. 2015. Diversity of Shiga Toxin-Producing Escherichia coli (STEC) O26:H11 Strains Examined via stx Subtypes and Insertion Sites of Stx and EspK Bacteriophages. *Appl Environ Microbiol,* 81**,** 3712-21.
BOQUET, P. 2000. Small GTP binding proteins and bacterial virulence. *Microbes Infect,* 2**,** 837-43.
BORDI, C., LAMY, M. C., VENTRE, I., TERMINE, E., HACHANI, A., FILLET, S., ROCHE, B., BLEVES, S., MEJEAN, V., LAZDUNSKI, A. & FILLOUX, A. 2010. Regulatory RNAs and the HptB/RetS signalling pathways fine-tune Pseudomonas aeruginosa pathogenesis. *Mol Microbiol,* 76**,** 1427-43.
BOSTICARDO, M., MARANGONI, F., AIUTI, A., VILLA, A. & GRAZIA RONCAROLO, M. 2009. Recent advances in understanding the pathophysiology of Wiskott-Aldrich syndrome. *Blood,* 113**,** 6288-95.
BRUNDAGE, L., HENDRICK, J. P., SCHIEBEL, E., DRIESSEN, A. J. & WICKNER, W. 1990. The purified E. coli integral membrane protein SecY/E is sufficient for reconstitution of SecA-dependent precursor protein translocation. *Cell,* 62**,** 649-57.
BULGIN, R., ARBELOA, A., GOULDING, D., DOUGAN, G., CREPIN, V. F., RAYMOND, B. & FRANKEL, G. 2009a. The T3SS effector EspT defines a new category of invasive enteropathogenic E. coli (EPEC) which form intracellular actin pedestals. *PLoS Pathog,* 5**,** e1000683.
BULGIN, R., RAYMOND, B., GARNETT, J. A., FRANKEL, G., CREPIN, V. F., BERGER, C. N. & ARBELOA, A. 2010. Bacterial guanine nucleotide exchange factors SopE-like and WxxxE effectors. *Infect Immun,* 78**,** 1417-25.
BULGIN, R. R., ARBELOA, A., CHUNG, J. C. & FRANKEL, G. 2009b. EspT triggers formation of lamellipodia and membrane ruffles through activation of Rac-1 and Cdc42. *Cell Microbiol,* 11**,** 217-229.
BUSTER, D. W., BAIRD, D. H., YU, W., SOLOWSKA, J. M., CHAUVIERE, M., MAZUREK, A., KRESS, M. & BAAS, P. W. 2003. Expression of the mitotic kinesin Kif15 in postmitotic neurons: implications for neuronal migration and development. *J Neurocytol,* 32**,** 79-96.
CAMPELLONE, K., ROBBINS, D. & LEONG, J. 2004a. EspF(U) is a translocated EHEC effector that interacts with Tir and N-WASP and promotes Nck-independent actin assembly. *Dev Cell.,* 7**,** 217-28.
CAMPELLONE, K. G., GIESE, A., TIPPER, D. J. & LEONG, J. M. 2002. A tyrosine-phosphorylated 12-amino-acid sequence of enteropathogenic Escherichia coli Tir binds the host adaptor protein Nck and is required for Nck localization to actin pedestals. *Mol Microbiol,* 43**,** 1227-41.
CAMPELLONE, K. G. & LEONG, J. M. 2005. Nck-independent actin assembly is mediated by two phosphorylated tyrosines within enteropathogenic Escherichia coli Tir. *Mol Microbiol,* 56**,** 416-32.

CAMPELLONE, K. G., RANKIN, S., PAWSON, T., KIRSCHNER, M. W., TIPPER, D. J. & LEONG, J. M. 2004b. Clustering of Nck by a 12-residue Tir phosphopeptide is sufficient to trigger localized actin assembly. *J Cell Biol,* 164**,** 407-16.

CAMPELLONE, K. G., WEBB, N. J., ZNAMEROSKI, E. A. & WELCH, M. D. 2008. WHAMM is an Arp2/3 complex activator that binds microtubules and functions in ER to Golgi transport. *Cell,* 134**,** 148-61.

CAMPELLONE, K. G. & WELCH, M. D. 2010. A nucleator arms race: cellular control of actin assembly. *Nat Rev Mol Cell Biol,* 11**,** 237-51.

CARON, E., CREPIN, V. F., SIMPSON, N., KNUTTON, S., GARMENDIA, J. & FRANKEL, G. 2006. Subversion of actin dynamics by EPEC and EHEC. *Curr Opin Microbiol.,* 9**,** 40-5.

CHAN, C., BELTZNER, C. C. & POLLARD, T. D. 2009. Cofilin dissociates Arp2/3 complex and branches from actin filaments. *Curr Biol,* 19**,** 537-45.

CHAVEZ, C. V., JUBELIN, G., COURTIES, G., GOMARD, A., GINIBRE, N., PAGES, S., TAIEB, F., GIRARD, P. A., OSWALD, E., GIVAUDAN, A., ZUMBIHL, R. & ESCOUBAS, J. M. 2010. The cyclomodulin Cif of Photorhabdus luminescens inhibits insect cell proliferation and triggers host cell death by apoptosis. *Microbes Infect,* 12**,** 1208-18.

CHEN, H. D. & FRANKEL, G. 2005. Enteropathogenic *Escherichia coli*: unravelling pathogenesis. *FEMS Microbiol Rev,* 29**,** 83-98.

CHEREAU, D., BOCZKOWSKA, M., SKWAREK-MARUSZEWSKA, A., FUJIWARA, I., HAYES, D. B., REBOWSKI, G., LAPPALAINEN, P., POLLARD, T. D. & DOMINGUEZ, R. 2008. Leiomodin is an actin filament nucleator in muscle cells. *Science,* 320**,** 239-43.

CHIU, H. J. & SYU, W. J. 2005. Functional analysis of EspB from enterohaemorrhagic *Escherichia coli*. *Microbiology,* 151**,** 3277-86.

CHRISTIE, P. J. & CASCALES, E. 2005. Structural and dynamic properties of bacterial type IV secretion systems (review). *Mol Membr Biol,* 22**,** 51-61.

CHRISTIE, P. J., WHITAKER, N. & GONZALEZ-RIVERA, C. 2014. Mechanism and structure of the bacterial type IV secretion systems. *Biochim Biophys Acta,* 1843**,** 1578-91.

CIANCIOTTO, N. P. 2005. Type II secretion: a protein secretion system for all seasons. *Trends Microbiol,* 13**,** 581-8.

CLEMENTS, A., SMOLLETT, K., LEE, S. F., HARTLAND, E. L., LOWE, M. & FRANKEL, G. 2011. EspG of enteropathogenic and enterohemorrhagic E. coli binds the Golgi matrix protein GM130 and disrupts the Golgi structure and function. *Cell Microbiol,* 13**,** 1429-39.

CONDE, C. & CACERES, A. 2009. Microtubule assembly, organization and dynamics in axons and dendrites. *Nat Rev Neurosci,* 10**,** 319-32.

CONDEELIS, J. 2001. How is actin polymerization nucleated in vivo? *Trends Cell Biol,* 11**,** 288-93.

COOPER, J. A. & SCHAFER, D. A. 2000. Control of actin assembly and disassembly at filament ends. *Curr Opin Cell Biol,* 12**,** 97-103.

COOPER, K. K., MANDRELL, R. E., LOUIE, J. W., KORLACH, J., CLARK, T. A., PARKER, C. T., HUYNH, S., CHAIN, P. S., AHMED, S. & CARTER, M. Q. 2014. Comparative genomics of enterohemorrhagic Escherichia coli O145:H28 demonstrates a common evolutionary lineage with Escherichia coli O157:H7. *BMC Genomics,* 15**,** 17.

CORNELIS, G. R. 2006. The type III secretion injectisome. *Nat Rev Microbiol,* 4**,** 811-25.

COTE, J. F. & VUORI, K. 2007. GEF what? Dock180 and related proteins help Rac to polarize cells in new ways. *Trends Cell Biol,* 17**,** 383-93.

COTE, R., KATANI, R., MOREAU, M. R., KUDVA, I. T., ARTHUR, T. M., DEBROY, C., MWANGI, M. M., ALBERT, I., RAYGOZA GARAY, J. A., LI, L., BRANDL, M. T., CARTER, M. Q. & KAPUR, V. 2015. Comparative analysis of super-shedder strains of Escherichia coli O157:H7 reveals distinctive genomic features and a strongly aggregative adherent phenotype on bovine rectoanal junction squamous epithelial cells. *PLoS One,* 10**,** e0116743.

CRAMER, L. P. 1997. Molecular mechanism of actin-dependent retrograde flow in lamellipodia of motile cells. *Front Biosci,* 2**,** d260-70.

CREASEY, E. A., DELAHAY, R. M., DANIELL, S. J. & FRANKEL, G. 2003a. Yeast two-hybrid system survey of interactions between LEE-encoded proteins of enteropathogenic *Escherichia coli. Microbiology,* 149**,** 2093-2106.

CREASEY, E. A., FRIEDBERG, D., SHAW, R. K., UMANSKI, T., KNUTTON, S., ROSENSHINE, I. & FRANKEL, G. 2003b. CesAB is an enteropathogenic Escherichia coli chaperone for the type-III translocator proteins EspA and EspB. *Microbiology,* 149**,** 3639-47.

CREPIN, V. F., HABIBZAY, M., GLEGOLA-MADEJSKA, I., GUENOT, M., COLLINS, J. W. & FRANKEL, G. 2015. Tir Triggers Expression of CXCL1 in Enterocytes and Neutrophil Recruitment during Citrobacter rodentium Infection. *Infect Immun,* 83**,** 3342-54.

CREPIN, V. F., PRASANNAN, S., SHAW, R. K., WILSON, R. K., CREASEY, E., ABE, C. M., KNUTTON, S., FRANKEL, G. & MATTHEWS, S. 2005. Structural and functional studies of the enteropathogenic Escherichia coli type III needle complex protein EscJ. *Mol Microbiol,* 55**,** 1658-70.

DAHAN, S., WILES, S., LA RAGIONE, R. M., BEST, A., WOODWARD, M. J., STEVENS, M. P., SHAW, R. K., CHONG, Y., KNUTTON, S., PHILLIPS, A. & FRANKEL, G. 2005. EspJ Is a prophage-carried type III effector protein of attaching and effacing pathogens that modulates infection dynamics. *Infect Immun,* 73**,** 679-86.

DANIELL, S. J., KOCSIS, E., MORRIS, E., KNUTTON, S., BOOY, F. P. & FRANKEL, G. 2003. 3D structure of EspA filaments from enteropathogenic *Escherichia coli. Mol Microbiol,* 49**,** 301-308.

DATSENKO, K. A. & WANNER, B. L. 2000. One-step inactivation of chromosomal genes in Escherichia coli K-12 using PCR products. *Proc Natl Acad Sci U S A,* 97**,** 6640-5.

DAUTIN, N. & BERNSTEIN, H. D. 2007. Protein secretion in gram-negative bacteria via the autotransporter pathway. *Annu Rev Microbiol,* 61**,** 89-112.

DE LA FUENTE, M. A., SASAHARA, Y., CALAMITO, M., ANTON, I. M., ELKHAL, A., GALLEGO, M. D., SURESH, K., SIMINOVITCH, K., OCHS, H. D., ANDERSON, K. C., ROSEN, F. S., GEHA, R. S. & RAMESH, N. 2007. WIP is a chaperone for Wiskott-Aldrich syndrome protein (WASP). *Proc Natl Acad Sci U S A,* 104**,** 926-31.

DEAN, P. & KENNY, B. 2009. The effector repertoire of enteropathogenic E. coli: ganging up on the host cell. *Curr Opin Microbiol,* 12**,** 101-9.

DEAN, P., MARESCA, M., SCHULLER, S., PHILLIPS, A. D. & KENNY, B. 2006. Potent diarrheagenic mechanism mediated by the cooperative action of three enteropathogenic Escherichia coli-injected effector proteins. *Proc Natl Acad Sci U S A,* 103**,** 1876-81.

DEAN, P., SCOTT, J. A., KNOX, A. A., QUITARD, S., WATKINS, N. J. & KENNY, B. 2010. The enteropathogenic E. coli effector EspF targets and disrupts the nucleolus by a process regulated by mitochondrial dysfunction. *PLoS Pathog,* 6**,** e1000961.

DEBROY, C., ROBERTS, E. & FRATAMICO, P. M. 2011. Detection of O antigens in Escherichia coli. *Anim Health Res Rev,* 12**,** 169-85.

DELEPELAIRE, P. 2004. Type I secretion in gram-negative bacteria. *Biochim Biophys Acta,* 1694**,** 149-61.

DENG, W., LI, Y., HARDWIDGE, P. R., FREY, E. A., PFUETZNER, R. A., LEE, S., GRUENHEID, S., STRYNAKDA, N. C., PUENTE, J. L. & FINLAY, B. B. 2005. Regulation of type III secretion hierarchy of translocators and effectors in attaching and effacing bacterial pathogens. *Infect Immun,* 73**,** 2135-46.

DENG, W., YU, H. B., LI, Y. & FINLAY, B. B. 2015. SepD/SepL-dependent secretion signals of the type III secretion system translocator proteins in enteropathogenic Escherichia coli. *J Bacteriol,* 197**,** 1263-75.

DERMARDIROSSIAN, C. & BOKOCH, G. M. 2005. GDIs: central regulatory molecules in Rho GTPase activation. *Trends Cell Biol,* 15**,** 356-63.

DEVINNEY, R., KNOECHEL, D. G. & FINLAY, B. B. 1999. Enteropathogenic *Escherichia coli*: cellular harassment. *Current Opinion in Microbiology,* 2**,** 83-8.

DOBRINDT, U., CHOWDARY, M. G., KRUMBHOLZ, G. & HACKER, J. 2010. Genome dynamics and its impact on evolution of Escherichia coli. *Med Microbiol Immunol,* 199**,** 145-54.
DOLEZAL, P., AILI, M., TONG, J., JIANG, J. H., MAROBBIO, C. M., LEE, S. F., SCHUELEIN, R., BELLUZZO, S., BINOVA, E., MOUSNIER, A., FRANKEL, G., GIANNUZZI, G., PALMIERI, F., GABRIEL, K., NADERER, T., HARTLAND, E. L. & LITHGOW, T. 2012. Legionella pneumophila secretes a mitochondrial carrier protein during infection. *PLoS Pathog,* 8**,** e1002459.
DONG, N., LIU, L. & SHAO, F. 2010. A bacterial effector targets host DH-PH domain RhoGEFs and antagonizes macrophage phagocytosis. *EMBO J,* 29**,** 1363-76.
DONNENBERG, M. S. & KAPER, J. B. 1992. Enteropathogenic Escherichia coli. *Infect Immun,* 60**,** 3953-61.
DOUZI, B., BALL, G., CAMBILLAU, C., TEGONI, M. & VOULHOUX, R. 2011. Deciphering the Xcp Pseudomonas aeruginosa type II secretion machinery through multiple interactions with substrates. *J Biol Chem,* 286**,** 40792-801.
DOVAS, A. & COUCHMAN, J. R. 2005. RhoGDI: multiple functions in the regulation of Rho family GTPase activities. *Biochem J,* 390**,** 1-9.
DOWNING, K. H. & NOGALES, E. 2010. Cryoelectron microscopy applications in the study of tubulin structure, microtubule architecture, dynamics and assemblies, and interaction of microtubules with motors. *Methods Enzymol,* 483**,** 121-42.
DRECHSLER, H., MCHUGH, T., SINGLETON, M. R., CARTER, N. J. & MCAINSH, A. D. 2014. The Kinesin-12 Kif15 is a processive track-switching tetramer. *Elife,* 3**,** e01724.
DRIESSEN, A. J. & NOUWEN, N. 2008. Protein translocation across the bacterial cytoplasmic membrane. *Annu Rev Biochem,* 77**,** 643-67.
ECHTENKAMP, F., DENG, W., WICKHAM, M. E., VAZQUEZ, A., PUENTE, J. L., THANABALASURIAR, A., GRUENHEID, S., FINLAY, B. B. & HARDWIDGE, P. R. 2008. Characterization of the NleF effector protein from attaching and effacing bacterial pathogens. *FEMS Microbiol Lett,* 281**,** 98-107.
ECONOMOU, A. & WICKNER, W. 1994. SecA promotes preprotein translocation by undergoing ATP-driven cycles of membrane insertion and deinsertion. *Cell,* 78**,** 835-43.
EDEN, S., ROHATGI, R., PODTELEJNIKOV, A. V., MANN, M. & KIRSCHNER, M. W. 2002. Mechanism of regulation of WAVE1-induced actin nucleation by Rac1 and Nck. *Nature,* 418**,** 790-3.
EDWARDS, D. C., SANDERS, L. C., BOKOCH, G. M. & GILL, G. N. 1999. Activation of LIM-kinase by Pak1 couples Rac/Cdc42 GTPase signalling to actin cytoskeletal dynamics. *Nat Cell Biol,* 1**,** 253-9.
EKLUND, M., LEINO, K. & SIITONEN, A. 2002. Clinical Escherichia coli strains carrying stx genes: stx variants and stx-positive virulence profiles. *J Clin Microbiol,* 40**,** 4585-93.
ELLIOTT, S. J., KREJANY, E. O., MELLIES, J. L., ROBINS-BROWNE, R. M., SASAKAWA, C. & KAPER, J. B. 2001. EspG, a novel type III system-secreted protein from enteropathogenic Escherichia coli with similarities to VirA of Shigella flexneri. *Infect Immun,* 69**,** 4027-33.
ELLIOTT, S. J., WAINWRIGHT, L. A., MCDANIEL, T. K., JARVIS, K. G., DENG, Y., LAI, L., MCNAMARA, B. P., DONNENBERG, M. S. & KAPER, J. B. 1998. The complete sequence of the locus of enterocyte effacement (LEE) from enteropathogenic *Escherichia coli* E2348/69. *Mol Microbiol,* 28**,** 1-4.
ETIENNE-MANNEVILLE, S. & HALL, A. 2002. Rho GTPases in cell biology. *Nature,* 420**,** 629-35.
EVDOKIMOV, A. G., TROPEA, J. E., ROUTZAHN, K. M. & WAUGH, D. S. 2002. Crystal structure of the Yersinia pestis GTPase activator YopE. *Protein Sci,* 11**,** 401-8.
FAIX, J. & ROTTNER, K. 2006. The making of filopodia. *Curr Opin Cell Biol,* 18**,** 18-25.
FASANO, A., NORIEGA, F. R., MANEVAL, D. R., JR., CHANASONGCRAM, S., RUSSELL, R., GUANDALINI, S. & LEVINE, M. M. 1995. Shigella enterotoxin 1: an enterotoxin of Shigella flexneri 2a active in rabbit small intestine in vivo and in vitro. *J Clin Invest,* 95**,** 2853-61.
FELISBERTO-RODRIGUES, C., DURAND, E., ASCHTGEN, M. S., BLANGY, S., ORTIZ-LOMBARDIA, M., DOUZI, B., CAMBILLAU, C. & CASCALES, E. 2011. Towards a structural comprehension of

bacterial type VI secretion systems: characterization of the TssJ-TssM complex of an Escherichia coli pathovar. *PLoS Pathog,* 7**,** e1002386.
FIDYK, N. J. & CERIONE, R. A. 2002. Understanding the catalytic mechanism of GTPase-activating proteins: demonstration of the importance of switch domain stabilization in the stimulation of GTP hydrolysis. *Biochemistry,* 41**,** 15644-53.
FILLOUX, A. 2004. The underlying mechanisms of type II protein secretion. *Biochim Biophys Acta,* 1694**,** 163-79.
FILLOUX, A., HACHANI, A. & BLEVES, S. 2008. The bacterial type VI secretion machine: yet another player for protein transport across membranes. *Microbiology,* 154**,** 1570-83.
FINLAY, B. B. 2005. Bacterial virulence strategies that utilize Rho GTPases. *Curr Top Microbiol Immunol,* 291**,** 1-10.
FRANKEL, G., PHILIPS, A. D., NOVAKOVA, M., BATCHELOR, M., HICKS, S. & DOUGAN, G. 1998a. Generation of Escherichia coli intimin derivatives with differing biological activities using site-directed mutagenesis of the intimin C-terminus domain. *Mol Microbiol,* 29**,** 559-70.
FRANKEL, G. & PHILLIPS, A. D. 2008. Attaching effacing Escherichia coli and paradigms of Tir-triggered actin polymerization: getting off the pedestal. *Cell Microbiol,* 10**,** 549-56.
FRANKEL, G., PHILLIPS, A. D., ROSENSHINE, I., DOUGAN, G., KAPER, J. B. & KNUTTON, S. 1998b. Enteropathogenic and enterohemorrhagic Escherichia coli: more subversive elements. *Mol Microbiol,* 30**,** 911-21.
FRANKEL, G., PHILLIPS, A. D., TRABULSI, L. R., KNUTTON, S., DOUGAN, G. & MATTHEWS, S. 2001. Intimin and the host cell - is it bound to end in Tir(s)? *Trends Microbiol,* 9**,** 214-218.
FRANZIN, F. M. & SIRCILI, M. P. 2015. Locus of enterocyte effacement: a pathogenicity island involved in the virulence of enteropathogenic and enterohemorragic Escherichia coli subjected to a complex network of gene regulation. *Biomed Res Int,* 2015**,** 534738.
FRONZES, R., CHRISTIE, P. J. & WAKSMAN, G. 2009a. The structural biology of type IV secretion systems. *Nat Rev Microbiol,* 7**,** 703-14.
FRONZES, R., SCHAFER, E., WANG, L., SAIBIL, H. R., ORLOVA, E. V. & WAKSMAN, G. 2009b. Structure of a type IV secretion system core complex. *Science,* 323**,** 266-8.
FU, Y. & GALAN, J. E. 1999. A salmonella protein antagonizes Rac-1 and Cdc42 to mediate host-cell recovery after bacterial invasion. *Nature,* 401**,** 293-7.
FUKATA, M., NAKAGAWA, M. & KAIBUCHI, K. 2003. Roles of Rho-family GTPases in cell polarisation and directional migration. *Curr Opin Cell Biol,* 15**,** 590-7.
GALAN, J. E., GINOCCHIO, C. & COSTEAS, P. 1992. Molecular and functional characterization of the Salmonella invasion gene invA: homology of InvA to members of a new protein family. *J Bacteriol,* 174**,** 4338-49.
GALAN, J. E. & WOLF-WATZ, H. 2006. Protein delivery into eukaryotic cells by type III secretion machines. *Nature,* 444**,** 567-73.
GARCIA-ANGULO, V. A., DENG, W., THOMAS, N. A., FINLAY, B. B. & PUENTE, J. L. 2008. Regulation of expression and secretion of NleH, a new non-locus of enterocyte effacement-encoded effector in Citrobacter rodentium. *J Bacteriol,* 190**,** 2388-99.
GARCIA-ANGULO, V. A., MARTINEZ-SANTOS, V. I., VILLASENOR, T., SANTANA, F. J., HUERTA-SAQUERO, A., MARTINEZ, L. C., JIMENEZ, R., LARA-OCHOA, C., TELLEZ-SOSA, J., BUSTAMANTE, V. H. & PUENTE, J. L. 2012. A distinct regulatory sequence is essential for the expression of a subset of nle genes in attaching and effacing Escherichia coli. *J Bacteriol,* 194**,** 5589-603.
GARMENDIA, J., CARLIER, M. F., EGILE, C., DIDRY, D. & FRANKEL, G. 2006. Characterization of TccP-mediated N-WASP activation during enterohaemorrhagic *Escherichia coli* infection. *Cell Microbiol.,* 8**,** 1444-55.
GARMENDIA, J. & FRANKEL, G. 2005. Operon structure and gene expression of the espJ--tccP locus of enterohaemorrhagic Escherichia coli O157:H7. *FEMS Microbiol Lett,* 247**,** 137-45.

GARMENDIA, J., FRANKEL, G. & CREPIN, V. F. 2005. Enteropathogenic and enterohemorrhagic Escherichia coli infections: translocation, translocation, translocation. *Infect Immun,* 73**,** 2573-85.

GAUTHIER, A., ROBERTSON, M. L., LOWDEN, M., IBARRA, J. A., PUENTE, J. L. & FINLAY, B. B. 2005. Transcriptional inhibitor of virulence factors in enteropathogenic *Escherichia coli*. *Antimicrob Agents Chemother,* 49**,** 4101-9.

GAUTHIER, A., THOMAS, N. A. & FINLAY, B. B. 2003. Bacterial injection machines. *J Biol Chem,* 278**,** 25273-6.

GAUTREAU, A., HO, H. Y., LI, J., STEEN, H., GYGI, S. P. & KIRSCHNER, M. W. 2004. Purification and architecture of the ubiquitous Wave complex. *Proc Natl Acad Sci U S A,* 101**,** 4379-83.

GIRAO, H., GELI, M. I. & IDRISSI, F. Z. 2008. Actin in the endocytic pathway: from yeast to mammals. *FEBS Lett,* 582**,** 2112-9.

GIRÓN, J. A., HO, A. S. & SCHOOLNIK, G. K. 1991. An inducible bundle-forming pilus of enteropathogenic Escherichia coli. *Science,* 254**,** 710-3.

GLOTFELTY, L. G., ZAHS, A., HODGES, K., SHAN, K., ALTO, N. M. & HECHT, G. A. 2014. Enteropathogenic E. coli effectors EspG1/G2 disrupt microtubules, contribute to tight junction perturbation and inhibit restoration. *Cell Microbiol,* 16**,** 1767-83.

GOLDMANN, W. H. 2008. Actin: A molecular wire, an electrical cable? *Cell Biol Int,* 32**,** 869-70.

GONZALEZ, E., KOU, R. & MICHEL, T. 2006. Rac1 modulates sphingosine 1-phosphate-mediated activation of phosphoinositide 3-kinase/Akt signaling pathways in vascular endothelial cells. *J Biol Chem,* 281**,** 3210-6.

GOODE, B. L. & ECK, M. J. 2007. Mechanism and function of formins in the control of actin assembly. *Annu Rev Biochem,* 76**,** 593-627.

GOOSNEY, D. L., CELLI, J., KENNY, B. & FINLAY, B. B. 1999. Enteropathogenic *Escherichia coli* inhibits phagocytosis. *Infect Immun,* 67**,** 490-95.

GOSSER, Y. Q., NOMANBHOY, T. K., AGHAZADEH, B., MANOR, D., COMBS, C., CERIONE, R. A. & ROSEN, M. K. 1997. C-terminal binding domain of Rho GDP-dissociation inhibitor directs N-terminal inhibitory peptide to GTPases. *Nature,* 387**,** 814-9.

GRISHIN, A. M., CHERNEY, M., ANDERSON, D. H., PHANSE, S., BABU, M. & CYGLER, M. 2014. NleH defines a new family of bacterial effector kinases. *Structure,* 22**,** 250-9.

GRUENHEID, S., DEVINNEY, R., BLADT, F., GOOSNEY, D., GELKOP, S., GISH, G. D., PAWSON, T. & FINLAY, B. B. 2001. Enteropathogenic E. coli Tir binds Nck to initiate actin pedestal formation in host cells. *Nat Cell Biol,* 3**,** 856-9.

GRUENHEID, S., SEKIROV, I., THOMAS, N. A., DENG, W., O'DONNELL, P., GOODE, D., LI, Y., FREY, E. A., BROWN, N. F., METALNIKOV, P., PAWSON, T., ASHMAN, K. & FINLAY, B. B. 2004. Identification and characterization of NleA, a non-LEE-encoded type III translocated virulence factor of enterohaemorrhagic Escherichia coli O157:H7. *Mol Microbiol,* 51**,** 1233-49.

GUIGNOT, J., PEIFFER, I., BERNET-CAMARD, M. F., LUBLIN, D. M., CARNOY, C., MOSELEY, S. L. & SERVIN, A. L. 2000. Recruitment of CD55 and CD66e brush border-associated glycosylphosphatidylinositol-anchored proteins by members of the Afa/Dr diffusely adhering family of Escherichia coli that infect the human polarized intestinal Caco-2/TC7 cells. *Infect Immun,* 68**,** 3554-63.

HALL, A. 1998. Rho GTPases and the actin cytoskeleton. *Science,* 279**,** 509-14.

HAMAGUCHI, M., HAMADA, D., SUZUKI, K. N., SAKATA, I. & YANAGIHARA, I. 2008. Molecular basis of actin reorganization promoted by binding of enterohaemorrhagic Escherichia coli EspB to alpha-catenin. *FEBS J,* 275**,** 6260-7.

HARDT, W. D., CHEN, L. M., SCHUEBEL, K. E., BUSTELO, X. R. & GALAN, J. E. 1998. S. typhimurium encodes an activator of Rho GTPases that induces membrane ruffling and nuclear responses in host cells. *Cell,* 93**,** 815-26.

HARRINGTON, S. M., DUDLEY, E. G. & NATARO, J. P. 2006. Pathogenesis of enteroaggregative Escherichia coli infection. *FEMS Microbiol Lett,* 254**,** 12-8.

HARTLAND, E. L., BATCHELOR, M., DELAHAY, R. M., HALE, C., MATTHEWS, S., DOUGAN, G., KNUTTON, S., CONNERTON, I. & FRANKEL, G. 1999. Binding of intimin from enteropathogenic Escherichia coli to Tir and to host cells. *Mol Microbiol,* 32**,** 151-8.

HAYASHI, T., MAKINO, K., OHNISHI, M., KUROKAWA, K., ISHII, K., YOKOYAMA, K., HAN, C. G., OHTSUBO, E., NAKAYAMA, K., MURATA, T., TANAKA, M., TOBE, T., IIDA, T., TAKAMI, H., HONDA, T., SASAKAWA, C., OGASAWARA, N., YASUNAGA, T., KUHARA, S., SHIBA, T., HATTORI, M. & SHINAGAWA, H. 2001. Complete genome sequence of enterohemorrhagic Escherichia coli O157:H7 and genomic comparison with a laboratory strain K-12. *DNA Res,* 8**,** 11-22.

HAYWARD, R. D., HUME, P. J., HUMPHREYS, D., PHILLIPS, N., SMITH, K. & KORONAKIS, V. 2009. Clustering transfers the translocated Escherichia coli receptor into lipid rafts to stimulate reversible activation of c-Fyn. *Cell Microbiol,* 11**,** 433-41.

HEASMAN, S. J. & RIDLEY, A. J. 2008. Mammalian Rho GTPases: new insights into their functions from in vivo studies. *Nat Rev Mol Cell Biol,* 9**,** 690-701.

HEMRAJANI, C., BERGER, C. N., ROBINSON, K. S., MARCHES, O., MOUSNIER, A. & FRANKEL, G. 2010. NleH effectors interact with Bax inhibitor-1 to block apoptosis during enteropathogenic Escherichia coli infection. *Proc Natl Acad Sci U S A,* 107**,** 3129-34.

HEMRAJANI, C., MARCHES, O., WILES, S., GIRARD, F., DENNIS, A., DZIVA, F., BEST, A., PHILLIPS, A. D., BERGER, C. N., MOUSNIER, A., CREPIN, V. F., KRUIDENIER, L., WOODWARD, M. J., STEVENS, M. P., LA RAGIONE, R. M., MACDONALD, T. T. & FRANKEL, G. 2008. Role of NleH, a type III secreted effector from attaching and effacing pathogens, in colonization of the bovine, ovine, and murine gut. *Infect Immun,* 76**,** 4804-13.

HENDERSON, I. R., NAVARRO-GARCIA, F., DESVAUX, M., FERNANDEZ, R. C. & ALA'ALDEEN, D. 2004. Type V protein secretion pathway: the autotransporter story. *Microbiol Mol Biol Rev.,* 68**,** 692-744.

HERNANDES, R. T., SILVA, R. M., CARNEIRO, S. M., SALVADOR, F. A., FERNANDES, M. C., PADOVAN, A. C., YAMAMOTO, D., MORTARA, R. A., ELIAS, W. P., DA SILVA BRIONES, M. R. & GOMES, T. A. 2008. The localized adherence pattern of an atypical enteropathogenic Escherichia coli is mediated by intimin omicron and unexpectedly promotes HeLa cell invasion. *Cell Microbiol,* 10**,** 415-25.

HEROLD, S., KARCH, H. & SCHMIDT, H. 2004. Shiga toxin-encoding bacteriophages--genomes in motion. *Int J Med Microbiol,* 294**,** 115-21.

HIROKAWA, N., PFISTER, K. K., YORIFUJI, H., WAGNER, M. C., BRADY, S. T. & BLOOM, G. S. 1989. Submolecular domains of bovine brain kinesin identified by electron microscopy and monoclonal antibody decoration. *Cell,* 56**,** 867-78.

HODGES, K., ALTO, N. M., RAMASWAMY, K., DUDEJA, P. K. & HECHT, G. 2008. The enteropathogenic Escherichia coli effector protein EspF decreases sodium hydrogen exchanger 3 activity. *Cell Microbiol,* 10**,** 1735-45.

HODGSON, A., WIER, E. M., FU, K., SUN, X., YU, H., ZHENG, W., SHAM, H. P., JOHNSON, K., BAILEY, S., VALLANCE, B. A. & WAN, F. 2015. Metalloprotease NleC suppresses host NF-kappaB/inflammatory responses by cleaving p65 and interfering with the p65/RPS3 interaction. *PLoS Pathog,* 11**,** e1004705.

HOFFMAN, G. R., NASSAR, N. & CERIONE, R. A. 2000. Structure of the Rho family GTP-binding protein Cdc42 in complex with the multifunctional regulator RhoGDI. *Cell,* 100**,** 345-56.

HOLLAND, I. B., SCHMITT, L. & YOUNG, J. 2005. Type 1 protein secretion in bacteria, the ABC-transporter dependent pathway (review). *Mol Membr Biol,* 22**,** 29-39.

HUANG, D. B., MOHANTY, A., DUPONT, H. L., OKHUYSEN, P. C. & CHIANG, T. 2006. A review of an emerging enteric pathogen: enteroaggregative Escherichia coli. *J Med Microbiol,* 55**,** 1303-11.

HUANG, Z., SUTTON, S. E., WALLENFANG, A. J., ORCHARD, R. C., WU, X., FENG, Y., CHAI, J. & ALTO, N. M. 2009. Structural insights into host GTPase isoform selection by a family of bacterial GEF mimics. *Nat Struct Mol Biol,* 16**,** 853-60.

IGUCHI, A., THOMSON, N. R., OGURA, Y., SAUNDERS, D., OOKA, T., HENDERSON, I. R., HARRIS, D., ASADULGHANI, M., KUROKAWA, K., DEAN, P., KENNY, B., QUAIL, M. A., THURSTON, S., DOUGAN, G., HAYASHI, T., PARKHILL, J. & FRANKEL, G. 2009. Complete genome sequence and comparative genome analysis of enteropathogenic Escherichia coli O127:H6 strain E2348/69. *J Bacteriol,* 191**,** 347-54.

IIZUMI, Y., SAGARA, H., KABE, Y., AZUMA, M., KUME, K., OGAWA, M., NAGAI, T., GILLESPIE, P. G., SASAKAWA, C. & HANDA, H. 2007. The enteropathogenic E. coli effector EspB facilitates microvillus effacing and antiphagocytosis by inhibiting myosin function. *Cell Host Microbe,* 2**,** 383-92.

INNOCENTI, M., GERBOTH, S., ROTTNER, K., LAI, F. P., HERTZOG, M., STRADAL, T. E., FRITTOLI, E., DIDRY, D., POLO, S., DISANZA, A., BENESCH, S., DI FIORE, P. P., CARLIER, M. F. & SCITA, G. 2005. Abi1 regulates the activity of N-WASP and WAVE in distinct actin-based processes. *Nat Cell Biol,* 7**,** 969-76.

IYODA, S., KOIZUMI, N., SATOU, H., LU, Y., SAITOH, T., OHNISHI, M. & WATANABE, H. 2006. The GrlR-GrlA regulatory system coordinately controls the expression of flagellar and LEE-encoded type III protein secretion systems in enterohemorrhagic *Escherichia coli*. *J. Bacteriol.,* 188**,** 5682-5692.

JAFFE, A. B. & HALL, A. 2005. Rho GTPases: biochemistry and biology. *Annu Rev Cell Dev Biol,* 21**,** 247-69.

JANK, T., GIESEMANN, T. & AKTORIES, K. 2007. Rho-glucosylating Clostridium difficile toxins A and B: new insights into structure and function. *Glycobiology,* 17**,** 15R-22R.

JELENSKA, J., KANG, Y. & GREENBERG, J. T. 2014. Plant pathogenic bacteria target the actin microfilament network involved in the trafficking of disease defense components. *Bioarchitecture,* 4**,** 149-53.

JENKINS, C., CHART, H., SMITH, H. R., HARTLAND, E. L., BATCHELOR, M., DELAHAY, R. M., DOUGAN, G. & FRANKEL, G. 2000. Antibody response of patients infected with verocytotoxin-producing Escherichia coli to protein antigens encoded on the LEE locus. *J Med Microbiol,* 49**,** 97-101.

JERSE, A. E., YU, J., TALL, B. D. & KAPER, J. B. 1990. A genetic locus of enteropathogenic Escherichia coli necessary for the production of attaching and effacing lesions on tissue culture cells. *Proc Natl Acad Sci USA,* 87**,** 7839-43.

KALMAN, D., WEINER, O. D., GOOSNEY, D. L., SEDAT, J. W., FINLAY, B. B., ABO, A. & BISHOP, J. M. 1999. Enteropathogenic E. coli acts through WASP and Arp2/3 complex to form actin pedestals. *Nat Cell Biol,* 1**,** 389-91.

KANACK, K. J., CRAWFORD, J. A., TATSUNO, I., KARMALI, M. A. & KAPER, J. B. 2005. SepZ/EspZ is secreted and translocated into HeLa cells by the enteropathogenic *Escherichia coli* type III secretion system. *Infect Immun.,* 73**,** 4327-37.

KAPER, J. B., ELLIOTT, S., SPERANDIO, V., PERNA, N. T., MAYHEW, G. F. & BLATTNER, F. R. Attaching and effacing intestinal histopathology and the locus of enterocyte effacement in *Escherichia coli* O157:H7 and other Shiga-toxin-producing *E. coli* strains. *In:* KAPER, J. B. & O'BRIEN, A. D., eds., 1998 Washington, DC. American Society for Microbiology, 163-82.

KAPER, J. B., NATARO, J. P. & MOBLEY, H. L. 2004. Pathogenic *Escherichia coli*. *Nat Rev Microbiol,* 2**,** 123-40.

KARCH, H., TARR, P. I. & BIELASZEWSKA, M. 2005. Enterohaemorrhagic *Escherichia coli* in human medicine. *Int J Med Microbiol,* 295**,** 405-18.

KAUFFMANN, F. 1974. On the significance of L antigens for the serology, immunology and pathogenicity of Escherichia species. *Zentralbl Bakteriol Orig A,* 229**,** 178-89.

KAUR, R., KAUR, G., GILL, R. K., SONI, R. & BARIWAL, J. 2014. Recent developments in tubulin polymerization inhibitors: An overview. *Eur J Med Chem,* 87**,** 89-124.

KELLY, M., HART, E., MUNDY, R., MARCHES, O., WILES, S., BADEA, L., LUCK, S., TAUSCHEK, M., FRANKEL, G., ROBINS-BROWNE, R. M. & HARTLAND, E. L. 2006. Essential role of the type III secretion system effector NleB in colonization of mice by Citrobacter rodentium. *Infect Immun,* 74**,** 2328-37.

KENNY, B. 1999. Phosphorylation of tyrosine 474 of the enteropathogenic Escherichia coli (EPEC) Tir receptor molecule is essential for actin nucleating activity and is preceded by additional host modifications. *Mol Microbiol,* 31**,** 1229-41.

KENNY, B. 2002. Mechanism of action of EPEC type III effector molecules. *Int J Med Microbiol,* 291**,** 469-77.

KENNY, B., DEVINNEY, R., STEIN, M., REINSCHEID, D. J., FREY, E. A. & FINLAY, B. B. 1997. Enteropathogenic *E. coli* (EPEC) transfers its receptor for intimate adherence into mammalian cells. *Cell,* 91**,** 511-20.

KENNY, B. & FINLAY, B. B. 1997. Intimin-dependent binding of enteropathogenic Escherichia coli to host cells triggers novel signaling events, including tyrosine phosphorylation of phospholipase C-gamma1. *Infect Immun,* 65**,** 2528-36.

KENNY, B. & JEPSON, M. 2000. Targeting of an enteropathogenic Escherichia coli (EPEC) effector protein to host mitochondria. *Cell Microbiol,* 2**,** 579-90.

KENNY, B. & VALDIVIA, R. 2009. Host-microbe interactions: bacteria. *Curr Opin Microbiol,* 12**,** 1-3.

KEPP, O., SENOVILLA, L., GALLUZZI, L., PANARETAKIS, T., TESNIERE, A., SCHLEMMER, F., MADEO, F., ZITVOGEL, L. & KROEMER, G. 2009. Viral subversion of immunogenic cell death. *Cell Cycle,* 8**,** 860-9.

KIM, J., THANABALASURIAR, A., CHAWORTH-MUSTERS, T., FROMME, J. C., FREY, E. A., LARIO, P. I., METALNIKOV, P., RIZG, K., THOMAS, N. A., LEE, S. F., HARTLAND, E. L., HARDWIDGE, P. R., PAWSON, T., STRYNADKA, N. C., FINLAY, B. B., SCHEKMAN, R. & GRUENHEID, S. 2007. The bacterial virulence factor NleA inhibits cellular protein secretion by disrupting mammalian COPII function. *Cell Host Microbe,* 2**,** 160-71.

KIM, M., OGAWA, M., FUJITA, Y., YOSHIKAWA, Y., NAGAI, T., KOYAMA, T., NAGAI, S., LANGE, A., FASSLER, R. & SASAKAWA, C. 2009. Bacteria hijack integrin-linked kinase to stabilize focal adhesions and block cell detachment. *Nature,* 459**,** 578-82.

KIM, O., YANG, J. & QIU, Y. 2002. Selective activation of small GTPase RhoA by tyrosine kinase Etk through its pleckstrin homology domain. *J Biol Chem,* 277**,** 30066-71.

KLEJNOT, M., FALNIKAR, A., ULAGANATHAN, V., CROSS, R. A., BAAS, P. W. & KOZIELSKI, F. 2014. The crystal structure and biochemical characterization of Kif15: a bifunctional molecular motor involved in bipolar spindle formation and neuronal development. *Acta Crystallogr D Biol Crystallogr,* 70**,** 123-33.

KNUTTON, S., BALDINI, T., KAPPER, J. B. & MCNEISH, A. S. 1987a. Role of plasmid-encoded adherence factors in adhesion of enteropathogenic *Escherichia coli* to HEp-2 cells. *Infect Immun,* 55**,** 78-85.

KNUTTON, S., BALDWIN, T., WILLIAMS, P. H. & MCNEISH, A. S. 1989. Actin accumulation at sites of bacterial adhesion to tissue culture cells: basis of a new diagnostic test for enteropathogenic and enterohemorrhagic *Escherichia coli*. *Infect Immun,* 57**,** 1290-98.

KNUTTON, S., LLOYD, D. R. & MCNEISH, A. S. 1987b. Adhesion of enteropathogenic Escherichia coli to human intestinal enterocytes and cultured human intestinal mucosa. *Infect Immun,* 55**,** 69-77.

KNUTTON, S., ROSENSHINE, I., PALLEN, M. J., NISAN, I., NEVES, B. C., BAIN, C., WOLFF, C., DOUGAN, G. & FRANKEL, G. 1998. A novel EspA-associated surface organelle of enteropathogenic *Escherichia coli* involved in protein translocation into epithelial cells. *EMBO J,* 17**,** 2166-2176.

KOLLMAN, J. M., MERDES, A., MOUREY, L. & AGARD, D. A. 2011. Microtubule nucleation by gamma-tubulin complexes. *Nat Rev Mol Cell Biol,* 12**,** 709-21.

KORONAKIS, V., ESWARAN, J. & HUGHES, C. 2004. Structure and function of TolC: the bacterial exit duct for proteins and drugs. *Annu Rev Biochem,* 73**,** 467-89.
KOROTKOV, K. V., SANDKVIST, M. & HOL, W. G. 2012. The type II secretion system: biogenesis, molecular architecture and mechanism. *Nat Rev Microbiol,* 10**,** 336-51.
KRESSE, A. U., ROHDE, M. & GUZMAN, C. A. 1999. The EspD protein of enterohemorrhagic *Escherichia coli* is required for the formation of bacterial surface appendages and is incorporated in the cytoplasmic membranes of target cells. *Infect Immun,* 67**,** 4834-42.
KUNDA, P., CRAIG, G., DOMINGUEZ, V. & BAUM, B. 2003. Abi, Sra1, and Kette control the stability and localization of SCAR/WAVE to regulate the formation of actin-based protrusions. *Curr Biol,* 13**,** 1867-75.
KUROKAWA, K., ITOH, R. E., YOSHIZAKI, H., NAKAMURA, Y. O. & MATSUDA, M. 2004. Coactivation of Rac1 and Cdc42 at lamellipodia and membrane ruffles induced by epidermal growth factor. *Mol Biol Cell,* 15**,** 1003-10.
KURUSHIMA, J., NAGAI, T., NAGAMATSU, K. & ABE, A. 2010. EspJ effector in enterohemorrhagic E. coli translocates into host mitochondria via an atypical mitochondrial targeting signal. *Microbiol Immunol,* 54**,** 371-9.
LAI, Y., ROSENSHINE, I., LEONG, J. M. & FRANKEL, G. 2013. Intimate host attachment: enteropathogenic and enterohaemorrhagic Escherichia coli. *Cell Microbiol,* 15**,** 1796-808.
LANZETTI, L. 2007. Actin in membrane trafficking. *Curr Opin Cell Biol,* 19**,** 453-8.
LECLAIRE, L. L., 3RD, BAUMGARTNER, M., IWASA, J. H., MULLINS, R. D. & BARBER, D. L. 2008. Phosphorylation of the Arp2/3 complex is necessary to nucleate actin filaments. *J Cell Biol,* 182**,** 647-54.
LEE, S. F., KELLY, M., MCALISTER, A., LUCK, S. N., GARCIA, E. L., HALL, R. A., ROBINS-BROWNE, R. M., FRANKEL, G. & HARTLAND, E. L. 2008. A C-terminal class I PDZ binding motif of EspI/NleA modulates the virulence of attaching and effacing Escherichia coli and Citrobacter rodentium. *Cell Microbiol,* 10**,** 499-513.
LEGG, J. A., BOMPARD, G., DAWSON, J., MORRIS, H. L., ANDREW, N., COOPER, L., JOHNSTON, S. A., TRAMOUNTANIS, G. & MACHESKY, L. M. 2007. N-WASP involvement in dorsal ruffle formation in mouse embryonic fibroblasts. *Mol Biol Cell,* 18**,** 678-87.
LEVINE, M. M., BERQUIST, E. J., NALIN, D. R., WATERMAN, D. H., HORNICK, R. B., YOUNG, C. R., STOMAN, S. & ROWE, B. 1978. *Escherichia coli* that cause diarrhoea but do not produce heat-labile or heat-stable enterotoxins and are non-invasive. *Lancet,* i**,** 119-122.
LINARDOPOULOU, E. V., PARGHI, S. S., FRIEDMAN, C., OSBORN, G. E., PARKHURST, S. M. & TRASK, B. J. 2007. Human subtelomeric WASH genes encode a new subclass of the WASP family. *PLoS Genet,* 3**,** e237.
LIU, L., JOHNSON, H. L., COUSENS, S., PERIN, J., SCOTT, S., LAWN, J. E., RUDAN, I., CAMPBELL, H., CIBULSKIS, R., LI, M., MATHERS, C., BLACK, R. E., CHILD HEALTH EPIDEMIOLOGY REFERENCE GROUP OF, W. H. O. & UNICEF 2012. Global, regional, and national causes of child mortality: an updated systematic analysis for 2010 with time trends since 2000. *Lancet,* 379**,** 2151-61.
LOMMEL, S., BENESCH, S., ROTTNER, K., FRANZ, T., WEHLAND, J. & KUHN, R. 2001. Actin pedestal formation by enteropathogenic *Escherichia coli* and intracellular motility of *Shigella flexneri* are abolished in N-WASP-defective cells. *EMBO Rep,* 2**,** 850-857.
LUIRINK, J., VON HEIJNE, G., HOUBEN, E. & DE GIER, J. W. 2005. Biogenesis of inner membrane proteins in Escherichia coli. *Annu Rev Microbiol,* 59**,** 329-55.
LUO, Y., FREY, E. A., PFUETZNER, R. A., CREAGH, A. L., KNOECHEL, D. G., HAYNES, C. A., FINLAY, B. B. & STRYNADKA, N. C. 2000. Crystal structure of enteropathogenic Escherichia coli intimin-receptor complex. *Nature,* 405**,** 1073-7.
MACHESKY, L. M., ATKINSON, S. J., AMPE, C., VANDEKERCKHOVE, J. & POLLARD, T. D. 1994. Purification of a cortical complex containing two unconventional actins from Acanthamoeba by affinity chromatography on profilin-agarose. *J Cell Biol,* 127**,** 107-15.

MACHUY, N., CAMPA, F., THIECK, O. & RUDEL, T. 2007. c-Abl-binding protein interacts with p21-activated kinase 2 (PAK-2) to regulate PDGF-induced membrane ruffles. *J Mol Biol,* 370**,** 620-32.

MAEKAWA, M., ISHIZAKI, T., BOKU, S., WATANABE, N., FUJITA, A., IWAMATSU, A., OBINATA, T., OHASHI, K., MIZUNO, K. & NARUMIYA, S. 1999. Signaling from Rho to the actin cytoskeleton through protein kinases ROCK and LIM-kinase. *Science,* 285**,** 895-8.

MARCHES, O., COVARELLI, V., DAHAN, S., COUGOULE, C., BHATTA, P., FRANKEL, G. & CARON, E. 2008. EspJ of enteropathogenic and enterohaemorrhagic Escherichia coli inhibits opsono-phagocytosis. *Cell Microbiol,* 10**,** 1104-15.

MARCHES, O., WILES, S., DZIVA, F., LA RAGIONE, R. M., SCHULLER, S., BEST, A., PHILLIPS, A. D., HARTLAND, E. L., WOODWARD, M. J., STEVENS, M. P. & FRANKEL, G. 2005. Characterization of two non-locus of enterocyte effacement-encoded type III-translocated effectors, NleC and NleD, in attaching and effacing pathogens. *Infect Immun,* 73**,** 8411-7.

MARTINEZ, E., SCHROEDER, G. N., BERGER, C. N., LEE, S. F., ROBINSON, K. S., BADEA, L., SIMPSON, N., HALL, R. A., HARTLAND, E. L., CREPIN, V. F. & FRANKEL, G. 2010. Binding to Na(+) /H(+) exchanger regulatory factor 2 (NHERF2) affects trafficking and function of the enteropathogenic Escherichia coli type III secretion system effectors Map, EspI and NleH. *Cell Microbiol,* 12**,** 1718-31.

MATSUZAWA, T., KUWAE, A. & ABE, A. 2005. Enteropathogenic *Escherichia coli* type III effectors EspG and EspG2 alter epithelial paracellular permeability. *Infect Immun,* 73**,** 6283-9.

MATSUZAWA, T., KUWAE, A., YOSHIDA, S., SASAKAWA, C. & ABE, A. 2004. Enteropathogenic *Escherichia coli* activates the RhoA signaling pathway via the stimulation of GEF-H1. *Embo J.,* 23**,** 3570-82.

MATULIENE, J., ESSNER, R., RYU, J., HAMAGUCHI, Y., BAAS, P. W., HARAGUCHI, T., HIRAOKA, Y. & KURIYAMA, R. 1999. Function of a minus-end-directed kinesin-like motor protein in mammalian cells. *J Cell Sci,* 112 (Pt 22)**,** 4041-50.

MCDANIEL, T. K., JARVIS, K. G., DONNENBERG, M. S. & KAPER, J. B. 1995. A genetic locus of enterocyte effacement conserved among diverse enterobacterial pathogens. *Proc Natl Acad Sci USA,* 92**,** 1664-8.

MCDANIEL, T. K. & KAPER, J. B. 1997. A cloned pathogenicity island from enteropathogenic Escherichia coli confers the attaching and effacing phenotype on E. coli K-12. *Mol Microbiol,* 23**,** 399-407.

MCNAMARA, B. P. & DONNENBERG, M. S. 1998. A novel proline-rich protein, EspF, is secreted from enteropathogenic Escherichia coli via the type III export pathway. *FEMS Microbiol Lett,* 166**,** 71-8.

MELLIES, J. L., BARRON, A. M. & CARMONA, A. M. 2007a. Enteropathogenic and enterohemorrhagic Escherichia coli virulence gene regulation. *Infect Immun,* 75**,** 4199-210.

MELLIES, J. L., ELLIOTT, S. J., SPERANDIO, V., DONNENBERG, M. S. & KAPER, J. B. 1999. The Per regulon of enteropathogenic *Escherichia coli*: Identification of a regulatory cascade and a novel transcriptional activator, the locus of enterocyte effacement (LEE)-encoded regulator (Ler). *Mol Microbiol,* 33**,** 296-306.

MELLIES, J. L., HAACK, K. R. & GALLIGAN, D. C. 2007b. SOS regulation of the type III secretion system of enteropathogenic Escherichia coli. *J Bacteriol,* 189**,** 2863-72.

MIKI, H., YAMAGUCHI, H., SUETSUGU, S. & TAKENAWA, T. 2000. IRSp53 is an essential intermediate between Rac and WAVE in the regulation of membrane ruffling. *Nature,* 408**,** 732-5.

MILLARD, T. H., SHARP, S. J. & MACHESKY, L. M. 2004. Signalling to actin assembly via the WASP (Wiskott-Aldrich syndrome protein)-family proteins and the Arp2/3 complex. *Biochem J,* 380**,** 1-17.

MIYAHARA, A., NAKANISHI, N., OOKA, T., HAYASHI, T., SUGIMOTO, N. & TOBE, T. 2009. Enterohemorrhagic Escherichia coli Effector EspL2 Induces Actin Microfilament Aggregation through Annexin 2 Activation. *Cell Microbiol,* 11 337-350.

MORIKAWA, H., KIM, M., MIMURO, H., PUNGINELLI, C., KOYAMA, T., NAGAI, S., MIYAWAKI, A., IWAI, K. & SASAKAWA, C. 2010. The bacterial effector Cif interferes with SCF ubiquitin ligase function by inhibiting deneddylation of Cullin1. *Biochem Biophys Res Commun,* 401**,** 268-74.

MOSELEY, J. B., SAGOT, I., MANNING, A. L., XU, Y., ECK, M. J., PELLMAN, D. & GOODE, B. L. 2004. A conserved mechanism for Bni1- and mDia1-induced actin assembly and dual regulation of Bni1 by Bud6 and profilin. *Mol Biol Cell,* 15**,** 896-907.

MOUGOUS, J. D., CUFF, M. E., RAUNSER, S., SHEN, A., ZHOU, M., GIFFORD, C. A., GOODMAN, A. L., JOACHIMIAK, G., ORDONEZ, C. L., LORY, S., WALZ, T., JOACHIMIAK, A. & MEKALANOS, J. J. 2006. A virulence locus of Pseudomonas aeruginosa encodes a protein secretion apparatus. *Science,* 312**,** 1526-30.

MUHLEN, S., RUCHAUD-SPARAGANO, M. H. & KENNY, B. 2011. Proteasome-independent degradation of canonical NFkappaB complex components by the NleC protein of pathogenic Escherichia coli. *J Biol Chem,* 286**,** 5100-7.

MULLER, M. 2005. Twin-arginine-specific protein export in Escherichia coli. *Res Microbiol,* 156**,** 131-6.

MUNDY, R., PETROVSKA, L., SMOLLETT, K., SIMPSON, N., WILSON, R. K., YU, J., TU, X., ROSENSHINE, I., CLARE, S., DOUGAN, G. & FRANKEL, G. 2004. Identification of a novel Citrobacter rodentium type III secreted protein, EspI, and roles of this and other secreted proteins in infection. *Infect Immun,* 72**,** 2288-2302.

MUNERA, D., CREPIN, V. F., MARCHES, O. & FRANKEL, G. 2010. N-terminal type III secretion signal of enteropathogenic Escherichia coli translocator proteins. *J Bacteriol,* 192**,** 3534-9.

NADLER, C., BARUCH, K., KOBI, S., MILLS, E., HAVIV, G., FARAGO, M., ALKALAY, I., BARTFELD, S., MEYER, T. F., BEN-NERIAH, Y. & ROSENSHINE, I. 2010. The type III secretion effector NleE inhibits NF-kappaB activation. *PLoS Pathog,* 6**,** e1000743.

NATALE, P., BRUSER, T. & DRIESSEN, A. J. 2008. Sec- and Tat-mediated protein secretion across the bacterial cytoplasmic membrane--distinct translocases and mechanisms. *Biochim Biophys Acta,* 1778**,** 1735-56.

NATARO, J. P. & KAPER, J. B. 1998. Diarrheagenic Escherichia coli. *Clin Microbiol Rev,* 11**,** 142-201.

NEVES, B. C., MUNDY, R., PETROVSKA , L., DOUGAN, G., KNUTTON, S. & FRANKEL, G. 2003. CesD2 of enteropathogenic Escherichia coli is a second chaperone for the type III secretion translocator protein EspD. *Infect Immun,* 71**,** 2130-2141.

NEWTON, H. J., PEARSON, J. S., BADEA, L., KELLY, M., LUCAS, M., HOLLOWAY, G., WAGSTAFF, K. M., DUNSTONE, M. A., SLOAN, J., WHISSTOCK, J. C., KAPER, J. B., ROBINS-BROWNE, R. M., JANS, D. A., FRANKEL, G., PHILLIPS, A. D., COULSON, B. S. & HARTLAND, E. L. 2010. The type III effectors NleE and NleB from enteropathogenic E. coli and OspZ from Shigella block nuclear translocation of NF-kappaB p65. *PLoS Pathog,* 6**,** e1000898.

NIEMANN, G. S., BROWN, R. N., MUSHAMIRI, I. T., NGUYEN, N. T., TAIWO, R., STUFKENS, A., SMITH, R. D., ADKINS, J. N., MCDERMOTT, J. E. & HEFFRON, F. 2013. RNA type III secretion signals that require Hfq. *J Bacteriol,* 195**,** 2119-25.

NOBES, C. D. & HALL, A. 1995. Rho, rac and cdc42 GTPases: regulators of actin structures, cell adhesion and motility. *Biochem Soc Trans,* 23**,** 456-9.

NOBES, C. D. & HALL, A. 1999. Rho GTPases control polarity, protrusion, and adhesion during cell movement. *J Cell Biol,* 144**,** 1235-44.

NOGALES, E. 2001. Structural insight into microtubule function. *Annu Rev Biophys Biomol Struct,* 30**,** 397-420.

NOGALES, E. & WANG, H. W. 2006. Structural intermediates in microtubule assembly and disassembly: how and why? *Curr Opin Cell Biol,* 18**,** 179-84.

OLOFSSON, B. 1999. Rho guanine dissociation inhibitors: pivotal molecules in cellular signalling. *Cell Signal,* 11**,** 545-54.

OLSON, M. A. & CUFF, L. 1997. Molecular docking of superantigens with class II major histocompatibility complex proteins. *J Mol Recognit,* 10**,** 277-89.

ORSKOV, F., WHITTAM, T. S., CRAVIOTO, A. & ORSKOV, I. 1990. Clonal relationships among classic enteropathogenic Escherichia coli (EPEC) belong to different O groups. *J Infect Dis,* 162**,** 76-81.

OTOMO, T., TOMCHICK, D. R., OTOMO, C., PANCHAL, S. C., MACHIUS, M. & ROSEN, M. K. 2005. Structural basis of actin filament nucleation and processive capping by a formin homology 2 domain. *Nature,* 433**,** 488-94.

PALLEN, M. J., BEATSON, S. A. & BAILEY, C. M. 2005. Bioinformatics analysis of the locus for enterocyte effacement provides novel insights into type-III secretion. *BMC Microbiol,* 5**,** 9.

PALLETT, M. A., BERGER, C. N., PEARSON, J. S., HARTLAND, E. L. & FRANKEL, G. 2014. The type III secretion effector NleF of enteropathogenic Escherichia coli activates NF-kappaB early during infection. *Infect Immun,* 82**,** 4878-88.

PAPANIKOU, E., KARAMANOU, S. & ECONOMOU, A. 2007. Bacterial protein secretion through the translocase nanomachine. *Nat Rev Microbiol,* 5**,** 839-51.

PAPATHEODOROU, P., DOMANSKA, G., OXLE, M., MATHIEU, J., SELCHOW, O., KENNY, B. & RASSOW, J. 2006. The enteropathogenic Escherichia coli (EPEC) Map effector is imported into the mitochondrial matrix by the TOM/Hsp70 system and alters organelle morphology. *Cell Microbiol,* 8**,** 677-89.

PARK, S. J., SUETSUGU, S., SAGARA, H. & TAKENAWA, T. 2007. HSP90 cross-links branched actin filaments induced by N-WASP and the Arp2/3 complex. *Genes Cells,* 12**,** 611-22.

PARSOT, C., HAMIAUX, C. & PAGE, A. L. 2003. The various and varying roles of specific chaperones in type III secretion systems. *Curr Opin Microbiol.,* 6**,** 7-14.

PEARSON, J. S., RIEDMAIER, P., MARCHES, O., FRANKEL, G. & HARTLAND, E. L. 2011. A type III effector protease NleC from enteropathogenic Escherichia coli targets NF-kappaB for degradation. *Mol Microbiol,* 80**,** 219-30.

PEARSON, J. S., ZHANG, Y., NEWTON, H. J. & HARTLAND, E. L. 2015. Post-modern pathogens: surprising activities of translocated effectors from E. coli and Legionella. *Curr Opin Microbiol,* 23**,** 73-9.

PECK, J., DOUGLAS, G. T., WU, C. H. & BURBELO, P. D. 2002. Human RhoGAP domain-containing proteins: structure, function and evolutionary relationships. *FEBS Lett,* 528**,** 27-34.

PELLEGRIN, S. & MELLOR, H. 2007. Actin stress fibres. *J Cell Sci,* 120**,** 3491-9.

PELLEGRINI, F. & BUDMAN, D. R. 2005. Review: tubulin function, action of antitubulin drugs, and new drug development. *Cancer Invest,* 23**,** 264-73.

PELLETIER, S., JULIEN, C., POPOFF, M. R., LAMARCHE-VANE, N. & MELOCHE, S. 2005. Cyclic AMP induces morphological changes of vascular smooth muscle cells by inhibiting a Rac-dependent signaling pathway. *J Cell Physiol,* 204**,** 412-22.

PENG, J., YANG, J. & JIN, Q. 2009. The molecular evolutionary history of Shigella spp. and enteroinvasive Escherichia coli. *Infect Genet Evol,* 9**,** 147-52.

PERNA, N. T., PLUNKETT, G., 3RD, BURLAND, V., MAU, B., GLASNER, J. D., ROSE, D. J., MAYHEW, G. F., EVANS, P. S., GREGOR, J., KIRKPATRICK, H. A., POSFAI, G., HACKETT, J., KLINK, S., BOUTIN, A., SHAO, Y., MILLER, L., GROTBECK, E. J., DAVIS, N. W., LIM, A., DIMALANTA, E. T., POTAMOUSIS, K. D., APODACA, J., ANANTHARAMAN, T. S., LIN, J., YEN, G., SCHWARTZ, D. C., WELCH, R. A. & BLATTNER, F. R. 2001. Genome sequence of enterohaemorrhagic Escherichia coli O157:H7. *Nature,* 409**,** 529-33.

PETTY, N. K., BULGIN, R., CREPIN, V. F., CERDENO-TARRAGA, A. M., SCHROEDER, G. N., QUAIL, M. A., LENNARD, N., CORTON, C., BARRON, A., CLARK, L., TORIBIO, A. L., PARKHILL, J., DOUGAN, G., FRANKEL, G. & THOMSON, N. R. 2010. The Citrobacter rodentium genome sequence reveals convergent evolution with human pathogenic Escherichia coli. *J Bacteriol,* 192**,** 525-38.

PHILLIPS, N., HAYWARD, R. D. & KORONAKIS, V. 2004. Phosphorylation of the enteropathogenic E. coli receptor by the Src-family kinase c-Fyn triggers actin pedestal formation. *Nat Cell Biol,* 6**,** 618-25.

PHILPOTT, D. J., EDGEWORTH, J. D. & SANSONETTI, P. J. 2000. The pathogenesis of Shigella flexneri infection: lessons from in vitro and in vivo studies. *Philos Trans R Soc Lond B Biol Sci,* 355**,** 575-86.

POLLARD, T. D. 1986. Rate constants for the reactions of ATP- and ADP-actin with the ends of actin filaments. *J Cell Biol,* 103**,** 2747-54.

POLLARD, T. D. 2007. Regulation of actin filament assembly by Arp2/3 complex and formins. *Annu Rev Biophys Biomol Struct,* 36**,** 451-77.

POLLARD, T. D. & COOPER, J. A. 2009. Actin, a central player in cell shape and movement. *Science,* 326**,** 1208-12.

PUKATZKI, S., MCAULEY, S. B. & MIYATA, S. T. 2009. The type VI secretion system: translocation of effectors and effector-domains. *Curr Opin Microbiol,* 12**,** 11-7.

QADRI, F., SVENNERHOLM, A. M., FARUQUE, A. S. & SACK, R. B. 2005. Enterotoxigenic Escherichia coli in developing countries: epidemiology, microbiology, clinical features, treatment, and prevention. *Clin Microbiol Rev,* 18**,** 465-83.

QUINLAN, M. E., HEUSER, J. E., KERKHOFF, E. & MULLINS, R. D. 2005. Drosophila Spire is an actin nucleation factor. *Nature,* 433**,** 382-8.

RASKO, D. A., WEBSTER, D. R., SAHL, J. W., BASHIR, A., BOISEN, N., SCHEUTZ, F., PAXINOS, E. E., SEBRA, R., CHIN, C. S., ILIOPOULOS, D., KLAMMER, A., PELUSO, P., LEE, L., KISLYUK, A. O., BULLARD, J., KASARSKIS, A., WANG, S., EID, J., RANK, D., REDMAN, J. C., STEYERT, S. R., FRIMODT-MOLLER, J., STRUVE, C., PETERSEN, A. M., KROGFELT, K. A., NATARO, J. P., SCHADT, E. E. & WALDOR, M. K. 2011. Origins of the E. coli strain causing an outbreak of hemolytic-uremic syndrome in Germany. *N Engl J Med,* 365**,** 709-17.

RATH, O. & KOZIELSKI, F. 2012. Kinesins and cancer. *Nat Rev Cancer,* 12**,** 527-39.

READING, N. C., TORRES, A. G., KENDALL, M. M., HUGHES, D. T., YAMAMOTO, K. & SPERANDIO, V. 2007. A novel two-component signaling system that activates transcription of an enterohemorrhagic Escherichia coli effector involved in remodeling of host actin. *J Bacteriol,* 189**,** 2468-76.

RIDLEY, A. J. 2001. Rho GTPases and cell migration. *J Cell Sci,* 114**,** 2713-22.

ROBERTS, P. J., MITIN, N., KELLER, P. J., CHENETTE, E. J., MADIGAN, J. P., CURRIN, R. O., COX, A. D., WILSON, O., KIRSCHMEIER, P. & DER, C. J. 2008. Rho Family GTPase modification and dependence on CAAX motif-signaled posttranslational modification. *J Biol Chem,* 283**,** 25150-63.

RODAL, A. A., SOKOLOVA, O., ROBINS, D. B., DAUGHERTY, K. M., HIPPENMEYER, S., RIEZMAN, H., GRIGORIEFF, N. & GOODE, B. L. 2005. Conformational changes in the Arp2/3 complex leading to actin nucleation. *Nat Struct Mol Biol,* 12**,** 26-31.

ROE, A. J., TYSALL, L., DRANSFIELD, T., WANG, D., FRASER-PITT, D., MAHAJAN, A., CONSTANDINOU, C., INGLIS, N., DOWNING, A., TALBOT, R., SMITH, D. G. & GALLY, D. L. 2007. Analysis of the expression, regulation and export of NleA-E in Escherichia coli O157 : H7. *Microbiology,* 153**,** 1350-60.

ROHATGI, R., MA, L., MIKI, H., LOPEZ, M., KIRCHHAUSEN, T., TAKENAWA, T., AND KIRSCHNER, M.W. 1999. The interaction between N-WASP and the Arp2/3 complex links Cdc42-dependent signals to actin assembly. *Cell,* 97**,** 221-231.

ROMERO, S., LE CLAINCHE, C., DIDRY, D., EGILE, C., PANTALONI, D. & CARLIER, M. F. 2004. Formin is a processive motor that requires profilin to accelerate actin assembly and associated ATP hydrolysis. *Cell,* 119**,** 419-29.

ROOF, R. W., HASKELL, M. D., DUKES, B. D., SHERMAN, N., KINTER, M. & PARSONS, S. J. 1998. Phosphotyrosine (p-Tyr)-dependent and -independent mechanisms of p190 RhoGAP-p120 RasGAP interaction: Tyr 1105 of p190, a substrate for c-Src, is the sole p-Tyr mediator of complex formation. *Mol Cell Biol,* 18**,** 7052-63.

ROSENSHINE, I., RUSCHKOWSKI, S., STEIN, M., REINSCHEID, D. J., MILLS, S. D. & FINLAY, B. B. 1996. A pathogenic bacterium triggers epithelials signals to form a functionnal bacterial receptor that mediates actin pseudopod formation. *EMBO J,* 15**,** 2613-24.

ROSSMAN, K. L., DER, C. J. & SONDEK, J. 2005. GEF means go: turning on RHO GTPases with guanine nucleotide-exchange factors. *Nat Rev Mol Cell Biol,* 6**,** 167-80.

RUSSO, T. A. & JOHNSON, J. R. 2000. Proposal for a new inclusive designation for extraintestinal pathogenic isolates of Escherichia coli: ExPEC. *J Infect Dis,* 181**,** 1753-4.

SASAKAWA, C. 2010. A new paradigm of bacteria-gut interplay brought through the study of Shigella. *Proc Jpn Acad Ser B Phys Biol Sci,* 86**,** 229-43.

SASAKI, N., MIKI, H. & TAKENAWA, T. 2000. Arp2/3 complex-independent actin regulatory function of WAVE. *Biochem Biophys Res Commun,* 272**,** 386-90.

SCHIEBEL, E., DRIESSEN, A. J., HARTL, F. U. & WICKNER, W. 1991. Delta mu H+ and ATP function at different steps of the catalytic cycle of preprotein translocase. *Cell,* 64**,** 927-39.

SCHLOSSER-SILVERMAN, E., ELGRABLY-WEISS, M., ROSENSHINE, I., KOHEN, R. & ALTUVIA, S. 2000. Characterization of Escherichia coli DNA lesions generated within J774 macrophages. *J Bacteriol,* 182**,** 5225-5230.

SCHRAIDT, O., LEFEBRE, M. D., BRUNNER, M. J., SCHMIED, W. H., SCHMIDT, A., RADICS, J., MECHTLER, K., GALAN, J. E. & MARLOVITS, T. C. 2010. Topology and organization of the Salmonella typhimurium type III secretion needle complex components. *PLoS Pathog,* 6**,** e1000824.

SEEGER, M. A., ZHANG, Y. & RICE, S. E. 2012. Kinesin tail domains are intrinsically disordered. *Proteins,* 80**,** 2437-46.

SELYUNIN, A. S. & ALTO, N. M. 2011. Activation of PAK by a bacterial type III effector EspG reveals alternative mechanisms of GTPase pathway regulation. *Small GTPases,* 2**,** 217-221.

SERVIN, A. L. 2005. Pathogenesis of Afa/Dr diffusely adhering Escherichia coli. *Clin Microbiol Rev,* 18**,** 264-92.

SHAMES, S. R., DENG, W., GUTTMAN, J. A., DE HOOG, C. L., LI, Y., HARDWIDGE, P. R., SHAM, H. P., VALLANCE, B. A., FOSTER, L. J. & FINLAY, B. B. 2010. The pathogenic E. coli type III effector EspZ interacts with host CD98 and facilitates host cell prosurvival signalling. *Cell Microbiol,* 12**,** 1322-39.

SHAW, R. K., SMOLLETT, K., CLEARY, J., GARMENDIA, J., STRAATMAN-IWANOWSKA, A., FRANKEL, G. & KNUTTON, S. 2005. Enteropathogenic Escherichia coli type III effectors EspG and EspG2 disrupt the microtubule network of intestinal epithelial cells. *Infect Immun,* 73**,** 4385-90.

SIITONEN, A. 1992. Escherichia coli in fecal flora of healthy adults: serotypes, P and type 1C fimbriae, non-P mannose-resistant adhesins, and hemolytic activity. *J Infect Dis,* 166**,** 1058-65.

SIMOVITCH, M., SASON, H., COHEN, S., ZAHAVI, E. E., MELAMED-BOOK, N., WEISS, A., AROETI, B. & ROSENSHINE, I. 2010. EspM inhibits pedestal formation by enterohaemorrhagic Escherichia coli and enteropathogenic E. coli and disrupts the architecture of a polarized epithelial monolayer. *Cell Microbiol,* 12**,** 489-505.

SIMPSON, N., SHAW, R., CREPIN, V. F., MUNDY, R., FITZGERALD, A. J., CUMMINGS, N., STRAATMAN-IWANOWSKA, A., CONNERTON, I., KNUTTON, S. & FRANKEL, G. 2006. The enteropathogenic *Escherichia coli* type III secretion system effector Map binds EBP50/NHERF1: implication for cell signalling and diarrhoea. *Mol Microbiol.,* 60**,** 349-63.

SMITH, T. K., HAGER, H. A., FRANCIS, R., KILKENNY, D. M., LO, C. W. & BADER, D. M. 2008. Bves directly interacts with GEFT, and controls cell shape and movement through regulation of Rac1/Cdc42 activity. *Proc Natl Acad Sci U S A,* 105**,** 8298-303.

SMOLLETT, K., SHAW, R. K., GARMENDIA, J., KNUTTON, S. & FRANKEL, G. 2006. Function and distribution of EspG2, a type III secretion system effector of enteropathogenic Escherichia coli. *Microbes Infect,* 8**,** 2220-7.

SPANGLER, B. D. 1992. Structure and function of cholera toxin and the related Escherichia coli heat-labile enterotoxin. *Microbiol Rev,* 56**,** 622-47.

STEFFEN, A., ROTTNER, K., EHINGER, J., INNOCENTI, M., SCITA, G., WEHLAND, J. & STRADAL, T. E. 2004. Sra-1 and Nap1 link Rac to actin assembly driving lamellipodia formation. *EMBO J,* 23**,** 749-59.

STENUTZ, R., WEINTRAUB, A. & WIDMALM, G. 2006. The structures of Escherichia coli O-polysaccharide antigens. *FEMS Microbiol Rev,* 30**,** 382-403.

SUETSUGU, S., KURISU, S., OIKAWA, T., YAMAZAKI, D., ODA, A. & TAKENAWA, T. 2006. Optimization of WAVE2 complex-induced actin polymerization by membrane-bound IRSp53, PIP(3), and Rac. *J Cell Biol,* 173**,** 571-85.

SUN, H. Q., YAMAMOTO, M., MEJILLANO, M. & YIN, H. L. 1999. Gelsolin, a multifunctional actin regulatory protein. *J Biol Chem,* 274**,** 33179-82.

TAIEB, F., NOUGAYREDE, J. P., WATRIN, C., SAMBA-LOUAKA, A. & OSWALD, E. 2006. Escherichia coli cyclomodulin Cif induces G2 arrest of the host cell cycle without activation of the DNA-damage checkpoint-signalling pathway. *Cell Microbiol,* 8**,** 1910-21.

TAKENAWA, T. & SUETSUGU, S. 2007. The WASP-WAVE protein network: connecting the membrane to the cytoskeleton. *Nat Rev Mol Cell Biol,* 8**,** 37-48.

TAUSCHEK, M., STRUGNELL, R. A. & ROBINS-BROWNE, R. M. 2002. Characterization and evidence of mobilization of the LEE pathogenicity island of rabbit-specific strains of enteropathogenic *Escherichia coli*. *Mol Microbiol,* 44**,** 1533-1550.

TCHERKEZIAN, J. & LAMARCHE-VANE, N. 2007. Current knowledge of the large RhoGAP family of proteins. *Biol Cell,* 99**,** 67-86.

THANABALASURIAR, A., KOUTSOURIS, A., HECHT, G. & GRUENHEID, S. 2010a. The bacterial virulence factor NleA's involvement in intestinal tight junction disruption during enteropathogenic E. coli infection is independent of its putative PDZ binding domain. *Gut Microbes,* 1**,** 114-118.

THANABALASURIAR, A., KOUTSOURIS, A., WEFLEN, A., MIMEE, M., HECHT, G. & GRUENHEID, S. 2010b. The bacterial virulence factor NleA is required for the disruption of intestinal tight junctions by enteropathogenic Escherichia coli. *Cell Microbiol,* 12**,** 31-41.

TOBE, T., BEATSON, S. A., TANIGUCHI, H., ABE, H., BAILEY, C. M., FIVIAN, A., YOUNIS, R., MATTHEWS, S., MARCHES, O., FRANKEL, G., HAYASHI, T. & PALLEN, M. J. 2006. An extensive repertoire of type III secretion effectors in Escherichia coli O157 and the role of lambdoid phages in their dissemination. *Proc Natl Acad Sci U S A,* 103**,** 14941-6.

TONIKIAN, R., ZHANG, Y., SAZINSKY, S. L., CURRELL, B., YEH, J. H., REVA, B., HELD, H. A., APPLETON, B. A., EVANGELISTA, M., WU, Y., XIN, X., CHAN, A. C., SESHAGIRI, S., LASKY, L. A., SANDER, C., BOONE, C., BADER, G. D. & SIDHU, S. S. 2008. A specificity map for the PDZ domain family. *PLoS Biol,* 6**,** e239.

TORRES, A. G., ZHOU, X. & KAPER, J. B. 2005. Adherence of diarrheagenic Escherichia coli strains to epithelial cells. *Infect Immun,* 73**,** 18-29.

TRABULSI, L. R., KELLER, R. & TARDELLI GOMES, T. A. 2002. Typical and atypical enteropathogenic *Escherichia coli*. *Emerg Infect Dis,* 8**,** 508-513.

TSENG, T. T., TYLER, B. M. & SETUBAL, J. C. 2009. Protein secretion systems in bacterial-host associations, and their description in the Gene Ontology. *BMC Microbiol,* 9 Suppl 1**,** S2.

TU, X., NISAN, I., YONA, C., HANSKI, E. & ROSENSHINE, I. 2003. EspH, a new cytoskeleton-modulating effector of enterohaemorrhagic and enteropathogenic Escherichia coli. *Mol Microbiol,* 47**,** 595-606.

TURNER, S. M., SCOTT-TUCKER, A., COOPER, L. M. & HENDERSON, I. R. 2006. Weapons of mass destruction: virulence factors of the global killer enterotoxigenic Escherichia coli. *FEMS Microbiol Lett,* 263**,** 10-20.

TZIPORI, S., KARCH, H., WACHSMUTH, K. I., ROBINS-BROWNE, R. M., O'BRIEN, A. D., LIOR, H., COHEN, M. L., SMITHERS, J. & LEVINE, M. M. 1987. Role of a 60-megadalton plasmid and Shiga-like toxins in the pathogenesis of infection caused by enterohemorrhagic Escherichia coli O157:H7 in gnotobiotic piglets. *Infect Immun,* 55**,** 3117-25.

VEGA, F. M. & RIDLEY, A. J. 2007. SnapShot: Rho family GTPases. *Cell,* 129**,** 1430.

VILJANEN, M. K., PELTOLA, T., JUNNILA, S. Y., OLKKONEN, L., JARVINEN, H., KUISTILA, M. & HUOVINEN, P. 1990. Outbreak of diarrhoea due to Escherichia coli O111:B4 in schoolchildren and adults: association of Vi antigen-like reactivity. *Lancet,* 336**,** 831-4.

VINGADASSALOM, D., KAZLAUSKAS, A., SKEHAN, B., CHENG, H. C., MAGOUN, L., ROBBINS, D., ROSEN, M. K., SAKSELA, K. & LEONG, J. M. 2009. Insulin receptor tyrosine kinase substrate links the E. coli O157:H7 actin assembly effectors Tir and EspF(U) during pedestal formation. *Proc Natl Acad Sci U S A,* 106**,** 6754-9.

VISWANATHAN, V. K., KOUTSOURIS, A., LUKIC, S., PILKINTON, M., SIMONOVIC, I., SIMONOVIC, M. & HECHT, G. 2004. Comparative analysis of EspF from enteropathogenic and enterohemorrhagic Escherichia coli in alteration of epithelial barrier function. *Infect Immun,* 72**,** 3218-27.

VLISIDOU, I., MARCHES, O., DZIVA, F., MUNDY, R., FRANKEL, G. & STEVENS, M. P. 2006. Identification and characterization of EspK, a type III secreted effector protein of enterohaemorrhagic Escherichia coli O157:H7. *FEMS Microbiol Lett,* 263**,** 32-40.

VOGELSGESANG, M., PAUTSCH, A. & AKTORIES, K. 2007. C3 exoenzymes, novel insights into structure and action of Rho-ADP-ribosylating toxins. *Naunyn Schmiedebergs Arch Pharmacol,* 374**,** 347-60.

WALKER, M. L., BURGESS, S. A., SELLERS, J. R., WANG, F., HAMMER, J. A., 3RD, TRINICK, J. & KNIGHT, P. J. 2000. Two-headed binding of a processive myosin to F-actin. *Nature,* 405**,** 804-7.

WANG, D., ROE, A. J., MCATEER, S., SHIPSTON, M. J. & GALLY, D. L. 2008. Hierarchal type III secretion of translocators and effectors from Escherichia coli O157:H7 requires the carboxy terminus of SepL that binds to Tir. *Mol Microbiol,* 69**,** 1499-512.

WANG, L., WANG, Y. M., YUE, J. J., LIANG, L. & HUANG, P. T. 2004. [Progress in type III secretion system]. *Wei Sheng Wu Xue Bao,* 44**,** 840-4.

WATERMAN-STORER, C. M. & SALMON, E. D. 1997. Microtubule dynamics: treadmilling comes around again. *Curr Biol,* 7**,** R369-72.

WEISS, S. M., LADWEIN, M., SCHMIDT, D., EHINGER, J., LOMMEL, S., STADING, K., BEUTLING, U., DISANZA, A., FRANK, R., JANSCH, L., SCITA, G., GUNZER, F., ROTTNER, K. & STRADAL, T. E. 2009. IRSp53 links the enterohemorrhagic E. coli effectors Tir and EspFU for actin pedestal formation. *Cell Host Microbe,* 5**,** 244-58.

WELCH, M. D., AND MULLINS, R.D. 2002. Cellular control of actin nucleation. *Ann Rev Cell Dev Biol,* 18**,** 247-288.

WHALE, A. D., HERNANDES, R. T., OOKA, T., BEUTIN, L., SCHULLER, S., GARMENDIA, J., CROWTHER, L., VIEIRA, M. A., OGURA, Y., KRAUSE, G., PHILLIPS, A. D., GOMES, T. A., HAYASHI, T. & FRANKEL, G. 2007. TccP2-mediated subversion of actin dynamics by EPEC 2 - a distinct evolutionary lineage of enteropathogenic Escherichia coli. *Microbiology,* 153**,** 1743-55.

WICKHAM, M. E., LUPP, C., MASCARENHAS, M., VAZQUEZ, A., COOMBES, B. K., BROWN, N. F., COBURN, B. A., DENG, W., PUENTE, J. L., KARMALI, M. A. & FINLAY, B. B. 2006. Bacterial genetic determinants of non-O157 STEC outbreaks and hemolytic-uremic syndrome after infection. *J Infect Dis,* 194**,** 819-27.

WICKHAM, M. E., LUPP, C., VAZQUEZ, A., MASCARENHAS, M., COBURN, B., COOMBES, B. K., KARMALI, M. A., PUENTE, J. L., DENG, W. & FINLAY, B. B. 2007. Citrobacter rodentium virulence in mice associates with bacterial load and the type III effector NleE. *Microbes Infect,* 9**,** 400-7.

WITKE, W. 2004. The role of profilin complexes in cell motility and other cellular processes. *Trends Cell Biol,* 14**,** 461-9.

WOLF, M. K. 1997. Occurrence, distribution, and associations of O and H serogroups, colonization factor antigens, and toxins of enterotoxigenic Escherichia coli. *Clin Microbiol Rev,* 10**,** 569-84.

WONG, A. R., CLEMENTS, A., RAYMOND, B., CREPIN, V. F. & FRANKEL, G. 2012a. The interplay between the Escherichia coli Rho guanine nucleotide exchange factor effectors and the mammalian RhoGEF inhibitor EspH. *MBio,* 3.

WONG, A. R., PEARSON, J. S., BRIGHT, M. D., MUNERA, D., ROBINSON, K. S., LEE, S. F., FRANKEL, G. & HARTLAND, E. L. 2011. Enteropathogenic and enterohaemorrhagic Escherichia coli: even more subversive elements. *Mol Microbiol,* 80**,** 1420-38.

WONG, A. R., RAYMOND, B., COLLINS, J. W., CREPIN, V. F. & FRANKEL, G. 2012b. The enteropathogenic E. coli effector EspH promotes actin pedestal formation and elongation via WASP-interacting protein (WIP). *Cell Microbiol,* 14**,** 1051-70.

WU, B., SKARINA, T., YEE, A., JOBIN, M. C., DILEO, R., SEMESI, A., FARES, C., LEMAK, A., COOMBES, B. K., ARROWSMITH, C. H., SINGER, A. U. & SAVCHENKO, A. 2010. NleG Type 3 effectors from enterohaemorrhagic Escherichia coli are U-Box E3 ubiquitin ligases. *PLoS Pathog,* 6**,** e1000960.

YAHR, T. L. & WICKNER, W. T. 2001. Functional reconstitution of bacterial Tat translocation in vitro. *EMBO J,* 20**,** 2472-9.

YANG, J., ZHANG, Z., ROE, S. M., MARSHALL, C. J. & BARFORD, D. 2009. Activation of Rho GTPases by DOCK exchange factors is mediated by a nucleotide sensor. *Science,* 325**,** 1398-402.

YANG, J. T., LAYMON, R. A. & GOLDSTEIN, L. S. 1989. A three-domain structure of kinesin heavy chain revealed by DNA sequence and microtubule binding analyses. *Cell,* 56**,** 879-89.

YAO, Q., ZHANG, L., WAN, X., CHEN, J., HU, L., DING, X., LI, L., KARAR, J., PENG, H., CHEN, S., HUANG, N., RAUSCHER, F. J., 3RD & SHAO, F. 2014. Structure and specificity of the bacterial cysteine methyltransferase effector NleE suggests a novel substrate in human DNA repair pathway. *PLoS Pathog,* 10**,** e1004522.

YEN, H., OOKA, T., IGUCHI, A., HAYASHI, T., SUGIMOTO, N. & TOBE, T. 2010. NleC, a type III secretion protease, compromises NF-kappaB activation by targeting p65/RelA. *PLoS Pathog,* 6**,** e1001231.

YEN, H., SUGIMOTO, N. & TOBE, T. 2015. Enteropathogenic Escherichia coli Uses NleA to Inhibit NLRP3 Inflammasome Activation. *PLoS Pathog,* 11**,** e1005121.

YIP, C. K., FINLAY, B. B. & STRYNADKA, N. C. 2005a. Structural characterization of a type III secretion system filament protein in complex with its chaperone. *Nat Struct Mol Biol,* 12**,** 75-81.

YIP, C. K., KIMBROUGH, T. G., FELISE, H. B., VUCKOVIC, M., THOMAS, N. A., PFUETZNER, R. A., FREY, E. A., FINLAY, B. B., MILLER, S. I. & STRYNADKA, N. C. 2005b. Structural characterization of the molecular platform for type III secretion system assembly. *Nature.,* 435**,** 702-7.

YOUNG, J. C., CLEMENTS, A., LANG, A. E., GARNETT, J. A., MUNERA, D., ARBELOA, A., PEARSON, J., HARTLAND, E. L., MATTHEWS, S. J., MOUSNIER, A., BARRY, D. J., WAY, M., SCHLOSSER, A., AKTORIES, K. & FRANKEL, G. 2014. The Escherichia coli effector EspJ blocks Src kinase activity via amidation and ADP ribosylation. *Nat Commun,* 5**,** 5887.

YOUNIS, R., BINGLE, L. E., ROLLAUER, S., MUNERA, D., BUSBY, S. J., JOHNSON, S., DEANE, J. E., LEA, S. M., FRANKEL, G. & PALLEN, M. J. 2010. SepL resembles an aberrant effector in binding to a class 1 type III secretion chaperone and carrying an N-terminal secretion signal. *J Bacteriol,* 192**,** 6093-8.

ZECHNER, E. L., LANG, S. & SCHILDBACH, J. F. 2012. Assembly and mechanisms of bacterial type IV secretion machines. *Philos Trans R Soc Lond B Biol Sci,* 367**,** 1073-87.

ZHAO, S., ZHOU, Y., WANG, C., YANG, Y., WU, X., WEI, Y., ZHU, L., ZHAO, W., ZHANG, Q. & WAN, C. 2013. The N-terminal domain of EspF induces host cell apoptosi after infection with enterohaemorrhagic Escherichia coli O157:H7. *PLoS One,* 8**,** e55164.

ZIGMOND, S. H. 2004. Beginning and ending an actin filament: control at the barbed end. *Curr Top Dev Biol,* 63**,** 145-88.

ZUCHERO, J. B., COUTTS, A. S., QUINLAN, M. E., THANGUE, N. B. & MULLINS, R. D. 2009. p53-cofactor JMY is a multifunctional actin nucleation factor. *Nat Cell Biol,* 11**,** 451-9.

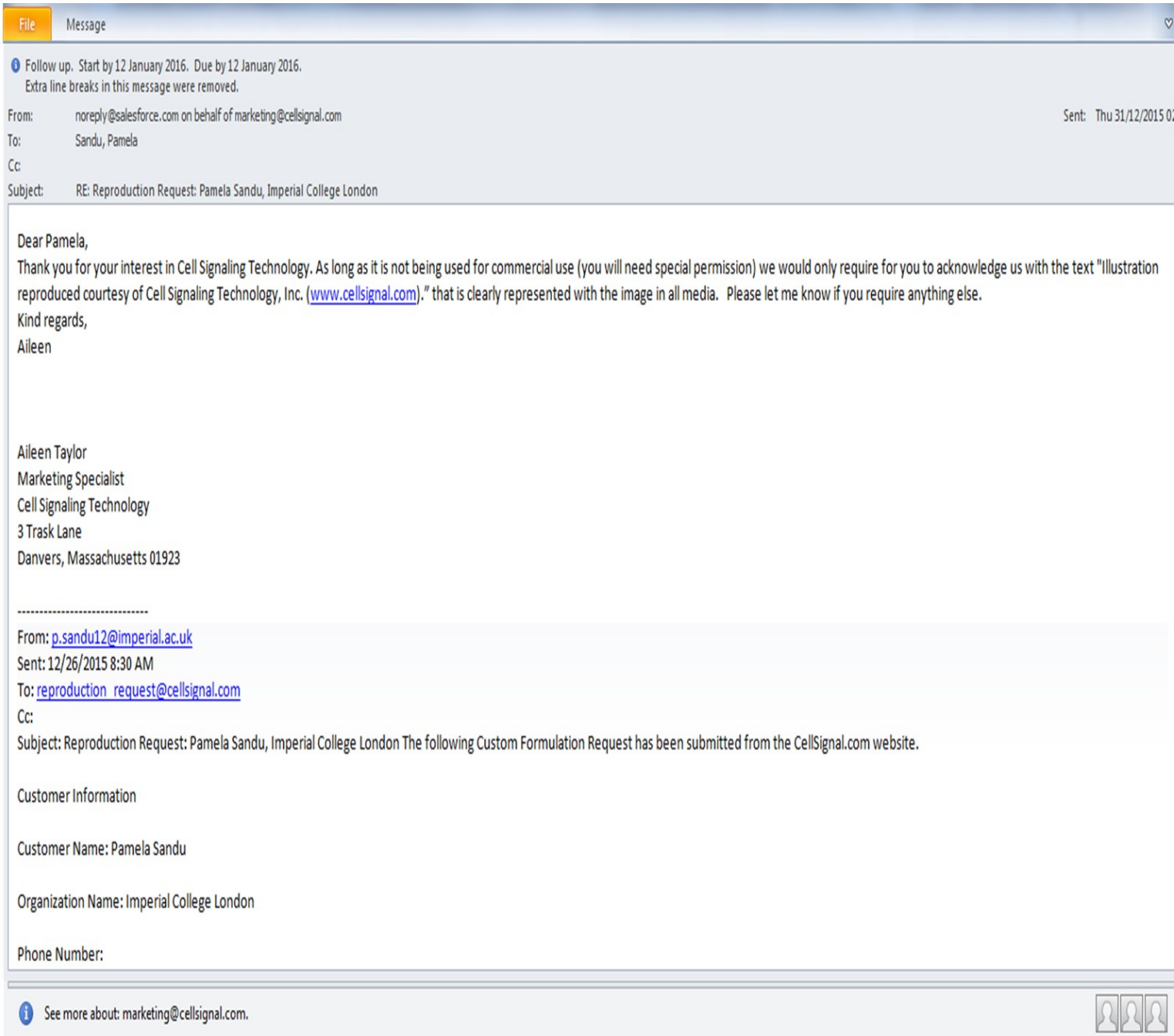

File Message

Follow up. Start by 12 January 2016. Due by 12 January 2016.
Extra line breaks in this message were removed.

From: noreply@salesforce.com on behalf of marketing@cellsignal.com Sent: Thu 31/12/2015 0

To: Sandu, Pamela

Cc:

Subject: RE: Reproduction Request: Pamela Sandu, Imperial College London

Dear Pamela,
Thank you for your interest in Cell Signaling Technology. As long as it is not being used for commercial use (you will need special permission) we would only require for you to acknowledge us with the text "Illustration reproduced courtesy of Cell Signaling Technology, Inc. (www.cellsignal.com)." that is clearly represented with the image in all media. Please let me know if you require anything else.
Kind regards,
Aileen

Aileen Taylor
Marketing Specialist
Cell Signaling Technology
3 Trask Lane
Danvers, Massachusetts 01923

From: p.sandu12@imperial.ac.uk
Sent: 12/26/2015 8:30 AM
To: reproduction_request@cellsignal.com
Cc:
Subject: Reproduction Request: Pamela Sandu, Imperial College London The following Custom Formulation Request has been submitted from the CellSignal.com website.

Customer Information

Customer Name: Pamela Sandu

Organization Name: Imperial College London

Phone Number:

See more about: marketing@cellsignal.com.


Rightslink® by Copyright Clearance Center - Google Chrome
https://s100.copyright.com/AppDispatchServlet#formTop
Copyright Clearance Center
RightsLink®
Home
Create Account
Help
Live Chat
ANNUAL REVIEWS
Title: Regulation of Actin Filament Assembly by Arp2/3 Complex and Formins
Author: Thomas D. Pollard
Publication: Annual Review of Biophysics and Biomolecular Structure
Publisher: Annual Reviews
Date: Jun 1, 2007
Copyright © 2007, Annual Reviews
LOGIN
If you're a copyright.com user, you can login to RightsLink using your copyright.com credentials. Already a RightsLink user or want to learn more?
Permission Not Required
Material may be republished in a thesis / dissertation without obtaining additional permission from Annual Reviews, providing that the author and the original source of publication are fully acknowledged.
BACK
CLOSE WINDOW
Copyright © 2016 Copyright Clearance Center, Inc. All Rights Reserved. Privacy statement. Terms and Conditions.
Comments? We would like to hear from you. E-mail us at customercare@copyright.com

IAI Accepted Manuscript Posted Online 19 June 2017 Infect. Immun. doi:10.1128/IAI.00244-17

1 The enterohaemorrhagic *Escherichia coli* effector EspW triggers actin remodeling in a 2 Rac1 dependent manner

3

4 Running title: EspW induces actin reorganization

5

6 Pamela Sandu [1] , Valerie F. Crepin [1] , Hauke Drechsler [2] , Andrew D. McAinsh [2] , Gad Frankel [1] , 7 Cedric N. Berger [1#]

8

- 9 [1] MRC Centre for Molecular Bacteriology and Infection, Department of Life Sciences,
- 10 Imperial College London, UK; [2] Centre for Mechanochemical Cell Biology, Division of
- 11 Biomedical Cell Biology, Warwick Medical School, University of Warwick, Coventry CV4
- 12 7AL, UK

13

14

- 15 Corresponding author:
- 16 Cedric N. Berger
- 17 MRC CMBI, Flowers Building
- 18 Imperial College
- 19 London, SW7 2AZ
- 20 Tel: +442075945300
- 21 c.berger@imperial.ac.uk

1

Abstract 22

Enterohaemorrhagic *Escherichia coli* (EHEC) is a diarrheagenic pathogen that 23 colonizes the gut mucosa and induces attaching-and-effacing lesions. EHEC employs a 24 type III secretion system (T3SS) to translocate 50 effector proteins that hijack and 25 manipulate host cell signalling pathways, which allow bacterial colonization, 26 subversion of immune responses and disease progression. The aim of this study was to 27 characterize the T3SS effector EspW. We found *espW* in the sequenced O157:H7 and 28 non-O157 EHEC strains as well as in *Shigella boydii*. Furthermore, a truncated version 29 of EspW, containing the first 206 residues is present in EPEC strains belonging to 30 serotype O55:H7. Screening a collection of clinical EPEC isolates revealed

that *espW* is 31 present in 52% of the tested stains. We report that EspW modulates actin dynamics in 32 a Rac1-dependant manner. Ectopic expression of EspW results in formation of unique 33 membrane protrusions. Infection of Swiss cells with an EHEC *espW* deletion mutant 34 induces a cell shrinkage phenotype that could be rescued by Rac1 activation via 35 expression of the bacterial GEF, EspT. Furthermore, using a yeast two hybrid screen 36 we identified the motor protein Kif15 as a potential interacting partner of EspW. Kif15 37 and EspW co-localized in co-transfected cells, while ectopically expressed Kif15 38 localized to the actin pedestals following EHEC infection. The data suggest that Kif15 39 recruits EspW to the site of bacterial attachment, which in turn activates Rac1, 40 resulting in modifications of the actin cytoskeleton that are essential to maintain cell 41 shape during infection. 42

Introduction 43

The human pathogens enterohemorrhagic *E. coli* (EHEC), enteropathogenic *E. coli* 44 (EPEC) (1) and the mouse pathogen *Citrobacter rodentium* (CR) (2) constitute a 45 bacterial family that colonize the intestinal mucosa and induce the formation of 46 attaching and effacing (A/E) lesions. The A/E lesions are characterized by effacement 47 of the brush border microvilli, intimate attachment of the bacteria to the apical 48 membrane of host epithelial cells and induction of actin polymerization beneath the 49 attached bacteria (3). EPEC, EHEC and *C. rodentium* employ a filamentous type III 50 secretion system (T3SS) (4), encoded within the locus of enterocyte effacement (LEE) 51 (5), to translocate a plethora of effector proteins directly from the bacterial cell into 52 host cell cytoplasm (6). Of the translocated effectors, five; Tir, EspZ, EspH, EspG and 53 Map, are LEE-encoded. The effector Tir plays a key role in formation of A/E lesions *in* 54 *vivo* (7) and actin rich pedestals in cultured cells (8). Following clustering by the LEE-55 encoded outer membrane adhesin intimin, Tir_{EPEC} and Tir_{CR} bind Nck while Tir_{EHEC} binds 56 the adaptor proteins IRTKS and/or IRSp53 (9, 10), and recruits the effector TccP/EspFu 57 (11, 12). The Tir signalling pathways then converge on N-WASP and the ARP2/3 58 complex, leading to actin polymerization (13).

The actin cytoskeleton, which is targeted by many bacterial pathogens, is essential for 60 cell integrity, motility, membrane trafficking and shape changes (14). Rho GTPases, 61 which belong to the family of Ras-related small GTPases, are key regulators of various 62 cellular processes including actin polymerization, microtubule dynamics, vesicle 63 trafficking, cell polarity and cytokinesis (15). The best-characterized members of the 64 Rho GTPases family are RhoA, Rac1 and Cdc42, activation of which leads to the 65 assembly of stress fibers, lamellipodia/ruffles and filopodia, respectively (16). 66 Switching of Rho GTPases from an inactive GDP bound state to an active GTP bound 67 state is mediated by guanine nucleotide exchange factors (GEFs). The switch back from 68 the active GTP to an inactive GDP bound state is regulated by GTPase-activating 69 proteins (GAPs). In their GTP-bound conformation Rho GTPases interact with and 70 activate downstream target effectors such as serine/threonine kinases, tyrosine 71 kinases, lipid kinases, lipases, oxidases and scaffold proteins (17). As Rho GTPases are 72 important regulators of the actin cytoskeleton, bacterial pathogens have evolved 73 strategies to subvert their signalling during infection. 74

Bacterial guanine nucleotide exchange factors, which belong to the SopE family, act as 75 bacterial Rho GEFs to activate the host Rho GTPase (18). The A/E pathogen effector 76 Map induces filopodia via Cdc42 at the site of attachment (19, 20), EspM promotes 77 stress fibres via RhoA activation (21), and EspT trigger ruffles and lamellipodia 78 formation by Rac1 (22). A/E pathogens also translocate effectors that inactivate Rho 79 GTPases. EspH globally inactivates DH-PH domain mammalian Rho-GEFs but not the 80 bacterial Rho-GEFs (23). Tir antagonizes the activity of Map as it down-regulates 81 filopodia formation (24), while EspO2 interact with EspM2 and blocks formation of the 82 stress fibres (25). 83

Using a transfection based screen, we recently identified that EspW $_{EHEC}$ as a regulator 84 of actin filaments organisation. EspW has been previously shown to be secreted by 85 EHEC and translocated into mammalian cells in a type 3-dependent manner (26). 86 However, until now, no function has been identified for this effector. The aim of this 87 study was to investigate the role of EspW during EHEC infection and its putative role as 88 Rho GTPases regulator. 89

Results 90

Screening of *espW* in EPEC clinical isolates 91

EspW is 352 amino acids effector and is located in the SP17 pathogenic island, which 92 also encodes EspM2 and members of the NleG family (Fig. S1A). So far, EspW has only 93 been reported in EHEC O157:H7 and EPEC B171 (O111:H-) strains, with no homologs 94 amongst other bacterial species. Using the BLAST algorithm with EspW as index 95 protein, we confirmed that it was present in the sequenced EHEC O157:H7 strains, in 96 five non-O157:H7 EHEC strains (O111:H-, O111:H11, O26:H11, O103:H2 and 97

O103:H25) as well as in *Shigella boydii* (Fig. S1B). Furthermore, a putative coding 98 sequence for a truncated version of EspW containing the N-terminal 206 amino acids 99 (EspW $_{1-206}$), was present in two EPEC strains (CB9615 and RM12579) belonging to 100 serotype O55:H7 (Fig. S2), a progenitor of EHEC O157:H7 (27). In order to determine if 101 either the long or short versions of *espW* are present in other EPEC strains, we 102 screened by PCR a collection of 132 clinical isolates available in our laboratory. This 103 revealed that the long version of *espW* is present in 52% of the tested stains (Table 1). 104 Furthermore, *espW* $_{1-206}$ was found in 10 of the 132 (8%) strains tested (Table 1). 105 Interestingly, nine of the 10 *espW* $_{1-206}$ genes belonged to serotype O55:H7. 106

Neither of the *espW* variants was found in *C. rodentium* and the prototype EPEC strain 107 E2348/69, while the prototype atypical EPEC strain E110019 (O111:H9) contains the 108 long version of *espW*. 109

EspW interacts with the C-terminus of Kif15 110

In order to identify the EspW host cell partner protein, we performed a yeast two 111 hybrid screen using HeLa cell cDNA library as bait and identified the carboxy terminus 112 of Kif15, Kif15 $_{1092-1368}$, as a putative partner. The interaction was confirmed by direct 113 Yeast-2-Hybrid (DY2H). Importantly, Kif15 $_{1092-1368}$ interacted with the full length EspW 114 (Fig. 1B) but not with EspW $_{1-206}$. To further map the binding site of EspW to Kif15, five 115 Kif15 truncation fragments were generated and tested by DY2H (Fig. 1A). An empty 116 pGAD-T7 plasmid was used as a negative

control. No growth was observed on selected 117 media (QDO) when yeast were co-transformed with EspW and Kif15 $_{1142\text{-}1347}$, Kif15 $_{1142\text{-}}$118 $_{1368}$ or with the negative control. In contrast, growth was seen following co-119 transformation with EspW and Kif15 $_{1092\text{-}1347}$ or Kif15 $_{1092\text{-}1142}$ (Fig. 1C), suggesting that 120 the C-terminus coil-coil domain of the Kif15 plays an important role in the interaction 121 with EspW. 122

Kif15 localizes to the pedestals and co-localizes with EspW 123

We aimed to determine the localization of Kif15 during EHEC infection. However, we 124 were unable to detect endogenous Kif15, and localization of overexpressed Kif15 was 125 difficult to detect due to poor tranfection efficiency. Accordingly, we determined the 126 localization of ectopically expressed Kif15 $_{1092\text{-}1368}$, used in the DY2H, following EHEC 127 infection of transfected Swiss 3T3 cells. Cells expressing myc-GFP were used as a 128 negative control. Immunofluorescence (IF) microscopy revealed that Kif15 $_{1092\text{-}1368}$, but 129 not GFP, localized to the actin pedestals at the site of EHEC attachment (Fig. 1D). 130 Interestingly, cells transfected with Kif15 $_{1092\text{-}1368}$ and infected with EHEC Δ*espW* present 131 a similar recruitment of Kif15 $_{1092\ 1368}$ into pedestal (Fig. S3) suggesting EspW is not 132 required for localization of Kif15 to the pedestal. 133

We next aimed to determine if Kif15 $_{1092\text{-}1368}$ and EspW co-localized. For this, we first 134 tried to HA-tagged EspW in EHEC, however; no signal could be detected by IF. 135 Therefore we cotransfected cells with pRK5-HA-*espW* and pRK5-Myc-*Kif15* $_{1092\text{-}1368}$. 136 pRK5-HA-*mCherry* served as a negative control. EspW and Kif15$_{1092\text{-}1368}$ co-localized, 137 whereas no co-localization was observed between mCherry and Kif15 $_{1092\text{-}1368}$, (Fig. 1E). 138 Interestingly, EspW and 139

Kif15 $_{1092\text{-}1368}$ were also present at membrane sites showing actin reorganisation. 140

EspW triggers actin remodelling in a Rac1 dependent manner 141

In order to determine if EspW is responsible for the observed actin reorganization (Fig. 142 1E), we transfected cells with pRK5-HA-*espW*, pRK5-HA-*espW* $_{1\text{-}206,}$ or pRK5 encoding 143 GFP as a negative control. Immunofluorescence straining (Fig. 2A) and scanning 144 electron microscopy (SEM; Fig. 2B) revealed that the full length EspW triggered either 145 formation of membrane ruffles (13% of transfected cells) or flower-shaped structures 146 (42% of transfected cells), which were rich in actin and co-localized with EspW (Fig 2A 147 to C). EspW $_{1\text{-}206}$ showed aggregative localisation dispersed within the cell with an actin 148 structure similar to those seen in the GFP control cells (Fig. 2A-B). 149

In order to determine if EspW-induced actin remodelling requires RhoA, Rac-1 or 150 Cdc42, we co-transfected HeLa cells with pRK5-HA-*espW* and a dominant negative of 151 each of the GTPases (Rac1 $_{N17}$, RhoA $_{N19}$ and Cdc42 $_{N17}$). The co-transfected cells were 152 assessed by IF for the presence of actin-rich flower-shaped structures. This revealed 153 that inactivation of either RhoA or Cdc42 had no effect on the ability of EspW to 154 induce actin reorganisation (Fig. 3A). In contrast, inhibition of Rac1 significantly 155 compromised the ability of EspW to induce actin rearrangements (Fig. 3A and B). 156

Deletion of *espW* induces cell shrinkage that could be overcome by Rac1 activation 157

To assess the role of EspW during infection, cells were infected for 3 h with wild-type 158 (WT) EHEC, EHEC Δ*espW* or EHEC Δ*espW* complemented with pEspW. 159 Immunofluorescence reveals that infection with EHEC Δ*espW* induced significant cell 160 shrinkage (56%) compared to infection with WT EHEC (12%; Fig. 4A). Partial 161 complementation was observed for the cell infected with EHEC Δ*espW* complemented 162 with pEspW (32%; Fig 4C). 163

To determine if the cell shrinkage was linked with lack of activation of Rac1, cells were 164 infected with EHEC Δ*espW* overexpressing EspT, an effector known to activate Rac1 165 (22). EspT $_{W/A}$ mutant, lacking the GEF activity of EspT, was used as a negative control 166 (Fig. 4B). 167

Expression of WT EspT significantly reduced cell shrinkage (31%) compared with cells 168 infected with EHEC Δ*espW* complemented with pEspT $_{W/A}$ (50%; Fig 4C). 169

5

In order to confirm that the cell shrinkage was caused by the lack of Rac1 activation, 170 we chemically induced activation of Rac1 during infection by adding 100nM S1P to the 171 culture medium (28) and quantified the number of shrunk cells after infection (Fig. 5A-172 B). S1P treatment significantly reduced cell shrinking of cells infected with EHEC Δ*espW* 173 from 53% to 33% (Fig. 5B). These results suggest that EspW activates Rac-1, which 174 stabilizes the shape of infected cells. 175

6

Discussion 176

In this study we found that *espW* is common amongst clinical EHEC and EPEC isolates; 177 an *espW* orthologue is also found in *Shigella boydii*. The majority of the EPEC strains 178 contain the full length *espW* gene, while others, mainly belonging to EPEC O55:H7, 179 encode a truncated EspW isoform. Although the truncated form of EspW does not 180 induce actin 181

reorganization, it is possible that it has other biological functions. 182

Using a two-hybrid screen we identified Kif15 as a specific partner of the full-length 183 EspW isoform. Human Kif15 is a multimeric protein of 1388 amino acids which belongs 184 to the kinesin family (29). It has an N-terminal motor domain (19–375) followed by a 185 long alpha helical rod-shaped stalk predicted to form an interrupted coiled coil. The C-186 terminal region has been shown to contain a putative actin interacting region 187 (residues 743–1333) (30). Moreover, in HeLa cells, Kif15 has been shown to 188 concentrate on spindle poles and microtubules in early mitosis and to localize with 189 actin in late mitosis (31). One possibility is that Kif15 switches binding from one 190 filament system to the other, while another possibility is that Kif15 may associate with 191 the most abundant cytoskeletal filament system (31). In this study we mapped the 192 EspW binding site to a segment of Kif15, amino acids 1092-1142. This segment is a 193 known binding site for both Ki-67 (1017-1237) and actin (743-1333). The exact role of 194 Kif15 during infection is still unclear as labelling of EspW in EPEC did not allow us to 195 localize the effector during infection. However, its recruitment to the pedestal during 196 EPEC infection is independent of EspW. We therefore hypothesize that Kif15 recruits 197 EspW

and determines its spatial distribution, similar to the function of NHERF1 or 198 NHERF2 towards the effector Map (32). 199

EPEC and EHEC, like many other enteric pathogens, target actin cytoskeleton as part of 200 their infection strategy. The hallmark of EPEC and EHEC infection of cultured cells is 201 formation of actin pedestal-like structures underneath the attached bacteria. In EPEC, 202 formation of these structures is dependent on the effector Tir and activation of N-203 WASP and independent of activation of mammalian Rho GTPases (33). However, EspH, 204 which is a global inhibitor of endogenous mammalian GEFs (23), is required for 205 efficient actin pedestal elongation (34) suggesting that Rho GTPases may be partially 206 involved in this process. Importantly, EPEC and EHEC translocate several effectors, 207 belonging to the SopE family, which have a GEF activity towards mammalian Rho 208 GTPases (18). *In vitro*, EspT which activates Rac1 triggers formation of ruffles or 209 lamelipodia and *in vivo* it induces expression of KC and TNF-α (35). In this study, we 210 found that EspW also appears to activate Rac1, either directly or indirectly, in 211 compartmentalised fashion; this is in contrast to EspT which has a more global effect. 212 Nonetheless, the phenotype of *espW* deletion could be partially complemented by 213

espT, suggesting some activity overlap. Due to a poor solubility, we were not able to 214 identify whether EspW directly activates Rac1. Importantly, multiple biological systems 215 revealed that activation or inhibition of the Rho GTPase has to be fine-tuned both 216 spatially and temporally. Their over activation or inhibition have detrimental effects 217 leading to activation of alarm signals (36) or apoptosis (37). During EPEC infection 218 activation of Cdc42 is limited to the bacterial binding sites (19); followed by rapid 219 inhibition by Tir (19). The effector EspO expressed by a selection of EPEC and EHEC 220 strains has been reported to inactivate EspM2 221

(RhoA GEF). Interestingly, deletion of *espO1* and *espO2* leads to cell shrinkage, in an 222 EspM2 dependant manner (25). Rac1 and RhoA have antagonistic effects (38). 223 Interestingly, we found that cells infected with EHEC expressing EspM1 and EspM2 but 224 missing EspW undergo cell shrinkage. This cell shrinkage phenotype was not 225 associated with decreased cell attachment or with any signs of cell death, including 226 nucleus condensation, loss of membrane permeability, or membrane blebbing, for the 227 duration of the experiment. Interestingly, we found that EPEC and EHEC strains 228 expressing EspM also express either EspT or EspW, suggesting that activation of RhoA 229 and Rac1 need to be coordinated during infection. 230

Furthermore, deletion of Rac1 impairs focal adhesion complex formation and cell 231 spreading (39). Taken together, these observations suggest that EPEC and EHEC have 232 developed a complex mechanism to control cell shape by manipulating the localization 233 and activation of RhoA and Rac1. Any dysregulation leading to an uncontrolled 234 activation leads to dramatic cell morphology changes. Further studies will be needed 235 in order to understand the spatiotemporal regulation of the Rho GTPase during EPEC 236 and EHEC infections. 237

238

Experimental procedures 239

Bacterial strains, growth conditions and cell culture 240

The bacterial strains used in this study and their origin are listed in Table 2. Bacteria 241 were grown from a single colony in Luria-Bertani (LB) broth in a shaking incubator (200 242 rpm) at 243

37°C for 18 h or on agar supplemented with ampicillin (100 µg/ml) or kanamycin (50 244 µg/ml). For cell infections, EHEC strains were grown in LB in a shaking incubator (200 245 rpm) at 37°C for 8 h and then subcultured (1/500) in DMEM with low glucose and 246 grown overnight at 37°C without agitation in 5% CO_2 incubator (primed culture). 247

Saccharomyces cerevisiae (AH109) were grown in YPDA medium (20 g/L Difco 248 peptone, 249

10 g/L yeast extract 2% glucose and 0.003% adenine hemisulfate) for 48 h at 30°C. For 250 the Yeast-2-hybrid screen, clones containing interaction partners were selected on 251 highstringency quadruple-dropout media (QDO) lacking leucine, tryptophan, histidine, 252 and adenine in the presence of X-α-Gal (Clontech Laboratories, Inc.). Successful 253 transformation with bait and prey plasmids was selected by plating on double-dropout 254 media (DDO) lacking leucine and tryptophan. Bait-prey interactions were assessed by 255 streaking the transformed clones from DDO onto QDO selection medium. 256

Swiss 3T3 and HeLa cells were maintained in DMEM with 4500 mg/ml glucose (Sigma) 257 or DMEM with 1000 mg/ml glucose (Sigma), respectively, supplemented with 10% 258 (vol/vol) heat-inactivated foetal bovine serum FCS (Gibco), 4 mM GlutaMAX (Gibco) 259 and 0.1 mM nonessential amino acids at 37°C in 5% CO2. 260

261

Plasmids and molecular techniques 262

Plasmids used in this study are listed in Table 2; primers are listed in Table S1. 263

The EHEC Δ*espW* (ICC1111) was generated using a Lambda red-based mutagenesis 264 system (40) in which *espW* was replaced by a kanamycin cassette. Plasmid pSB315 was 265 the source of the kanamycin resistance gene (*aphT*) which was purified following 266 *EcoRI* restriction digest. Primer pair P23/P24 was used to PCR-amplify *espW* with 267 500bp upstream and downstream flanking regions, from *E. coli* O157:H7 (85-170) 268 genomic DNA. The PCR product was cloned into TOPO Blunt II vector (Invitrogen) and 269 *espW* was removed by inverse PCR using the primer pair P25/P26. The linear PCR 270 product was then *EcoRI* digested to allow ligation of the kanamycin cassette. The 271 insert was then amplified using the primer pair P23/P24 and the PCR product 272

electroporated into WT EHEC containing pKD46 encoding the lambda Red 273 recombinase. Transformants were selected on kanamycin plates and the deletion of 274 *espW* was confirmed by PCR and DNA sequencing (using primer pair P27/P28). 275

EspW and *espW* $_{1-206}$ were cloned into the bacterial expression vector pRK5-HA 276 following amplification from 85-170 genomic DNA using primer pairs P1/P2 and P1/P3 277 generating plasmid pICC1727 and pICC1728. *mCherry* was amplified from pmcherry-278 miniSOG-C1(41) using primers P4/P5 generating plasmid pICC1396. Plasmid pICC1727 279 was used as template to amplify *espW* (P10/P11) and further cloned into pSA10 (42) 280 generating plasmid pICC1732. 281

EspW and *espW* $_{1-206}$ were amplified using primers P10/P12 with plasmids pICC1727 282 and pICC1728 respectively and cloned them into the *EcoRI/BamHI* restriction sites of 283 pGBT9 (Clonetech), generating plasmids pICC1714 and pICC1715. Kif15 $_{1092-1368}$ was 284 identified as a binding partner for EspW by Yeast-2-Hybrid screen (Clonetech). 285 *kif15* $_{1092-1368}$ was amplified by PCR with primers P13/P14 and cloned into pGAD-T7-AD 286 (Clonetech) using *NdeI/XhoI* as restriction sites, generating plasmid pICC1723. We 287 used plasmid pICC1723 as a template to amplify *kif15* $_{1142-1347}$, *kif15* $_{1092–1347}$ and 288 kif15 $_{1142–1368}$ with primers P15/P16, P17/P16 and P15/P18 respectively. The genes were 289 cloned into pGAD-T7 using *NdeI/XhoI* restriction sites generating plasmids pICC1724, 290 pICC1725 and pICC1726. Plasmid pICC1752 containing *kif15* $_{1092–1142}$ was generated by 291 inverse PCR using plasmid pICC1723 as template and phosphorylated primers 292 P19/P20. *kif15* $_{1092-1368}$ was cloned into the *EcoRI/HindIII* sites of the bacterial protein 293 expression vector pRK5-Myc (Clonetech) following amplification using primer pair 294 P21/P22 and plasmid pICC1723 as a template, generating plasmid pICC1914. EPEC 295 clinical isolates were screened first for the presence of *espW* by PCR using pair primers 296 P29/P30. We further screen all the *espW* negative strains for the presence of *espW* $_{1-}$ 297

$_{206}$ using primer pair P31/P32. 298

Yeast Two-Hybrid assays 299

Yeast Two-Hybrid screen using EspW as prey and cDNA library as bait was performed 300 as described previously (43). Briefly, a pre-transformed MATCHMAKER HeLa cell cDNA 301 library (Clontech) was screened according to the manufacturer's protocol for proteins 302 interacting with EspW. The LiAc method was used to transform pGBT9-espW 303 (pICC1714) (Table 2) into yeast strain AH109 (MATa) and transformants were selected 304 on Trp minus SD agar plates. Following mating with Y187 (MATα) yeast strain 305 containing the cDNA library, diploids cells were selected on DDO and QDO for 306 selection of protein interactions. The cDNA-containing pGADT7 plasmid was rescued 307 from positive clones and the cDNA identified by DNA sequencing. The prey plasmid 308 and derivatives (Table 2) were then retransformed into AH109 either on its own to 309

determine possible self-activation or with pICC1714 or pICC1715 to confirm 310 interaction by direct yeast-two hybrid. 311

Infection of Swiss 3T3 and HeLa cells 312

Forty-eight hours prior to infection, Swiss 3T3 or HeLa cells were seeded in 24-well 313 plates containing 13-mm glass coverslips (VWR International) at a density of 5.10 $_5$ cells 314 per well. 315

Infection and Immunity

Before infection the cells were washed 3 times with PBS and the medium was replaced 316 with fresh DMEM without FCS. Cells in 24-well plates were infected with 20 µl of 317 primed cultures. The plates were then centrifuged at 200 rpm for 5 min at room 318 temperature and infections were carried out for 3 h at 37°C in 5% CO_2 without 319 agitation. After infection, monolayers were washed at least ten times in PBS to remove 320 the bacteria and were fixed for immunofluorescence (to assess cell morphology) as 321 described below. 322

For Sphingosine 1-phosphate (S1P) (Sigma-Aldrich) treatment, S1P was dissolved in 323 dimethyl sulfoxide (DMSO) (Sigma-Aldrich) was added to DMEM medium to attain a 324 final concentration of 100 nM. 325

Transfection 326

Swiss 3T3 and HeLa cells were transfected for 24 h using Lipofectamine 2000 327 (Invitrogen) and GeneJuice (Merck Millipore), respectively, according to the 328 manufacturer's instructions. 329

Immunofluorescence and microscopy 330

Coverslips were fixed with 3% Paraformaldehyde (PFA) for 15 min before washing 3 331 more times with PBS. Cells were quenched for 10 min with 50 mM NH_4Cl then 332 permeabilized for 4 min in PBS 0.2% Triton X-100, and washed 3 times in PBS. The 333 coverslips were blocked for 15 min in 0.2% bovine serum albumin (BSA)-PBS before 334 incubation with primary and secondary antibodies. The primary antibody mouse anti 335 Haemagglutinin (HA) (Cambridge 336

Bioscience), chicken anti-Myc (Millipore), rabbit polyclonal anti O157 (Roberto la 337 Ragione, Veterinary Laboratory Agency, United Kingdom) were used at a dilution of 338 1:500. Coverslips were incubated with the primary antibody for 1 h, washed 3 times in 339 PBS and incubated with the secondary antibodies. AMCA-, Cy2-, RRX- or Cy5-340 conjugated donkey anti-mouse, antichicken and anti-rabbit antibodies (Jackson 341 ImmunoResearch) were used as secondary antibodies. All dilutions were in PBS 0.2% 342 BSA. Actin was detected with tetramethyl rhodamine isothiocyanate (TRITC)-343

conjugates phalloidin (1:500 dilution) (Sigma), Phalloidin Alexa Fluor® 350 or with 344 Phalloidin Oregon Green® 488 (1:100 dilution) 345

(Invitrogen). DNA was stained with 4',6-diamidino-2-phenylindole (DAPI) (1:1,000 346 dilution). Coverslips were mounted on slides using ProLong® Gold antifade reagent 347

(Invitrogen) and examined by conventional epifluorescence microscopy using a Zeiss 348 Axio LSM-510 microscope. Images were deconvoluted, processed using the Axio 349 Vision 4.8 LE software (Zeiss) and trimmed using Adobe Photoshop CS4. 350

Scanning electron microscopy 351

Cells were washed 3 times in phosphate buffer pH 7.4 and then fixed with 2.5% 352 glutaraldehyde in phosphate buffer pH 7.4. Cells were washed 3 times in phosphate 353 buffer before being post fixed in 1% Osmium Tetroxide for 1 h. Cells were then washed 354 3 times in phosphate buffer and dehydrated for 15 min in graded ethanol solutions 355 from 50% to 100%. The cells were then transferred to an Emitech K850 Critical Point 356 drier and processed according to the manufacturer's instructions. The coverslips were 357 coated in gold/palladium mix using an Emitech Sc762 mini sputter. Samples for 358 scanning electron microscopy (SEM) were then examined blindly at an accelerating 359 voltage of 25 kV using a Jeol JSM-6390. 360

Statistical analysis 361

All data were analysed with GraphPad Prism software, using one-way analysis of 362 variance (ANOVA). Results were expressed as means and standard deviations. 363 Statistical significance was determined by a two-tailed Student *t* test. A *P* value of 364 <0.05 was considered significant. 365

366

- 339 **Acknowledgements**
- 340 This work was supported by grants from The Wellcome Trust, the BBSRC and MRC.

References 340

- 1. Chen HD, Frankel G. 2005. Enteropathogenic *Escherichia coli*: unravelling 341 pathogenesis. FEMS Microbiol Rev 29:83-98. 342
- 2. Collins JW, Keeney KM, Crepin VF, Rathinam VA, Fitzgerald KA, Finlay BB, Frankel 343 G. 2014. *Citrobacter rodentium*: infection, inflammation and the microbiota. Nat 344 Rev Microbiol 12:612-23. 345
- 3. Knutton S, Lloyd DR, McNeish AS. 1987. Adhesion of enteropathogenic 346 *Escherichia coli* to human intestinal enterocytes and cultured human intestinal 347 mucosa. Infect Immun 55:69-77. 348
- 4. Knutton S, Rosenshine I, Pallen MJ, Nisan I, Neves BC, Bain C, Wolff C, Dougan G, 349 Frankel G. 1998. A novel EspA-associated surface organelle of enteropathogenic 350

Escherichia coli involved in protein translocation into epithelial cells. EMBO J 351 17:2166-76. 352

- 5. McDaniel TK, Jarvis KG, Donnenberg MS, Kaper JB. 1995. A genetic locus of 353 enterocyte effacement conserved among diverse enterobacterial pathogens. 354 Proc Natl Acad Sci U S A 92:1664-8. 355
- 6. Wong AR, Pearson JS, Bright MD, Munera D, Robinson KS, Lee SF, Frankel G, 356 Hartland EL. 2011. Enteropathogenic and enterohaemorrhagic *Escherichia coli:* 357 even more subversive elements. Mol Microbiol 80:1420-38. 358

- 7. Crepin VF, Girard F, Schuller S, Phillips AD, Mousnier A, Frankel G. 2010. 359 Dissecting the role of the Tir:Nck and Tir:IRTKS/IRSp53 signalling pathways in 360 vivo. Mol Microbiol 75:308-23. 361

- 8. Kenny B, Finlay BB. 1997. Intimin-dependent binding of enteropathogenic 362 *Escherichia coli* to host cells triggers novel signaling events, including tyrosine 363 phosphorylation of phospholipase C-gamma1. Infect Immun 65:2528-36. 364
- 9. Vingadassalom D, Kazlauskas A, Skehan B, Cheng HC, Magoun L, Robbins D, 365 Rosen MK, Saksela K, Leong JM. 2009. Insulin receptor tyrosine kinase substrate 366 links the *E. coli* O157:H7 actin assembly effectors Tir and EspF(U) during pedestal 367 formation. Proc Natl Acad Sci U S A 106:6754-9. 368
- 10. Weiss SM, Ladwein M, Schmidt D, Ehinger J, Lommel S, Stading K, Beutling U, 369 Disanza A, Frank R, Jansch L, Scita G, Gunzer F, Rottner K, Stradal TE. 2009. IRSp53 370 links the enterohemorrhagic *E. coli* effectors Tir and EspFU for actin pedestal 371 formation. Cell Host Microbe 5:244-58. 372
- 11. Campellone KG, Robbins D, Leong JM. 2004. EspFU is a translocated EHEC 373 effector that interacts with Tir and N-WASP and promotes Nck-independent actin 374 assembly. Dev Cell 7:217-28. 375
- 12. Garmendia J, Phillips AD, Carlier MF, Chong Y, Schuller S, Marches O, Dahan S, 376 Oswald E, Shaw RK, Knutton S, Frankel G. 2004. TccP is an enterohaemorrhagic 377 *Escherichia coli* O157:H7 type III effector protein that couples Tir to the 378 actincytoskeleton. Cell Microbiol 6:1167-83. 379
- 13. Caron E, Crepin VF, Simpson N, Knutton S, Garmendia J, Frankel G. 2006. 380 Subversion of actin dynamics by EPEC and EHEC. Curr Opin Microbiol 9:40-5. 381
- 14. Millard TH, Sharp SJ, Machesky LM. 2004. Signalling to actin assembly via the 382

WASP (Wiskott-Aldrich syndrome protein)-family proteins and the Arp2/3 383 complex. Biochem J 380:1-17. 384

- 15. Heasman SJ, Ridley AJ. 2008. Mammalian Rho GTPases: new insights into their 385 functions from in vivo studies. Nat Rev Mol Cell Biol 9:690-701. 386
- 16. Hall A. 1998. Rho GTPases and the actin cytoskeleton. Science 279:509-14. 387
- 17. Nayak RC, Chang KH, Vaitinadin NS, Cancelas JA. 2013. Rho GTPases control 388 specific cytoskeleton-dependent functions of hematopoietic stem cells. Immunol 389 Rev 256:255-68. 390
- 18. Bulgin R, Raymond B, Garnett JA, Frankel G, Crepin VF, Berger CN, Arbeloa A. 391

2010. Bacterial guanine nucleotide exchange factors SopE-like and WxxxE 392 effectors. Infect Immun 78:1417-25. 393

- 19. Berger CN, Crepin VF, Jepson MA, Arbeloa A, Frankel G. 2009. The mechanisms 394 used by enteropathogenic *Escherichia coli* to control filopodia dynamics. Cell 395 Microbiol 11:309-22. 396

- 20. Jepson MA, Pellegrin S, Peto L, Banbury DN, Leard AD, Mellor H, Kenny B. 2003. 397 Synergistic roles for the Map and Tir effector molecules in mediating uptake of 398 enteropathogenic *Escherichia coli* (EPEC) into non-phagocytic cells. Cell 399 Microbiol 5:773-83. 400
- 21. Arbeloa A, Bulgin RR, MacKenzie G, Shaw RK, Pallen MJ, Crepin VF, Berger CN, 401 Frankel G. 2008. Subversion of actin dynamics by EspM effectors of attaching and 402 effacing bacterial pathogens. Cell Microbiol 10:1429-41. 403

16

- 22. Bulgin RR, Arbeloa A, Chung JC, Frankel G. 2009. EspT triggers formation of 404 lamellipodia and membrane ruffles through activation of Rac-1 and Cdc42. Cell 405 Microbiol 11:217-29. 406
- 23. Dong N, Liu L, Shao F. 2010. A bacterial effector targets host DH-PH domain 407

RhoGEFs and antagonizes macrophage phagocytosis. EMBO J 29:1363-76. 408

- 24. Kenny B, Ellis S, Leard AD, Warawa J, Mellor H, Jepson MA. 2002. Co-ordinate 409 regulation of distinct host cell signalling pathways by multifunctional 410 enteropathogenic *Escherichia coli* effector molecules. Mol Microbiol 44:1095-411 1107. 412
- 25. Morita-Ishihara T, Miura M, Iyoda S, Izumiya H, Watanabe H, Ohnishi M, Terajima 413 J. 2013. EspO1-2 regulates EspM2-mediated RhoA activity to stabilize formation 414 of focal adhesions in enterohemorrhagic *Escherichia coli*-infected host cells. 415 PLoS One 8:e55960. 416
- 26. Tobe T, Beatson SA, Taniguchi H, Abe H, Bailey CM, Fivian A, Younis R, Matthews 417 S, Marches O, Frankel G, Hayashi T, Pallen MJ. 2006. An extensive repertoire of 418 type III secretion effectors in Escherichia coli O157 and the role of lambdoid 419 phages in their dissemination. Proc Natl Acad Sci U S A 103:14941-6. 420
- 27. Wick LM, Qi W, Lacher DW, Whittam TS. 2005. Evolution of genomic content in 421 the stepwise emergence of *Escherichia coli* O157:H7. J Bacteriol 187:1783-91. 422
- 28. Gonzalez E, Kou R, Michel T. 2006. Rac1 modulates sphingosine 1-423 phosphatemediated activation of phosphoinositide 3-kinase/Akt signaling 424 pathways in vascular endothelial cells. J Biol Chem 281:3210-6. 425

17

- 29. Drechsler H, McHugh T, Singleton MR, Carter NJ, McAinsh AD. 2014. The Kinesin- 426

12 Kif15 is a processive track-switching tetramer. Elife 3:e01724. 427

- 30. Klejnot M, Falnikar A, Ulaganathan V, Cross RA, Baas PW, Kozielski F. 2014. The 428 crystal structure and biochemical characterization of Kif15: a bifunctional 429 molecular motor involved in bipolar spindle formation and neuronal 430 development. Acta Crystallogr D Biol Crystallogr 70:123-33. 431
- 31. Buster DW, Baird DH, Yu W, Solowska JM, Chauviere M, Mazurek A, Kress M, 432 Baas PW. 2003. Expression of the mitotic kinesin Kif15 in postmitotic neurons: 433 implications for neuronal migration and development. J Neurocytol 32:79-96. 434

- 32. Martinez E, Schroeder GN, Berger CN, Lee SF, Robinson KS, Badea L, Simpson N, 435 Hall RA, Hartland EL, Crepin VF, Frankel G. 2010. Binding to Na(+) /H(+) exchanger 436 regulatory factor 2 (NHERF2) affects trafficking and function of the 437 enteropathogenic Escherichia coli type III secretion system effectors Map, EspI 438 and NleH. Cell Microbiol 12:1718-31. 439
- 33. Ben-Ami G, Ozeri V, Hanski E, Hofmann F, Aktories K, Hahn KM, Bokoch GM, 440 Rosenshine I. 1998. Agents that inhibit Rho, Rac, and Cdc42 do not block 441 formation of actin pedestals in HeLa cells infected with enteropathogenic 442 Escherichia coli. Infect Immun 66:1755-8. 443
- 34. Tu X, Nisan I, Yona C, Hanski E, Rosenshine I. 2003. EspH, a new 444 cytoskeletonmodulating effector of enterohaemorrhagic and enteropathogenic 445 Escherichia coli. Mol Microbiol 47:595-606. 446

- 35. Raymond B, Crepin VF, Collins JW, Frankel G. 2011. The WxxxE effector EspT 447 triggers expression of immune mediators in an Erk/JNK and NF-kappaB-448 dependent manner. Cell Microbiol 13:1881-93. 449
- 36. Keestra AM, Winter MG, Auburger JJ, Frassle SP, Xavier MN, Winter SE, Kim A, 450

Poon V, Ravesloot MM, Waldenmaier JF, Tsolis RM, Eigenheer RA, Baumler AJ. 451

2013. Manipulation of small Rho GTPases is a pathogen-induced process 452 detected by NOD1. Nature 496:233-7. 453

- 37. Fiorentini C, Falzano L, Travaglione S, Fabbri A. 2003. Hijacking Rho GTPases by 454 protein toxins and apoptosis: molecular strategies of pathogenic bacteria. Cell 455 Death Differ 10:147-52. 456
- 38. Chauhan BK, Lou M, Zheng Y, Lang RA. 2011. Balanced Rac1 and RhoA activities 457 regulate cell shape and drive invagination morphogenesis in epithelia. Proc Natl 458 Acad Sci U S A 108:18289-94. 459
- 39. Guo F, Debidda M, Yang L, Williams DA, Zheng Y. 2006. Genetic deletion of Rac1 460 GTPase reveals its critical role in actin stress fiber formation and focal adhesion 461 complex assembly. J Biol Chem 281:18652-9. 462
- 40. Datsenko KA, Wanner BL. 2000. One-step inactivation of chromosomal genes in 463

Escherichia coli K-12 using PCR products. Proceedings of the National Academy 464 of Sciences of the United States of America 97:6640-6645. 465

- 41. Shu X, Lev-Ram V, Deerinck TJ, Qi Y, Ramko EB, Davidson MW, Jin Y, Ellisman MH, 466 Tsien RY. 2011. A genetically encoded tag for correlated light and electron 467 microscopy of intact cells, tissues, and organisms. PLoS Biol 9:e1001041. 468

- 42. Schlosser-Silverman E, Elgrably-Weiss M, Rosenshine I, Kohen R, Altuvia S. 2000. 469 Characterization of Escherichia coli DNA lesions generated within J774 470 macrophages. J Bacteriol 182:5225-30. 471
- 43. Simpson N, Shaw R, Crepin VF, Mundy R, FitzGerald AJ, Cummings N, 472 StraatmanIwanowska A, Connerton I, Knutton S, Frankel G. 2006. The 473 enteropathogenic *Escherichia coli* type III secretion system effector Map binds 474 EBP50/NHERF1: implication for cell signalling and diarrhoea. Mol Microbiol 475 60:349-63. 476
- 44. Tzipori S, Karch H, Wachsmuth KI, Robins-Browne RM, O'Brien AD, Lior H, Cohen 477 ML, Smithers J, Levine MM. 1987. Role of a 60-megadalton plasmid and Shiga-478 like toxins in the pathogenesis of infection caused by enterohemorrhagic 479 Escherichia coli O157:H7 in gnotobiotic piglets. Infect Immun 55:3117-25. 480
- 45. Dolezal P, Aili M, Tong J, Jiang JH, Marobbio CM, Lee SF, Schuelein R, Belluzzo S, 481

Binova E, Mousnier A, Frankel G, Giannuzzi G, Palmieri F, Gabriel K, Naderer T, 482 Hartland EL, Lithgow T. 2012. Legionella pneumophila secretes a mitochondrial 483 carrier protein during infection. PLoS Pathog 8:e1002459. 484

- 46. Clements A, Smollett K, Lee SF, Hartland EL, Lowe M, Frankel G. 2011. EspG of 485 enteropathogenic and enterohemorrhagic E. coli binds the Golgi matrix protein 486 GM130 and disrupts the Golgi structure and function. Cell Microbiol 13:1429-39. 487
- 47. Li X, Saint-Cyr-Proulx E, Aktories K, Lamarche-Vane N. 2002. Rac1 and Cdc42 but 488 not RhoA or Rho kinase activities are required for neurite outgrowth induced by 489 the Netrin-1 receptor DCC (deleted in colorectal cancer) in N1E-115 490 neuroblastoma cells. J Biol Chem 277:15207-14. 491

- 48. Galan JE, Ginocchio C, Costeas P. 1992. Molecular and functional characterization 492 of the *Salmonella* invasion gene invA: homology of InvA to members of a new 493 protein family. J Bacteriol 174:4338-49. 494

495

Figures and tables legends 496

Table 1. Distribution of *espW* and *espW* $_{1\text{-}206}$ among 132 clinical EPEC isolates. 497

Serogroup	*espW*	Serotype (no. of strains)
ONT (3)	3	H7(1/1) ; H45(1/1); H-(1/1)
O13(1)	1	H-(1/1)
O26 (13)	9	H-(4/8); H11(5/5)
O49(1)	1	H-(1/1)
O55(24)	10	H-(3/11); H6(5/5); H7(1/5); H34(1/3)
O86(5)	3	H8(0/2); H34(3/3)

O104(1)	1	H2(1/1)
O109(1)	1	H9(1/1)
O111(12)	5	H-(2/4); H2(3/3); H9(0/1); H12(0/1); H21(0/1); H25(0/2)
O114(3)	2	H-(0/1); H2(2/2)
O119(29)	14	H2(4/11); H4(0/1); H6(10/17)
O123(1)	1	H-(1/1)
O125(3)	1	H6(1/3)
O126(4)	1	H-(1/1); H27(0/3)
O127(8)	3	H-(1/1); H6(2/3); H27(0/1); H40(0/3)
O128(6)	4	H-(0/1); H2(4/4); H35(0/1)
O142(7)	5	H6(3/3); H34(2/4)
O153(1)	1	H-(1/1)
O154(1)	1	H9(1/1)
O177(1)	1	H11(1/1)

espW was present in 68 out of 132 EPEC strains screened; 10 out of the 64 PCR 498 negative strains (O26:H-(1), O55:H-(5) and O55:H7(4)) were *espW* $^{1-206}$ positive. The 499 following strains were *espW* and *espW* $^{1-206}$ negative: O2:H49(1), O6:H19(2), O45:H-(1); 500 O85:H-(1) and 501

O118:H5(2). 502

22

503 **Table 2. List of strains and plasmids.**

Strain	**Description**	**Source/Reference**
85-170	EHEC O157:H7, stx-	(44)
ICC1111	85-170 Δ*espW*	This study
AH109	*S. cerevisiae* MATα mating type with ADE2, HIS3, MEL1 and LacZ reporters for interaction and TRP1 and LEU2 selection markers	Clontech
Y187	*S. cerevisiae* MATα mating type with MEL1 and LacZ reporters and TRP1 and LEU2 selection markers	Clontech
Plasmids	**Description/function**	**Source/Reference**
pRK5-HA (Amp $_r$)	Eukaryotic expression vector of HA tagged protein	(45)
pICC1396	pRK5- expression of HA tagged mCherry	This study
pICC1727	pRK5- expression of HA tagged EspW	This study
pICC1728	pRK5- expression of HA tagged EspW $^{1-206}$	This study
pRK5-myc (Amp $_r$)	Eukaryotic expression vector of Myc tagged protein	Clontech
pICC563	pRK5- expression of myc tagged GFP	(46)
pRK5-myc-Rac1 ^{N17}	pRK5- expression of myc tagged Rac1 ^{N17}	(47)
pRK5-myc-	pRK5- expression of myc tagged RhoA ^{N19}	(47)

RhoA ^{N19}		
pRK5-myc-Cdc42 ^{N17}	pRK5- expression of myc tagged Cdc42 ^{N17}	(47)
pICC1914	pRK5- expression of myc tagged Kif15 $^{1092-1368}$	This study
pSA10 (Amp ^{r})	pKK177-3 derivative containing *lac I*	(42)
pICC1732	pSA10 derivative expressing espW	This study
pICC461	pSA10 derivative expressing espT	(22)
pICC1205	pSA10 derivative expressing espT $^{W/A}$	(22)
pKD46 (Amp ^{r})	Coding the lambda red recombinase	(40)
pSB315 (Kan ^{r})	Coding the kanamycin resistance *aphT* cassette	(48)
TOPO Blunt II (Kan ^{r})	Plasmid for TOPO cloning of blunt PCR products	Invitrogen
pGBT9	Gal4 DNA binding domain, selective for –Trp media expression for proteins in yeast	Clontech
pICC1714	pGBT9 derivative expressing espW	This study
pICC1715	pGBT9 derivative expressing espW $^{1-206}$	This study
pGAD-T7-AD	Yeast two-hybrid prey expression vector	Clontech
pICC1723	pGAD derivative expressing Kif15 $^{1092-1368}$	This study
pICC1724	pGAD derivative expressing Kif15 $^{1142-1347}$	This study
pICC1725	pGAD derivative expressing Kif15$^{1092-1347}$	This study
pICC1726	pGAD derivative expressing Kif15 $^{1142-1368}$	This study
pICC1752	pGAD derivative expressing Kif15 $^{1092-1142}$	This study

504

23

Figures legends 504

Fig. 1 Kif15 interacts with EspW 505

A. Schematic representation of Kif15. **B**. Direct yeast two hybrid assay revealed that 506 EspW 507

but not EspW $^{1-206}$, interacts with Kif15 $^{1092-1368}$. **C.** EspW interacts with Kif15 $^{1092-1368}$, 508 Kif15$^{1092–1347}$ and Kif15$^{1092–1142}$ but not Kif15$^{1142–1368}$ and Kif15$^{1142-1347}$, by direct yeast two 509 hybrid. **D**. Following infection of transfected Kif15 $^{1092-1368}$ (green) cells, Kif15 $^{1092-1368}$ 510 localized at the actin (red) pedestals (white arrows), under adherent EHEC (magenta). 511 DNA was visualized by Hoechst staining (blue). **E**. Ectopically expressed Kif15 $^{1092-1368}$ 512 (green) colocalized with EspW (red) and actin (magenta) but not mCherry in Swiss 3T3 513 cells. Bar = 10 μm 514

515

Fig. 2: EspW induces actin rearrangement 516

A. Ectopic expression of HA-EspW (green) induces either actin (red) ruffles or flower-517 shape structures. No actin modification can be observed with HA-EspW $_{1\text{-}206}$ or GFP 518 (green). DNA was visualized by Hoechst staining (blue). White arrows indicate co-519 localization of EspW with actin. Bar = 5 µm. **B**. SEM of transfected cell. **C**. 520 Quantification of actin structure observed in transfected cells. 521

522

Fig. 3 EspW-induced actin reorganisation is Rac1 dependant 523

A. Co-transfection of HA-EspW (red) with myc-Rac1 $_{N17}$ (green), but not with GFP, 524 MycCdc42 $_{N17}$ and Myc-RhoA $_{N19}$, inhibited actin (blue) rearrangement (white arrow). 525 Bar = 10 µm. **B**. Quantification of co-transfected cells showing actin rearrangement. 526 Percentage was calculated by counting 100 transfected cells (in triplicate) from three 527 independent experiments. Results are presented as means ± SD. * $p < 0.05$ 528

529

Fig.4 EHEC Δ*espW* induces cells shrinkage 530

A. Shrinking of cells (visualised by IF with actin in green / DNA in blue and SEM) was 531 observed following infection with EHEC Δ*espW* in comparison to cell uninfected or 532 infected with WT EHEC (red) or EHEC Δ*espW* complemented with pEspW. Bar = 5 µm. 533

B. Cells infected with EHEC Δ*espW* expressing EspT $_{W/A}$ shrunk compared to cells 534 infected with EHEC Δ*espW* expressing WT EspT. Bar = 5 µm. **C**. Quantification of 535 phenotype observed in panel B (100 infected cells in triplicate) following infection with 536 WT EHEC, EHEC Δ*espW*, 537

EHEC Δ*espW* expressing EspW (Δ*espW*/EspW), EspT (Δ*espW*/EspT) and EspT W/A 538 (Δ*espW*/EspT W/A). * $p < 0.05$ 539

540

Fig.5 Rac1 activation prevent cell shrinkage 541

A. Immunofluorescence microscopy of Swiss cells (visualised with actin in green / DNA 542 in blue) infected (magenta) with WT EHEC or EHEC Δ*espW* in the presence or absence 543 of 100 nM of S1P. The presence of S1P prevented cell shrinkage. Bar = 10 µm. **B.** 544 Quantification of phenotype observed in panel B (100 cells in triplicate) infected with 545 WT EHEC, EHEC Δ*espW* in presence (white bar) or absence (black bar) of S1P. * $p <$ 546 0.05 547

548

549

Infection and Immunity

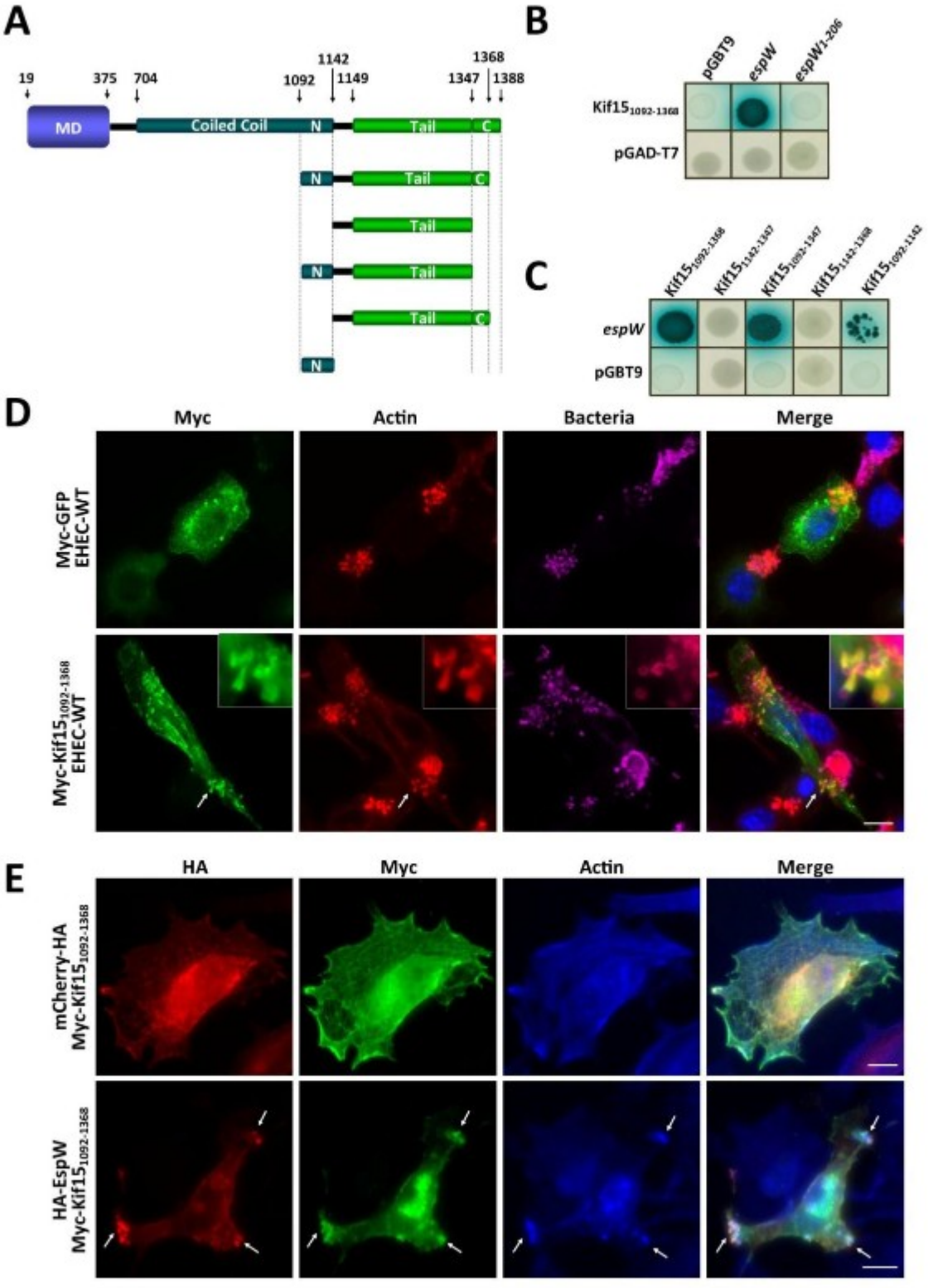

Fig. 1

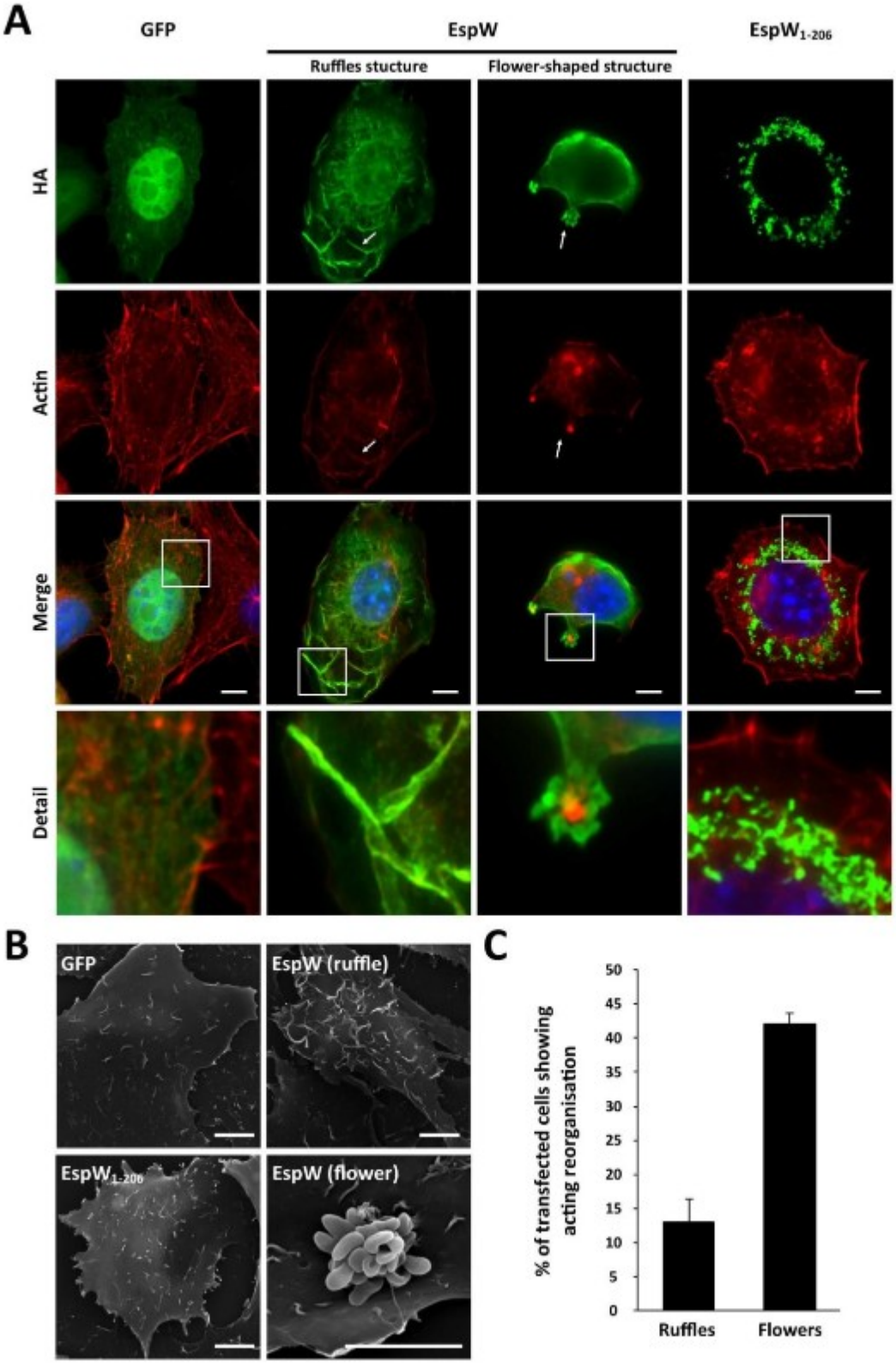

Fig. 2

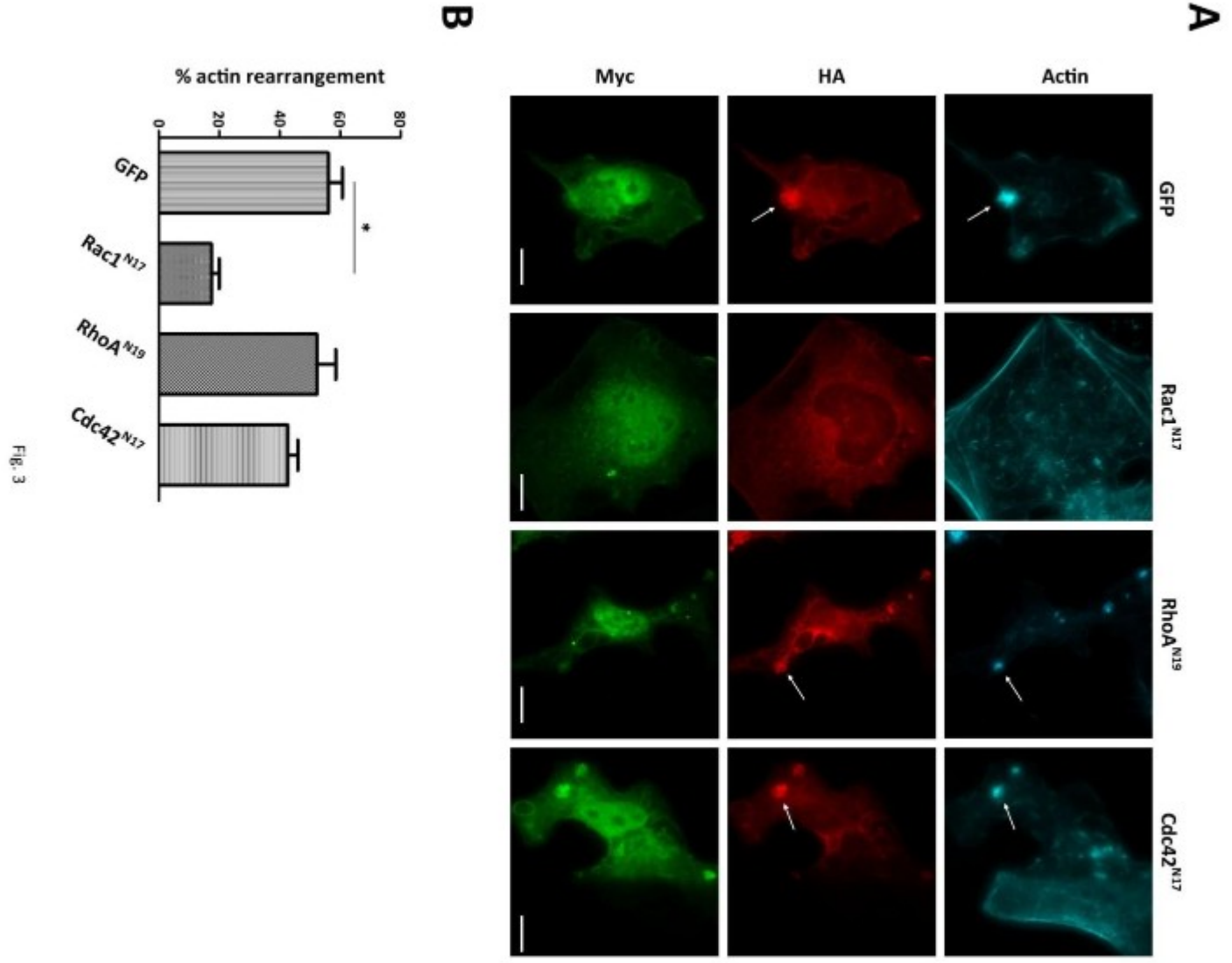
A
Myc
HA
Actin
GFP
Rac1N17
RhoAN19
Cdc42N17
B
% actin rearrangement
0
20
40
60
80
GFP
Rac1N17
RhoAN19
Cdc42N17
*

Fig. 3

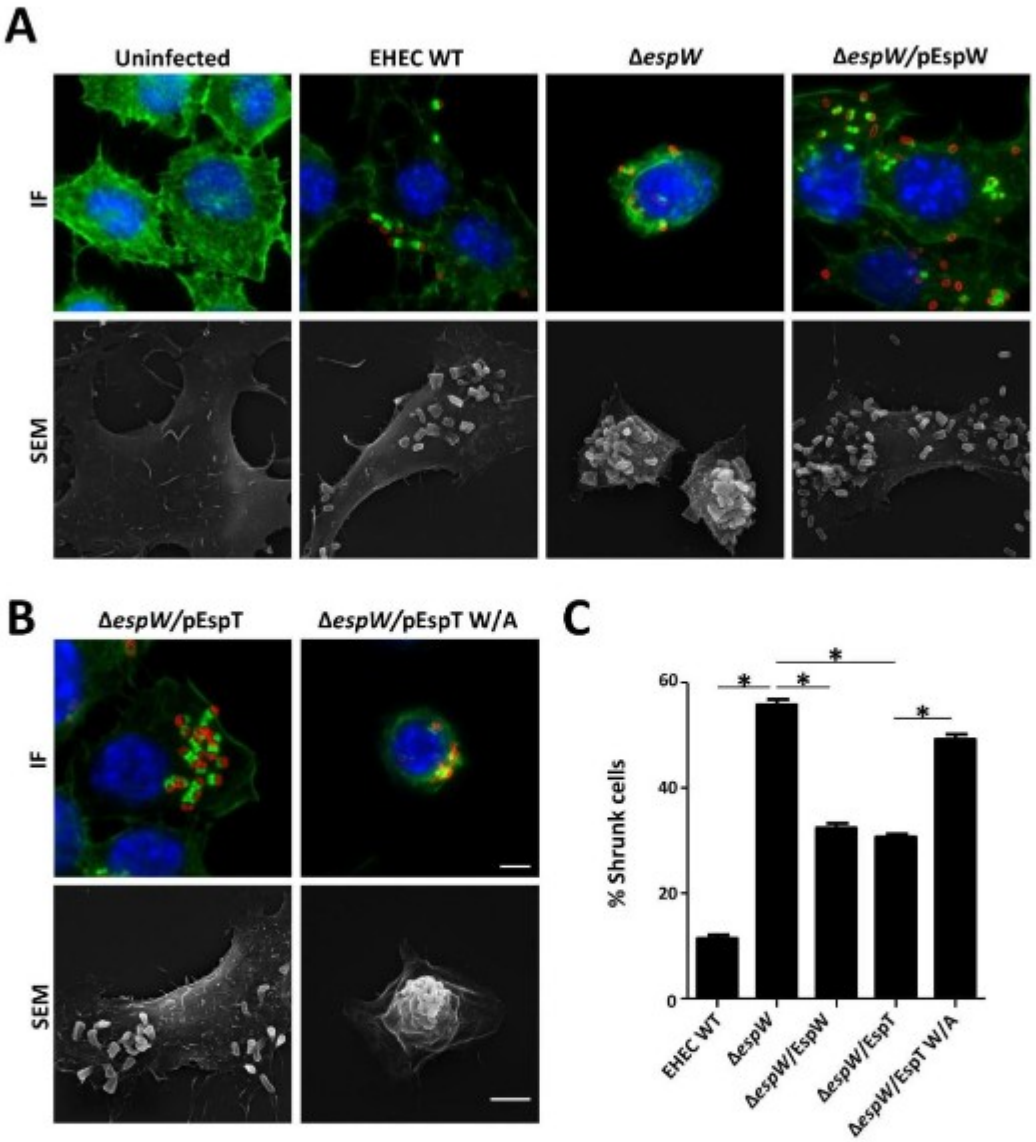

Fig. 4